Initial Probabilistic Seismic Hazard model for France's southeast 1/4

Inputs to SIGMA Project for tests and improvements

AUTHORS			REVIEW			APPROVAL		
NOM	DATE	VISA	NOM	DATE	VISA	NOM	DATE	VISA
D. Carbon S. Drouet C. Gomes A. Leon Ch. Martin R. Secanell GEOTER	13/02/2012	In attachment	F. Scherbaum Postdam University Member of the SIGMA Scientific Committee J. Savy Risk Consulting USA Member of the SIGMA Scientific Committee	Review done during the Scientific Committee 17-18 Nov 2011		G. Senfaute SIGMA Project Leader		

DISSEMINATION: Authors; Steering Committee; Work Package leaders, Scientific Committee, Archiving.

	Research and Development Programme on Seismic Ground Motion	**Ref : SIGMA-2012-D4-41** **Version : 01**
EDF cea AREVA Enel Σigma	CONFIDENTIAL *Restricted to SIGMA scientific partners and members of the consortium, please do not pass around*	**Date : 13/02/2012** **Page : 121 (report)** **8 (annex 1)** **22 (annex 2)**

Summary

The objective of the task 4-1 was to produce maps and hazard curves, based on available data and models and using current state of practice in the country, at the beginning of the project and to provide necessary inputs (maps, hazard curves and response spectra) to the others tasks of the project.
The results of the initial PSHA will be used in the future to appreciate the benefits of SIGMA at the end of the project.

The PSHA level is comparable to a SSHAC level 2. The conceptual logic tree tries to capture a representative range of possibilities, especially regarding the seismotectonic sources and ground motion prediction equations, based on the available data at the beginning of the project.

The epistemic branches of the logic tree refer to the seismic source models, the GMPEs, the catalogue of seismicity and associated completeness periods and Gütenberg-Richter parameters, and to the maximum magnitudes. The other uncertainties represent the aleatory variability of the earthquakes distribution within the seismic source (location and depth), of the time of occurrence and of the ground motion.

A zoneless model was implemented to compare the results obtained with the logic tree based on source zones models.

All the numeric results are made available to the SIGMA partners on a DVD. The results will be tested and shortcomings will be solved in order to improve the PSHA model within the further steps of the project.

SIGMA. WP4 T4-1.

Initial Probabilistic Seismic Hazard model

for France's southeast ¼

Inputs to SIGMA Project for tests and

improvements

Type of document :	identification :
Final report	Report GTR/ARE/0212-924

Revisions

Ind.	Date	Modifications
0	13/02/2012	First emission of the report

Client : **AREVA**	Type of document : **Final report**	Identification : **GTR/ARE/0212-924**	
Contact : **Jean-Michel THIRY**	GEOTER archive (text and figures): Serveur\affaire\2011\1411	Reference date: 13/02/2012	Number of pages: 119 p.

REPORT TITLE :

SIGMA. WP4 T4-1.

Initial Probabilistic Seismic Hazard model

for France's southeast ¼

Inputs to SIGMA Project for tests and improvements

Realization :

GEOTER international

Espace 890
Route Nationale 96
13360 ROQUEVAIRE
France

Tél. : (33) 04 42 36 08 60
Fax : (33) 04 42 36 08 61
Email :
geoter.international@geoter.fr
Site Web : www.geoter.fr

Contract : n° 40047900

date : 21/03/2011

CLIENT approval:
Jean-Michel THIRY
AREVA
69456 LYON Cedex 06
Email : jeanmichel.thiry@areva.com

Date	Prepared by	Checked by	Approved by
February 13, 2012	D. CARBON S. DROUET C. GOMES A. LEON C. MARTIN R. SECANELL	C. MARTIN	P. COMBES
Visas			

CONTENTS

LIST OF FIGURES

> # SIGMA. WP4 T4-1.
> # Initial Probabilistic Seismic Hazard model for France's southeast ¼
> ## Inputs to SIGMA Project for tests and improvements

1. Introduction

1.1 Foreword

This report provides hazard curves, seismic hazard maps covering the south east of France, and uniform hazard response spectra at 20 sites, calculated for the purpose of providing a preliminary probabilistic hazard assessment at the beginning of the SIGMA project.

The deliverables produced in this study for each main branches of the logic tree, are contained in the DVD annexed to the report.

Several maps are provided, for return periods of 100, 475, 975, 5000 and 10000 years and for spectral periods of 0, 0.2 and 1 second. The spectral ordinates are defined as the geometric mean of the two horizontal components.

The PSHA model has been proposed by the technical integration team, composed by engineers and scientists from GEOTER. Two intermediate reports were produced during the task WP4-1:

- The models and parameters proposed for building a preliminary "classical" hazard map for France's southeast ¼ were detailed in the SIGMA report SIGMA-2011-D4-08 and discussed during the first scientific committee (Ref: SIGMA-2011-CR11) ;

- Refinements of the model were introduced and presented in the SIGMA report SIGMA-2011-D4-18, to consider the action items and recommendations issued by the SIGMA scientific committee.

Adjustements and modeling decisions were taken considering:

- The comments and written documents prepared by the two reviewers of the task WP4-1, Jean Savy and Frank Sherbaum ;

- Suggestions of the scientific committee ;

- Decisions taken together and convened with the SIGMA project manager and the WP4 leader after the second scientific committee of 17-18 November 2011.

To develop a probabilistic seismic hazard analysis (PSHA), the full range of uncertainty should be addressed (Budnitz et al 1997). This is generally implemented in identifying the epistemic and aleatory

uncertainties. The level of detail of the analysis may significantly vary as a function of the objective of the PSHA study. As detailed in Budnitz et al. (1997) SSHAC level 3 or level 4 study is designed to encompass the full range of technically defensible interpretationson all the issues that the conception of a PSHA model has to address. In the preliminary PSHA, this level of refinement is not introduced.

However, the model tries to take into account different interpretations of the scientific seismic hazard community in France. We tried to capture the range of possibilities, considering seismotectonic models developed following different criteria, and selecting ground motion prediction equations built from different databases and model definitions.

Compared to a site-specific study, shortcomings may exist, the objective being to obtain preliminary hazard maps at the beginning of the project, as much representative as the state of practice in the country, and not to define seismic ground motions at specific sites, for the design of buildings. The model try to respect, as much as possible, the principle of independence and exhaustiveness, but also to optimize the model and the computational time limitations, within the contractual framework of the project.

1.2 Organization of the report

The report is self-supporting. It partly incorporates the presentation of the models and parameters described in the progress reports SIGMA-2011-D4-08 and SIGMA-2011-D4-18. The logic tree and the nature of uncertainties considered in the hazard assessment are described in chapter 2. Chapter 3 presents the ground motion prediction equations (GMPEs). Chapter 4 presents the definition of the seismotectonic models. The method of combination of the different branches is developed in chapter 5. The results of the PSHA (maps, hazard curves and uniform response spectra) are given in chapter 6, with a sensitivity analysis.

All the numerical results are available on the DVD attached to the report. The user is encouraged to read the file "readme.doc" before using the DVD or the annex 1 of this report.

1.3 Calculation grid and selected sites

The PSHA computations were made for points distributed on a grid at approximately 10 km intervals in both directions, and this defines the spatial resolution of the maps (Figure 1).

Hazard curves and uniform hazard response spectra are calculated at 20 selected sites.

The sites selection obey the following criteria :

- The sites are located at strategic locations to allow pertinent comparisons, either with recorded accelerometric data or with macroseismic observations. The comparisons are planed in other tasks of the workpackage ;

- They are sufficiently distant to provided enough independence between the different sites of observations (accelerations/intensities) ;

- They cover as homogeneously as possible the whole region of interest, in which relatively stable and more active areas exist ;

- Some sites present a specific interest for models checks and comparisons (location at zones boundaries)
- Suggestion made by scientific committee members.

The 20 suggested sites are presented inTable 1 and Figure 1.

Site	Type	Longitude	Latitude
CALF Plateau de Calern (06)	Accelerometric station	6.9218	43.7528
OGAG L'Argentieres La Bessee (05)	Accelerometric station	6.5400	44.7880
OGAN Annecy DRASSM (74)	Accelerometric station	6.1360	45.8920
OGCA Beaumont de Pertuis (84)	Accelerometric station	5.6718	43.7323
OGMO Modane (73) France	Accelerometric station	6.6850	45.2084
OGMU Grenoble Musee Dauphinois (38)	Accelerometric station	5.7265	45.1954
STET Saint-Etienne de Tinee (06) France	Accelerometric station	6.9287	44.2595
Ville de Lyon	City	4.8352	45.7664
Ville de Valence	City	4.8952	44.9270
Ville de Digne	City	6.2348	44.0946
Ville d'Avignon	City	4.8099	43.9456
Ville de Nice	City	7.2618	43.7063
Ville de Marseille	City	5.3691	43.2964
Ville d'Albertville	City	6.3865	45.6742
Ville de Donzere	City	4.7125	44.4434
Ville de Gap	City	6.0768	44.5584
Ville de Draguignan	City	6.4665	43.5388
Ville de La Mure	City	5.7871	44.9046
Commune de Vinon Sur Verdon	City	5.8137	43.7246
Ville de Fos sur Mer (Site industriel)	City	4.9458	43.4352

Table 1 : The twenty pre-selected sites and their geographic coordinates.

Figure 1 : Calculation grid (blue dots) and the twenty selected sites (accelerometric stations or cities) superposed to the two seismoctectonic models 1 and 2.
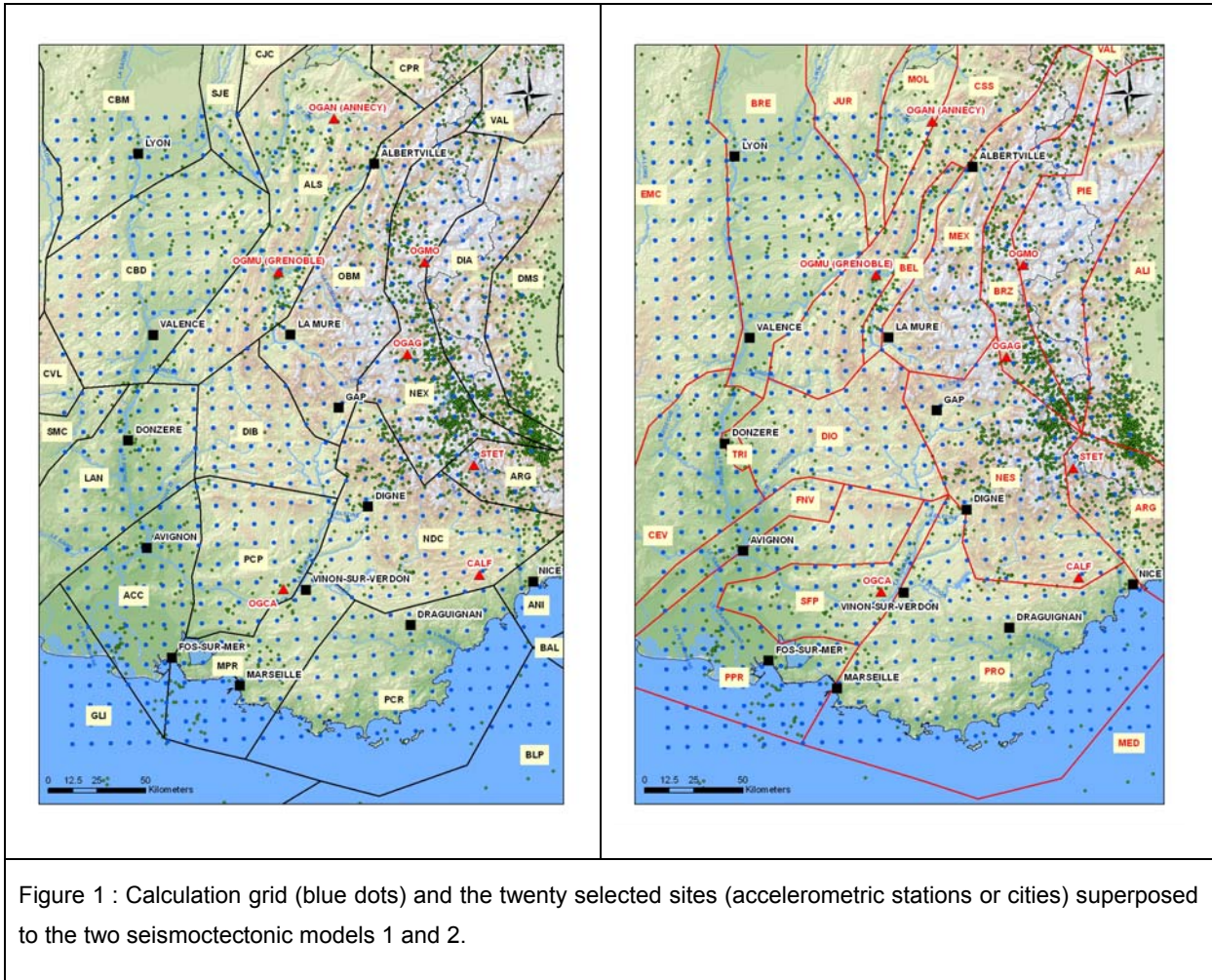
2.   Presentation of the logic tree

2.1 Uniform soil condition

The site condition is usually considered in any seismic hazard assessment. The objective being to produce hazard maps at the scale of the region of interest, only a uniform and constant soil condition is assumed. The Vs30 parameter is assumed equivalentto 800 m/s.

2.2 Nature and treatment of the uncertainties

2.2.1 Terminology

In our model, the epistemic uncertainty represents the different scientific interpretations of the same phenomenon or process and is considered by alternative models or alternative branches of the logic tree.

The branches of the logic tree are either defined by the technical integration team or generated using sampling technics. The number and nature of the seismotectonic zonations, the number and nature of the

ground motion prediction equations or the number of homogeneized magnitude and completeness periods, result from an analysis of the state of knowledge in the area of interest. For other epistemic parameters like the maximum magnitude or the recurrence parameters, Monte Carlo sampling technics are used to generate a number of epistemic branches reflecting the range of possibilities, according to the available data and the methods adopted to define quantitive values and their associated uncertainties.

The analysis and specification of the seismic hazard requires to consider, for each seismic source, the earthquake magnitude distribution, the distance distribution from the earthquakes to the site that includes randomness in the depth of the earthquakes and the ground motion distribution that present and intrinsic and random variability. This aleatory variability is accounted for directly in the hazard equations or is treated numerically using Monte Carlo sampling.

2.2.2 Identification of the uncertainties

2.2.2.1   Epistemic uncertainties

Conceptual approach

Recognizing the efficiency of different PSHA approaches, this study utilizes the capabilities of two different approaches:

- The classical Cornell-McGuire approach (Cornell, 1968; McGuire, 1976) based on the definition of seismogenic zones. In this approach the geological and seismological databases are interpreted to delineate seismic sources (areas, faults, systems of faults) of homogeneous activity.

- The zoneless method developed by Woo (1996). Compared to the previous method, the kernel estimation method is intended to avoid the ambiguities related to seismic zone delineation of seismic zones of uniform seismicity, that araise when the association between seismicity and geological structures remains unclear.

The zoneless approach was not intended to be integrated in the logic-tree. The objective was to compare the results from the zoning and the zoneless approaches for assessing the hazard variability. The comparison is done in chapter 6.2.5.

Seismotectonic zonations

Because of the lack of information and knowledge to define an accurate and homogeneized representation of seismic sources in terms of individual faults and associated seismogenic process in the total region of interest, all the seismotectonic models are based on area sources delineation. The area sources represent regions exhibiting the same seismotectonic regime and seismicity occurrence features. They are modeled assuming that the seismicity is homogenously distributed over their extent and the occurrence parameters are calculated by processing the subset of events that occurred within the polygon describing the seismic source. This procedure necessarilycreates a trade off between the need, for small areas, to guarantee that the underlying seismogenic process is properly considered, and the need, for large enough area sources, to select large sample of seismicity to reliably compute the Gutenberg-Richter parameters.

One major criticism to area sources is that subjectivity is implicitly assumed in the definition of their geometry, especially when a unique team is responsible for the model elaboration.

To overcomethis difficulty, three seismic source models are developed considering different criteria for the seismic sources delineation. The objective of the preliminary PSHA was not to develop new seismotectonic models (even if it has been the case for the model 2), which is one of the objectives of WP1, but to base the development of three source zone models on existing seismotectonic zonations, keeping in mind that the model should be as independent and exhaustive as possible. The principles for the selection of models are detailed in section 4.4 and briefly recalled bellow:

-    The model 1 is an area sources model based on previous Geoter works ;
-    The model 2 is a new model much more based on the identification of fault systems like the Belledone Fault, the Nime fault, the Provence faults system and the specific cluster of Tricastin.
-    The model 3 is an area sources model based on previous IRSN works, and significantly differs from model 1 and 2 by the size of the seismic sources.

We believe that the three models constitutea representation of the possible interpretations existing in the informed community, at the beginning of the SIGMA project and according to our scope of works. Additionnaly, and to avoid the subjectivity of the area sources models, one branch of the logic tree is based on a zoneless approach.

Each seismotectonic model constitutes a branch of thethe logic-tree.

Ground motion prediction equations

Four ground motion prediction equations are considered. The selected set was discussed during the two scientific committees and with the workpackage 2, with the objtective to respect as much as possible the principle of "mutually exclusiveness and collectively exhaustiveness of the GMPEs", with a limited number of models, one of which being mandatory.

The ranking process developed in the workpackage 2 and sensitivity tests were conducted to appreciate the hazard variability and to select three other models in complement of the mandatory model of Berge-Thierry et al. (2003).

The four are GMPEs:

-    Berge-Thierry et al. (2003) as the mandatory model;
-    Akkar and Bommer (2010) ;
-    Boore and Atkinson (2008, modified in 2011) ;
-    Zhao et al. (2006).

Each model constitutes an epistemic branch of the logic tree.

Seismic catalogue and completeness period

Two catalogues are considered. The first catalogue is homogeneized in moment magnitude scale (Mw) using the original instrumental catalogue and macroseismic database available for France. The homogenization procedure was described in the report SIGMA-2011-D4-18. The second one is a synthetic

catalogue to take into account the variability on the magnitude estimations (considering a possible perturbation of 0.3 on instrumental magnitudes and 0.5 on historical magnitudes) and location (considering a perturbation of 0.05° of epicenters). The synthetic catalogue is produced using a Monte Carlo sampling and a posteriori completeness periods and seismic parameters as well as new standard deviations on these parameters are calculated to serve as another epistemic branch of the logic tree.

Maximum magnitude

The maximum magnitude that is expected to be possible within each source zone is defined, in our approach by a range of magnitudes [Mmax$_{min}$ - Mmax$_{max}$] that represents the epistemic uncertainty. Due to the lack of data no discrete value of maximum magnitude can be identified within this range. Consequently a uniform distribution is used to propagate the uncertainty, through Monte Carlo sampling, each sample being a sub-branch.

Minimum magnitude

No uncertainty is considered on the minimum magnitude. The definition of the minimum magnitude was discussed with the scientific committee and a value Mw=4.5 was adopted to remain consistent with the validity domain of the selected GMPEs and because the likelihood of an earthquake of smaller magnitude causing damage to current constructions can be discounted. The sensitivity tests on this parameters are described in the SIGMA report SIGMA-2011-D4-18.

Recurrence parameters

In our approach, the propagation of uncertainties on the λ-β pairs is done using the two above mentioned seismic catalogues :

- – The Mw homogenized catalogue used to calculate a first set ofactivity parameters;
- – a synthetic catalogue thattakes into account the variability on the earthquakes characteristics. The synthetic catalogue is produced using a Monte Carlo sampling and a posteriori completeness periods and seismic parameters as well as new standard deviations are calculated to serve as another epistemic branch of the logic tree.

For each catalogue a Monte Carlo sampling, considering a gaussian probability distribution, is used to generate 100 correlated λ-β pairs. For half of the pairs, a β value is generated and a λ value is calculated and the opposite is done for the other half, each constituting an alternative branch. The complete procedure is described in th section 7.2 of the SIGMA report SIGMA-2011-D4-18.

Depth of the seismogenic layer

Two types of uncertainty are considered for the depth :

- Epistemic : which represents the depth and thickness of the seismogenic layer;
- Aleatory, that represents the random variability of earthquakes depth within the seismogenic layer.

The epistemic uncertainty can be introduced as individual branches, if the state of knowledge allows us to determine significantly different seismogenic layer depths. In our case however, we estimate that a discrete representation is not appropriate (due to the lack of justification) and the thickness and depth of the seismogenic layer in each area source is define by a range of values [Hmin-Hmax], between which the depth distribution obey to a random process.

At the scale of the region of interest, differences in the depth distribution can be discerned from an area to another. The estimation of the depth of the seismic source is done independently for each seismotectonic zonation.

2.2.2.2   Aleatory variability

The earthquake magnitude, the distance and the ground motion are characterized by aleatory probability distributions, and are treated in the hazard equation.

However the treatment of the depth in the software is not appropriately considered in the hazard integral and the random variability of depth within the seismogenic layer is adressedusing a Monte Carlo sampling, with a uniform distribution, each sample being assigned a weight. The sum of the weights being equal to unity.

The result of the aleatory uncertainties propagation in the calculation process leads to a single hazard curve, while each epistemic branch hypothesis gives its own hazard curve.

2.3 Logic tree

The epistemic branches that represent the alternative models are treated by the logic tree presented in Figure 2.

Each node of the logic tree represents an alternative way. The nodes correspond to :

-    3 seismotectic models in area sources for the zoning approach
-    2 catalogues of seismicity with associated completeness periods ;
-    4 attenuation models ;
-    100 combinations of maximum magnitude and recurrence parameters for each seismic source of 1 model.

2.4 Weight assignments

As a single team was in charge of the preliminary PSHA, the logic tree relies on a composition of alternative models that represents what that team believes suitable to develop an a priori hazard model for the region of interest, keeping in mind that it had to manage the trade off bewteen:

-    The volunty to develop a model that fulfills as much as possible the criteria of inclusiveness and exhaustiveness ;

-    The constraints to implement the preliminary PSHA with a limited number of source zones models and ground motion prediction equations.

The weights definition remains subjective since it reflects the judgment of the alternatives that the technical team decided to include, even if it tried to consider the opinions prevaling in the informed community. A representative example of this subjectivity can be found in the definition of the maximum magnitude. It is our believe, based on the criteria that we have adopted for this parameter, that the Mmax

associated to each large seismotectonic province is distributed between a narrow range of values (for instance 6.7-7.2 for the region 4, see chapter 4.6), rather than by discrete but not justifiable values. We are convinced that other participants would have defined the epistemic uncertainty in a different way or with different values, would they have had the responsibility of this task.

Notwithstanding this subjectivity, we believe that the model includes a reasonable representation of the possible range of interpretations, even if not all the possible range of extreme interpretations. It is precisely the objective of the different workpackages of the SIGMA project to justify new and different hypothesis, the benefit of which will be appreciate at a later stage of the project. The weights are discussed below. At a later stage, one may define new weights and recomputed the resulting hazard from the results provided in this study by simply recomputing average, median and percentiles of ground-motion including the new weights.

2.4.1 Conceptual models

The zonless approach is only used for comparison purpose with the zoning approach. The zoneless model can be seen as a subsidiary to zoning approach which aims at counterbalancing the subjectivity in the source zones delineation. However if the zonless approach were to be included, we would propose to assign a limited weight of 0.25 to this model. The reason is basically that all the guidelines, especially for nuclear applications, insist on the importance of developing geologic and seismologic databases, and to interpret them in coherent models of source zones. Part of subjectivity is also introduced in zoneless approach, for instance by the choice of the kernel functions parameters.

2.4.2 Catalogue of seismicity

Variability in the magnitudes and locations of the earthquakes is incorporated in the model through the use of two catalogues, the weights being equivalent for each catalogue

2.4.3 Seismotectonic models

Our degree of believe is stronger in the seismotectonic models 1 and 2 than in model 3, not only because we were involved in the developpement of these models, but because the model 3 represents a simplification of the tectonic process, combining very different seismic patterns within thesame areas, which leads to hazard smoothing. The model 3 has been assigned a weight of 0.2, while the two first models have an equivalent weight of 0.4.

2.4.4 Ground motion prediction equation

The weighing scheme adopted for the GMPEs relies on an internal process implemented by the technical integration team.
Four engineers of the Geoter team with experience in the field were requested to provide weights associated to the four selected GMPEs, without distinguishing the return periods of interest (i.e. from 100 to 10000 years) nor the spectral periods, and to justify their choice. The weights assigned by the

evaluators are summarized in Table 2, the last columns being the proposed weight for the PSHA calculations.

GMPE	Weight E1	Weight E2	Weight E3	Weight E3	Proposed Weight
Berge-Thierry et al. (2003)	0.3	0.35	0.3	0.3	0.3
Akkar & Bommer (2010)	0.2	0.3	0.2	0.3	0.2
Boore & Atkinson (2008/2011)	0.25	0.25	0.3	0.25	0.3
Zhao et al. (2006)	0.25	0.1	0.2	0.15	0.2

Table 2 : Weights assigned by the four evaluators and "consensual" weights proposed.

Since the Berge-Thierry (2003) model was imposed, this introduces a bias in the weighting process. The relation has a significant weight for all evaluators, because the model remains mandatory in all seismic hazard assessment studies in France and allows for comparisons with previous probabilistic seismic hazard assessments. Its calibration in Ms magnitude and focal distance, and the absence of consideration of focal mechanism are factors that significantly differ from the three other relationships. The adopted weight is 0.3.

As shown in Delavaud et al. (2012) the Akkar and Bommer (2010) GMPE fits well with the European and worldwide data. In our application the equation suffers from an application outside its validity domain in the small magnitude range and at distances greater than 100 km; the weights vary between 0.2 and 0.3, and the adopted weight is 0.2.

The proposed weight for the Boore and Atkinson (2008, extended in 2011 to small magnitudes) vary between 0.25 and 0.3. The validity domain of this relationship is fully consistent with the minimum magnitude and integration distance adopted in the PSHA model. The adopted weight is 0.3.

The Zhao et al.(2006) has a weight (0.2), two evaluators arguing that the database includes a majority of earthquakes in a too different context than the Alpine context.

2.4.5 Maximum magnitude and recurrence parameters

Allowance for variation in the maximum magnitude and recurrence parameters in all zones are incorporated in the seismic model by assigning weights equivalent to 1/N to each branch, N being the number of samples used in the Monte-Carlo sampling for each source zone. Tests of stability were implemented and lead to the choice of 100 samples for each seismic source.

Logic tree proposed to implement the task 4-1. PSHA level 0 of the SIGMA project

FIGURE: 2

	SEISMOTECTONIC MODEL	Mmax	SEISMOGENIC LAYER DEPTH	EARTHQUAKE CATALOG	SEISMICITY PARAMETERS	GMPES	UNCERTAINTY PROPAGATION THROUGH MONTE CARLO SAMPLING
UNCERTAINTY	Epistemic: - model definition	Epistemic: - Mmax value	Epistemic and aleatory: - Depth value	Epistemic: - magnitude scale and value - earthquake localisation	Epistemic: - parameters values	Epistemic AND aleatory	Epistemic OR aleatory

MODEL

SEISMOTECTONIC MODEL

Model 1, Model 2, Model 3 — SOURCE AREA MODELS

ZONELESS MODELS

FAULTS MODELS

Model I

Mmax

Mmax 1 — $W_{Mmax, 1}$
Mmax 2 — $W_{Mmax, 2}$
Mmax 3 — $W_{Mmax, 3}$
Mmax J — $W_{Mmax, J}$

OR

Mmax $\in$ [$Mmax_{min}$; $Mmax_{max}$] — W_{Mmax}

SEISMOGENIC LAYER DEPTH

Depth 1 — $W_{Depth, 1}$
Depth 2 — $W_{Depth, 2}$
Depth 3 — $W_{Depth, 3}$
Depth K — $W_{Depth, K}$

OR

Depth $\in$ [$Depth_{min}$; $Depth_{max}$] — W_{Depth}

EARTHQUAKE CATALOG

Catalog 1 — $W_{Cat, 1}$
Catalog 2 — $W_{Cat, 2}$
Catalog 3 — $W_{Cat, 3}$
Catalog L — $W_{Cat, L}$

SEISMICITY PARAMETERS

GR parameters for area models and zoneless models

$\lambda 1, \beta 1$ — $W_{SP, 1}$
$\lambda 2, \beta 2$ — $W_{SP, 2}$
$\lambda 3, \beta 3$ — $W_{SP, 3}$
$\lambda M, \beta M$ — $W_{SP, M}$

SOURCE AREA AND ZONELESS MODELS

OR

$\beta \pm \sigma_\beta$; $\lambda = f(\beta)$
$\lambda \pm \sigma_\lambda$; $\beta = f(\lambda)$

Caracterisctic model or GR parameters for fault models

$\lambda 1, \beta 1$ — $W_{SP, 1}$
$\lambda M, \beta M$ — $W_{SP, M}$
$Mcar_1, sliprate_1, Tcar_1$ — $W_{SP,1}$
$Mcar_M, sliprate_M, Tcar_M$ — $W_{SP,M}$

FAULT MODELS

OR

$\beta + \sigma_\beta$; $\lambda = f(\beta)$
$\lambda \pm \sigma_\lambda$; $\beta = f(\lambda)$
Mcar ; sliprate ; Tcar = f (Mcar, sliprate)

GMPES

GMPE 1 — $W_{GMPE, 1}$
GMPE 2 — $W_{GMPE, 2}$
GMPE 3 — $W_{GMPE, 3}$
GMPE N — $W_{GMPE, N}$

UNCERTAINTY PROPAGATION THROUGH MONTE CARLO SAMPLING

Propagation of uncertainty on:
- Seismicity parameters
- Mmax
- Depth

Available ditributions

MC 1 — $W_{MC,1=1/P}$
MC 2 — $W_{MC,2=1/P}$
MC 3 — $W_{MC,3=1/P}$
MC P — $W_{MC,P=1/P}$

OUR ASSUMPTION

3 sources models / 3 zoneless models for comparison	Mmax between $Mmax_{min}$ and $Mmax_{max}$	Depth between $Depth_{min}$ and $Depth_{max}$	2 catalogs - 1 original - 1 synthetic Both with Mw and Ms	GR parameters $\beta + \sigma_\beta$; $\lambda = f(\beta)$ $\lambda \pm \sigma_\lambda$; $\beta = f(\lambda)$	4 GMPES Akkar & Bommer (2010) Berge-Thierry *et al.* (2003) Boore & Atkinson (2008) Zhao *et al.* (2006)

100 MC samples

- Seismicity parameters: Gaussian distribution for β and λ correlated ($f(\beta)$)

- Mmax: uniform distribution

- Depth: uniform distribution

Date: 26-01-2012   Author: Amelie LEON   File: LogicTree2.ai   Source: GEOTER, 2011

3.   **Ground motion prediction equations**

The GMPE pre-selection process implemented in interaction with WP2, leaded to a set of 4 GMPEs described in Table 3.

GMPE	Magnitude range	Distance Range	Period range	Site	Fault type	H Comp.
Akkar & Bommer (2010)	M_w=5.0-7.6	R_{JB}=0-99 km	PGA ; 0.01-3 sec	3 classes	Yes	GM
Boore & Atkinson (2008, 2011)	M_w=3.5-7.9	R_{JB}=0-280 km	PGA ; 0.02-10 sec	Function of v_{S30}	Yes	GMrotI50
Berge-Thierry et al. (2003)	M_S=4.0-7.9 M_w=4.5-7.9	R_{hyp}=4-330 km	PGA ; 0.03-10 sec	2 classes	No	Both
Zhao et al. (2006)	M_w=5.0-8.3	R_{rup}=0-300 km	PGA ; 0.05-5 sec	5 classes	Yes	GM

Table 3 : List of GMPEs selected for PSHA for Southern France

3.1 **Berge-Thierry et al. (2003).**

This GMPE is based on European data mainly and data from California which were added in order to increase the number of records from large magnitude events. It is somehow superseded by most recent pan-European GMPEs, like Akkar & Bommer (2010), which used updated databases with better quality information on the earthquakes, recording sites, and more adapted functional forms. It is however important to consider this GMPE in the French context since it is the mandatory GMPE used for any seismic hazard assessment for nuclear facilities, in application of the safety fundamental rule RFS 2001-01.

The list of input parameters is:

- The surface-wave magnitude (M_S)
- The hypocentral distance in km (R_{hyp})
- The average S-wave velocity in the top 30 meters (v_{S30}) in m/s

The general form of the equation is:

$$\log_{10}(PSA) = a \times M_S + b \times R_{hyp} - \log_{10}(R_{hyp}) + c$$

Where:

- PSA is in cm/s²
- Site conditions are described through 2 classes ($300 < v_{S30} < 800$ m/s in which case $c=c_2$, $800 < v_{S30}$ in which case $c=c_1$)

Although coefficients are given to periods as high as 10 sec, the validity of the long period predictions is doubtful. Indeed as indicated in Bommer et al. (2011) the accelerograms used in Berge-Thierry et al. (2003) GMPE have been filtered at 4 sec and the high-period filter affect very much spectral amplitudes.

Recently, Douglas & Boore (2011) have shown that low-period filters have a much smaller influence on spectral amplitudes.
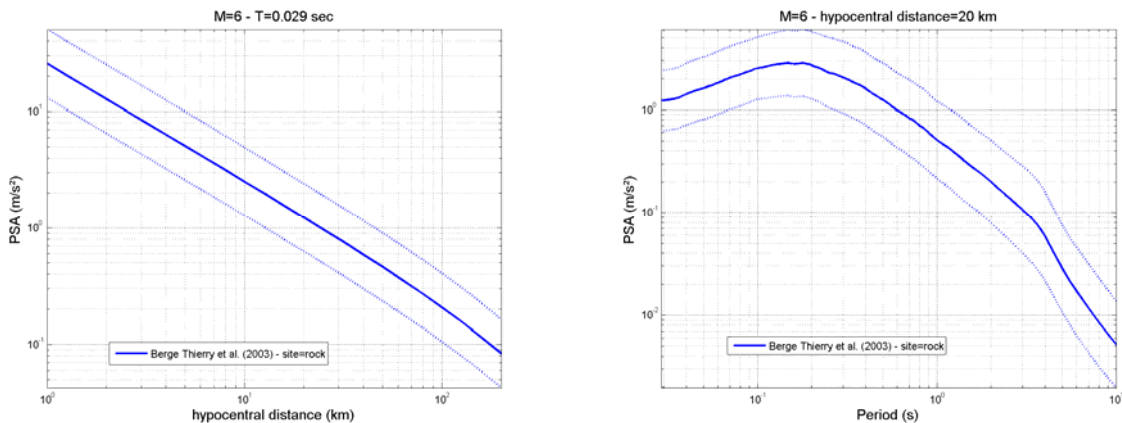
Figure 3: Exemple of predictions using Berge-Thierry et al. (2003). Attenuation of PGA (defined at 0.029 sec) with distance for M=6 (left); Response spectra for M=6 at 20 km (right).

One can note that this equation lacks a short-distance saturation term. Although data with hypocentral distance as low as 4 km were considered, the validity domain of this model is limited to 7 km in the French Regulation, and a magnitude/distance adjustment is imposed for sources closer than 7 km (RFS2001-01). The Berge-Thierry et al. (2003) GMPE (Figure 3) also lacks a magnitude squared term, and uses surface wave magnitude. For all these reasons the Berge-Thierry et al. (2003) GMPEs does not pass the exclusion criteria of Cotton et al. (2006) which are used to pre-select GMPEs for PSHA applications.

Some adjustements are necessary to homogeneize the predictor variables and are described in section 3.7.

3.2 Boore & Atkinson (2008, modified in 2011)

This relation is one of the 5 developed during the NGA project. They are all based on the same database, with records mainly from California and Taiwan. However, as shown in Abrahamson et al. (2008), the different groups did not use exactly the same data. For example, Boore & Atkinson (2008) excluded data from aftershocks while Abrahamson & Silva (2008) used those data. Consequently, the data used to build the GMPEs are coming from the same database but all the models do not useexactely the same number of data.

The list of input parameters is:

- The moment magnitude (M_w)
- The Joyner-Boore distance in km (R_{JB})
- The average S-wave velocity in the top 30 meters (v_{S30}) in m/s
- The style-of-faulting (normal, reverse or strike-slip fault mechanisms are considered)

The general form of the equation is:

$$\ln(Y) = F_M(M_w) + F_D(R_{JB}, M_w) + F_S(v_{S30}, R_{JB}, M_w)$$

Where:

- Y is in g

- F_M is a magnitude scaling term
- F_D is a distance scaling term
- F_S is a site term including non-linearity, and is a continuous function of v_{S30}

This model has recently been modified by Atkinson & Boore (2011). Since 2008, comparisons of the GMPEs including Boore & Atkinson (2008) with data from small to moderate earthquakes with magnitudes lower than 4/5 have shown the general tendency of over-prediction of ground-motion produced by small to moderate magnitude events (Bommer et al., 2007; Chiou et al., 2010; Atkinson & Boore, 2011). Consequently, Atkinson & Boore (2011) used data from small to moderate events in order to define correction functions to be applied to Boore & Atkinson (2008) GMPE in order to extend its validity domain toward small magnitude. The correction function has the following form:

$$\log_{10}\left(F_{BA08}\right) = a(M_w) + b(M_w) \times \log_{10}\left(R_{JB} + 10\right)$$

The correction is then applied to adjust Boore & Atkinson (2008) predictions (noted Y):

$$Y_{adjusted} = Y \times F_{BA08}$$

The validity domain of the adjusted model in terms of magnitude is M_w=4.0-7.9.
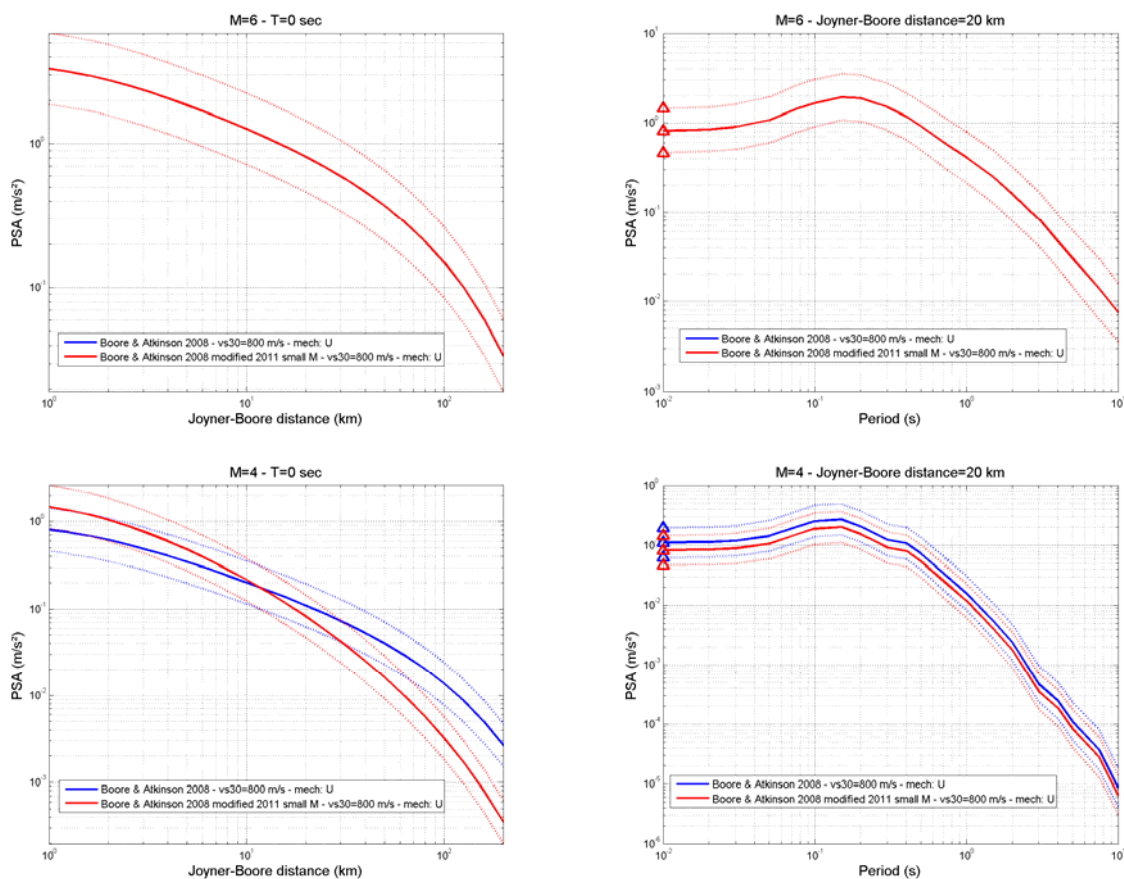
Figure 4: Exemple of predictions using Boore & Atkinson (2008) (blue) and Boore & Atkinson (2008) as modified in Atkinson & Boore (2011) (red). Attenuation of PGA with distance for M=6 (top left) and M=4 (bottom left); Response spectra for M=6 at 20 km (top right) and M=4 (bottom right). PGA is plotted at 0.01 s (triangle).

3.3 **Akkar & Bommer (2010)**

This GMPE is the most recent pan-European equation; it is an update of the 2007 equation from the same authors. Bommer et al. (2011) also published a high-frequency extension for the 2010 GMPE which is presented in this report.

The list of input parameters is:

- The moment magnitude (M_w)
- The Joyner-Boore distance in km (R_{JB})
- The average S-wave velocity in the top 30 meters (v_{S30}) in m/s
- The style-of-faulting (normal, reverse or strike-slip fault mechanisms are considered)

The general form of the equation is:

$$\log_{10}(PSA) = b_1 + b_2 \times M_w + b_3 \times M_w^2 + (b_4 + b_5 \times M_w) \times \log_{10}\left(\sqrt{R_{JB}^2 + b_6^2}\right) + b_7 \times S_S + b_8 \times S_A$$
$$+ b_9 \times F_N + b_{10} \times F_R$$

Where:

- PSA is in m/s²
- Site conditions are described through 3 classes (v_{S30}<360 m/s, 360≤v_{S30}<750 m/s, 750<v_{S30})
- Attenuation with distance is magnitude dependent

The reader is referred to Akkar & Bommer (2010), Akkar & Bommer (2007), and Bommer et al. (2011) for more details.
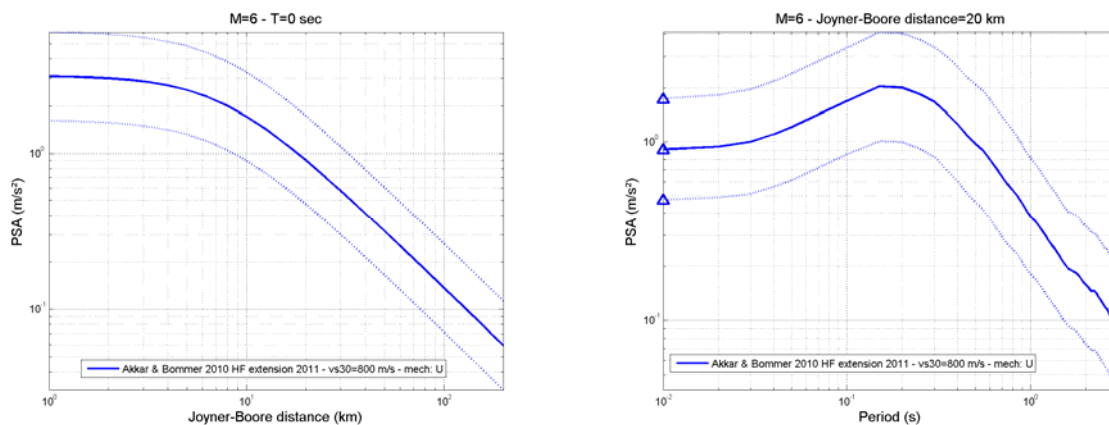
Figure 5: Exemple of predictions using Akkar & Bommer (2010). Attenuation of PGA with distance for M=6 (left); Response spectra for M=6 at 20 km (right). PGA is plotted at 0.01 s (triangle).

3.4 **Zhao et al. (2006)**

This GMPE is based on Japanese data recorded at the KiK-net network. It is developed for both crustal and subduction tectonic environments. In this report, we focus on the shallow active crustal model.

The list of input parameters is:

- The moment magnitude (M_w)
- The rupture distance in km (R_{rup})

- The average S-wave velocity in the top 30 meters (v_{S30}) in m/s
- The style-of-faulting (normal, reverse or strike-slip fault mechanisms are considered)
- The hypocentral depth (in km)

The general form of the equation is:

$$\ln(Y) = aM_w + bR_{rup} - \ln\left(R_{rup} + c\exp(dM_w)\right) + e(h - h_c)\delta_h + F_R + C_k$$

Where:

- Y is in cm/s²
- F_R is a term for reverse crustal events
- Site conditions are described through 5 classes ($v_{S30} \leq 200$ m/s, $200 < v_{S30} \leq 300$ m/s, $300 < v_{S30} \leq 600$ m/s, $600 < v_{S30} \leq 1100$ m/s, $v_{S30} > 1100$ m/s)
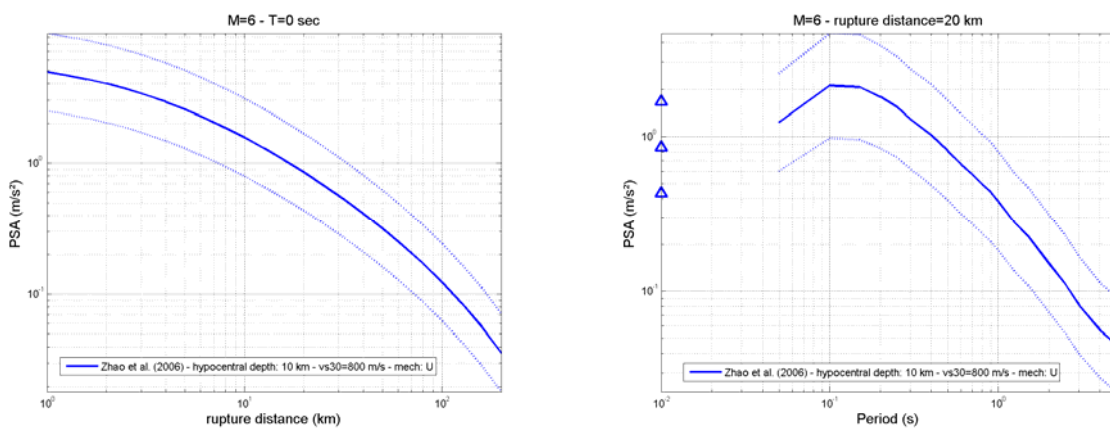
Figure 6: Exemple of predictions using Zhao et al. (2006). Attenuation of PGA with distance for M=6 (left); Response spectra for M=6 at 20 km (right). PGA is plotted at 0.01 s (triangle).

3.5 Comparison of the selected GMPEs

The pre-selected GMPEs are compared for both attenuation with distance and response spectral shape in Figure 7. In Figure 7, we assumed the equivalence between hypocentral distance (used in Berge-Thierry et al. 2003 GMPE) and rupture distance (used in Zhao et al. 2006 GMPE) which is valid for the small magnitudes. However, Figure 7 shows that the predictions from the model using hypocentral distance (Berge-Thierry et al., 2003) are consistent with the other models. One can also note that extrapolating the Akkar & Bommer (2010) model up to 200 km, while it is valid up to 100 km is not a source of large variability. The extrapolation to low magnitude for the Akkar & Bommer (2010), Zhao et al (2006), Berge-Thierry et al. (2003) GMPEs is probably a larger source of uncertainty as suggested by the results of recent studies to adjust GMPEs to small magnitude events (see section 3.2 for an illustration of the effect of such adjustment on Boore & Atkinson, 2008 GMPE).
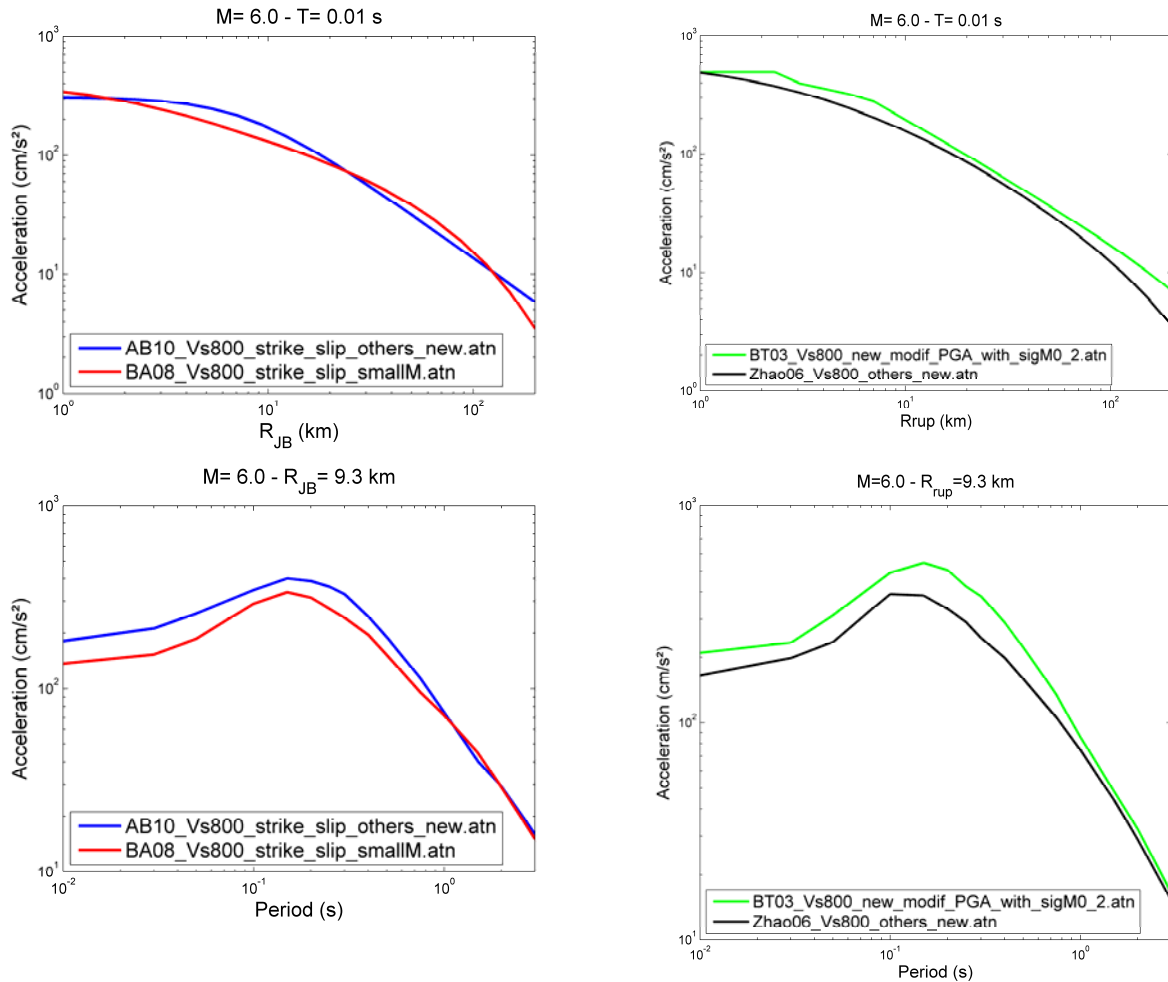
Figure 7: PGA for Mw=6 and PGA versus distance (top) for Akkar & Bommer (2010) and Boore & Atkinson (2008) GMPEs (left) which use Joyner-Boore distance, and Berge-Thierry et al. (2006) and Zhao et al. (2006) (right) which use hypocentral and rupture distance, respectively. Response spectra (bottom) for Mw=6 and R=9.3 km for the same GMPEs as above.

Figure 8 compares the standard deviations predicted by the four GMPEs. The Figure shows the lower standard deviation predicted by Boore & Atkinson (2008), followed by Akkar & Bommer (2010), and the other two models. At low spectral period (T<0.2 sec), the standard deviation predicted by Zhao et al. (2006) is higher than the other ones, while at high period (T>0.2 sec), the highest values are coming from Berge-Thierry et al. (2003). Note that for this model, the standard deviation has been modified to account for uncertainty propagation of the magnitude conversion (Mw to Ms, see section 3.7.3).
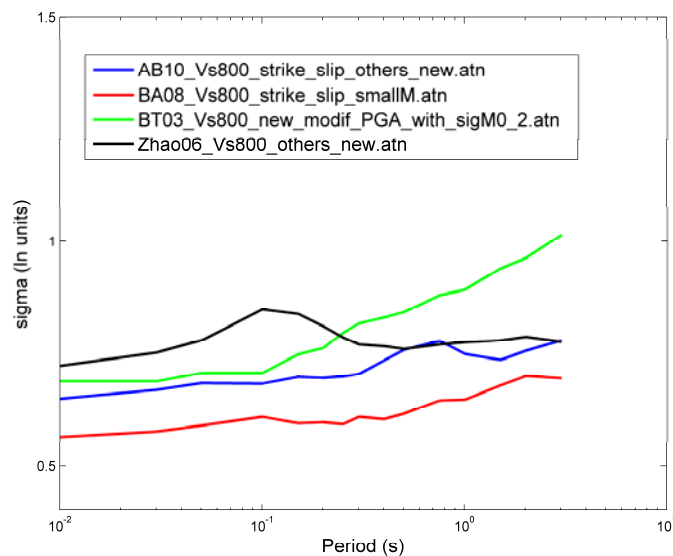
Figure 8: Standard deviations in natural log unit for the four selected GMPEs as a function of period.

Sensitivity tests were implemented to appreciate the hazard variability as a function of the GMPE choice (SIGMA report SIGMA-2011-D4-18).

3.6 Number of standard-deviations considered in the calculation process

In the PSHA software, the truncation is introduced by two possible ways: at a maximum value of acceleration (depending of the spectral period) or at a given number of standard deviations.

The distribution of acceleration values for a given magnitude and distance, as predicted by the GMPEs, is assumed to follow a lognormal probability function. In the probabilistic calculations, the whole distribution is integrated over a fixed number of standard deviations set to 3 σ in the original hazard model, based on tests and analysis done during previous PSHA studies in France.

We, however, performed additional sensitivity tests using integration from 2 σ to no truncation. The results are shown for two sites in different environments; the first (OGCA) is close to the Provence zone were the variability on the seismic activity parameters is high, and the other one (OGAG) is in the Alps were the activity is better constrained. Figure 9 shows the Uniform Hazard Spectra obtained using different levels of integration for the two sites, and Table 4 gives the accelerations predicted and the % of variation with respect to the no truncation case. From these results, it is clear that a 2 σ truncation leads to hazard underestimation, and that above 5 σ truncation, there is no difference in the hazard computed even at large return periods (i.e. 10000 years).
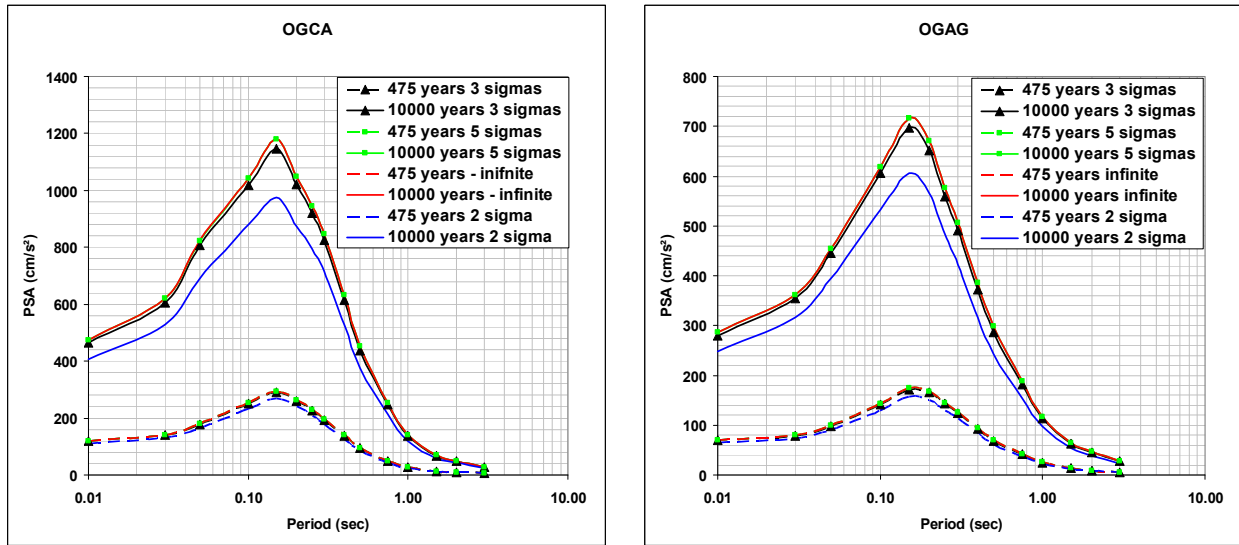
Figure 9: Uniform Hazard Spectra using the first seismotectonic model and the Akkar & Bommer (2010) GMPEs with different levels of integration for two sites.

Integration level	PGA (cm/s²)		PSA(0.2s) (cm/s²)		PSA(1.0s) (cm/s²)	
	475 years	10000 years	475 years	10000 years	475 years	10000 years
OGAG						
Infinite	70.21	286.00	168.26	671.24	25.34	116.98
5 σ	70.21 *(-0%)*	285.99 *(-0%)*	168.25 *(-0%)*	671.21 *(-0%)*	25.34 *(-0%)*	116.97 *(-0%)*
3 σ	69.35 *(-1%)*	279.87 *(-2%)*	165.74 *(-1%)*	652.21 *(-3%)*	24.97 *(-1%)*	113.17 *(-3%)*
2 σ	64.04 *(-9%)*	248.22 *(-13%)*	150.93 *(-10%)*	565.30 *(-16%)*	22.62 *(-11%)*	97.05 *(-17%)*
OGCA						
Infinite	119.90	473.27	264.06	1049.92	27.24	141.77
5 σ	119.90 *(-0%)*	473.26 *(-0%)*	264.06 *(-0%)*	1049.89 *(-0%)*	27.23 *(-0%)*	141.77 *(-0%)*
3 σ	118.85 *(-1%)*	463.20 *(-2%)*	261.30 *(-1%)*	1020.82 *(-3%)*	26.91 *(-1%)*	137.88 *(-3%)*
2 σ	110.88 *(-8%)*	405.70 *(-14%)*	241.67 *(-8%)*	873.22 *(-17%)*	24.57 *(-10%)*	120.36 *(-15%)*

Table 4: Influence of the level of integration on the spectral accelerations PGA and PSA at 0.2 and 1.0 s for the sites OGAG and OGCA.

A 3 σ truncation seems to be the best choice since it is supported by the data. When considering the original strong ground motion databases, as the database considered by Berge-Thierry et al. (2003), 99% of the data are in the intervalle -3 σ – 3 σ of the lognormal distribution (99,7% for the Berge-Thierry et al. (2003) relationship, Figure 10).

As there is no empirical justification to consider a lower value than 3 σ, we suggest to keep considering our initial choice of 3 standard-deviations. This choice is in agreement with the current practice (Abrahamson, 2006).

Probably much more than this choice, which is here at least to consider the number of standard deviation allowing to consider 99% of the distribution of observed data in the GMPEs database, the question of the physical limit of the acceleration has probably a greatest influence, which is not solved at the moment.
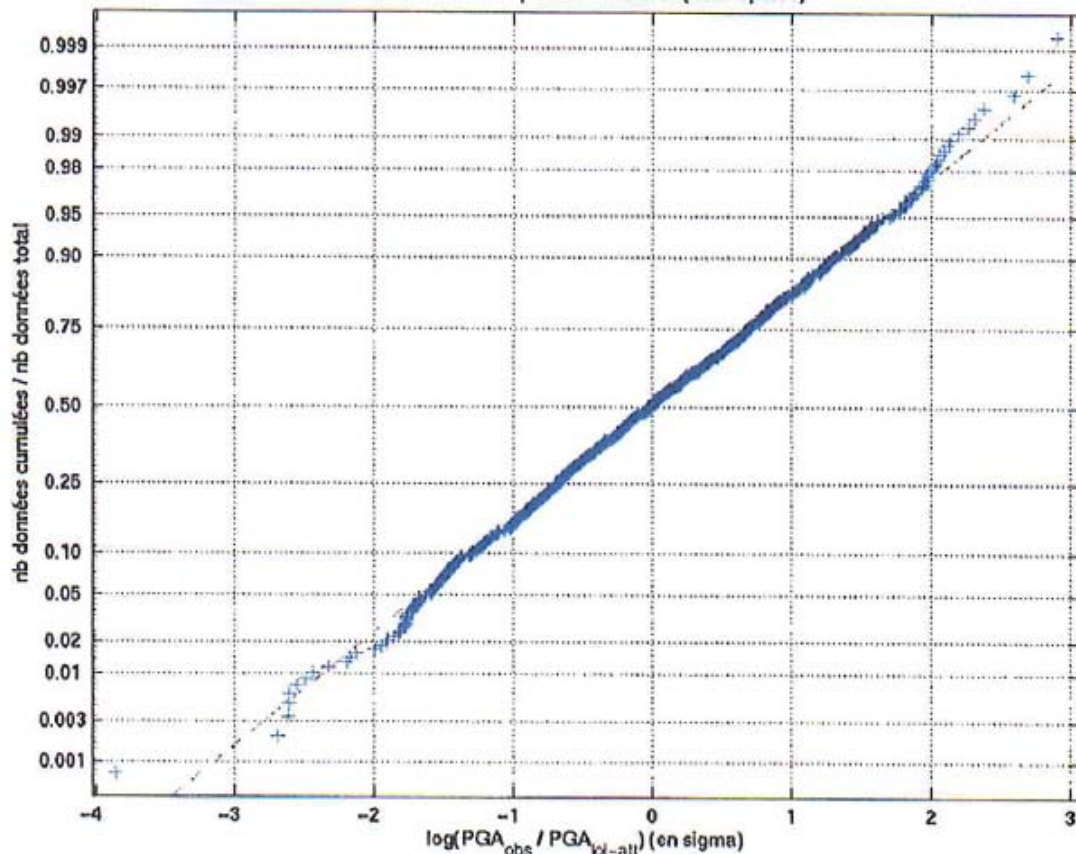
Figure 10 Residual distribution in terms of number of sigma of the Berge-Thierry et al. (2003) attenuation relationship. Y axis shows the number of cumulated data over the total number of data (Rey and Berge-Thierry, 2005).

3.7 Procedure to unify the predictor variables used in the GMPEs

Predictor variables may differ from one GMPE to the other, and procedures to unify the differences are generally accounted for through appropriate conversions (Bommer et al., 2005). When calculating seismic hazard using a suite of GMPEs, it may be necessary to make adjustments to some of the ground motion results to harmonize values determined for different conditions or using different approaches. In the current analysis, the selection of GMPEs has mitigated the need to make such adjustments. However, it was not possible to select GMPEs that completely eliminated the need for adjustments. This section addresses the need for ground motion adjustments and, in cases for which they are required, how they are implemented.

3.7.1 Adjustement for PGA of the Berge-Thierry et al. (2003) GMPE

Some adjustement was necessary because the Berge-Thierry et al. (2003) GMPE gives coefficients up to 34 Hz. Recent results (Bommer et al. 2011) show that the equivalence between PGA and PSA at low period is not obtained at 34 Hz but rather around 100 Hz in most cases. Consequently we decided to adjust the Berge-Thierry et al. (2003) GMPE in order to predict PGA around 100 Hz. A correction factor was computed using the ratios of PSA(0.03 sec)/PGA using Campbell & Bozorgnia (2008) GMPE (*Figure 11*) and Abrahamson & Silva 2008 (GMPE) which leaded to similar results.

From *Figure 11*, it is clear that the ratio PSA(0.03 sec)/PGA depends on distance for all magnitudes and slightly on magnitude at close distances. In the adjustment, we ignore the magnitude dependence which is very weak, and the final adjustment only depends on distance (red curve in the left hand frame of *Figure 11*). We do not adjust the standard deviation since it usually slightly decreases from PSA(0.03 s) to PGA and consequently we assume σ(0.03 sec)=σ(PGA) for the Berge-Thierry et al. (2003) GMPE, which is a conservative assumption.
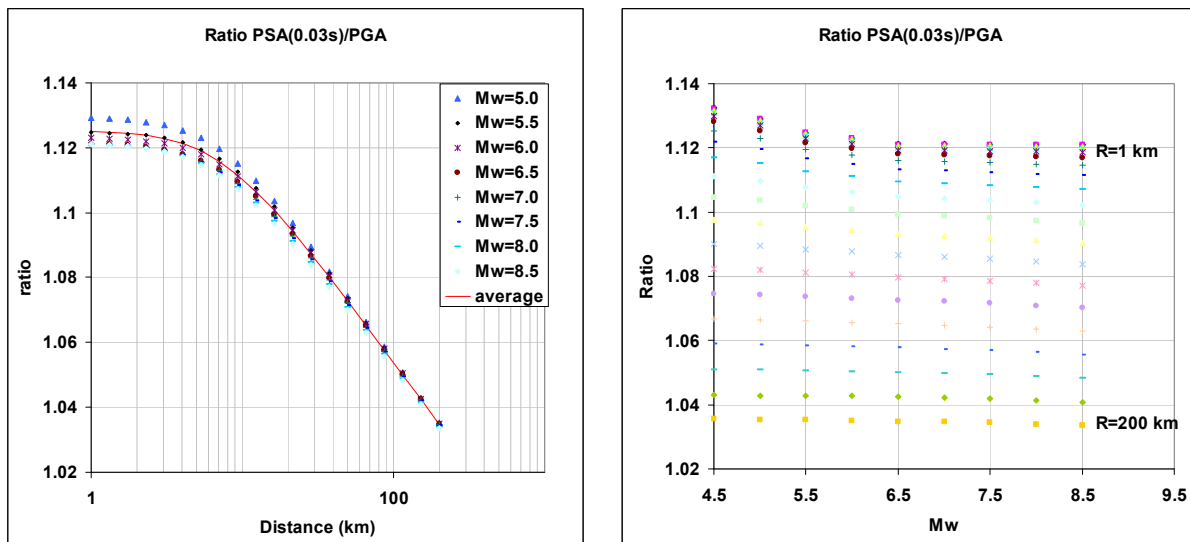
Figure 11 : Ratios PSA(0.03 sec)/PGA against distance (left) and magnitude (right) using Campbell & Bozorgnia (2008) GMPE.

3.7.2 Procedure to synchronize the common structural periods of the GMPEs

The list of periods used in the hazard computation is PGA (or 0 s), 0.03, 0.05, 0.1, 0.15, 0.20, 0.25, 0.30, 0.40, 0.50, 0.75, 1.0, 1.5, 2.0, 3.0 s. This number of spectral periods allows us to compute uniform hazard spectra for the selected sites with enough spectral values to obtain a satisfactory description of the ground motion. In order to save computation time, the maps are only generated for PGA and for the periods 0.2 and 1.0 s.

Some of the selected GMPEs do not provide coefficients at all the period considered. Zhao et al. (2006) model is missing the periods 0.03 and 0.75 s, and Berge-Thierry et al. (2003) made the assumption that PGA is equivalent to PSA at 34 Hz, which has been shown recently to not be valid (Bommer et al., 2011).

The adjustment for PGA of Berge-Thierry et al. (2003) has been exposed previously. For the Zhao et al. (2006) model, we choose to interpolate directly the coefficients for the missing periods and compute the prediction with these new coefficients. Another solution would have been to interpolate directly the Uniform Hazard Spectra or the hazard curves, but this procedure is less flexible. We consequently used a linear interpolation against period and logarithm of period since both can lead to different results in some cases (Bommer et al. 2011). Figure 12 shows the response spectra obtained for the original model and using interpolated coefficients. Note that for the original model, PGA is plotted at 0.01 s, which assumption has also been used for the log(T) interpolation. This assumption is at the origin of the slight differences in the predictions at 0.01 s. However, at the targets periods of 0.03 and 0.75 s, both interpolations lead to the same results.
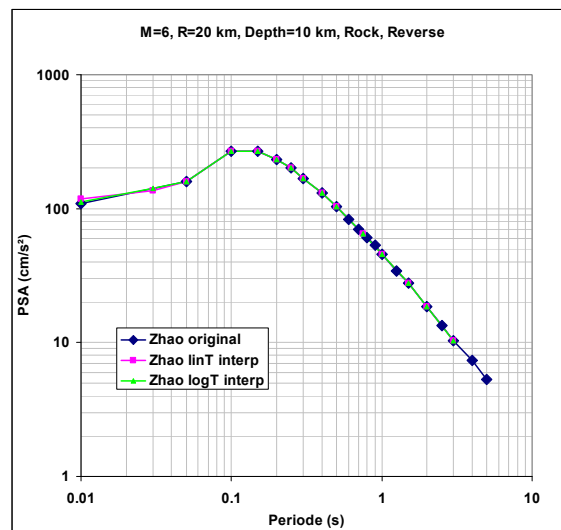
Figure 12: Response spectra predicted using Zhao et al. (2006) for a specific scenario before and after interpolation against both T and log(T).

3.7.3 Adjustment for the definitions of magnitude

When GMPEs are developed using a magnitude scale different from the one used for the earthquake catalog, the results need to be adjusted to take into account the effect of the different scales. Except the Berge-Thierry et al. (2003) relationship, which uses the Ms magnitude scale, all the other GMPEs use moment magnitude. This is consistent with the use of Mw in the earthquakes catalog.

When using the Berge-Thierry et al. (2003) model, a magnitude conversion is applied directly in the GMPE model that should involve a modification of the standard deviation. However, the quantification of the standard deviation increment is not obvious because part of the standard deviation of the GMPE already accounts for magnitude conversions that have been used to create the underlying database (RFS 2001-01). This quantification would require a specific work that could be envisaged in the WP2 if thought necessary. We consider here that we have not the means to develop a consistent analysis.

We performed a simple test in order to estimate the influence of the propagation of magnitude conversion uncertainties on the PSHA (SIGMA report SIGMA-2011-D4-18). We assume in the PSHA a constant magnitude uncertainty of $\sigma_M=0.2$ which has to be added to the uncertainty predicted by the Berge-Thierry et al. (2003) GMPE. The adjusted uncertainty is computed as follows:

$$\sigma_{adjusted} = \sqrt{\sigma_{GMPE}^2 + \left(\frac{\partial \log_{10}(Y)}{\partial M} \right)^2 \times \sigma_M^2}$$

Where Y is the ground-motion parameter predicted by the GMPE.

The effect of this adjustment on the sigma model of Berge-Thierry et al. (2003) GMPE is shown in Figure 13. The increase in sigma is higher at higher period due to a larger magnitude coefficient in the GMPE.
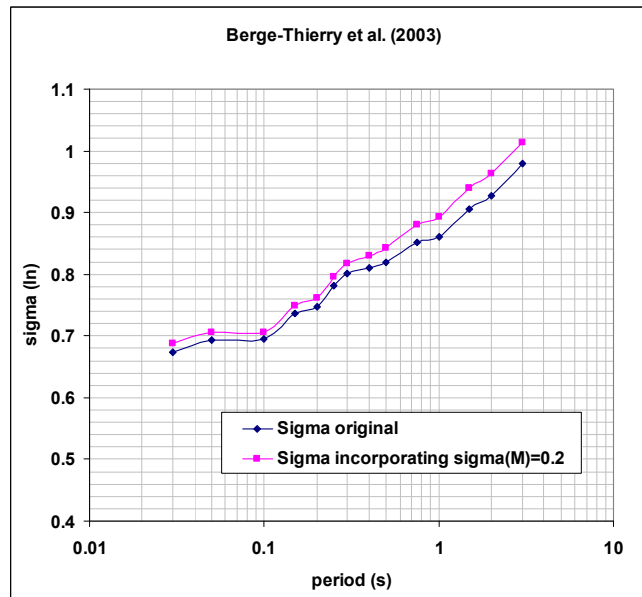
Figure 13: Sigma model of the Berge-Thierry et al. (2003) GMPE before and after adjustement
in order to take into account uncertainties in magnitude conversion.

3.7.4 Adjustment to unify the horizontal component expressions

For the definition of the horizontal component of motion, the GMPEs use either geometric mean (Akkar and Bommer, 2010 and Zhao et al., 2006), both components (Berge-Thierry et al., 2003), or GMRotI50 (Boore and Atkinson, 2008). Results in our study will be for geometric mean of the horizontal components. Beyer and Bommer (2006) report that the ratio of the median PGA determined using either both components or GMRotI50 to the median PGA using geometric mean is 1.00 with a small standard deviation.

Thus, the results of the selected GMPEs that are not defined for the geometric mean horizontal component are considered to be equivalent to results for that definition. Therefore, no adjustment is planed for the differing definitions of horizontal component.

3.7.5 Adjustment for site conditions

The four GMPEs used in the PSHA provide ground motion for different site conditions that are specified in terms of the VS30 value of the site material. The consideration of site conditions can be a function of VS30 directly entered in the attenuation model (Boore and Atkinson, 2008), or coefficients that are

determined for each considered soil class (Berge-Thierry et al., 2003; Zhao et al., 2006; and Akkar and Bommer 2010).

For the current PSHA, a uniform Vs30=800 m/s is considered on all the territory, the objective being not to consider the site effects in the preliminary map. There is no need to introduce a corrective action, because this value is included in the validity domain of the four GMPEs.

However, we point out that for the Berge-Thierry et al. (2003) model, the site classification was based on very rough information on the sites and many stations are found ill-classified considering more recent information on site condition (Drouet et al., 2007). The rock site class includes in reality sites characterized by vs30's lower than 800 m/s.

3.7.6 Adjustment for missing style-of-faulting

Among the GMPEs, only the Berge-Thierry et al. (2003) model does not take into account style-of-faulting. One could make an adjustment based on the study of Bommer et al. (2003).

However, the requested input for such an adjustment are the proportion of normal and reverse faulting earthquakes within the underlying database. Such information is not available. Moreover, the adjustment is based on empirical ratios between ground-motions produced by normal, reverse or strike-slip events. These ratios would need to be refined as well as the associated uncertainty in order to perform robust conversions. Consequently, we decided not to use the style-of-faulting adjustment.

3.8 Validity domain in terms of magnitude

All the earthquakes with magnitudes between the minimum magnitude (Mw4.5, Ms4.0) and the maximum magnitude (that doesn't exceed 7/7.3 in the French context) contribute to the hazard. This means that Akkar and Bommer (2010) and Zhao et al. (2006) GMPEs are used beyond their validity domain for the lowest magnitudes, while the Boore & Atkinson (2008) and Berge-Thierry et al. (2003) GMPEs are used within their validity domains.

A disagregation analysis allowed us to control that the range of dominant magnitudes is within the validity domain of the GMPEs at the largest return periods, and reach the lower limit of the validity domain at the shortest return periods. Figure 14 presents the results of the disagregation analysis for the seismotectonic model 3 (the one for which the influence of farthest sources is the higher), the Akkar & Bommer (2010) GMPE and for two sites (OGAG and OGCA). This figure shows that at close distance, small scenario earthquakes are dominant, especially for PGA and at the two return periods considered (i. e. 475 and 10000 years).

At 475 years of return period, the most significant contribution comes from magnitudes between Mw 4.5 and 5. These magnitudes are outside the validity domaine of the Akkar and Bommer (2010) and Zhao et al. (2006) models. The extrapolation to low magnitude can be a source of hazard overestimation, that could be analyzed when the results of the WP2 on the adjustment of GMPE towards small magnitudes will be available.
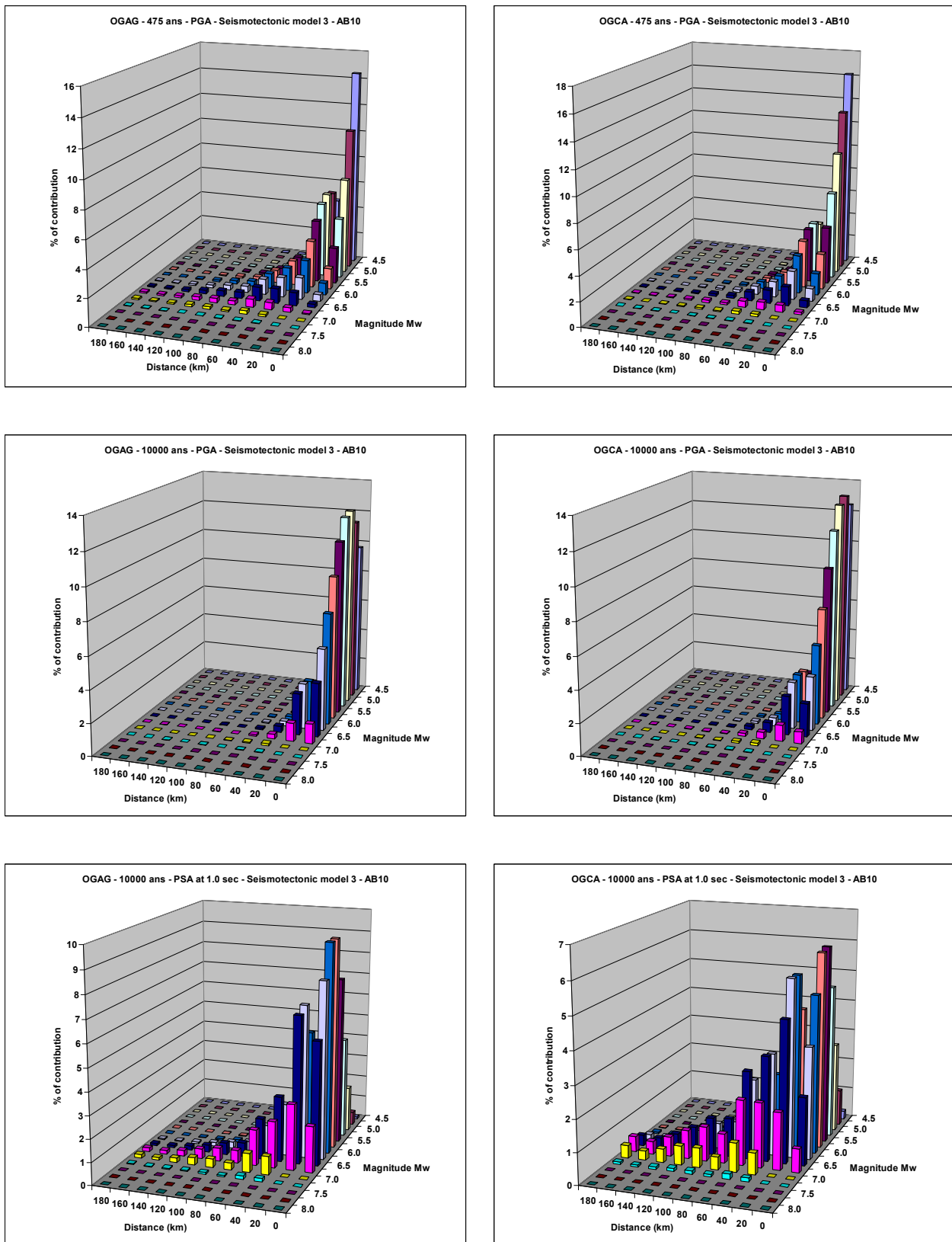
Figure 14: Percentage of contribution to the hazard per magnitude-distance scenarios using seismotectonic model 3 and Akkar & Bommer (2010) at the sites OGAG (left) and OGCA (right) and for PGA at 475 years RP (top), PGA at 10000 RP (middle), and PSA(1.0s) at 10000 RP (bottom)

3.9 Consideration of distances and validity domain in terms of distance

Four types of metric distances are considered in CRISIS and are specified for each seismic source : epicentral distance, focal distance, R_{JB} and R_{RUP} depending the GMPE used.

This avoids the introduction of a distance correction term, the definition of which may lead to increase the uncertainty.

CRISIS allows us to model finite ruptures using magnitude-length/area scaling relationships. When the rupture is assigned to a specific fault surface or seismic source, the rupture is not allowed to extend outside. The calculation of R_{JB} and R_{RUP} require to compute a rupture surface or a rupture length.

For Area sources: $A = k1\ e^{\,k2\,M}$

For line sources: $L = k3\ e^{\,k4\,M}$

Where M is the magnitude and k1 to k4 are constants given by the user or chosen from a set of constants for different types of fault models (Brune, 1970; Singh et al, 1980) or rupture size-magnitude relationship (Wells and Coppersmith, 1994).

When area sources are considered (which is the case in our model), Crisis implements an integration procedure based on a triangulation algorithm used for the seismic sources discretization. When working with a calculation grid, this solution optimizes the calculation time while maintaining a reliable description of source geometry and seismicity. Additionally, the distance of integration is defined, which allows us to exclude from the calculation discretized sources that are located farther than the fixed integration distance. This means that, for the third model, characterized by a small set of large source areas, discretized sources (triangles), with center farther than 200 kilometers from the calculation point, are not considered in the hazard integration, which limits the use of GMPE far beyond their validity domain.

The choice of the integration distance was mainly done to consider, for the most seismically stable regions of the model, the contribution of distant and more active areas which contribution could become dominant at high spectral periods. We first adopted as principle to eliminate from the GMPEs selection, the relationships with a too limited domain (i.e. the Chiou and Youngs 2008 relationship with a R_{JB} limited to 70 km). Among the GMPEs selected, all but one have a distance validity domain at least up to the integration distance (i.e. 200 km). The remaining problem was with the Akkar and Bommer (2010) GMPE with a limited R_{JB} of 99 km.

The disaggregation (Figure 14) shows that the contribution of seismic sources located at grestest distance than 100 km is very low in the region of interest.

Instead of introducing an arbitrary increase of the standard deviation (it is pointed out that the database contains a limited number of distances as long as 200 km), the choice was done to appreciate the impact of using the equation in the range 100-200 km through a sensitivity test.

We computed the PSHA using the Akkar & Bommer (2010) GMPE with two integration distances, 100 and 200 km. The resulting uniform hazard spectra for the two sites considered (OGAG and OGCA) at return periods of 475 and 10000 years are shown in Figure 15. This Figure shows that except for OGCA at a

return period of 475 years and spectral period above 0.5 seconde, the integration distance has no influence on the hazard. This is consistent with the tests that have been performed to obtain a hazard disagregation scheme indicating that the hazard is governed by sources at rather short distances.
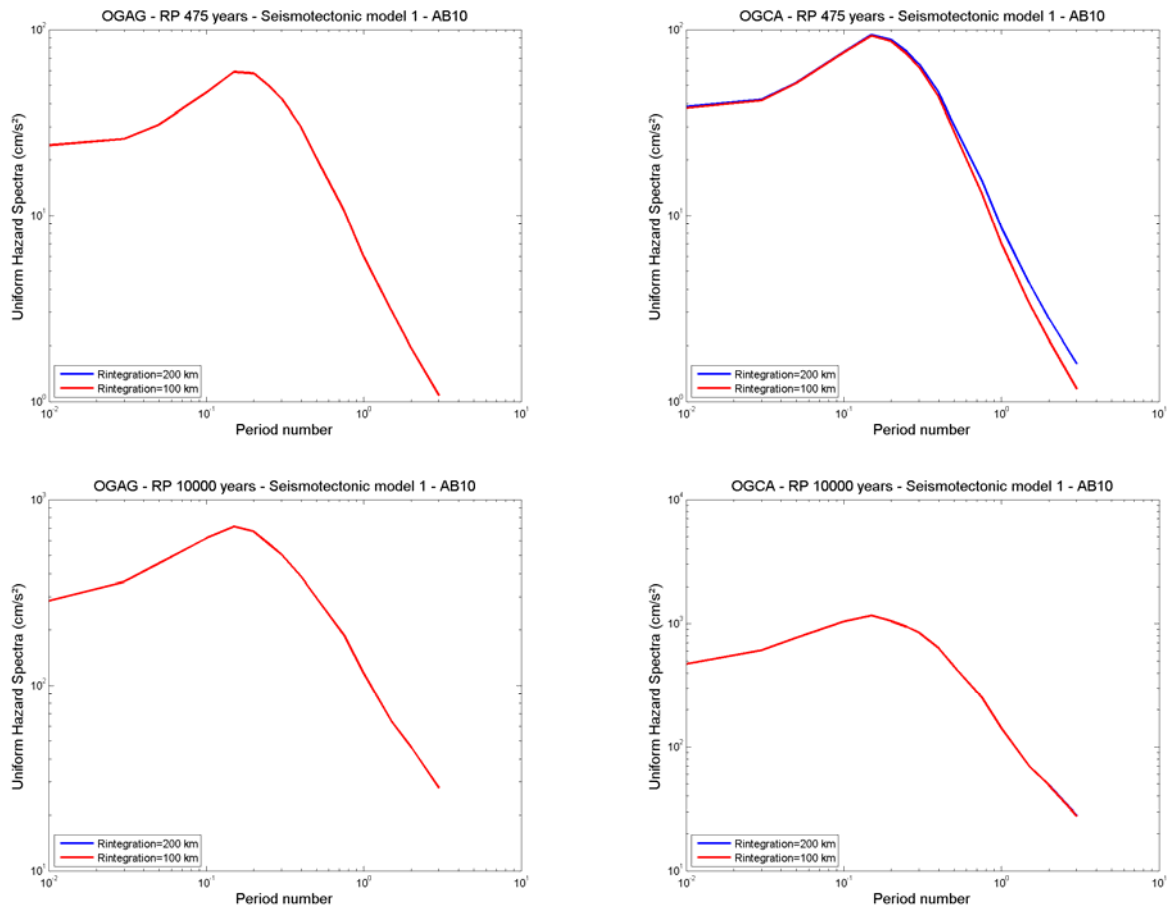
Figure 15: Uniform Hazard Spectra at 475 (top) and 10000 (bottom) years for sites OGAG (left) and OGCA (right), computed using seismotectonic model 1 and Akkar & Bommer (2010) GMPE with two integration distances: 100 and 200 km.

Indeed, Figure 14 shows that for the two sites and for PGA, the contribution of scenarios corresponding to distances larger than 100 km is small (a couple of %) for the two return periods considered in the test, namely : 475 and 10000 years return period. Since the contribution of farthest sources is usually larger at longer spectral periods, Figure 14 also shows the results for PSA at 1.0 s and for 10000 years return period. The contribution of the farthest sources is larger as expected but their cumulative contribution is limited to less than 10%. This result and the fact that the extrapolation of the Akkar & Bommer (2010) at distances larger than 99 km gives consistent results with other GMPEs (see Figure 7) justify our choice to use Akkar & Bommer (2010) GMPE beyond its distance validity domain.

3.10 **Spectral acceleration peak**

Preliminary comparisons between response spectra obtained from GMPEs with observed response spectra seem to indicate that the GMPEs underestimate the frequency where the maximum spectral acceleration is observed. F. Scherbaum suggested in his review that this could be due to a difference in kappas that could be addressed using kappa conversions within the hybrid empirical approach of

Campbell (2003, 2004 and 2006). We also pointed out during the SC meeting that this could be due to an effect related to stress drop and that this observation should be confirmed by other comparisons since only two earthquakes were used to establish the comparison. The comparison between the predicted and the 2 observed response spectra is not sufficient to draw conclusion. As many recordings as possible should be used to demonstrate that the observed tendency is stable (or not).

We believe that it is not possible for the preliminary PSHA to develop a specific attenuation model to account for this effect which must be addressed in the WP2, the objective of which being precisely to select and develop an appropriate set of GMPEs for the SIGMA project.

The benefit of such a development will then be appreciated in the benefit of SIGMA, when comparing new results obtained considering the WP2 results with the initial PSHA.

4.   Seismotectonic models

4.1 Geological database

At the scale of the region of interest, several seismic hazard assessment studies already exist. Scientific publications and/or reports have been compiled and analyzed to create a bibliographical database:

-   More than 40 scientific publications for the last 15 years concern the geology and seismotectonic context of the region of interest;

-   Seismotectonic zonations developed and published by French (IRSN, BRGM, LDG, EDF) or European institutions (ESC-SESAME zonation, Jimenez *et al.,* 2003; On-going SHARE zonation, Grünthal *et al.,* 2010);

-   Deterministic and probabilistic seismic hazard assessment studies realized during the last 10 years for different industrial facilities (ICPE, INB, NPP, Dams…) sites.

These studies and scientific publications are used as input data to select three seismotectonic models. As defined in the terms of reference, three models are chosen or developed with the objective to capture a significant range of the epistemic uncertainties based on the interpretation of the geological and seismological databases.

4.2 Earthquake catalogue

Following the Scientific committee of May 24th a revision of the catalogue was implemented for two reasons :

-   The activity rates of Mw and Ms magnitudes obtained after application of the selected conversions, were inconsistent with the recognized assumption that Ms is lower than Mw for magnitudes bellow Mw 6 ;

-   A tendency is observed in the new catalogue of historical earthquakes with Mw, Ms and depths determinations, developed by IRSN (oral communication), that increases the magnitudes of major events and decreases the magnitudes of smallest events.

The IRSN (Baumont and Scotti, 2008), developed a method to account for uncertainty in historical magnitude and depth evaluations: the macroseismic data are exploited to establish an intensity-magnitude attenuation model according to different binning strategies used and to jointly calculate the Mw and Ms magnitudes and depth of historical events.

The access to this information was thought to be important for the project and an attempt was done to obtain the new Mw magnitudes and use the corresponding catalogue in the preliminary PSHA. However it was not possible to obtain the catalogue and the available bibliography was analyzed, to appreciate the possibility to improve the definition of the magnitudes from macroseismic data.

The adopted conversions rely on the works of Grünthal et al. (2009a and 2009b). These authors have analyzed the historical and intrumental data within the central, northern and northwestern Europe and have proposed a procedure for the harmonization of Mw for historical and instrumental earthquakes.

For historical events, the database is composed by 41 master events covering a range of epicentral intensity between V and IX-X, Mw magnitudes between 3.1 and 6.4 and depth between 5 and 22 km. An empirical relation of Mw as a function of the epicentral intensity Io and the focal depth h is derived from the exploitation of the database :

$$Mw = 0.667 \, Io + 0.30 \log(h) - 0.1 \quad \sigma = 0.31$$

For the specific case of LDG ML magnitudes, that are larger than the local magnitudes defined by other observatories, a preliminar regression was defined to calibrate the MLldg magnitude into a coherent ML :

$$ML = 1.31 \, MLldg - 1.44 \quad \sigma = 0.40 \text{ for MLldg} < 4.65$$

$$ML = MLldg \text{ for MLldg} \geq 4.65$$

The relationship between Mw and ML is derived from a data set of 221 events with Mw-ML pairs in the range 2-6 :

$$Mw = 0.0376 \, ML^2 + 0.646 \, ML + 0.53 \quad \sigma = 0.29$$

This procedure was adopted to generate the catalogue in moment magnitude.

The Ms magnitude was then obtained using the calibration procedure of Ambraseys and Free (1997) :

$$Ms = -45.61 + 3.252 \log (Mo) - 0.048 \, [\log(Mo)]^2 \quad \sigma = 0.283$$

The application of these relationships leads to Ms magnitudes lower than Mw magnitudes in the range of magnitudes included in the catalogue of the region of interest (Mw$\leq$6.2).

4.3   Synthesis of data and publications

The knowledge of the geodynamic and seismotectonic context of Northwestern European platform took advantage, these last years, from many university or institutional works. They allowed in particular to better understanding the current mechanisms of deformation of the alpine region and its foreland domain.

The results of national and European scientific research and many recent Ph.D. theses provide new information and knowledge that enable the characterization of the recent geodynamic evolution and updating of seismotectonic models. In particular:

4.3.1 Static parameters of the crust:

- The Isobaths map of the Moho discontinuity (Dèzes and Ziegler, 2002; Cloetingh *et al.,* 2005) indicates the thickness of the crust and provides information on the isostatic state of the crust regarding major geodynamic phenomena (isostatic thickening in mountain ranges such as Alps,

thinning in areas of crustal stretching as in the Gulf of Lion and its margin and the area of Limagne grabens in Massif Central);

- The ECORS-CROP Alps and NFP-20 European Geo-Traverse geophysical programs have allowed to find explanations for the deep geometry of geological features, such as rifts, mountains ranges or sedimentary basins. Several deep seismic surveys were carried out across the western Alpine chain, giving useful information on the complex crustal structures. These deep seismic profiles have been exploited by several research teams in order to propose coherent structural and geological interpretations of the crustal structures that characterize the west European alpine chain (*e.g.* Tardy *et al.,* 1990; Nicolas *et al.,* 1990; Mugnier *et al.,* 1990, 1996; Marchant, 1993; Pfiffner *et al.,* 1997; Schmid and Kissling, 2000).

- The gravimetric data (New gravimetric map of France, Martelet *et al.*, 2009) give a good picture of the deep structures and of the discontinuities associated with structural contacts between two blocs.

- The data on the structure of the Hercynian Orogen (*e.g.* Matte, 1986; 1991; Matte and Hirn, 1988) are used to characterize the structural inheritance of the crust. Many crustal-scale accidents inherited from the Hercynian Orogen have been reactivated during subsequent tectonic episodes that have affected the West-European platform and can potentially be reactivated.

- Several old petroleum seismic profiles were recently reprocessed and reinterpreted in Provence in order to characterize the geometry and history of the main regional tectonic structures:

  o About ten seismic profiles were reinterpreted in the framework of the ANDRA research works in the Rhône Valley in the 1990s (Seguret et al., 1997; Mouroux and Brulhet, 1997);

  o 25 petroleum seismic profiles (more than 370 km for the total length) were reinterpreted in the region of the Middle Durance fault system by CASHIMA research team led by CEA (Cushing *et al.*, 2007; Hollender *et al.,* 2005; 2007);

  o And 10 petroleum seismic profiles were reinterpreted by Terrier *et al.* (2006, 2008) in Provence. These profiles intersect the main tectonic structures of Western Provence (Luberon thrust, Eiguilles Thrust, Cavaillon fault, Alpilles thrust);

4.3.2 Dynamic parameters of the crust:

- The PALEOSIS project of the European Commission [1998-2000] ("*Evaluation of the potential for large earthquakes in regions of present-day low seismic activity in Europe*") which concerns the use of paleoseismology in various geological domains (Alps, Pyrenees, lower and upper Rhine graben).

- The SAFE project of the European Commission [2001-2003] ("*Slow Active Faults in Europe*"), which is an integrated project aiming to indentify and characterize active faults for hazard assessment in low to medium activity areas.

- The GEOFRANCE 3D project "*Characterization of the recent and current deformations*", which is a scientific program led by the BRGM, based on 3D modeling of various geological structures, recently tectonically activated.

- The ENTEC project [2001-2004] ("*Environmental Tectonics, The Northern Alpin Foreland Natural Laboratory*") that concerns the tectonic interpretation, understanding the mechanisms of deformation and evolution of intraplate continental lithosphere in the Alpine foreland. (*e.g.* Cloetingh & Cornu, 2005 ; Cloetingh *et al.,* 2002, 2005, 2006 ; Tesauro *et al.*, 2005, 2006).

- The EUCOR-URGENT project [1999-2003] ("*Upper Rhine Graben Evolution & Neotectonics*"), a network of 25 European universities and government agencies that conduct researches on the seismic hazard, on the neotectonics of the Cenozoic rift system of western European and interaction with the Pyrenean and Alpine orogens (*e.g.* Dèzes *et al.*, 2004, Cloetingh *et al.*, 2005, 2006, Ziegler & Dèzes, 2005, 2006, Bourgeois et al., 2007).

- Databases on neotectonic evidences and paleoseismic ruptures:

    o Inventory of rupture evidences affecting the Quaternary in relation with major tectonic structures known in France and neighboring regions (contribution of GEOTER and IRSN; Baize *et al.*, 2002);

    o National Database of recent deformations and paleoearthquakes led by the BRGM (NEOPAL http://www.neopal.net);

    o The Database of neotectonic rupture evidences build and regularly updated by GEOTER (2011).

- Updated database of in situ stress measurements and focal mechanisms compiled by GEOTER. It allows a calculation of regional stress tensors to characterize the dominant deformation mechanism in various seismotectonic zones.

- Geodetic data also provide an essential contribution to the knowledge of the current strain field and strain rate at regional scale and understanding of deformation mechanisms (*e.g.* Vigny *et al.* 2006; Nocquet and Calais, 2003, 2004; Walpersdorf *et al.*, 2006).

- The distribution and characteristics of historical (SISFRANCE) and instrumental seismicity (LDG, RENASS).

Analysis of these tectonic deformations allows us to evaluate the rate of deformation and the kinematics of active accidents and to approach the characteristics of major earthquakes causing surface ruptures and for which the return periods are much greater than the period covered by the historical events.

- The follow-up of the Research and Development works undertaken by the CEA (LDG) and IRSN in the framework of nuclear safety (*e.g.* : Marin *et al.* 2004 ; Beauval, 2003 ; Scotti et Beauval, 2003; Beauval and Scotti, 2004; Scotti *et al.*, 2003; Clément *et al.*, 2003, 2004);

- The new probabilistic seismic zonation of France realized by GEOTER (Martin *et al.*, 2002). This zonation (EPAS 2002) is based on the geological and tectonic parameters listed and validated in France by a group of experts of the French Association for Earthquake Engineering (AFPS) in the framework of the EPAS working group (Autran *et al.*, 1998);

- The new Seismic Hazard Assessment of Switzerland realized by the Swiss Seismological Service of the Federal Institute of Technology in Zurich (SED) (Giardini *et al.*, 2004);

In addition, many recent scientific thesis were carried out at regional scale on the Western Alps and its foreland domain. They concern in particular:

- Works of Jean-Mathieu Nocquet on the measurement of crustal deformation in Western Europe using spatial geodesy (Nocquet et Calais, 2003, 2004) ;

- Bastien Delacou "Current tectonic and geodynamic setting of the alpine arc - Insights from seismotectonics and numerical modelling" (Thesis, Universities of Neuchatel and Nice-Sophia Antipolis 2004; Delacou *et al.*, 2004, 2005);

- Jean-Daniel Champagnac "Brittle tectonics of the inner parts of the W-Alpine belt; geodynamic implications" (Thesis, University of Neuchatel and Grenoble 1, 2004; Champagnac *et al.*, 2006);

- Pierre-Jean Alasset "Seismotectonic and identification of seismic sources in slow deformation context: the case of western Pyrenees and Northern Alps (France)" (Thesis, University of Strasbourg 1, 2005).

- Gwendolyn Peters "Active Tectonics in the Upper Rhine Graben: Integration of paleoseismology, geomorphology and geomechanical modelling" (Thesis, University of Amsterdam, 2007);

- Marielle Collombet (Thesis Grenoble university, 2001) on the cinematic and rotation of Western Alps;

- Works of Bonnet (Thesis Montpellier II, 2007) on the interactions between tectonics and surface deformation in the Alpine foreland.

4.3.3 Evolution of the 2000 models

The main results of these recent studies were exploited to develop or select the seismotectonic models for the preliminary PSHA.

The main evolutions concern:

- The revision of zones boundaries

  - New zones are included

  - Modifications of boundaries justified by new knowledge ;

- The maximum magnitudes

  - Revision of the definition procedure that leads to a significant increase

- The revision of the seismogenic layer depth

– The consideration of deformation mechanism which is included in the ground motion equations as focal mechanism.

4.4 Basis for the selection of the seismotectonic models

The objective was not to develop new seismotectonic models (treated in WP1), but rather to select and to modify existing models that have been published or used recently in France and that represent the current state of practice at the beginning of the SIGMA project. The specific objective discussed during the kick-off meeting, was to select a limited number of independent models developed on the basis of different interpretation criteria, to include significant epistemic uncertainty in the model and appreciate the respective influence of each model on the hazard levels.

Several models have also been developed in European projects like the SESAME-ESC project (Jimenez *et al.,* 2003) or the SHARE European seismic source zone model (Grünthal *et al.,* 2010; Arvidsson and Grünthal, 2010). However, these models are developed at another scale of investigation and are based, for the region of interest, on the existing French models, without new interpretation. This is the reason why we prefered to directly use the national sources of information.

All the available seismotectonic models in the region of interest identify seismotectonic zones that are defined as volumes of the earth's crust with homogenous seismogenic potential. Few of them consider individual faults with a precise geometry. This is because the seismogenic character of individual faults is very difficult to demonstrate, except in few parts of the territory. However, a seismotectonic zone may consist of several separate volumes modeling systems of faults with the same structural and seismotectonic properties. This is why it was decided to use at least one model that focuses on the identification of such systems, in the region of interest.

The three seismotectonic models are issued from a coherent interpretation of available seismological and geological databases at the beginning of the SIGMA project, and are based on the works of different national institutions or specialized entities (EDF, IRSN, BRGM, Universities, GEOTER).

According to the authors understanding and interpretation of the active tectonics and to the criteria adopted to identify the seismic sources, the size of the seismic sources may significantly vary. In an area of moderate seismic activity, like the region of interest, seismogenic and known faults are far from accounting for all observed seismic activity. This is because seismogenic structures may exist without recognized surface or subsurface manifestations and because of the time scales involved. The fault displacements may have long recurrence intervals with respect to seismological observation periods. The link between the strongest historical earthquakes and known tectonic structures is even difficult to establish.

With the objective to fit as well as possible the pincipe of model independence and competeness of interpretation, with the constraint of a limited number of models, we propose to adopt the three models described in the following chapters based on the following considerations:

- The first model (SZM1) is based on GEOTER studies and results from our own interpretation of the available databases in the region of interest and combines the parameters characterizing the static and dynamic states of the crust;

- The second model (SZM2) gives more emphasis to known or assumed fault systems and to the seismic activity as identified by the distribution of historical and instrumental earthquakes. It is much more based on original models from other institutions (BRGM, EDF, IRSN) that were developed to carry out deterministic assessments in application of the French RFS 2001-01 rule. The size of the source zones is reduced compared to the first model;

- The third model (SZM3), based on IRSNS works (Clement et al., 2004) is much more based on the identification of a coherent structural scheme and deformation scheme under the present state of stress. It overpasses the ambiguity that affects the seismogenic potential and seismic activity in small areas, the delineation of which, is sometimes based on unclear tectonic or structural limits. Seismic sources are larger than in the two first models and allow to work with a more complete seismic sample.

The seismic sources of these three seismotectonic models consist to greater or lesser extents, in two types of seismic sources:

- Systems of seismogenic structures such as faults systems that can be identified using the available database; this is the case of the model 2, with identification of three specific systems : the Belledone fault system; the Provence fault systems including the Middle Durance fault and the compressive structures (Trevaresse, Coste, Luberon thrusts), and the Tricastin cluster ;

- Area sources of diffuse seismicity, based on homogeneous tectonic and seismic character. They represent zones in which the correlation between seismicity and fault systems is not obvious. They consist in large volumes of the earth crust submitted to the same deformation scheme under the actual state of stress (model 1 and model 3).

Before entering in the details of each seismotectonic model, we briefly make some clarification on the consideration of the depth of the seismic source, which was one of the concerns of the Sceintific Committee.

4.5 Consideration of the depth of the seismic sources.

A major issue with the earthquake data is the large number of events associated with unreported depths (0 km or -2 km in the instrumental catalog, unknown depth for most of historical events) or catalogue default depths, which constitute 45% of the catalogue.

For the instrumental data, the epicenter is generally well determined with an uncertainty less than 5 km, whereas the depth is not well constrained: the uncertainty is of the order of 5 km or more. Depending on the institute in charge of the location and on the type of magnitude considered, the magnitude estimation is strongly scattered, even for large earthquakes. The magnitude uncertainty can reach 0.5 up to 1 degree

even for large earthquakes. A demonstrative example is the St Dié earthquake, one of the strongest recorded on the territory in the last decade with an important magnitude scatter : ML(RENASS) =5,4; ML(LDG)=5,8; ML(INGV)=4,6; Mw= 4,8.

The instrumental depth is poorly constrained and there is no real mean, from the available documentation, to appreciate the quality of the determination. In the location procedure, the depth can be a free parameter, or imposed at a fixed depth (5, 10, 15 km), when the localization algorithm do not converge.

For the historical event, numerous hypothesis can be formulated which can lead to significantly different results in terms of magnitude and depth estimates. The methods rely on the consideration of an attenuation model in intensity which analytical formulation requires to adjust different parameters. Different catalogues of historical seismicity can be constructed depending on the choices made.

The characteristics (magnitude and depth) of historical earthquakes can vary within a large range of values, according to the available bibliographical sources. Different complementary methods have been applied to determine the magnitudes and focal depths of the historical earthquakes. Those estimations were implemented in France, in order to apply the RFS 2001-01 or the rules for seismic hazard assessment for critical facilities sites, that impose a deterministic assessment.

The different methods used in the last decades were :

- The Kövesligethy-Sponheuer method (1960) for the calculation of the depth, and the Levret et al. (1996) method for the magnitude determination, used up to 2000. They allow the use of the individual determination of macroseismic intensities associated to an earthquakes (punctual measurement or isoseismal lines), and are based on an attenuation model in intensity specific to each earthquake ;

- The coupled method for the determination of the magnitude and the depth published by Scotti et al., 1999 ;

- The more recent method introduced by IRSN, that uses a binning strategy, is calibrated on instrumental events and allows for a determination of Ms and Mw magnitudes.

In the region of interest, the magnitude and depth have been published by different authors (mainly BRGM Blès *et al.* (1998) and IRSN Levret *et al.* (1996)). Geoter made its own assessment for some earthquakes, that are identified as reference earthquakes in the DSHA methodology.

The Table 5 summarizes the values calculated by those different authors. It is pointed out that the IRSN prepared a new catalogue of historical with simultaneous determination of depth and Ms and Mw magnitudes. This new source of information could bring new significant knowledge on the chracteristics of histrorical earthquakes. Unfortunately, the data were not made available for the preliminary SIGMA PSHA. The exploitation of this source of information would be of major interest during the project, if the data become in the public domain.

Earthquake Date			BRGM Bles et al. (1998) Parameters				Levret et al. (1996) parameters		IRSN (2010) parameters		Geoter parameters	
Year	month	day	Mmacro	H(km)	Seismic region	Zone	Mmacro	H(km)	Ms	H(km)	Mmacro	H(km)
1939	5	16	4.9	15	Sud Massif Central	D12						
1957	3	25	4.4	7	Limagnes	D13	4.5	5				
1878	6	24	5.2	18	Est Massi Central	D14	5.4	15				
1889	2	18	4.9	9	Fosse Nord Rhodanien	D16						
1881	1	27	5	10	Avant Fosse molassique Alpine	D19						
1984	2	19	4.2	5	Domaine provencal	D21	4.2	5				
1982	12	23	4.1	10	Camargue	D22						
1950	6	28	5	13	Bas Languedoc Ouest	D24	5	15			5	10
1903	4	20	4.7	12	Golfe du Lion	D25						
1822	2	19	5.4	13	Faille du Vuache	F7	5.6	15				
1996	7	15	5.2	5	Faille du Vuache	F7						
1708	8	14	4.9	4	Faille Moyenne Durance	F14			4.7	4		
1952	6	08	4	2	Faille Ventoux Lure	F12						
1887	11	14	4.2	4	Faille Salon Cavaillon	F13					4.2	5
1922	12	28	4.4	7	Faille Tet Cerdagne	F16						
1490	3	01	5.7	15	Failles Limagne Cezallier	S14						
1887	11	26	4.3	6	Axe CBS	S15						
1772	6	24	5	20	Failles Velay	S16						
1873	7	19	4.5	3	Tricastin	S17						
1971	6	21	4.3	3	Failles Jura Central	S18	4.3	5				
1962	4	25	5	6	Zones ext alpines septentrionales	S20	5	5				
1905	4	29	5.5	15	Zones ext alpines septentrionales	S20	5.7	15			5.7	14
1601	9	18	5.9	20	Zones ext alpines helvetiques	S21						
1774	9	10	5.5	10	Zones ext alpines helvetiques	S21						
1855	7	25	6	11	Valais	S22					6.2	12
1959	4	05	5.2	9	Alpes internes occidentales	S23	5.2	10				
1884	11	27	5.5	20	Alpes internes occidentales	S23						
1808	4	02	5.5	10	Corps d'ivree	S24						
1935	3	19	5	9	Ubaye Mercantour	S25W	5.3	10				
1887	2	23	6.3	8	Alpes ligures meridionales	S25E						
1644	2	15	5.7	15	Alpes meridionales et arcs DCN	S26						
1855	12	12	4.7	3	Alpes meridionales et arcs DCN	S26						
1909	6	11	5.5	5	Chevauchements Nord Provencaux	S27	5.5	10	6	6	5.9	5

Table 5 : Calculated magnitudes and depths of most of reference earthquakes in the region of interest, and used in DSHA analysis.

Several observations can be made :

- The magnitude of reference earthquakes (historical earthquakes that are used in the French deterministic approach to define the seismic ground motion on a site) varies between 4 and 6.3 and the depth between 3 and 20 kilometers. They are the range of values that were considered as representative of known historical earthquake in most of the deterministic assessement performed until now ;

- The mean depth (considering all the reference earthquakes) is close to 10 km. Some regions show specific characteristics : the depth of reference earthquakes in the Western Provence region is close to 5 km, while it is sensitively higher in the Alps, close to 12 km ;

- A given region can be characterized by different reference earthquakes (small magnitude at small depth, higher magnitude at greater depth) ;

- Some earthquakes present characteristics probably in relation with fault mechanism and tectonics (The Tricastin cluster with small magnitudes and low depths, the faults of Jura Central with similar properties).

An analysis can also be implemented including the instrumental earthquakes even if the depth is rarely determined by the national network with a precision better than 5 km. The depth distribution of earthquakes with Mw $\geq$3.5 and reported depth, in the region of interest, is shown Figure 16. It is observed that the majority of the earthquakes in the study area occurred at very shallow depths, although there are some deeper earthquakes mainly located beneath the Alps.
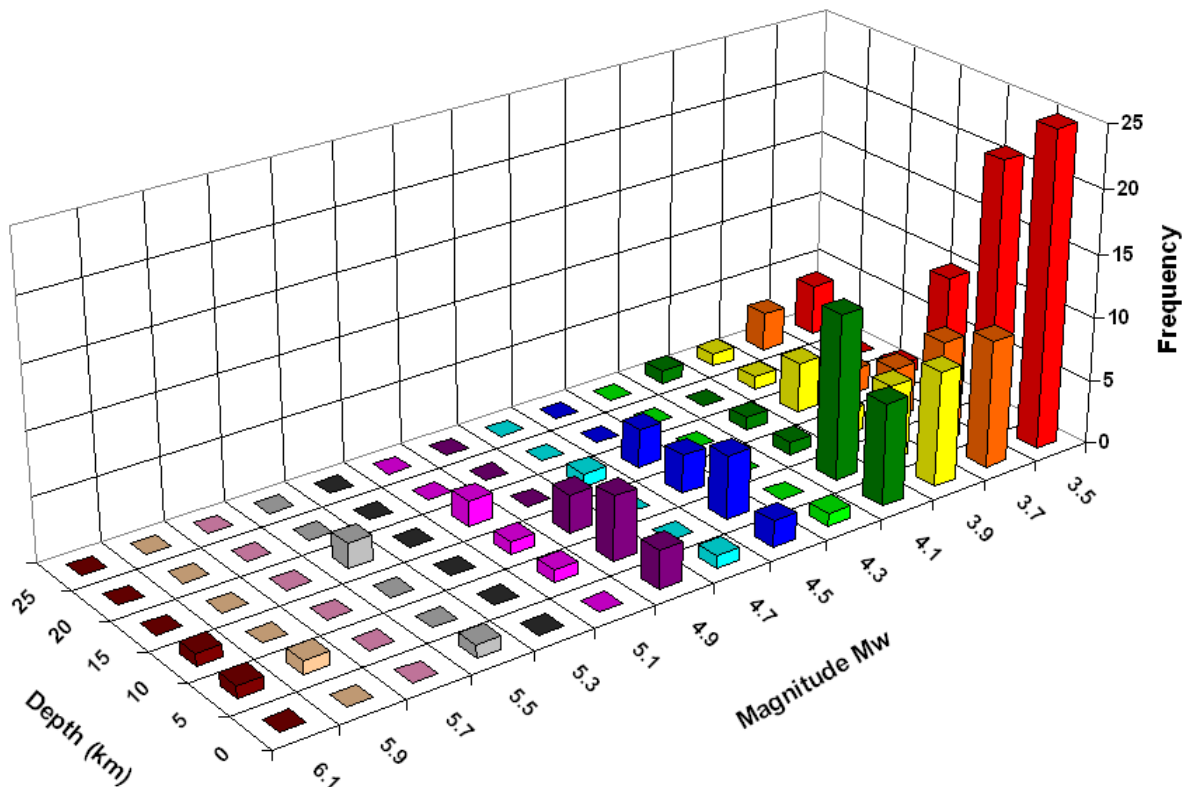
Figure 16 : Depth distribution of magnitudes $\geq$ 3.5 in the region of interest.

If we consider the depth distribution of earthquakes with Mw magnitudes greater than the adopted minimum magnitude for the PSHA analysis (4.5), the earthquakes depths do not exceed 20 km and 60% are in the range 5-15 km, without any justification to identify a predominant depth.

In our model, the depth is the depth on the fault rupture where the earthquake is assumed to be initiated. The depth of the seismic sources has an impact in the hazard calculation when the distance of the GMPEs corresponds to the focal distance or the shortest distance to the rupture area.

It is common in PSHA to use a depth distribution, to allow for the uncertainty consideration in the depth distribution input. This is generally done assuming a probability distribution of weights associated with different depths, for each seismic source : for instance 5 km (40%), 10 km (40%) and 20 km (20%), each value being an epistemic alternative.

However, due to the scarcity of the depth determination in the data set, additional criteria are often use to determine the possible range of values, like the geologic knowledge of tectonic structures at depth or the interpretation of seismic profiles.

We believe that without a specific work on the earthquakes relocations, including the determination of regional-dependent velocity models, the definition of a justified depth distribution, with weight assignements to specific depths has no scientific founding. This is the reason why, in our model, the epistemic uncertainty attached to the depth parameter, is defined by a range of values.

An independent approach, based on different criteria, is implemented for each seismotectonic model.

4.6 Maximum magnitude estimation.

Regardless of the different available approaches, the determination of maximum earthquake magnitude remains significantly uncertain, and the uncertainty needs to be described.

In a country of moderate seismicity, the method of applying an arbitrary increment on the observed maximum magnitudes in each seismic source is not adapted when considering the large uncertainties associated with the historical and instrumental magnitudes, with the incompleteness of the catalogue, with the potential source dimensions and with the physical parameters like stress drop. The uncertainty associated with the observed maximun magnitude is also significant because it is generally derived from macroseismic observations. However, one of the basic principles that is adopted here, is that the maximum magnitude considered in a zone, has a minimum value, that is at least the maximum observed magnitude increased by 0.5. This principle is adopted to remain coherent with RFS 2001-01 rule and the consecutive definition of the magnitude of reference earthquakes.

The maximum magnitude that is expected to be possible within each source zone is defined, in our approach by a range of magnitudes ($Mmax_{min}$, $Mmax_{max}$). Sensitivity tests that have been implemented on the French territory (Martin et al., 2002, Beauval, 2003, GZAFPS, 2006) have shown that as a result, the under-estimation of Mmax uncertainties can introduce a bias in the hazard assessment, especially for low annual probability of exceedance. To cover the range of possibilities, our approach of magnitude definition

is not based on a source by source analysis, but at the scale of large domains of similar tectonic history and process. Its definition results from the combined exploitation of :

- seismological scale laws in the seismic domains where the knowledge of faults dimensions provide the appropriate information ;

- the maximum observed magnitudes (to control that the proposed value is higher than the observed one) ;

- the recurrence laws in large areas of homogeneous deformation;

- the magnitudes assigned to the few paleoearthquakes ;

- the maximum magnitudes considered by the authors of the seismotectonic models.

Different criteria are adopted for each seismotectonic model and described in the following sections.

4.7 Seismotectonic Model 1 based on combined interpretation of static and dynamic parameters

4.7.1 Main characteristics of Model 1

The main parameters used to characterize the static and dynamic states of the earth crust and to identify the area sources are:

- The structural inheritance;

- The major tectonic features and tectonic episodes;

- The geometry of structures;

- The thickness of the crust and the thickness of the sedimentary cover;

- The lithological nature of the crust;

- The rates of convergence and the kinematics of the major boundaries;

- The epicenters distribution;

- The historical and instrumental seismic activity and the related earthquakes focal mechanisms;

- The slip rates determined on some faults;

- The stress field;

- The neotectonic evidences and paleoearthquakes studies.

The seismotectonic model 1 is based on the previous model developed in 2002 to elaborate the new probabilistic seismic zonation for Eurocode 8 application (Martin *et al.,* 2002). This model has continuously evolved in the framework of different PSHA studies in France, to integrate the results of new research and development programs, mentioned in chapter 4.3. In particular, the definition of the seismic parameters (*e.g.* seismogenics depths and maximum magnitudes was strongly revised for the SZM1 model.

The seismic zonation consists in 39 regional seismotectonic zones (Figure 17). It is mainly constrained by the main structural limits, the distribution of the seismicity, the kinematics of the recent and current

deformations (neotectonic data, earthquake focal mechanisms), and by the geometry and characteristics of the main regional fault systems.

4.7.1 Input parameters for Model 1

4.7.1.1 Determination of maximum magnitudes of the seismic zones

Historical and instrumental seismicity as well as sparse neotectonic evidences and palaeoseismic faulting are analyzed to determine the regional distribution of the strongest observed or assumed past earthquakes. The analysis, conducted in each large domain, provides information on the occurence and magnitude of major earthquakes, from the earthquake catalog and the possible existence of paleoseismic and neotectonic evidences issued from the bibliography.

The analysis of the seismic activity zone by zone, highlights strong contrasts in the observed maximum magnitudes between some adjacent zones, especially in the inner Alps. To ensure greater consistency in the definition of maximum magnitudes, GEOTER has developed a comprehensive approach (at the scale of France and surrounding areas), bringing face to face geophysical, geological and seismological data that characterize crustal deformations at large scale. This approach resulted in identifying large seismotectonic activity domains according to the static state of the crust, the geodynamic context and the seismotectonic activity. In particular the following parameters are taken into account:

- The composition and thickness variations of the continental crust (Moho);

- The geographical extension of the Alpine range (Alps and Pyrenees) and the zones of active rifting (Rhine graben, Limagne, Languedoc…);

- The localization of large Meso-Cenozoic sedimentary basins (Basin of Paris, Aquitain basin, Liguro-provençal basin);

- The zones characterized by strong Hercynian structural inheritance (Armorican massif, Massif Central, Ardennes, Vosges);

- The present relief, etc.

In our model, four large seismotectonic domains are identified (*cf.* Figure 18):

- **Domain 1** corresponds to the stable zones of meso-cenozoic sedimentary basins with a crust characterized by fossil Moho in isostatic equilibrium. For the region of interest, the identified stable zones correspond to the Liguro-Provençal basin and southern Massif-Central (Grand Causse region).

- **Domain 2** includes the stable zones with a crust characterized by fossil Moho in isostatic equilibrium, but characterized by a strong Hercynian structural inheritance, and a nonexistent or very thin Meso-Cenozoic cover. The seismic activity of these zones appears significantly stronger than that of the zones of large sedimentary basin. These zones concern the Armorican massif, North of France and Hercynian Corsica. They do not concern the region of interest.

- **Donain 3** encompasses the transition zones between the active and stable domains, with a thinned of intermediate thickness. Within the region of interest, It concerns the Alps foreland (Jura, Rhône valley, Provence), the rifting zones (Northeastern Massif Central), and the domains currently rather in extension (Languedoc). Some neotectonic or paleosismic evidences are known in these active zones (Figure 18).

- **Domain 4** includes the active areas characterized with deep crustal roots. This crust thickening reflects the insertion of continental foreland crust into the mantle and the development of mantle back-stops involving an offset of the upper and lower plate crust-mantle boundary (Ziegler and Dèzes, 2005). For the region of interest, it concerns the axial zone of the western alpine belt. The seismic activity of these zones is important and many neotectonic evidences are known (*cf.* Figure 18).

The maximum magnitude of the seismotectonic domains is expressed between two bounds to express the uncertainties related to the evaluation of this parameter.

Source zones model 1 (SZM1) - GEOTER model based on the combined interpretation of static and dynamic parameters characterizing the earth crust	FIGURE: 17

Background map: Geological map of France at 1:1 000 000 (BRGM, 2003)

Magnitude

○ [2 - 3 [

○ [3 - 4 [

○ [4 - 5 [

○ [5 - 6 [

○ [6 - 7 [

▭ Seismotectonic zones

▭ Area of interest

▭ Regional scale

Code	Name of the seismotectonic zone	Code	Name of the seismotectonic zone
ACC	ALPILLE, CRAU, CAMARGUE	LAN	LANGUEDOC
ALP	ALPES LEPONTINE	LBO	NORD LIMAGNE BOURBONNAIS
ALS	ZONE EXTERNE ALPINE SEPTENTRIONALE	LIF	LIMAGNES ET FOREZ
ANI	ARC DE NICE	LIN	LIGURIE NORD
ARG	ARGENTERA	LIS	LIGURIE SUD
BAL	BASSIN LIGURE	LOM	LOMBARDIE PLAINE DU PAU
BLP	BASSIN LIGURO-PROVENCAL	MPR	MARGE PROVENCALE
BMS	BASSIN MOLASSIQUE SUISSE	NDC	NAPPE DIGNE-CASTELLANNE
BOU	BOURGOGNE	NEX	NAPPE EXTERNE (BRIANCONNAIS VANOISE)
CBD	CISAILLEMENT NE BASSIN BAS-DAUPHINE	OBM	MASSIFS EXTERNES OISAN, BELLEDONNE, MONT BLANC
CBM	BASSINS PERMO-CARBONIFERES DE BRESSE ET NE MASSIF CENTRAL	OCC	PYRENEES ORIENTALES CATALANES COTIERES
CHY	CORSE HERCYNIENNE	PCP	PANNEAU DE COUVERTURE PROVENCAL
CJC	BASSINS PERMO-CARBONIFERES DU JURA CENTRAL	PCR	PROVENCE CRISTALLINE
CNP	CHEVAUCHEMENTS NORD PYERENEENS	PRO	PREALPES ROMANDES
CPR	CHABLAIS PREALPES ROMANDES	SJE	ZONE DE FAILLES SUBMERIDIENNES JURA EXTERNE
CVL	CANTAL VELAY	SMC	SUD MASSIF CENTRAL
DIA	DOMAINE INTERNE ALPES	TAA	INTERSECTION FAILLE DE LA MARCHE-SILLON HOUILLER-FAILLE TAUVES AIGUEPERSE
DIB	DIOIS BARRONIES	TRR	ZONE OUEST TRANFORNANTE RHIN-SAONE
DMS	DORA MAIRA ET SESIA	VAL	VALAIS
ERN	EMILIA ROMAGNA NORD	ZAO	BASSINS DU ROUSSILLON et D'EMPURDAN et ZONE AXIALE ORIENTALE
GLI	GOLFE DU LION	ZSA	ZONE SUD ALPINE OCCIDENTALE

Date: 14-10-2011	Author: Amélie LEON	File: V2_SZM1.mxd	Source: GEOTER, 2011

The evaluation of maximum magnitudes (Mmax) is based on a comparison of maximum magnitudes obtained by different methods and data:

- In a first step, within each seismotectonic domain, it is considered that the lower bound of the Mmax cann't be lower than the maximum observed magnitude, increased by a fixed value. Table 8 reports the date and magnitude of the maximum historical earthquakes (MHE) for the four large domains. The magnitudes of these MHE are increased by 0.5, according to French deterministic practice for nuclear facilities (RFS 2001-01).

- The published paleoseismic ruptures are compiled at national scale and gathered by seismotectonic domains. The published magnitudes associated with these paleoseismic ruptures are listed in Table 8. It is considered that the upper bound of Mmax in each seismotectonic domain cann't be lower than the upper bound of the paleoseismic magnitudes.

- For the two most active domains (domains 3 and 4) that concern the region of interest (1/4 Southeast of France) the length of the major fault segments is evaluated in order to determine the maximum magnitude, using empirical relationships such as Wells and Coppersmith (1994); Wesnousky (2008); Papazachos *et al.,* (2004). Empirical relationships based on the maximum rupture length and maximum surface rupture are used:

  o Results of this evaluation for the best known and largest active faults located in the seismotectonic domain 3 are presented in Table 6. The geometry of fault segmentation (length, width, dip) is examined in order to evaluate the maximum magnitude associated to each fault segment. The fault geometry is based on numerous published studies and synthetized in Terrier (2006) for the PACA region. The empirical relationships of Wells & Coppersmith (1994); Wesnousky (2008); Papazachos *et al.,* (2004) area applied considering the maximum rupture area and the maximum rupture length of each fault segment (Table 6). The average value of the calculated Mmax for each fault is provided in the last column. The maximum average value of Mmax is 6.5. The case of an unlikely rupture of two consecutive segments is considered for the Middle Durance fault system which is considered as the most active fault system in SE of France. In this case, the maximum value of Mmax is 6.8±0.2. According to this approach, a Mmax=7.0 is considered for the seismotectonic domain 3 for the Mmax upper bound. This value corresponds to the maximum average value of Mmax+0.5.

  o For the most active seismotectonic domain (domain 4), considering the presence of crustal-scale accidents of potentially more than 100 km length (*e.g.* Penninic front fault, Belledonne fault…), we consider the possibility of magnitude upper than 7.0 that may occur on these structures. Using the empirical relationships listed above, we determined the average values of length for magnitude of 6.7, 7.0 and 7.3 (Table 7). Following this approach, it appears that for a Mmax=6.7, the average maximum rupture length ranges between 28 and 35 km; for a Mmax=7.0, the maximum rupture length is ~40-60 km and between ~60 and ~100 km for Mmax=7.3. An upper bound Mmax value

of 7.3 is then considered as a reasonable value. For this seismotectonic domain a Mmax of 7.0±0.3 is considered.

4.7.1.2   Depth of the seismic sources

The depth of the source zones has an influence on the hazard calculations when the attenuation laws are parameterized with a distance metric which integrates this parameter, like the hypocentral distance or the distance to the rupture.

As mentioned in chapter 4.5, the analysis of the focal depth of earthquakes can constrain the depths of the seismic sources. Nevertheless, it should be considered magnitudes enough high and consistent with the magnitudes used for calculations (M≥Mmin). In France, the use of instrumental data to characterize the depth of seismic sources remains difficult, because the number of earthquakes above magnitude 4.0 with determined depth value is very limited. At the scale of France and surrounding areas, only 33 earthquakes with Mw≥4.0 are provided with a depth value in the LDG catalog, and only 10 earthquakes for the region of interest. Geological and tectonic criteria are used in complement, to characterize the seismogenic depths of the zones.

For the model 1, the depths of the source zones are, at the origin, those debated and validated by the scientific committee of the probabilistic zoning of France (Martin *et al.,* 2002). The depth values that were adopted, for this PSHA, resulted from discussions and consensus between the members of the scientific committee.

In order to take into account more recent data and knowledge, these values are revised and updated according to:

-   The in-depth geometry of the major tectonic structures deduced from the interpretation of deep seismic profiles such as those of programs ECORS-CROP and NFP20 West, in the Western Alps;

-   The analysis of cross-sections considering the events for which the depth was calculated. Particularly, some cross-sections of seismicity were built through western alpine arch. Some cross-sections of seismicity could be superimposed on the geological cross-sections interpreted from the ECORS-CROP and NFP20 West seismic profiles.

-   The analysis of scientific publications about the distribution of the seismicity (*like in.* Delacou *et al.*, 2004).

The depths of the model 1 seismic zones are reported in Table 10.

ZSM1 – Zonation of large seismotectonic domains for the definition of the maximal magnitudes

FIGURE: 18

Seismotectonic activity zones

🟩	1
🟧	2
🟥	3
🟪	4

Regional scale

Area of interest

Magnitude

- ∘ [2 - 3 [
- ∘ [3 - 4 [
- ○ [4 - 5 [
- ○ [5 - 6 [
- ○ [6 - 7 [

▲ Paleoseismic evidence

∘ Neotectonic evidence
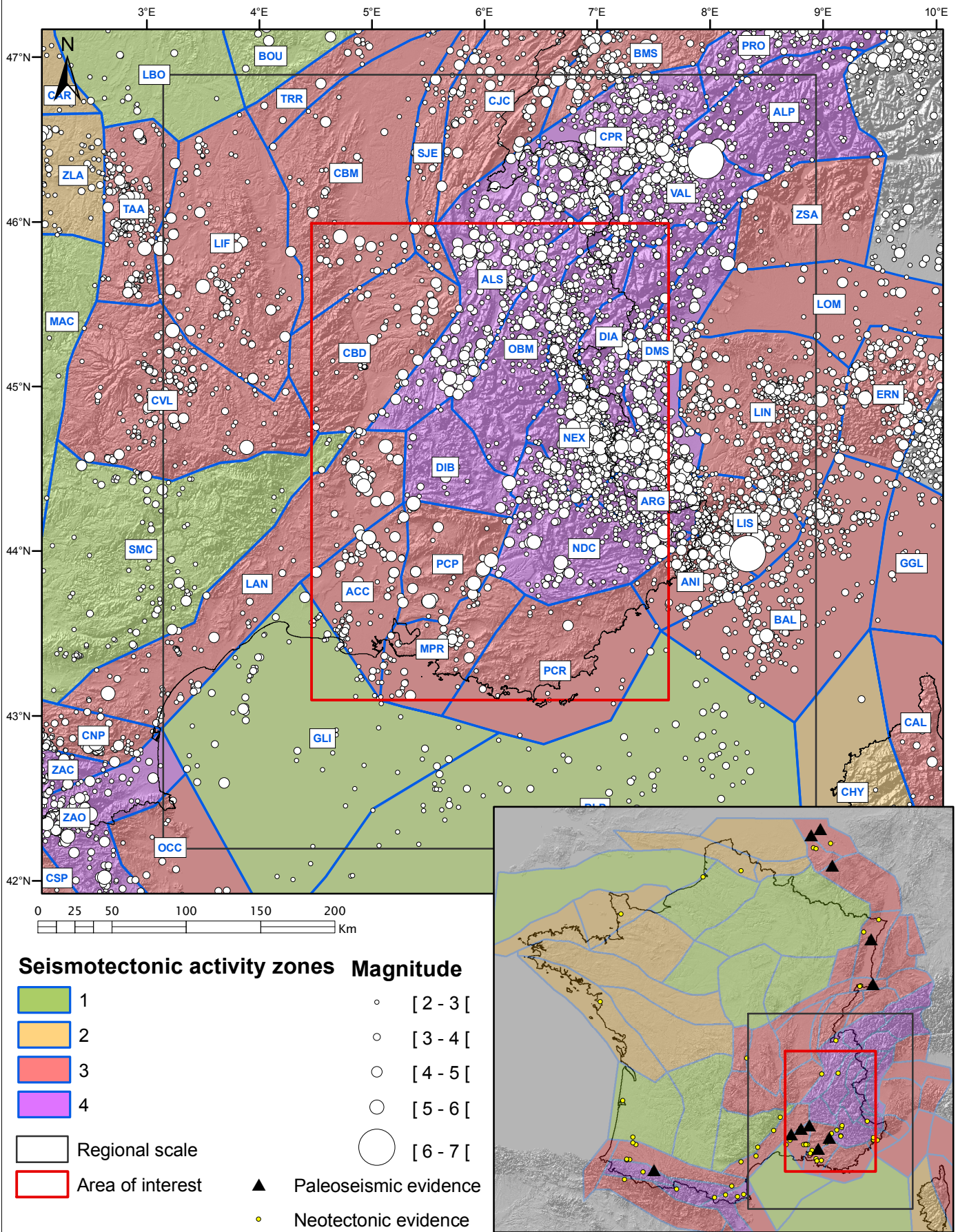
Date: 08-09-2011	Author: Amélie LEON	File: V2_SZM1_ZA.mxd	Source: GEOTER, 2011

Id Fault	Name of the fault	Main Segmentation	Length of segments	Estimated width of fault	Average dip	Mmax using Wells & Coppersmith (1994) relationships (maximum rupture area)	Mmax using Wesnousky (2008) relationships (maximum rupture length)	Mmax using Papazachos et al. (2004) relationships (maximum rupture area)	Average value of Mmax
F01	Ventoux thrust		25 km	10 km	80°S	6.5±0.3	6.7±0.2	6.4±0.2	**6.5**
F02	Lure thrust		F01a : 23 km F01b : 20 km	6 km	80°S	6.3±0.3	6.7±0.2 6.6±0.2	6.0±0.2	6.3
F03	Middle Durance fault	Château-Arnoux – La Brillanne	21 km	4 à 6 km	80°O	6.1±0.3	6.7±0.2	6.0±0.2	6.3
F04		Manosque thrust	17 km	4 à 6 km	60°NO	6.0±0.3	6.6±0.2	5.8±0.2	6.1
F05		Pierrevert-La Bastide des Jourdans	13 km	4 à 7 km	80°NO	6.0±0.3	6.5±0.2	5.8±0.2	6.1
		La Brillanne – Sainte Tulle	21 km	3 à 6 km	80°NO	6.1±0.3	6.7±0.2	6.0±0.2	6.3
F06		Sainte-Tulle – Mirabeau	19 km	3 à 6 km	60°NO	6.1±0.3	6.7±0.2	5.9±0.2	6.2
F07		Mirabeau – Venelles	16 km	3 à 6 km	70°O	6.0±0.3	6.6±0.2	5.8±0.2	6.1
		In case of rupture along two segments	*30 to 40 km*	*~6km*	*80°NO*	*6.3+/-0.3 to 6.4+/-0.3*	***6.8±0.2* to 6.9±0.2**	*6.1+/-0.2 to 6.3+/-0.2*	*6.4 to* **6.5**
F08	Trévaresse thrust		17 km	5 à 10 km	60°N	6.3±0.3	6.6±0.2	6.1±0.2	6.3
F09	Costes thrust		F12a : 12 km F12b : 10 km	10 à 12 km	60°N	6.2±0.3	6.1±0.2	6.1±0.2	6.3
F10	Lubéron thrust		F13a : 15 km F13b : 20 km	7 à 10 km	45°N	6.3±0.3	6.6±0.2	6.2±0.2	6.4
F11	Alpilles thrust		F14a : 14 km F14b : 14 km	11 à 12 km	60°N	6.3±0.3	6.3±0.2	6.1±0.2	6.2
F13	Nîmes fault	Rhône valley – Ouvèze	21 km	8 à 12 km	70°SE	6.4±0.3	6.7±0.2	6.4±0.2	**6.5**
F14		Châteauneuf-du-Pape - Nîmes	F18a : 24 km F18b : 23 km	6 à 8 km		6.3±0.3	6.8±0.2	6.2±0.2	6.4

Table 6 : Maximum magnitudes evaluated for the main active fault systems within the region of interest and for the seismotectonic domain 3

Maximum magnitude	Kinematics	Wells & Coppersmith (1994)		Wesnousky (2008)	Papazachos et al.(2004)		Average fault length
		Subsurface Rupture Length [RLD]	Rupture Area [RA]	Rupture length [L]	Fault Length [L]	Fault Area [RA]	
6.7	Reverse	29 km	377 km²	24 km	31 km	470 km²	28 km
	Strike-slip	38 km	407 km²	21 km	45 km	510 km²	35 km
	All	33 km	405 km²	24 km			29 km
7	Reverse	43 km	741 km²	38 km	45 km	800 km²	42 km
	Strike-slip	59 km	759 km²	45 km	68 km	900 km²	57 km
	All	46 km	759 km²	45 km			46 km
7.3	Reverse	65 km	1459 km²	50 km	62 km	1350 km²	59 km
	Strike-slip	90 km	1413 km²	100 km	100 km	1600 km²	97 km
	All	74 km	1422 km²	90 km			82 km

Table 7: Maximum magnitude versus fault length and fault area

Seismo-tectonic activity domains	Main characteristics	Main seismotectonic entities (national scale)	Date and magnitude of maximum observed historical earthquake (MHE) and correspondant seismic zone	M_{MHE}+0.5	Paleoseismic evidence *(Seismotectonic structure)*	Ref. Paleoseismic Magnitude	Paleoseismic magnitude	Rupture lengths and areas	Mmax chosen Min-Max
1	Stable meso-cenozoic sedimentary basins with crust being characterized by a fossil Moho in isostatic equilibrium	Paris and Aquitain Basins, Liguro-Provençal Basin	10/08/1759 [5.2 Mw] Entre-deux Mers Earthquake Aquitain Basin [ZNA]	5.7 Mw	-				5.7-6.3
2	Stable zones with crust being characterized by a fossil Moho in isostatic equilibrium, with strong Hercynian and /or Cadomian structural inheritance and a thin of inexistent meso-cenozoic cover	Armorican Massif, Brabant block and North-Artois/Midi shear zone, Hercynian Corsica	25/01/1799 [5.6 Mw] Marais Breton (Bouin) Earthquake South Armorican zone [SAR]	6.1 Mw	-				6.1-6.5
3	Transition zone between active zones and stable zones with an intermediate or thinned crust	Foreland domains of Alps and Pyrenees, Rift zones (Limagnes, Rhin Graben) and distensive tectonic domains (Languedoc, Tyrrhenian basin)	23/02/1887 [6.2 Mw] Riviera Di Ponente (Italy) Earthquake Southern Liguria [LIS]	6.7 Mw	Pont de la Lône *(Nîmes fault)*	Volant et al., 2008	Mw≥6.0	6.8±0.2 (Cf. Table 6)	6.7-7.0
					Courthézon-Latour *(Nîmes Fault)*	Combes et al., 1993 Blès et al., 1995	Mw≥6.0 Mw=6.1		
					La Fauchonne *(Trévaresse Fault)*	Chardon et al., 2005	Mw=6.2 à 6.4		
					Malaucène *(Ventoux Thrust)*	Dutour et al., 2002	Mw≥6.0		
					Valveranne *(Middle-Durance Fault)*	Blès et al., 1995 Sébrier et al., 1997	Mw=6.4 à 6.6 Mw=6.5 à 6.9		
					Bâle-Reinach *(Bâle-Reinach Fault)*	Ferry et al., 2005	Mw=6.4 à 6.7		
					Achenheim/Hangenbieten *(Achenheim Fault)*	Lemeille et al., 1999 Cushing et al., 2000	Mw=6.0 à 6.5		
					Bree *(Feldsbiss Fault)*	Camelbeeck & Meghraoui, 1998	Mw=6.0 à 6.3		
					Neer *(Peel Fault)*	Van Den Berg et al., 2002	Mw=6.0 à 6.6		
					Jülich *(Rurrand fault)*	Lehmann et al., 2001 Vanneste & Verbeek, 2001	Mw~6.8		
4	Domains with thickened crust and significant isostatic disequilibrium	Pyrenean axial zone and internal alps	21/06/1660 [5.9 Mw] Bagnères de Bigorre Earthquake Occidental North-Pyrenean zone [NPO] 25/07/1855 [6.2 Mw] Valais (zwitserland) Earthquake Valais [VAL]	6.7 Mw	Arcizac *(Lourdes Fault)*	Alasset & Meghraoui, 2005	Mw=6.5 à 7.1	7.0±0.3 (Cf. Table 7)	6.7-7.3

Table 8 : Comparison of the maximal magnitudes for the large domains of seismotectonic activity (SZM1)

4.7.1.1   Dominant deformation mechanism

The new generation of attenuation laws allows to consider the "deformation mechanism" or "focal mechanism" as one of the input parameters.

A dominent mechanism of deformation is assigned to each zone, using the available data (focal mechanisms, in-situ stress measurements, regionalized maps of stress field…).

A database of focal mechanisms and in-situ stress measurements was built for this analysis, from various data sources (scientific publications, reports, online catalogues…). For each seismic zone, the dominant deformation mechanism results from the calculation of a regional stress tensor, using the TENSOR software (Delvaux, 1993, Delvaux & Sperner, 2003), based on data inversion of focal mechanisms of earthquakes and in-situ stresses data.

Since that all intermediate stress fields exist, between a purely extensive mode and purely compressive regime, five categories of tectonic regime are defined to characterize the dominant focal mechanism of each seismic zone:

-    Extensive regime (E);
-    Extensive Strike-slip regime (ED);
-    Strike-slip regime (D);
-    Compressive Strike-slip regime (CD);
-    Compressive regime (C).

The following table indicates the equivalence between the dominant mechanism of deformation of the zones and the parameters used in the selected attenuation laws:

CODE DEF	MECADEF	Akkar & Bommer 2010	Boore & Atkinson 2008	Zhao et al., 2006
C	Compressive	Reverse Fr=1	Reverse RS=1	Reverse SR>0
CD	Compressive strike-slip			
D	Strike-slip	Others Fr=0 Fn=0	Strike-slip SS=1	Others SR=0
ED	Extensive strike-slip	Normal Fn=1	Normal NS=1	
E	Extensive			
I	Undefined	Others Fr=0 Fn=0	U=1	

Table 9: Parameter « mechanism of deformation » of the selected attenuation laws

4.7.1.2   Synthesis of the zones parameters

The Table 10 presents the synthesis of the seismic parameters assigned to the zones of model 1. In this table each zone name is identified, with the dominant mechanism of deformation (MECADEF), the stronger historical earthquake parameters (date, magnitude, intensity), the seismotectonic activity domain and input parameters used for the probabilistic assessment (lower and upper bounds of maximum magnitudes and depths, and zone area in km²).

IDENT.	NAME OF ZONE	Date Observed Mmax	observed Mmax	Epicentral intensity Io	Activity Domain	Mmax min	Mmax max	H min (km)	H max (km)	Dominant mechanism of deformation	DEF	AREA (Km²)
ACC	Alpille, Crau, Camargue	18 november 1769, 21 december 1769	4.9	VII	3	6.7	7.0	3	15	Normal Strike-slip	E	4652
ALP	Alpes Lepontine	14 march 1964, 05 november 1987	3.2		4	6.7	7.3	3	15	Strike-slip Reverse	D	7034
ALS	Zone externe Alpine Septentrionale	19 february 1822, 25 april 1962	5.2	VII-VIII	4	6.7	7.3	3	15	Reverse Strike-slip to Strike-slip	C	9102
ANI	Arc de Nice	29 december 1854	5.2	VII-VIII	3	6.7	7.0	3	15	Reverse Strike-slip	C	2833
ARG	Argentera	7 april 1966	4.5	VI	4	6.7	7.3	5	15	Reverse Strike-slip	C	2035
BAL	Bassin Ligure	19 july 1963	5.5		3	6.7	7.0	3	10	Reverse	C	12702
BLP	Bassin Liguro-provençal	6 september 1972	4.4		1	5.7	6.3	3	10	Undetermined	I	65430
BMS	Bassin Molassique Suisse	27 january 1881	4.9	VII	3	6.7	7.0	3	10	Strike-slip Reverse (SW) à Strike-slip Normal (NE)	D	6581
CBD	Cisaillement NE Bassin Bas-Dauphiné	18 february 1889	4.5	VI-VII	3	6.7	7.0	5	15	Strike-slip	D	8282
CBM	Bassins Permo-Carbonifères de Bresse et NE Massif Central	24 june 1878	5.0	VI-VII	3	6.7	7.0	5	15	Strike-slip Normal	D	13102
CJC	Bassins Permo-Carbonifères du Juran Central	21 june 1971	4.9	VII	3	6.7	7.0	3	15	Strike-slip Reverse	D	8919
CNP	Chevauchement Nord Pyrénéens	18 february 1996	5.0	VI	3	6.7	7.0	5	15	Reverse Strike-slip	C	15650
CPR	Chablais Préalpes Romandes	29 april 1905	5.4	VII-VIII	4	6.7	7.3	3	15	Strike-slip Normal	D	6661
CVL	Cantal Velay	18 october 1833	4.9	VII	3	6.7	7.0	5	15	Strike-slip Normal	D	13262
DIA	Domayne Interne Alpes	12 September 1785	5.2	VII	4	6.7	7.3	5	15	Normal (S) à Strike-slip Normal (N)	E	5168
DIB	Diois Barronies	19 may 1866	5.2	VII-VIII	4	6.7	7.3	3	8	Reverse Strike-slip	C	3746
DMS	Dora Mayra et Sesia	02 april 1808	5.5	VIII	4	6.7	7.3	5	20	Reverse Strike-slip (N) to Oblique Normal (S)	C	5493
ERN	Emilia Romagna Nord	09 october 1828	5.5	VIII	3	6.7	7.0	5	15	Strike-slip Normal	D	5190
GLI	Golfe du Lion	20 april 1903	4.3	VI	1	5.7	6.3	5	15	Normal Strike-slip	E	22864
LAN	Languedoc	23 january 1773, 19 july 1873	5.2	VI-VII	3	6.7	7.0	3	15	Normal	E	12296
LIF	Limagnes et Forez	29 june 1477	5.2	VI-VII	3	6.7	7.0	5	15	Normal Strike-slip	E	13248
LIN	Ligurie Nord	21 august 2000	5.0		3	6.7	7.0	5	15	Strike-slip Reverse	D	10608
LIS	Ligurie Sud	23 february 1887	6.2	IX	3	6.7	7.0	3	15	Strike-slip	D	3263

IDENT.	NAME OF ZONE	Date Observed Mmax	observed Mmax	Epicentral intensity Io	Activity Domain	Mmax min	Mmax max	H min (km)	H max (km)	Dominant mechanism of deformation	DEF	AREA (Km²)
LOM	Lombardie Plaine du Pô	07 february 1977, 20 november 2005	3.5		3	6.7	7.0	5	15	Strike-slip	D	7685
MPR	Marge Provençale	05 february 1803, 12 may 1846, 01 may 1932 et 19 february 1984	4.2	VI	3	6.7	7.0	3	8	Reverse	C	4585
NDC	Nappe Digne-Castelanne	26 june 1494, 20 july 1564, 18 january 1618, 15 february 1644 et 12 december 1855	5.5	VIII	4	6.7	7.3	5	15	Reverse Strike-slip	C	7131
NEX	Nappe Externe (Briançonnais Vanoise)	5 april 1959	5.2	VII	4	6.7	7.3	5	15	Strike-slip Normal to Strike-slip	E	6145
OBM	Massifs Externes Oisan, Belledonne, Mont Blanc	11 march 1817, 22 july 1881, 13 august 1905 25 april 1963	4.9	VII	4	6.7	7.3	5	15	Strike-slip Reverse (S) to Normal Strike-slip (N)	D	6525
OCC	Pyrénées Orientales Catalanes Côtières	26 october 1973	3.2		3	6.7	7.0	5	15	Normal Strike-slip	E	7179
PCP	Panneau de couverture Provençal	11 june 1909	6.0	VIII-IX	3	6.7	7.0	3	8	Reverse Strike-slip	C	4357
PCR	Provence cristalline	29 july 1899	3.8	V	3	6.7	7.0	3	8	Strike-slip Reverse	D	9915
PRO	Préalpes Romandes	14 march 1964	4.9		4	6.7	7.3	3	15	Strike-slip Reverse to Reverse	D	5591
SJE	Zone de failles Submeridiennes Jura Externe	09 september 1879	4.2	VI	3	6.7	7.0	3	15	Strike-slip	D	3404
SMC	Sud Massif central	16 may 1939	4.2	VI	1	5.7	6.3	5	15	Strike-slip Normal	D	19381
TAA	Intersection Faille de La Marche – Sillon houiller – Faille Tauves Aigueperse	01 march 1490	5.5	VIII	3	6.7	7.0	5	15	Normal Strike-slip	E	5176
TRR	Zone Ouest Transformatne Rhin-Saône	30 october 1828	4.9	VII	3	6.7	7.0	5	15	Strike-slip	D	6094
VAL	Valais	25 july 1855	6.2	IX	4	6.7	7.3	5	15	Normal to Normal Strike-slip	E	4166
ZAO	Bassins du Roussillon et d'Empurdan et Zone Axiale Orientale	02 february 1428	6.2	IX	4	6.7	7.3	5	15	Normal Strike-slip	E	9186
ZSA	Zone Sud Alpine occidentale	14 june 1993	4.2		3	6.7	7.0	5	20	Strike-slip Reverse	D	6081

Table 10 : Input Seismic parameters of the regional model SZM 1 (Figure 17)

4.8   Seismotectonic model 2 based on highest consideration of the seismicity distribution and fault systems

4.8.1   Main characteristics of Model 2

One of the objectives of the workpackage 1 of SIGMA is to improve the knowledge of active faults and the characterization of their activity. It is planned to focus on different active fault systems at different scale:

- The Belledonne fault system, that is considered as a potential mega-structure with the objective to address the issue of the potential impact of long-extension faults;

- The western Provence area, where the actual state of knowledge reveals the presence of quite well identified structures like the Durance fault and east-west thrusts.

It was not the objective, in the task 1 of WP4, to develop a pure and homogeneous fault model (precise geometry of faults, slip rates, proportion of seismic/aseismic deformation, characteristic magnitudes, and return periods) at the scale of the region of interest. However, the WP4 leaders wished to make an attempt at developing a branch of the logic tree aiming at better identifying the potential relationships between the seismicity distribution and tectonic faults in three specif areas of the region of intrest:

- The alpine west front, (*e.g.* the Belledonne fault);

- The western Provence;

- The Tricastin cluster.

As the results of WP1 are not available to implement the task 4-1, we used different scientific works and existing seismotectonic models to better constrain the delineation of seismic sources of these fault systems.

For the Provence region, a probabilistic seismic hazard assessment was done by Clement *et al.* (2009) based on a faults seismotectonic model. Other recent synthetic works concerning the seismotectonic structures of Southern Alps and Provence are used to characterize the seismic zones. These include the following research works:

- Identification and characterization of the active faults of the Provence-Alps-Côte d'Azuyr Region realized by the BRGM (Terrier, 2006);

- The results of the multidisciplinary research works of the Collège de France and CEREGE of Aix-en-Provence about the geodynamic of the France Southeast Basin, thematic issue published in a special volume of the *Bulletin de la Société Générale de France* in 2010 (Le Pichon and Rangin, 2010 ; Rangin *et al.,* 2010).

These publications are used to identify the fault systems characterized by the same type of seismic deformation. This model involves seismic sources localized along the main faults of Western Provence identified as potentially active during the Plio-Quaternary period (*Figure 19* and Figure 20).
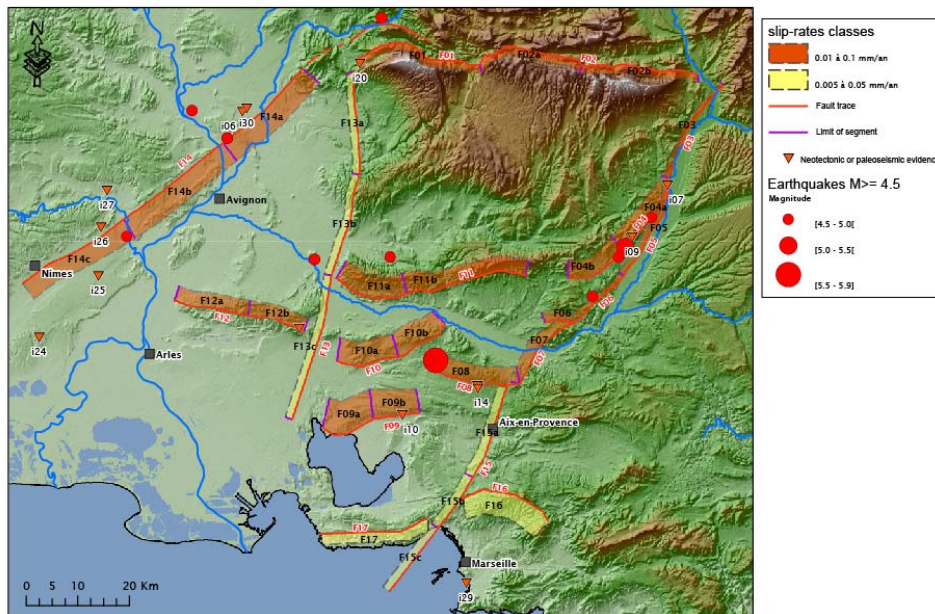
Figure 19: Fault model of Clement et al., (2009) used to develop a probabilistic seismic hazard assessment in western Provence

For the alpine western front, it is more complicated than in Provence to clearly identify the relationships between the seismicity and faults. The research works of the Grenoble university (Thouvenot *et al.,* 2003), who made a detailed study of the instrumental seismicity in the region between Grenoble and Chambery using the Sismalp database, is used. Thouvenot *et al.* (2003) suggests that the recent seismicity in this region could be associated to a bordering N30° fault of the Belledonne massif that was unidentified before, because of the important sedimentary cover, but was revealed thanks to the precise focus locations of the Sismalp network (Figure 21).

For the Tricastin cluster, the models developed by Clement *et al.* (2004) and Secanell *et al.* (2011) together with the analysis of instrumental seismicity done by Thouvenot *et al.* (2009) is used to assign the seismicity to a hypothetic fault zone.

For the remaining zones, the seismotectonic models developed by EDF, BRGM (Blès et al., 1998) and IRSN (Baize et al., 2011) to implment DSHA analysis, provide also a complementary highlighting approach to develop the seismotectonic model 2. This model gives more emphasis on the historical seismicity distribution and fault systems than the GEOTER model 1.

The second seismotectonic model is presented in Figure 22.

Figure 20 : Synthetic seismotectonic map of SE France after Terrier, 2006

4.8.2 Input parameters for the model 2

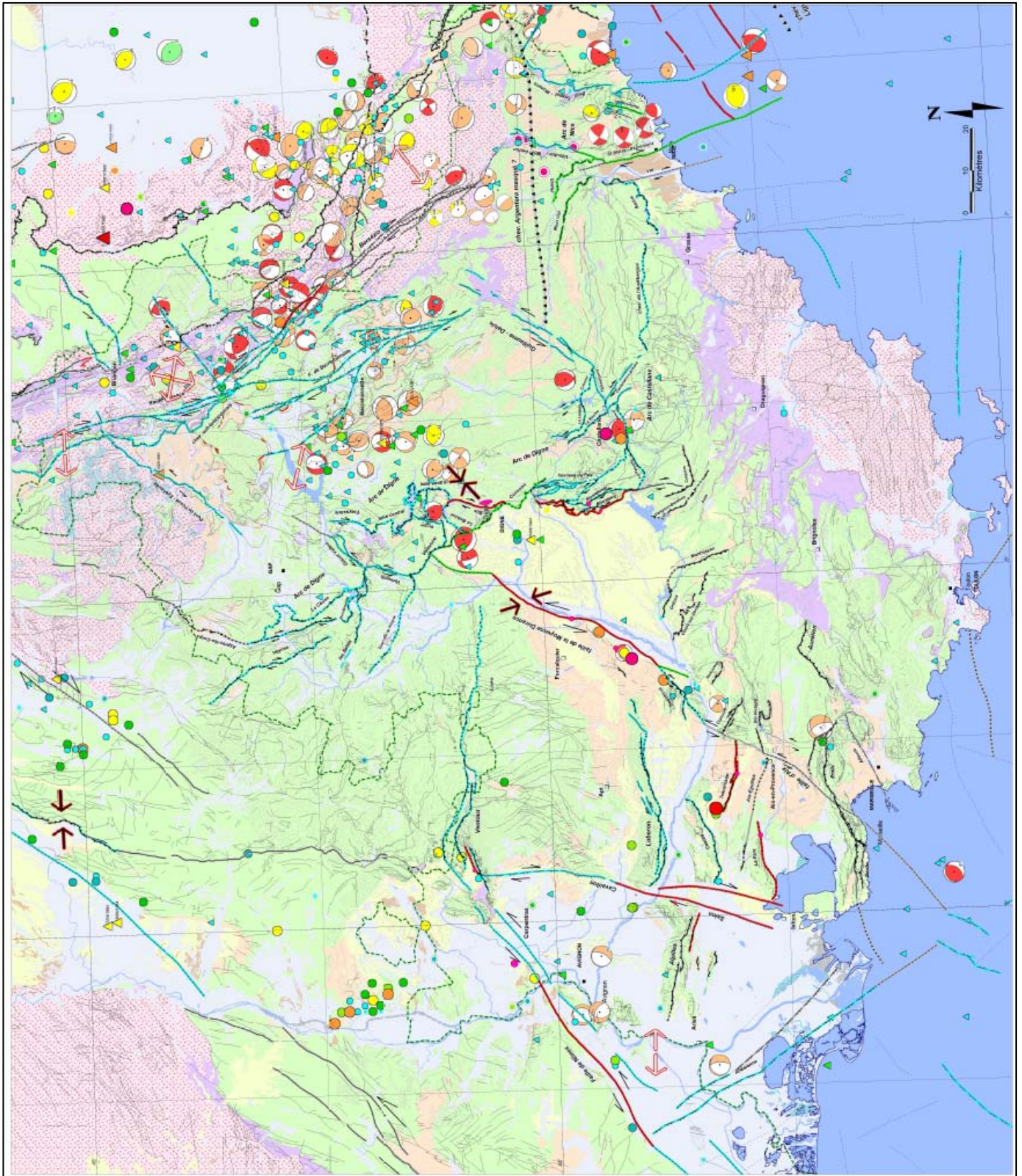#### 4.8.2.1 Determination of maximal magnitudes

In the same perspective that for the seismic model 1, the maximum magnitude of the seismic sources is defined in a global way between a lower and upper bound, to avoid strong contrasts that can occur between adjacent sources, when a zone by zone approach is adopted.

Three seismotectonic activity domains are defined (Figure 23), instead of four in the model 1. For the study area these are the following:

1. Low deformation domain – Gulf of Lion (MED zone);

2. Intermediate deformation domain – alpine foreland zones, Massif Central and eastern Provence;

3. Active deformation domain- Alps and western Provence.

In a second step and for each seismotectonic domains, we completed the analysis done for the model 1, applying the statistical procedure of Kijko (2002) and the HA software, that use three different periods of data characterizing the seismic activity (instrumental, historical and paleoseismicity).

Here again the lower bound of the minimum magnitude is not lower than the maximum observed magnitude increased by 0.5, and the upper bound corresponds to the highest magnitude resulting from the application of the different methods.

The values of the maximum magnitudes are presented in the Table 11.

4.8.2.2 Depth of the seismic sources

The depth values of the source zones used in the hazard calculation are reported in Table 11 for each seismic zone. Compared to the criteria adopted for the model 1, we tried to implement a statistical analysis of the depth distribution using the instrumental and historical data.

For each seismic zone the following parameters were considered:

1. The minimum, median and maximum values of the depth sample associated to each zone defined as follow :

- Selection of earthquakes of the earthquake catalogue for which the depth is defined and the magnitude is higher or equal to Mw 4.0;

- If the number of earthquakes is lower than 10, the filter on the magnitude is reduced to 3.5, then to 3.0, to 2.5, up to 2.0 to obtain a sufficient sample of earthquakes;

- Calculation of the centiles 15%, 50% and 85 % of the distriution.

2. The mean depth resulting from the regional attenuation models in intensity calculated for different French regions, in a PSHA assessment in intensity developed for EDF in 2007 (Secanell *et al.*, 2007). The mean depths in the region of interest are 11 km for the Alps, 4 km in Provence and 12 km for the rest of regions.

	Seismotectonic activity domains	Main seismotectonic entities (national scale)	Date and magnitude of maximum observed historical earthquake (MHE) and associated seismic zone	$M_{MHE}+0.5$	Paleoseismic evidence *(Seismotectonic structure)*	Ref. Paleoseismic Magnitude	Paleoseismic magnitude	Mmax Kijko	Mmax chosen Min-Max
1	Low	Paris and Aquitain Basins, Ardennes, Gulf of Lion, Manche	10/08/1759 [5.2 Mw] Entre-Deux Mers Earthquake Entre-Deux Mers zone [ENT]	5.7 Mw	-			5.6-6.4	5.7-6.4
2	Moderate	Armorican Massif, Central Massif, Foreland domain of Alps, Rift zones (Limagnes, Rhin Graben)	18/10/1356 [6.2 Mw] Bâle Earthquake Bâle zone [BAL]	6.7 Mw	Bâle-Reinach *(Bâle-Reinach Fault)*	Ferry et al., 2005	Mw=6.4 à 6.7	6.0-7.0	6.7-7.0
					Achenheim/Hangenbieten *(Achenheim Fault)*	Lemeille et al., 1999 Cushing et al., 2000	Mw=6.0 à 6.5		
					Bree *(Feldsbiss Fault)*	Camelbeeck & Meghraoui, 1998	Mw=6.0 à 6.3		
					Neer *(Peel Fault)*	Van Den Berg et al., 2002	Mw=6.0 à 6.6		
					Jülich *(Rurrand fault)*	Lehmann et al., 2001 Vanneste & Verbeek, 2001	Mw~6.8		
3	Active	Pyrenees and alps domains, Provence	23/02/1887 [6.2 Mw] Riviera Di Ponente (Italy) Earthquake Argentera and Liguria zone [ARG]	6.7 Mw	Arcizac *(Lourdes Fault)*	Alasset & Meghraoui, 2005	Mw=6.5 à 7.1	6.4-7.2	6.7-7.2
					La Fauchonne *(Trévaresse Fault)*	Chardon et al., 2005	Mw=6.2 à 6.4		
					Valveranne *(Middle-Durance Fault)*	Blès et al., 1995 Sébrier et al., 1997	Mw=6.4 à 6.6 Mw=6.5 à 6.9		
					Pont de la Lône *(Nîmes fault)*	Volant et al., 2008	Mw≥6.0		
					Courthézon-Latour *(Nîmes Fault)*	Combes et al., 1993 Blès et al., 1995	Mw≥6.0 Mw=6.1		
					Malaucène *(Ventoux Thrust)*	Dutour et al., 2002	Mw≥6.0		

Table 11 : Comparison of the maximal magnitudes for the large domains of seismotectonic activity (SZM2)

Seismotectonic map of the alpine west front (Thouvenot *et al.,* 2003) and identification of the Belledonne fault system

FIGURE: 21

Source zones model 2 (SZM2) – Alternative model based on highest consideration of the seismicity distribution and fault systems

FIGURE: 22
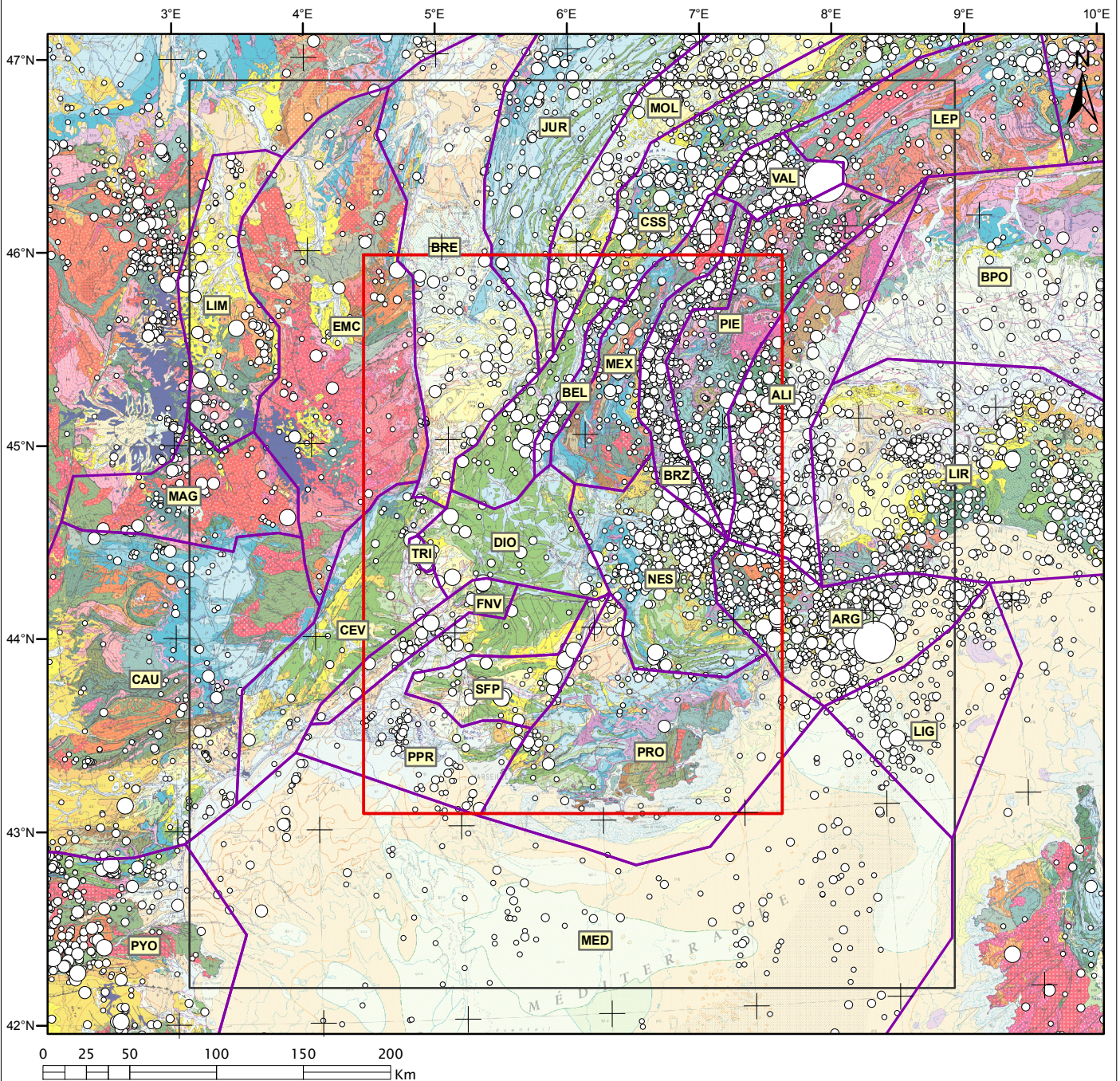
Magnitude

∘	[2 - 3 [
∘	[3 - 4 [
∘	[4 - 5 [
○	[5 - 6 [
○	[6 - 7 [

Area of interest

Regional scale

Background map: Geological map of France at 1/1.000.000
BRGM, 2003

NUMERO	NOM	CODE	NUMERO	NOM	CODE
1	Ligurie du Nord	LIR	16	Zone Briançonnaise	BRZ
2	Jura	JUR	17	Alpes lepontines	LEP
3	Bassin molassique	MOL	18	Nappes externes Sud	NES
4	Cévennes Languedoc	CEV	19	Bassin Ligure	LIG
5	Diois	DIO	20	Alpes italiennes	ALI
6	Bordure Est Massif Central	EMC	21	Bassin du Pô	BPO
7	Bresse et Dauphiné	BRE	22	Failles Nîmes Ventoux	FNV
8	Chaînes subalpines	CSS	23	Système de failles Provence	SFP
9	Golfe du Lion	MED	24	Tricastin	TRI
10	Provence orientale	PRO	25	Panneau provençal	PPR
11	Massifs cristallins externes	MEX	26	Faille de Belledonne	BEL
12	Zone Piémontaise	PIE	27	Pyrénées Orientales	PYO
13	Margeride	MAG	28	Limagne	LIM
14	Causses	CAU	29	Valais	VAL
15	Argentera et Ligurie	ARG			

Date: 14-10-2011	Author: David CARBON	File: V2_SZM2.mxd	Source: GEOTER, 2011

The 15% and 85% centiles are adopted to define the lower and upper bounds of the depth parameter. In the model 2 we decided to adopt an asymmetric triangular distribution to modelize the depth distribution, the highest probability being associated with the mean value between the centile 50% of the distribution and the mean depth value resulting from the attenuation model in intensity.

4.8.2.3   Dominant mechanism of deformation

The dominant mechanism of deformation is defined using the same methodology as for the first model.

4.8.2.4   Synthesis of the zones parameters

The Table 12 presents the synthesis of the seismic parameters assigned to the zones of model 2.

ZSM2 – Zonation of the seismic activity for the definition of the maximal magnitudes   FIGURE: 23

Seismotectonic activity zones

Zone	
1	
2	
3	

Regional scale

Area of interest

▲ Paleoseismic evidence

Magnitude

∘ [2 - 3 [

∘ [3 - 4 [

○ [4 - 5 [

○ [5 - 6 [

○ [6 - 7 [
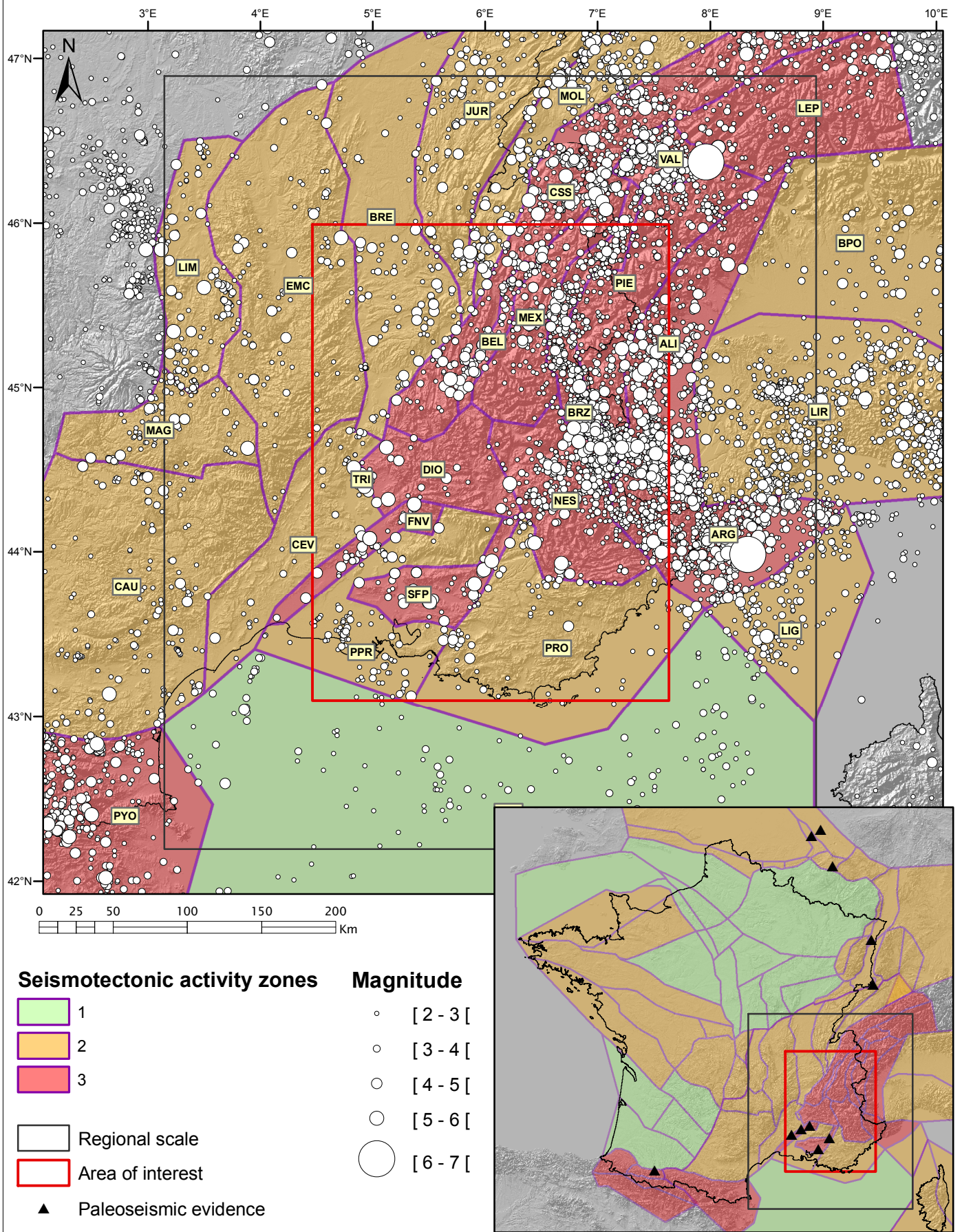
Date: 08-09-2011	Author: Amélie LEON	File: V2_SZM2_ZA.mxd	Source: GEOTER, 2011

NUM.	NAME OF ZONE	CODE	DATE Mmax observed	Magnitude Max observed	Io	A.Z.	Mmax min	Mmax max	Hmin	Hmean	Hmax	Dominant mechanism of deformation	DEF
1	Ligurie du Nord	LIR	09 october 1828	5.5	VIII	2	6.7	7.0	5	9	14	Strike-slip Reverse	CD
2	Jura	JUR	21 june 1971	4.9	VI-VII	2	6.7	7.0	3	8	11	Strike-slip Reverse	CD
3	Bassin molassique	MOL	19 february 1822	5.2	VII-VIII	2	6.7	7.0	3	8	15	Strike-slip Reverse	CD
4	Cévennes Languedoc	CEV	24 september 1924	4.5	VI-VII	2	6.7	7.0	5	9	20	Normal	E
5	Diois	DIO	13 may 1901 10 april 1905	4.9	VII	3	6.7	7.2	3	7	14	Strike-slip Reverse	CD
6	Bordure Est Massif Central	EMC	24 june 1878	5.0	VI-VIII	2	6.7	7.0	4	10	17	Strike-slip Normal	ED
7	Bresse et Dauphiné	BRE	12 january 1754 18 february 1889	4.5	VI-VIII	2	6.7	7.0	3	8	15	Strike-slip	D
8	Chaînes subalpines	CSS	29 april 1905 et 25 april 1962	5.4	VII-VIII	3	6.7	7.2	3	8	16	Strike-slip Reverse	CD
9	Golfe du Lion	MED	6 september 1972	4.4	VI	1	5.7	6.4	5	10	15	Normal	E
10	Provence orientale	PRO	25 february 2001	4.4	VI	2	6.7	7.0	5	8	14	Strike-slip Reverse	CD
11	Massifs cristallins externes	MEX	11 march 181, 22 july 1881 et 13 aout 1905	4.9	VII	3	6.7	7.2	3	10	18	Strike-slip Reverse	CD
12	Zone Piémontaise	PIE	12 september 1785	5.2	VII-VIII	3	6.7	7.2	3	9	15	Normal	E
13	Margeride	MAG	17 january 1924	4.6	V-VI	2	6.7	7.0	3	9	15	Strike-slip Normal	ED
14	Causses	CAU	28 june 1950	4.7	VI-VII	2	6.7	7.0	3	9	15	Strike-slip Normal	ED
15	Argentera et Ligurie	ARG	23 february 1887	6.2	IX	3	6.7	7.2	3	8	13	Strike-slip Reverse	CD
16	Zone Briançonnaise	BRZ	5 april 1959	5.2	VII-VIII	3	6.7	7.2	3	10	18	Normal	E
17	Alpes lepontines	LEP	20 november 1991	4.8		3	6.7	7.2	3	9	15	Strike-slip Normal	CD
18	Nappes externes Sud	NES	12 december 1855	5.5	VIII	3	6.7	7.2	3	10	18	Strike-slip Reverse	CD
19	Bassin Ligure	LIG	19 july 1963	5.5		2	6.7	7.0	5	10	15	Compressif	C
20	Alpes italiennes	ALI	02 april 1808	5.5	VIII	3	6.7	7.2	3	9	15	Compressif	C
21	Bassin du Pô	BPO	9 february 1979	4.5		2	6.7	7.0	5	10	15	Strike-slip Reverse	CD
22	Failles Nîmes Ventoux	FNV	18 november 1769, 21 december 1769, 24 july 1927 et 18 june 1952	4.9	VII	3	6.7	7.2	3	5	8	Strike-slip Reverse	CD
23	Système de failles Provence	SFP	11 june 1909	6.0	VIII-IX	3	6.7	7.2	3	5	8	Strike-slip Reverse	CD
24	Tricastin	TRI	23 january 1773 et 19 july 1873	5.2	VII-VIII	2	6.7	7.0	2	4	8	Strike-slip	D
25	Panneau provençal	PPR	18 october 1738, 05 february 1803, 08 december 1863, 12 november 1886, et 1 may 1932	4.2	VI	2	6.7	7.0	3	5	8	Strike-slip Reverse	CD
26	Faille de Belledonne	BEL	25 april 1963	4.9	VII	3	6.7	7.2	3	10	18	Strike-slip Reverse	CD

NUM.	NAME OF ZONE	CODE	DATE Mmax observed	Magnitude Max observed	Io	A.Z.	Mmax min	Mmax max	Hmin	Hmean	Hmax	Dominant mechanism of deformation	DEF
27	Pyrénées Orientales	PYO	02 february 1428	6.2	IX	3	6.7	7.2	3	9	15	Strike-slip Reverse	CD
28	Limagne	LIM	29 june 1477	5.2	VII-VIII	2	6.7	7.0	4	8	12	Strike-slip Normal	ED
29	Valais	VAL	25 july 1855	6.2	IX	3	6.7	7.2	5	10	15	Strike-slip Normal	ED

Table 12 : Input seismic parameters of the regional model SZM 2

4.9 Seismotectonic model 3 based on large areas of homogeneous deformation

The third seismotectonic model presented Figure 24, is included in the preliminary PSHA to consider the occurrence of more diffuse seismicity distributed in large zones of homogeneous deformation. It is based on the approach developed by the IRSN (Clément *et al.,* 2004). The authors re-interpreted and simplified the French seismotectonic model EPAS (Autran *et al.,* 1998), that was the basis model of the PSHA developed for Eurocode 8 applications in 2002 (Martin *et al*. 2002), in 10 large seismotectonic source zones of diffuse seismicity covering the metropolitan territory (Figure 24).

The source zones delineation allow to gather all the main structural features and the associated seismicity in a same zone of homogeneous deformation (Clement *et al.,* 2004). Compared to the two previous models, the size of source zones is significantly larger. It allows to decrease the uncertainty on the recurrence parameters thanks to a more exhaustive seismic sample per seismic source and to avoid splitting the seismicity in the two adjacent parts of unclear structural boundaries of the two previous models.

Five zones of this model cover the region of interest. They are listed in the Table 13. Mmax of the zones provided by Clément *et al*. (2004) are used and summarized in the Table 13. A similar depth is adopted for all sources with a range of values between 5 and 15 km, while the authors considered a depth range 5-10 km.

Zone	Identification	Mmax	Depth (km)
1	Basin of Paris	7.0 – 7.2	5 – 15 km
2	Rift	7.2 – 7.6	5 – 15 km
3	Alpes	7.2 – 7.6	5 – 15 km
4	Southern France	7.0 – 7.0	5 – 15 km
5	Liguria	7.0 – 7.0	5 – 15 km

Table 13 : Seismic parameters of the model 3 zones (after Clément et al., 2004)

Source zones model 3 (SZM3) - IRSN interpretation (Clément *et al.*, 2004) based on the identification of large homogenous deformation zones

FIGURE: 24
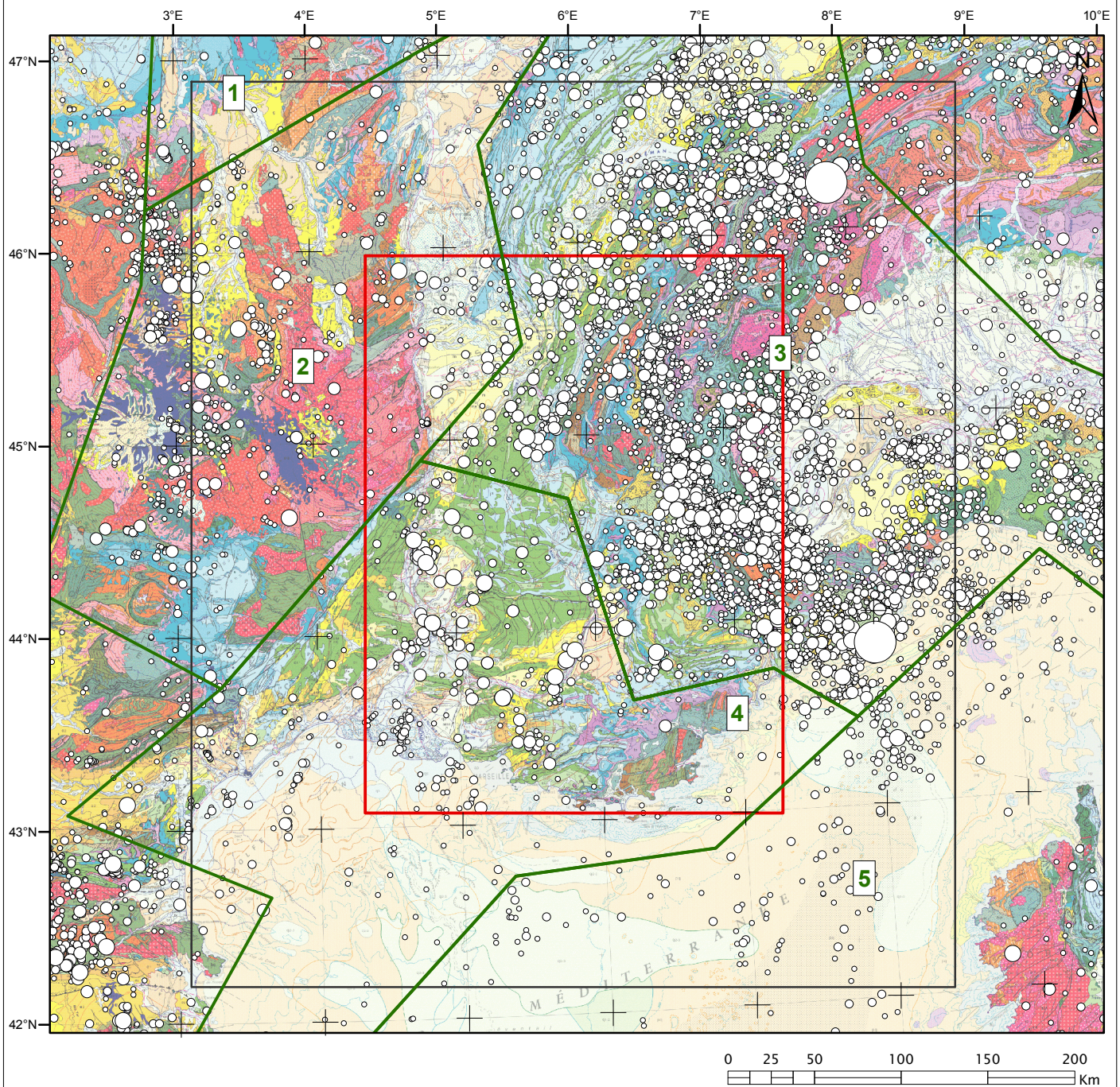
Magnitude

○	[2 - 3 [
○	[3 - 4 [
○	[4 - 5 [
○	[5 - 6 [
○	[6 - 7 [

▭	Seismotectonic zones
▭	Area of interest
▭	Regional scale

Code	Name of the seismotectonic zone
1	Basin of Paris
2	Rift zone
3	Alps
4	Southern France
5	Liguria

Carte géologique de la France à 1/1.000.000,
BRGM, 6ème édition révisée, 2003

Date: 14-10-2011	Author: Amélie LEON	File: V2_SZM3.mxd	Source: GEOTER, 2011

4.10 Comparison of the three models

4.10.1 Comparison of boundaries

The comparison of boundaries of the seismic zones of the three seismotectonic models is presented Figure 25. This superposition of the seismic zonations shows the significant differencies between the models.

The SZM3 zonation is the model that has the most differences with the other two models. Compared to the two previous models, the size of source zones is significantly larger.

The SZM1 and SZM2 zonations present also several significative differences. The SZM1 zonation is mainly constrained by the main structural limits, the distribution of the seismicity, and the kinematics of the recent and current deformations. The boundaries of certain zones correspond to major accidents that separate distinct crustal blocks. On the contrary, the zones of the SZM2 model include the most active faults and fault systems of SE France like the Belledonne fault, the Nimes fault system, the Middle Durance fault, the east-west thrusts of western Provence and the Tricastin cluster.

4.10.2 Comparison of the maximum magnitudes with surrounding countries

A comparison of the maximum magnitudes that are assigned to the seismic zones of the SZM1 model is realized, with the maximum magnitudes assigned to the seismic zones of the zonations published for surrounding countries (Italy and Switzerland).

The comparison between the Mmax of the SZM1 model with the Mmax of the Italian probabilistic ZS9 zonation published by Stucchi *et al.* (2011) for the Italian Building Code, is presented in Figure 26. The same comparison with the Swiss zonation (Giardini *et al.*, 2004) is provided in Figure 27.

Considering the SZM1 model, values of Mmax parameter were defined according to explicit criteria, mainly based on our own seismotectonic interpretation, but trying to consider other point of view. The uncertainties are explained by a range of values rather than by discrete set of more subjective values. It is obvious that other teams would have conducted different analysis to determine the maximum magnitude of the seismic sources of their models. Indeed, large discrepancies appear for the adopted values in the SIGMA region of interest between our zonation (SZM1) and the Italian ZS9 zonation (Figure 27).

For the Italian SZ9 zonation, maximum magnitude is defined by two sets of magnitudes called $M_w$max1 and $M_w$max2 for each source zone. In the first set ($M_w$max1), the maximum magnitude has been defined as the maximum between the magnitude bin to which the maximum historical earthquake belongs and the magnitude bin of the earthquake associated with an individual seismogenic source from the database of seismogenic sources (DISS, Valensise and Pantosti, 2001). The second set ($M_w$max2) is similar to $M_w$max1, except a more conservative assumption was adopted; in this case, the maximum magnitude is Mw 6.14±0.115 (Stucchi *et al.,* 2011).

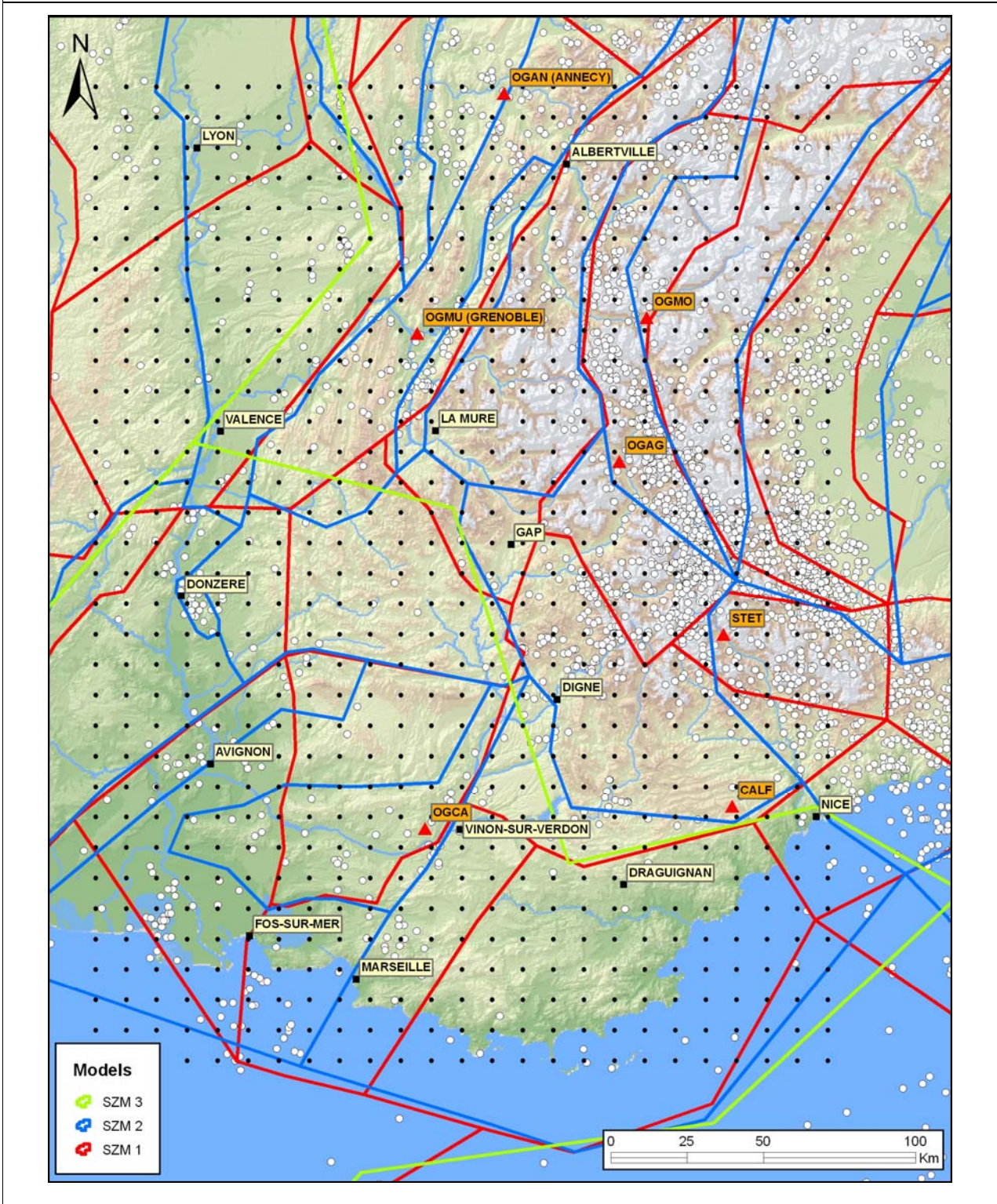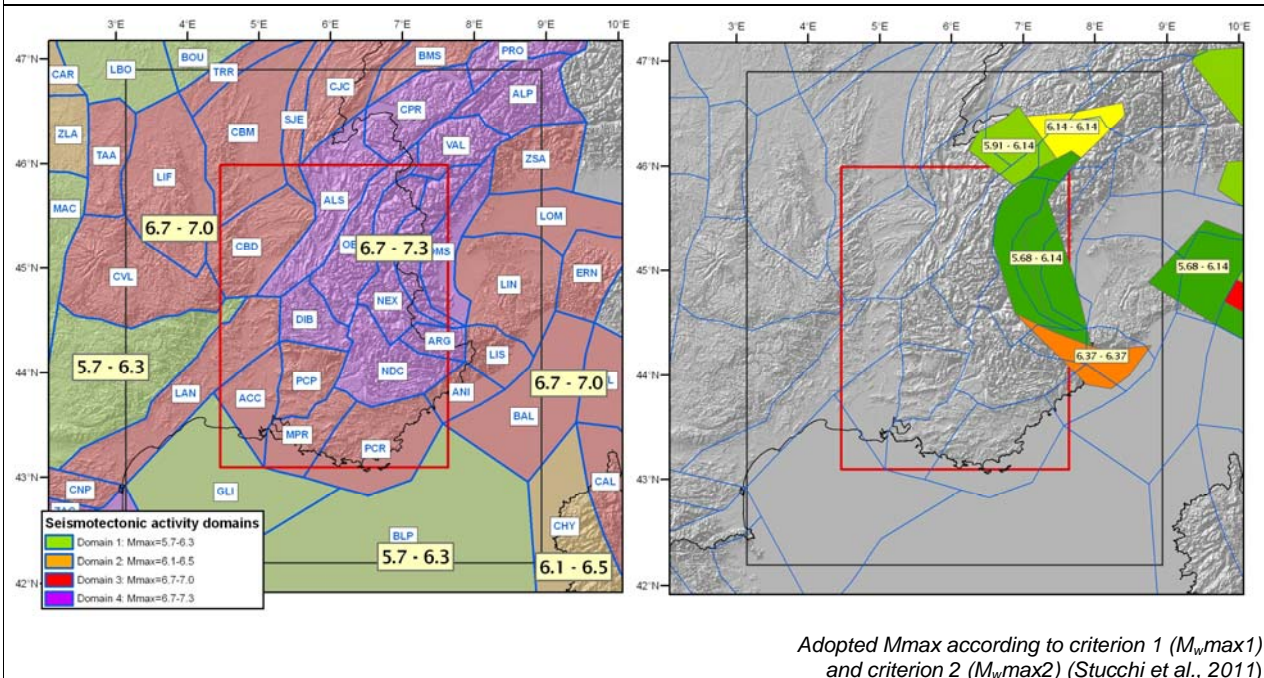Figure 25: Comparison of boundaries between the three seismotectonic models

Figure 26: Comparison of the maximum magnitudes between SZM1 zonation and the Italian ZS9 model (Stucchi et al., 2011) in the SIGMA region of interest

Adopted Mmax according to criterion 1 ($M_w$max1) and criterion 2 ($M_w$max2) (Stucchi et al., 2011)

The comparison between the Italian SZ9 zonation and the SZM1 model shows clearly that the values of the maximum magnitude sets of the SZ9 seismic zone in the SIGMA region of interest are significantly lower than the range of Mmax proposed in our model:

| Model	Lower bound of Mmax	Upper bound of Mmax
Italian SZ9 (Stucchi et al. 2011)	5.91 to 6.37	6.14 to 6.37
SZM1 (domains 3 and 4)	6.7	7.0 to 7.3

A sensitivity test is done in our study assigning a maximum magnitude of 6.3 to all seismic sources instead of the larger values that we propose (see section **Erreur ! Source du renvoi introuvable.**).

For Swizerland, and according to Giardini *et al.* (2004), the main guiding principles applied for the Mmax determination for the Swiss zonation (SEIS zonation) are the following:

- Mmax should be relatively large, because they see no evidence from worldwide studies or seismotectonic constraints that rule out M6 class events in any region of Switzerland. This kind of events may have recurrence rates exceeding 10'000 years in most zones and might not be traceable in the historical or geological record;

- The *Mmax* assessment should somewhat reflect the uncertainty that exists in this parameter;

- Mmax should not vary between zones; the choice of Mmax being in their opinion a generic one. This reflects the believe that no fundamental differences between tectonic regions exist that would justify a different behavior when it comes to Mmax.

To incorporate these principles, and to keep a simplistic model, Giardini *et al.* (2004) use only two different Mmax in their model as logic tree branches: Mmax = 7.2 and Mmax = 7.5. According to the authors, this model has the advantage of being simple, yet allowing to capture the influence of Mmax for sensitivity analysis. It should be verified in WP1 and if the documentation is available what are the Mmax values considered in the Pegasos project to verify if a marger epistemic uncertainty has been considered.

Figure 27: Comparison of the maximum magnitudes between SZM1 zonation and the SEIS Swiss model (Giardini et al., 2004) in the SIGMA region of interest
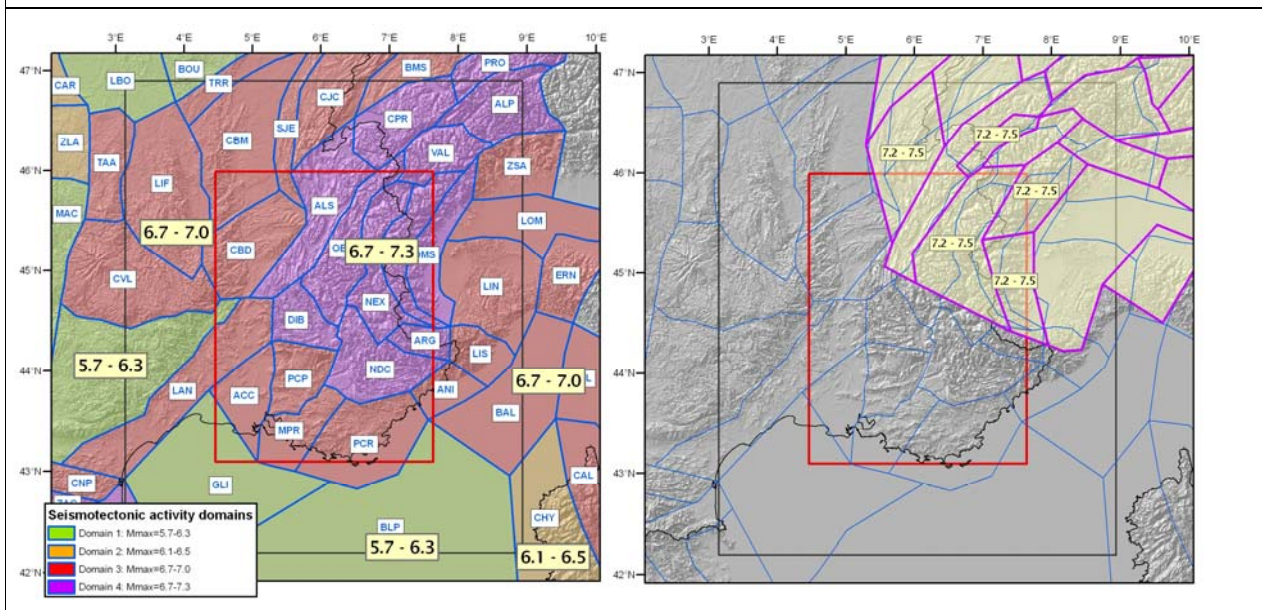
5.   Method of combination of the independent branches

The CRISIS software does not provide an environment to manage the propagation of uncertainties with the required level of completeness, but permits sequential execution of various individual models. This is the reason why we developed internal softwares in Geoter (Geosis and GeocrisisTools) to prepare the individual runs and perform a post-processing analysis to obtain aggregated results (i.e. mean, median and fractiles of the distribution).

Uncertainties (both epistemic and aleatory) are generally propagated from a coupled methodology combining logic tree (for the epistemic uncertainties) and integration procedures over the probability distributions of the aleatory parameters or Monte Carlo approaches (for the aleatory uncertainties). However Monte Carlo techniques can also be used to propagate epistemic uncertainties depending on the confidence we have in input data or interpretations of input data.

Each end branch of a logic tree combined with a Monte Carlo sampling represents in our model a calculation model. There are as many branches as the sum of logic-tree branches multiplied by the Monte Carlo sampling.

As an example if we consider a specific branch with three independent variables (seismic sources model, maximum magnitude, GMPE), each affected with a weight W1, W2, W3, the weight Pi associated to the specific branch is the product of the weights Pi=W1 W2 W3. Now considering that some parameters are explored through Monte Carlo sampling (depth, maximum magnitude, distribution laws) with N samplings, each resulting calculation is affected with a weight Pi/N. In our model the sum of Pi/N=1.

Hazard curves are computed for all sub-branches of such trees with associated weighting at all common spectral periods of the GMPEs (one sub-branch means one specific branch associated with one Monte Carlo run). For a given annual probability of occurrence the ground motion calculated for each spectral period is obtained from the hazard curves. These ground motions values are then used through a statistical process using the weights of the sub branches to build the equal hazard spectra corresponding respectively to the mean and median values and the percentiles values.

5.1 Test of results stability

When working with a calculation grid, an important challenge is to limit the computation time and optimize the number of iterations. Each of them corresponds to a calculation model where parameters result from a random combination of the logic tree branches.

It is obvious that, the greater the number of iterations, the better the exploration of the tail-ends of the distribution, even if the mean or median remains quite stable. In our model and for each independent seismic source the terminal branches of the logic tree are sampled with different values of Mmax, depth and recurrence parameters. To appreciate the impact of the number of explorations we implemented a sensitivity test with the initial logic tree (report SIGMA-2011-D4-18) to appreciate the variability of statistical values and the evolution of the coefficient of variation versus the number of iterations.

Two calculations points were chosen in two regions: station OGMU in the Alps and station OGCA, in Provence. PSHA was computed for seismotectonic model 1 and the Akkar & Bommer (2010) GMPE, and the input parameters associated to a given seismic source (i.e. GR-curve parameter, depth, maximum magnitude) are explored using 100, 200, 500, and 5000 Monte Carlo samples. The computed distributions of accelerations and the associated parameters (minimum, maximum, mean, standard deviation, and percentiles) are plotted on Figure 28 and given in Table 14, in which the percentage of variation compared to the reference (5000 samples) are given in brackets.

From this test, it appears that extreme values of the distribution (Min and Max in Table 20) vary, while the variation of percentiles remain bellow 5%. This test also shows that the stability for the first percentiles (i.e. 14-86%) is higher than larger percentiles. As a conclusion, 100 samples seem to be enough to capture the median and 1 standard deviation characteristics of the distribution, however, if larger values are requested a larger number of samples may be required.

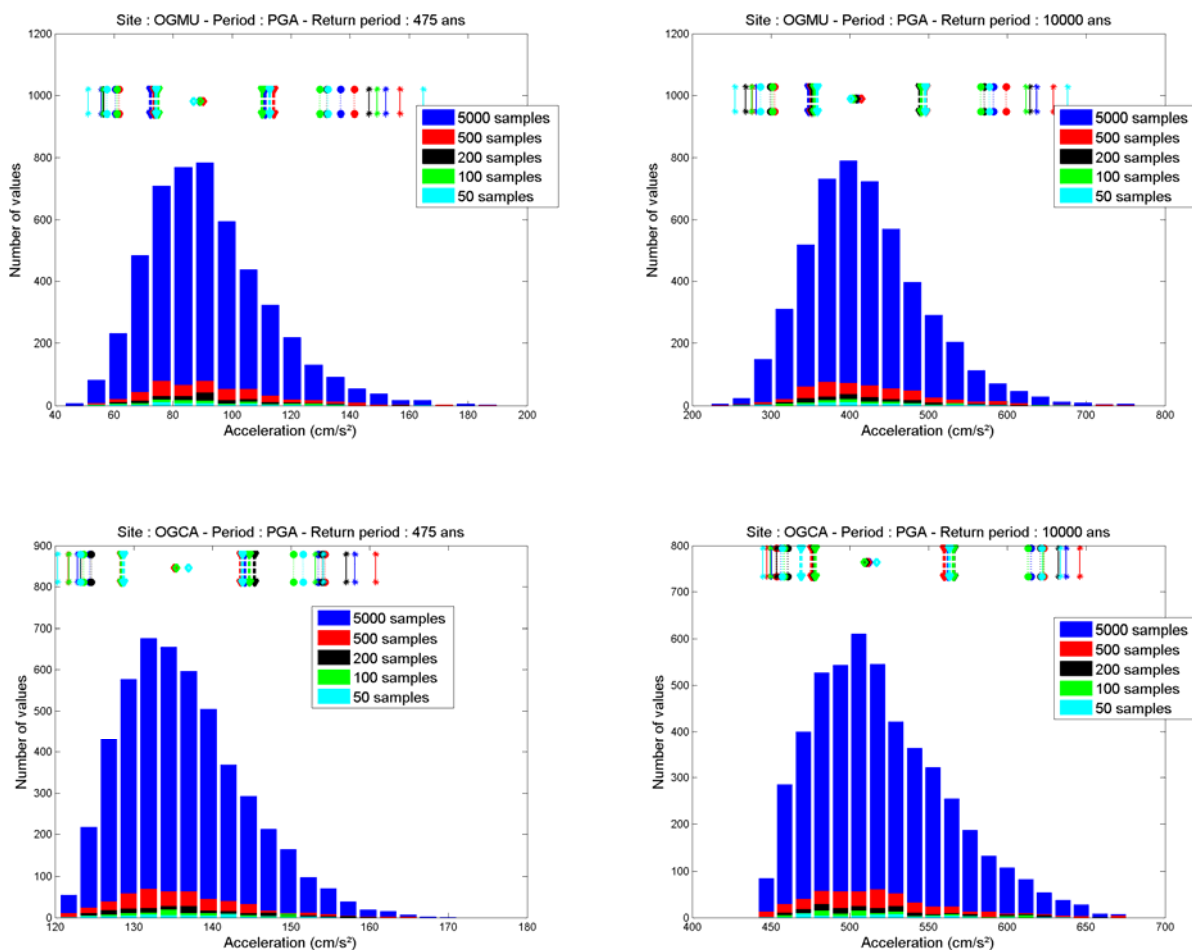The obtained distributions follow a log-normal distribution (Figure 28).

Figure 28 : Distributions of the accelerations for PGA at sites OGMU (top) and OGCA (bottom) and for two return periods (left : 475 years ; right : 10000 years) as a function of the number of samples used in the uncertainty propagation. The diamonds indicate the median value, and triangles, circles and stars are the percentiles 14-86%, 3-97% and 1-99%, respectively

Number of samples	Max (cm/s²)	Min (cm/s²)	Mean (cm/s²)	Std (cm/s²)	Coef. var	Per 1% (cm/s²)	Per 3% (cm/s²)	Per 16% (cm/s²)	Per 50% (cm/s²)	Per 84% (cm/s²)	Per 97% (cm/s²)	Per 99% (cm/s²)
OGMU – PGA – 475 years													
5000	190.27	42.96	91.79	20.42	4.50	55.70	60.52	72.38	89.15	111.25	136.81	152.08
500	185.75 (-2%)	51.15 (19%)	93.47 (2%)	21.46 (5%)	4.36	56.56 (2%)	61.70 (2%)	73.56 (2%)	90.29 (1%)	114.19 (3%)	141.52 (3%)	157.01 (3%)
200	163.15 (-14%)	53.27 (24%)	91.55 (0%)	19.27 (-6%)	4.75	56.53 (1%)	61.13 (1%)	74.06 (2%)	89.16 (0%)	110.19 (-1%)	132.13 (-3%)	146.46 (-4%)
100	160.97 (-15%)	53.00 (23%)	91.28 (-1%)	19.57 (-4%)	4.67	56.23 (1%)	61.00 (1%)	75.00 (4%)	89.19 (0%)	110.14 (-1%)	129.88 (-5%)	149.18 (-2%)
50	164.90 (-13%)	51.24 (19%)	91.33 (-1%)	22.17 (9%)	4.12	51.24 (-8%)	57.60 (-5%)	74.32 (3%)	87.06 (-2%)	112.72 (1%)	132.54 (-3%)	164.90 (8%)
OGMU – PGA – 10000 years													
5000	763.70	221.99	419.24	74.89	5.60	281.54	299.53	348.16	410.69	490.90	582.75	637.57
500	766.28 (0%)	247.81 (12%)	425.28 (1%)	79.51 (6%)	5.35	276.55 (-2%)	304.46 (2%)	351.35 (1%)	414.86 (1%)	496.58 (1%)	598.53 (3%)	658.50 (3%)
200	664.52 (-13%)	256.15 (15%)	417.78 (0%)	72.43 (-3%)	5.77	268.23 (-5%)	299.71 (0%)	352.52 (1%)	408.62 (-1%)	488.96 (0%)	570.95 (-2%)	628.72 (-1%)
100	647.94 (-15%)	260.23 (17%)	418.92 (0%)	71.56 (-4%)	5.85	275.41 (-2%)	302.41 (1%)	354.75 (2%)	404.54 (-1%)	490.79 (0%)	566.51 (-3%)	624.03 (-2%)
50	676.71 (-11%)	254.77 (15%)	421.07 (0%)	80.80 (8%)	5.21	254.77 (-10%)	286.73 (-4%)	358.82 (3%)	401.55 (-2%)	496.05 (1%)	577.20 (-1%)	676.71 (6%)
OGCA – PGA – 475 years													
5000	171.22	120.48	136.34	7.85	17.36	122.87	124.38	128.67	135.27	144.14	153.51	158.15
500	164.75 (-4%)	119.37 (-1%)	136.22 (0%)	8.08 (3%)	16.85	121.68 (-1%)	123.53 (-1%)	128.40 (0%)	135.22 (0%)	143.63 (0%)	154.29 (1%)	160.77 (2%)
200	159.30 (-7%)	119.73 (-1%)	136.45 (0%)	7.90 (1%)	17.27	123.28 (0%)	124.60 (0%)	128.72 (0%)	135.43 (0%)	145.39 (1%)	154.02 (0%)	157.01 (-1%)
100	153.08 (-11%)	120.32 (0%)	136.4 (0%)	7.46 (-5%)	18.28	121.75 (-1%)	123.63 (-1%)	128.47 (0%)	135.44 (0%)	144.72 (0%)	150.34 (-2%)	153.07 (-3%)
50	154.11 (-10%)	120.34 (0%)	136.78 (0%)	7.95 (1%)	17.22	120.34 (-2%)	123.24 (-1%)	128.72 (0%)	136.95 (1%)	143.84 (0%)	151.52 (-1%)	154.11 (-3%)
OGCA – PGA – 10000 years													
5000	676.29	441.06	519.44	42.77	12.14	450.38	456.47	477.01	512.39	562.62	615.06	637.47
500	678.97 (0%)	439.14 (0%)	517.72 (0%)	44.38 (4%)	11.67	447.52 (-1%)	453.57 (-1%)	475.88 (0%)	511.63 (0%)	560.02 (0%)	623.18 (1%)	645.88 (1%)
200	655.90 (-3%)	441.15 (0%)	518.83 (0%)	44.37 (4%)	11.69	453.55 (1%)	460.68 (1%)	477.37 (0%)	510.26 (0%)	566.06 (1%)	621.37 (1%)	632.37 (-1%)
100	628.97 (-7%)	443.98 (1%)	518.93 (0%)	42.48 (-1%)	12.22	449.93 (0%)	458.44 (0%)	478.27 (0%)	509.35 (-1%)	565.82 (1%)	613.05 (0%)	622.68 (-2%)
50	633.72 (-6%)	444.85 (1%)	518.75 (0%)	43.48 (2%)	11.93	444.85 (-1%)	457.24 (0%)	468.99 (-2%)	517.23 (1%)	563.26 (0%)	621.96 (1%)	633.72 (-1%)

Table 14: Parameters of the acceleration distributions obtained after propagation of uncertainties as a function of the number of samples explored, for PGA at 475 and 10000 years return period and for sites OGMU and OGCA.

5.2 Combination of the independent branches

Recommendation: *It is recommended to be careful in selecting an appropriate method of combination of the independent branches of the epistemic Logic-Tree for the purpose of re-calculating the total hazard when one or several branches have been changed. Particular attention must be given to the derivation of the full probability distribution of the hazard, including the percentiles of the distribution. The committee recommends that a description/ clarification of the planned method of combination be provided to the committee prior to the final derivation of results.*

The logic tree approach allows the use of alternative models. Each is assigned a weighting factor that is interpreted as the relative confidence of that specific model being correct. The logic tree consists of a series of nodes, representing points at which models are specified, and branches that represent the different models specified at each node. The sum of the probabilities of all branches connected to a given node is 1.

The construction of the logic tree is done as follow :

- The basic core of the logic tree is a specific source zone model (using area sources or grid sources in the case of the zoneless approach). A weight W_{mi} is assigned to each model ;

- Two catalogues are considered (a priori and synthetic) to calculate the recurrence parameters; An equivalent weight W_{cj} is assigned to each catalogue ;

- Each of the four GMPEs is assigned a weight W_{lk} ;

- For a specific model and each source of a specific model a number N of models is then built, each of them being assigned with a given depth, maximum magnitude and recurrence parameters, that respectively follow a triangular, uniform and Gaussian probability distribution. A weight 1/N is assigned to each model.

The weight assigned to a given branch of the logic tree as a weight :

$$W_{ijkn} = W_{mi} \times W_{cj} \times W_{lk} \times 1/N$$

The complete tree is composed by Y branches and the seismic hazard curves are calculated by statistical treatment of individual results (annual probabilities of exceedance at 40 points of the hazard curves) :

- A weighted mean is calculated considering the Y individual values and associated W_x values. The branches with a high weights contribute more to the weighted mean than branches with low weight. The weights are all positive and some of them can be zero if chosen by the operator (not the case here).

  The weighted mean is the quantity : $\overline{x} = \dfrac{\sum_{i=1}^{Y} w_i x_i}{\sum_{i=1}^{Y} w_i}$

- The percentiles are calculated considering the weights of the branches, using a weights classification. The x_i and w_i values are ordered with increasing values of w_i and summation of w_i values is implemented. The median value of the distribution is the first value x_i, where the summation is equal or exceeds 0.5.

- The process is equivalent for the definition of weighted percentiles, the target value of the summation being different.

Once the statistical hazard curves are calculated for a specific point of interest, the response spectra are defined from the hazard curves. The acceleration value associated to a specific return period T is calculated by logarithmic interpolation on the seismic hazard curve.

6.   **PSHA results**

All the PSHA results are computed for a minimum magnitude M_w=4.5 and with an integration up to 3 standard deviation of the GMPEs. The results presented graphically in this report are provided with the intention to compare the different branches of the logic-tree and assess the influence of the different hypothesis used in this study. Some global results are also shown. All the results will however be provided digitally which allows the computation of any specific result (maps, hazard curves or uniform response spectra).

The results corresponding to the total logic-tree take into account the zone models. The weights for each of the branches have been defined in section 2.4. The zoneless models are only used for comparison purpose and are not included in the total logic-tree.

6.1 **Organization of the results**

The numerical results are provided in two main directories. One of these contain the results computed for a grid of 858 points covering the region of interest. The first points (bottom left of the grid) has the following coordinates: latitude 43.05°N, longitude 4.3°E. The latitude and longitude steps are 0.09° and 0.12°, respectively. In this case the results are provided for 3 spectral periods: PGA, 0.2 and 1.0 sec. The second directory contains the results for the 20 points of special interest defined in section 1.3. For this set of results, 15 spectral periods are considered: PGA, 0.03, 0.05, 0.1, 0.15, 0.2, 0.25, 0.3, 0.4, 0.5, 0.75, 1.0, 1.5, 2.0, 3.0 sec.

In each of the main directories, the structure of the directories follows the structure of the logic tree. Firstly, 6 directories contain the results for each of the zones/zoneless models: M1 to M3 for the 3 zone models, and Zl1 to Zl3 for the 3 zoneless models. Under each of these directory, to more directories contain results for the original seismicity catalog and the synthetic one (C1 and C2). Then four directories contain the results obtained using different GMPEs: L1 for Akkar & Bommer (2010), L2 for Berge-Thierry et al. (2003), L3 for Boore & Atkinson (2008), and L4 for Zhao et al. (2006). Note that in the case of the zoneless approach, only the Berge-Thierry et al. (2003) is used and consequently, only directory L2 exists.

The contents of the end directories differ slightly for the zones models and the zoneless models. For the zones models, 2 files are included: one parameter file for Crisis2007 which correspond to mean parameters computation and the hazard curve file which is the ouput of Crisis2007. A directory is also included (MC) which contains the results of the uncertainty propagation on the seismicity parmaters, Mmax and depth. This directory includes 4 .tir files which contain the different values of the seismicity parameters (λ and β), Mmax and depth used in each source zones (these files are used to build the 100 Crisis2007 input files for uncertainty propagation), two .rar archives with the Crisis2007 input and output files (.gra files). 8 more files are included which correspond to the statistics (mean or average, median and percentiles 16% and 84%) for the specific end branch. From these 8 files, 4 are .gra files with the same format as the Crisis2007 output files (hazard curves) and 4 .iap files with the acceleration levels for a given return period at the different spectral periods (uniform hazard spectra).

Consequently, any hazard curve or response spectra can be plotted for each of the 858 points of the grid or for the 20 points of interest.

The detailed format and structure of the numerical results are described in Annex 1.

6.2 Hazard maps

All hazard maps are presented with the same scale of of acceleration values. This allows to compare the maps for the different return periods and spectral periods. An interval of 50 cm / s ² is considered between each class. Choosing other values could lead to different contours. To appreciate the specific values at specific calculation points, it is necessary that the user operates the output files from the DVD.

The interpolation method used to draw the maps is a kriging method which is an advanced geostatistical procedure of the Arcgis GIS, that generates an estimated surface from a scattered set of points with z-values. Other interpolation technique could lead to slight differences in the produced maps. The user can use its own technic applied to the numeric files of the DVD.

There are about 1500 maps to be produced, taking into account the number of branches of the logic tree, the number of return period, the number of spectral periods, the number of statistical quantities, and about 250,000 curves hazard.

It was decided during the meeting of December 14, 2011, to represent these maps for some representative parameters and to define at a later stage, what would be the exploitation and analysis of the results, all of them being stored in digital format and available for the SIGMA members.

6.2.1 Mean hazard maps

The mean hazard maps for the total logic-tree are presented in Figure 29 for two spectral periods (PGA and 0.2 sec), and for two return periods (475 and 10000 years). As expected the acceleration ration between 0.2 sec and PGA is close to 2.5. Within the area of interest, the PGA doesn't exceed 100 cm/s² at 475 years of return periods and varies from 100 to 450 cm/s² at 10000 years of return period. The PSA at 0.2 sec varies from from 50 to 250 cm/s² and from 251 to 900 cm/s² at return periods of 475 and 10000 years, respectively. The maps also show that the highest hazard is obtained in the Provence area and near to the border between France and Italy to the East.

If we compare with previous PSHA maps developed for the French territory at 475 years of return period, the PGA values are significantly lower than the values obtained in the MEDD 2002 study, and lower than the values obtained by the AFPS working group in 2006. The hazard pattern is also different which is due to the evolution of the seismotectonic models used this study.
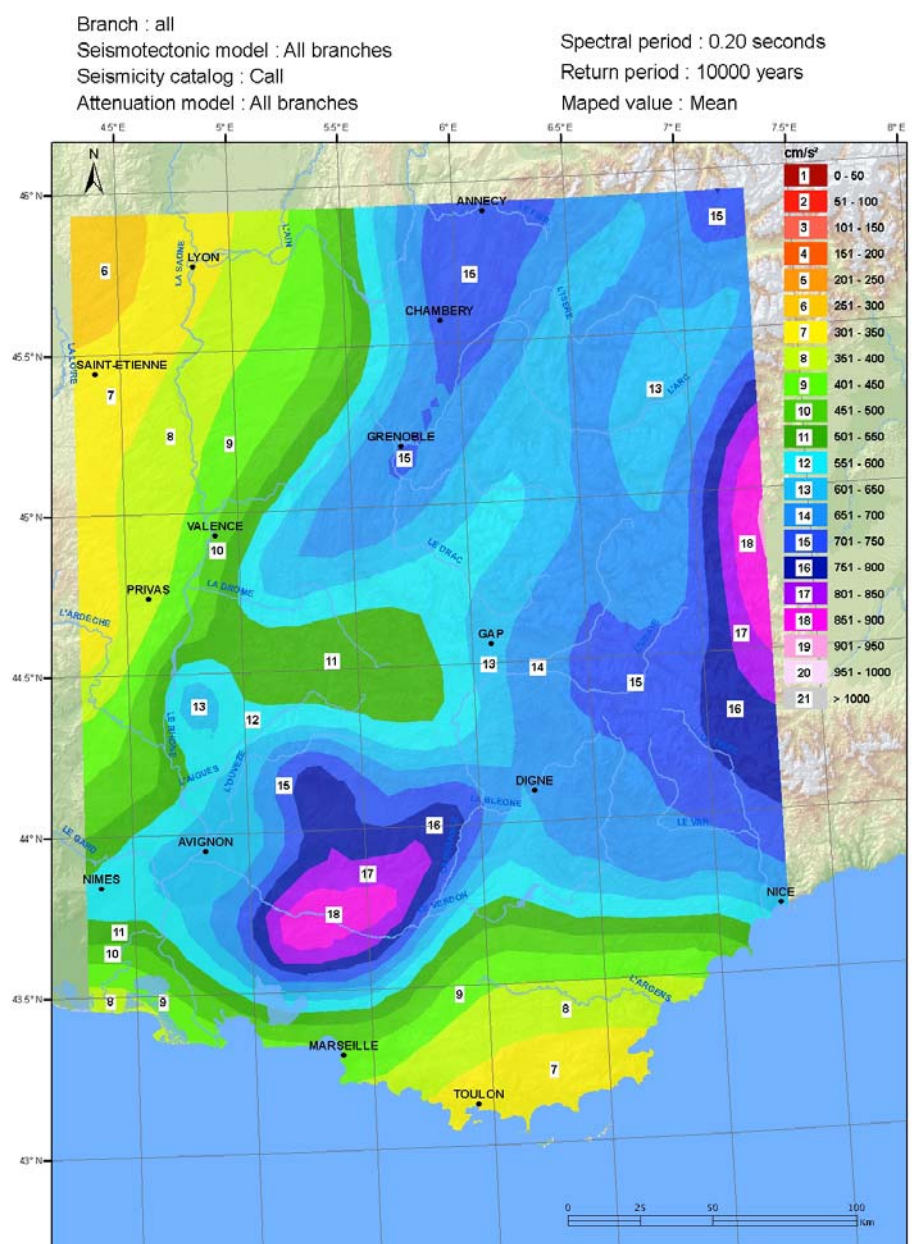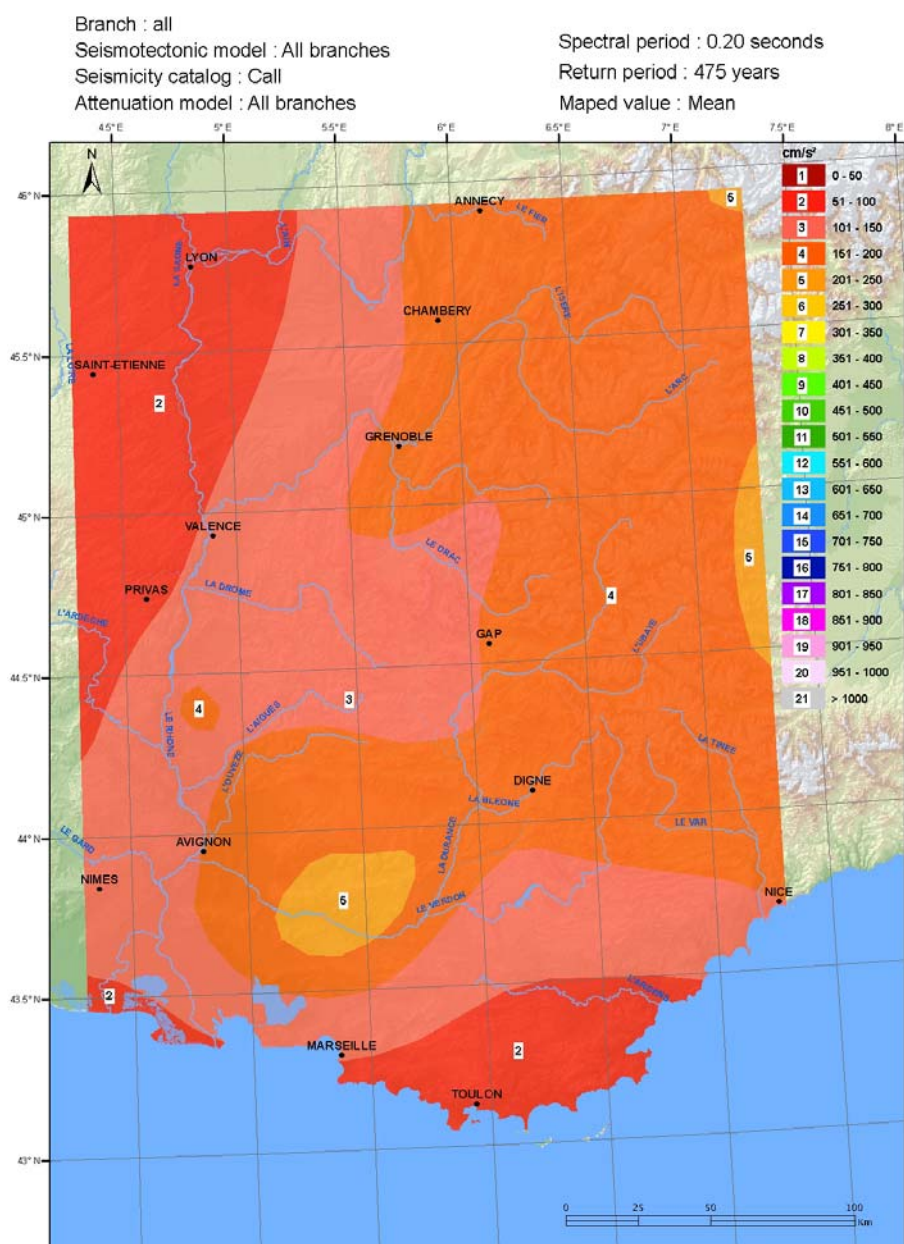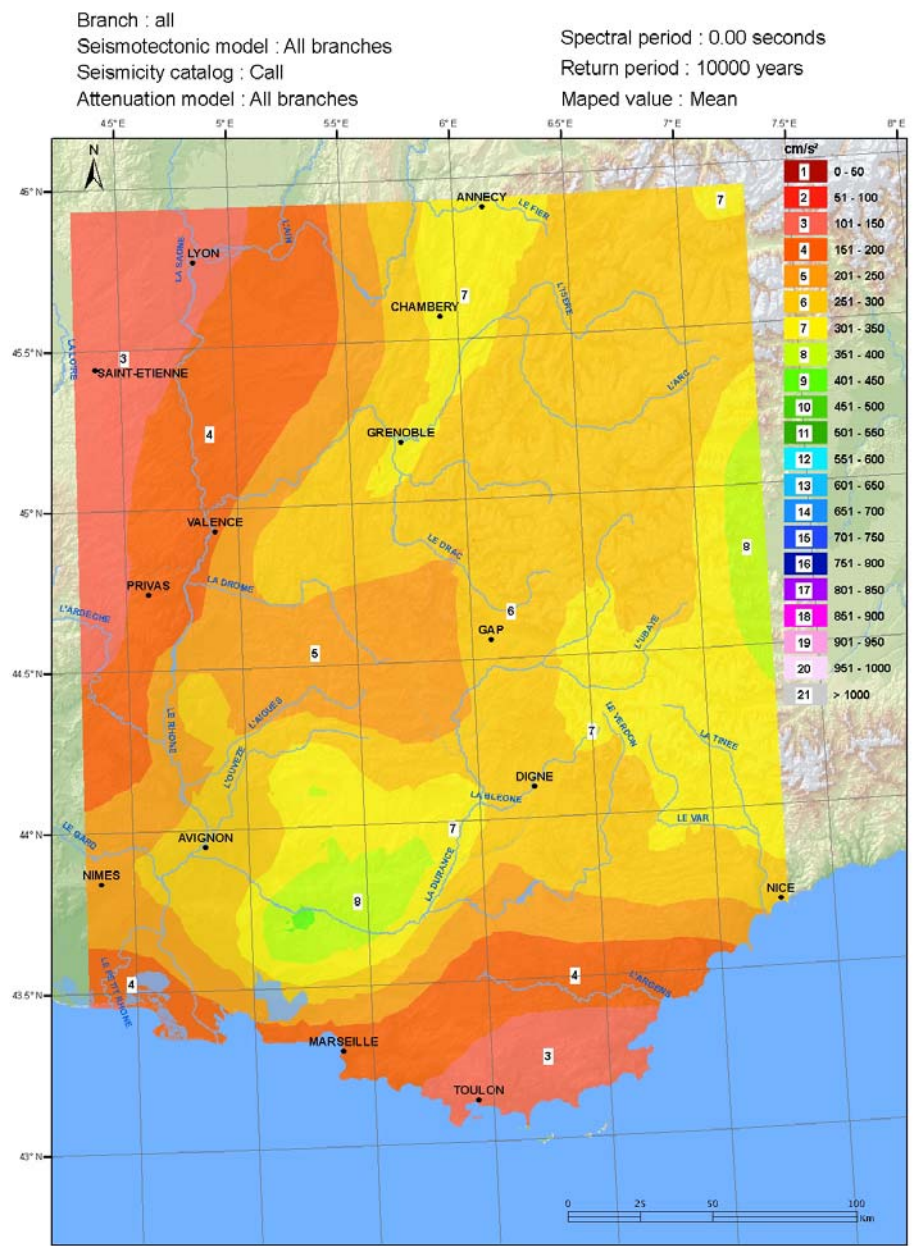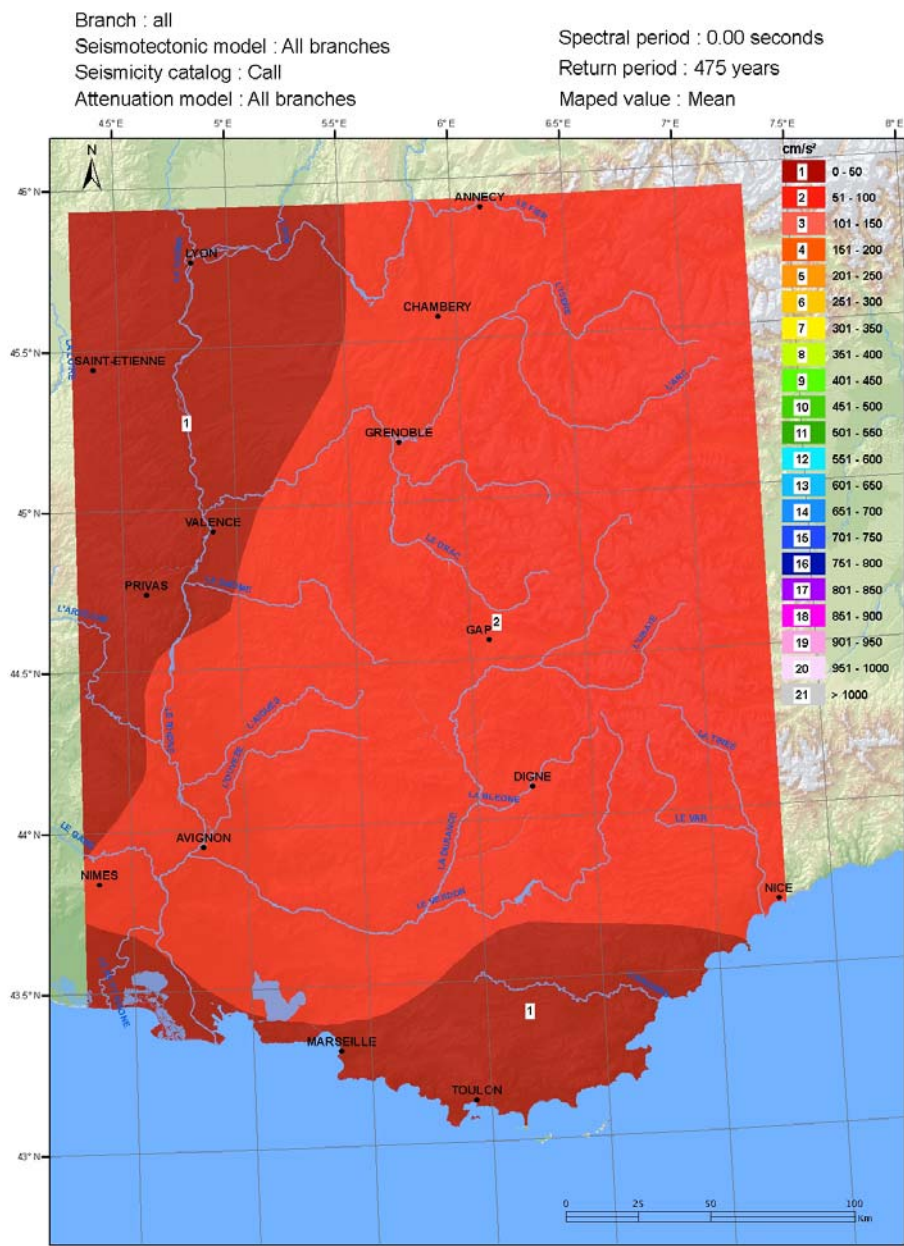
Figure 29 - Mean hazard maps for PGA (top) and 0.2 s (bottom) and for two return periods (left: 475 years ; right: 10000years)

6.2.2 Variability of hazard maps

The variability is assessed by calculating the percentage change between the 15% fractile and the median (negative values), and 85% fractile and the median (positive values).

The variability of the predicted acceleration is presented in Figure 30 and Figure 31. These maps show the percentage of variation from the median to the percentiles 16% and 84% (negative and positive values, respectively). Figure 30 presents the variations for PGA at return periods of 475 and 10000 years, while Figure 31 shows the same results for the spectral period 0.2 s.

Depending on the region, the variations of both PGA and PSA at 0.2 sec varies from about 10-15% to around 40-50% for the negative values and from 15-25% to 70-75% for the positive values. The regional variations are much quicker than for the mean values. The largest variations appear to occur in the Provence region and close the the French-Italian border, and there is an area almost in the middle of the region of interest where the variability appears to be relatively low around 15%. The pattern of variation is nearly the same whatever the percentile, the return period, or the spectral period considered.
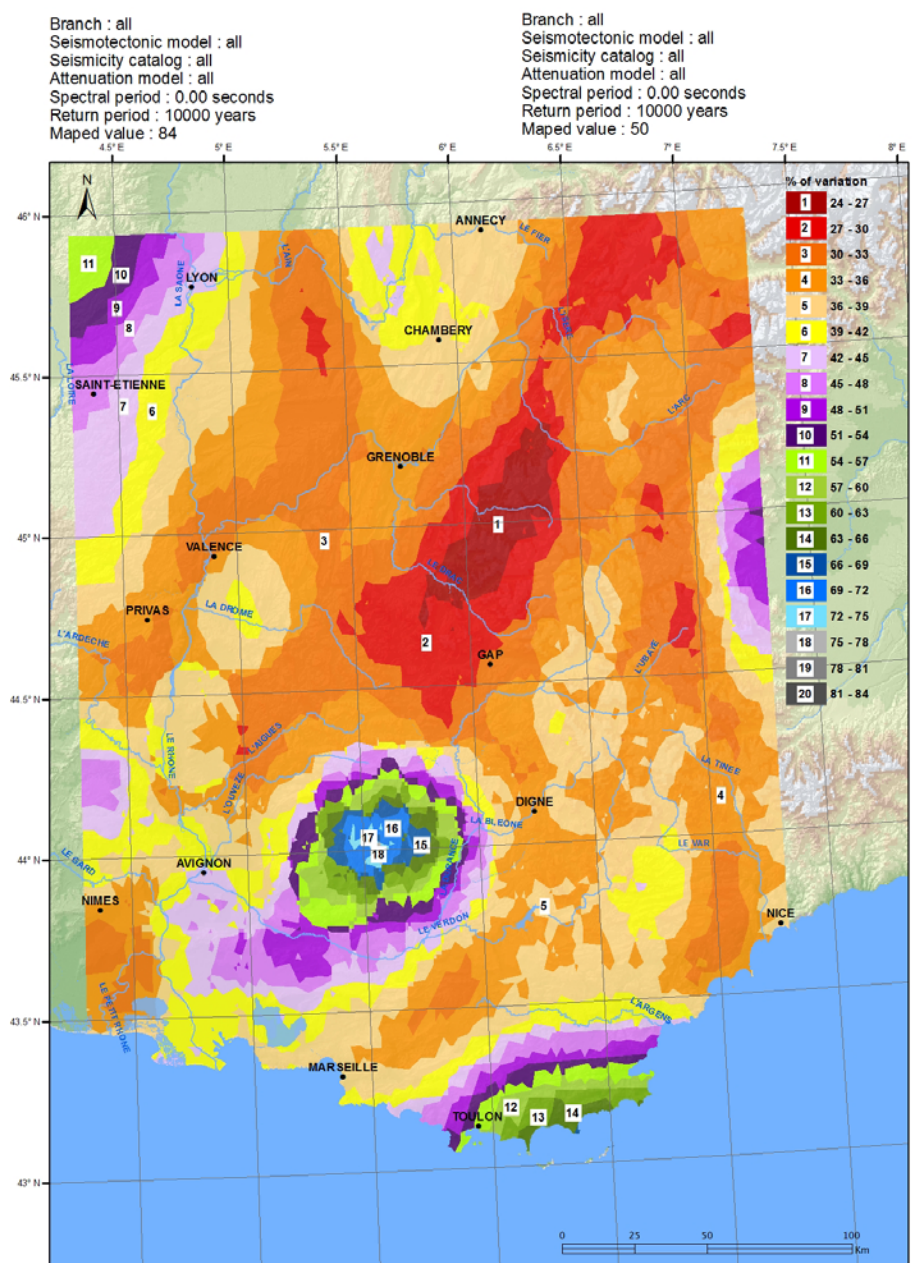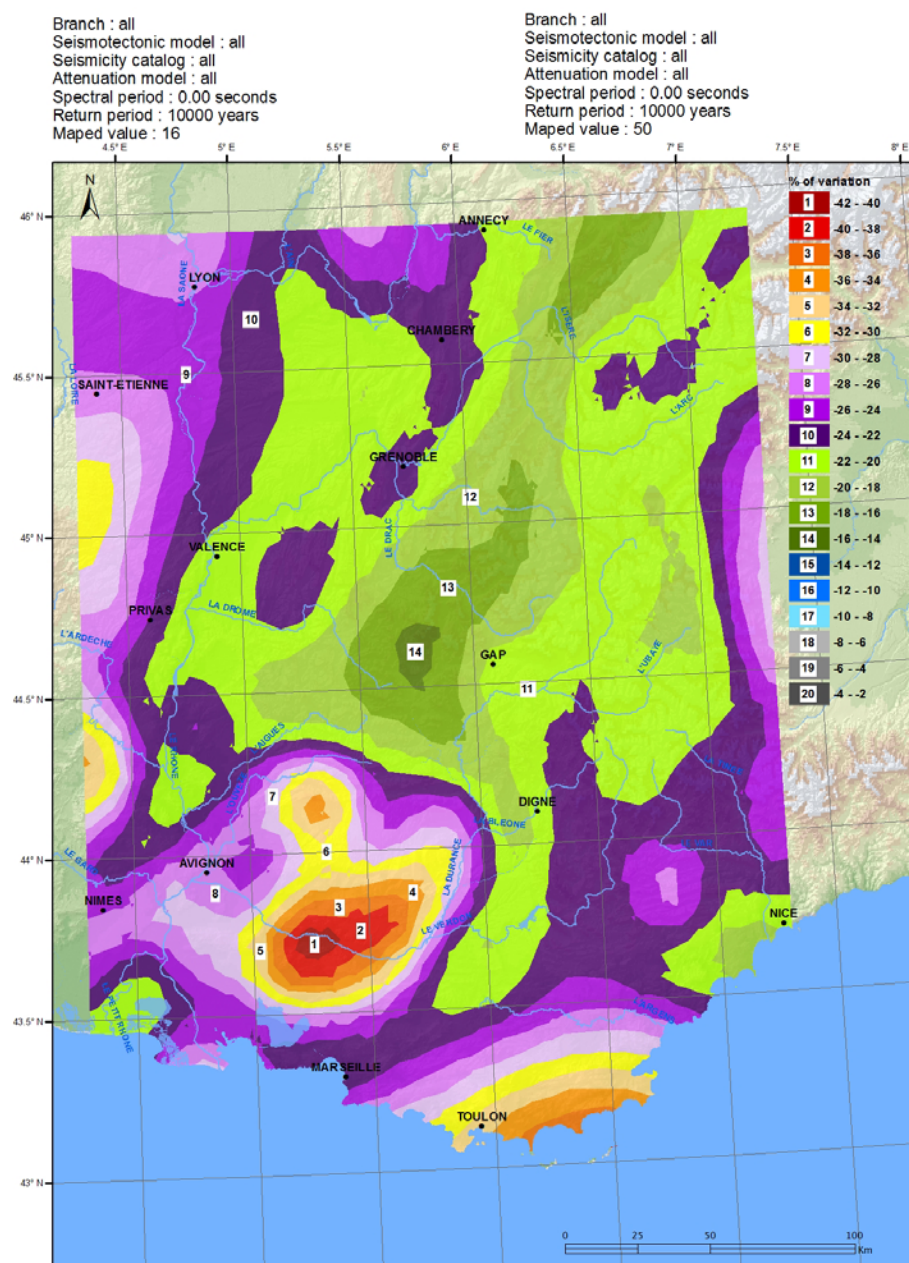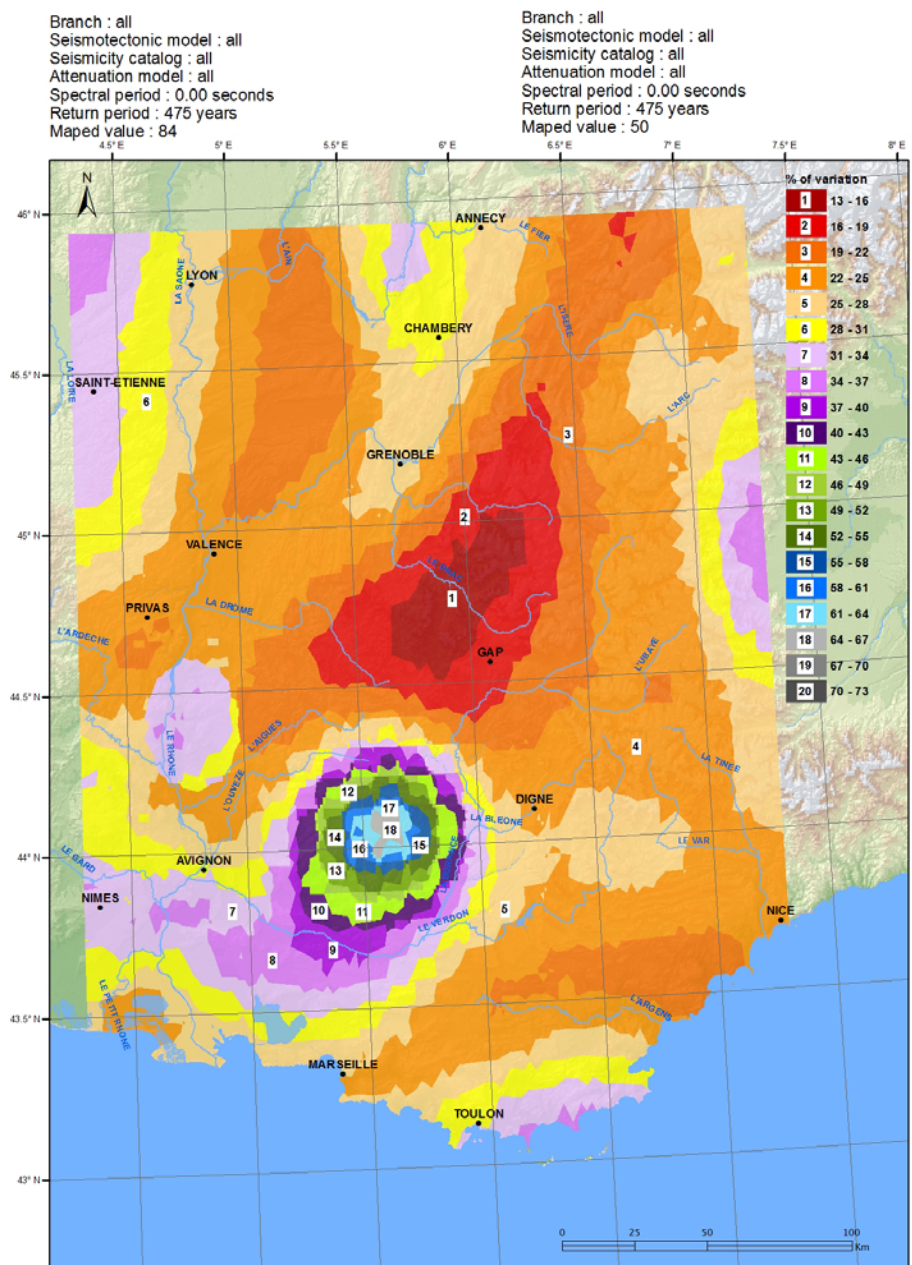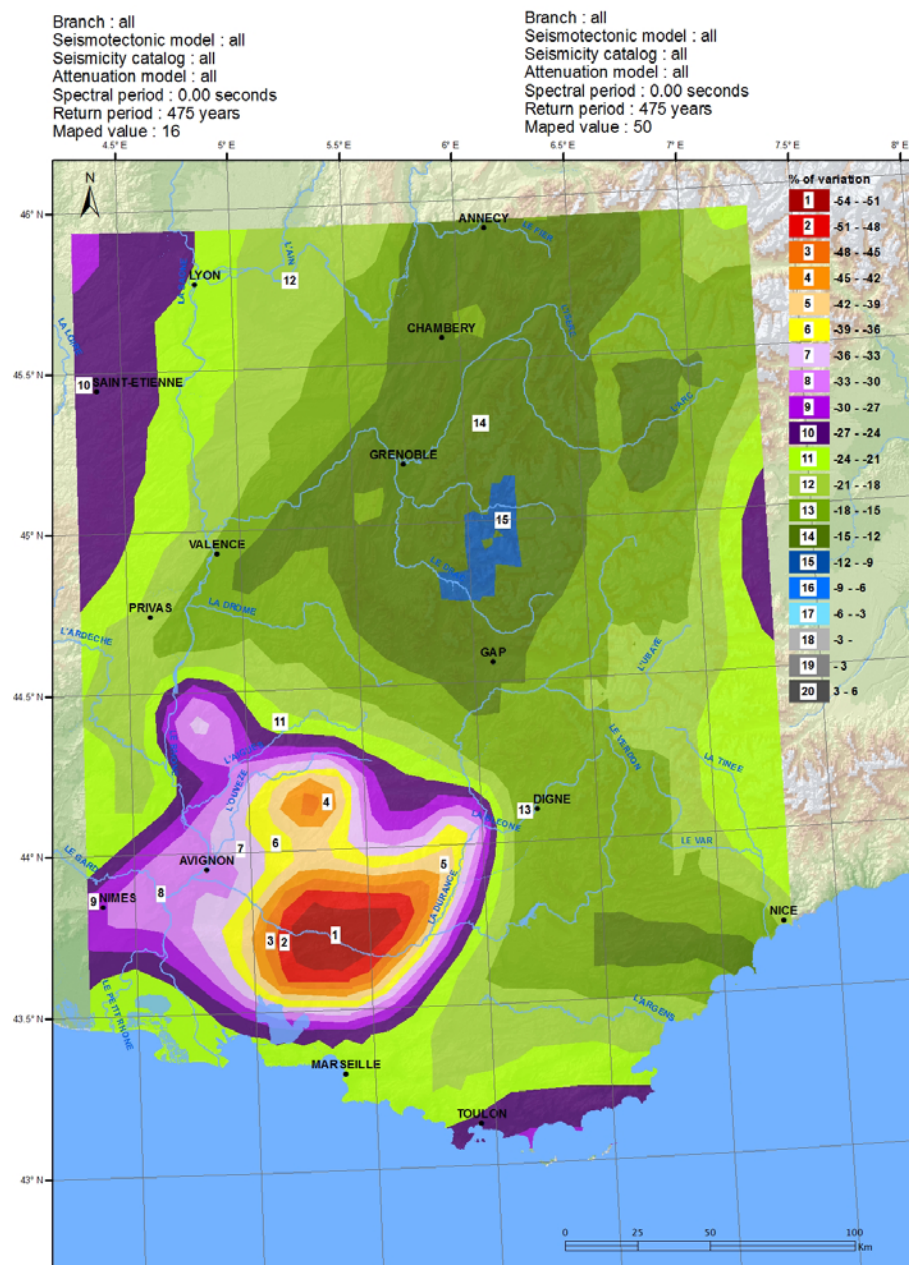
Figure 30 - *Percentage of variation between percentile 16 and median (top) and between percentile 84 and median, for PGA and two return periods (left: 475 years; right: 10000 years)*
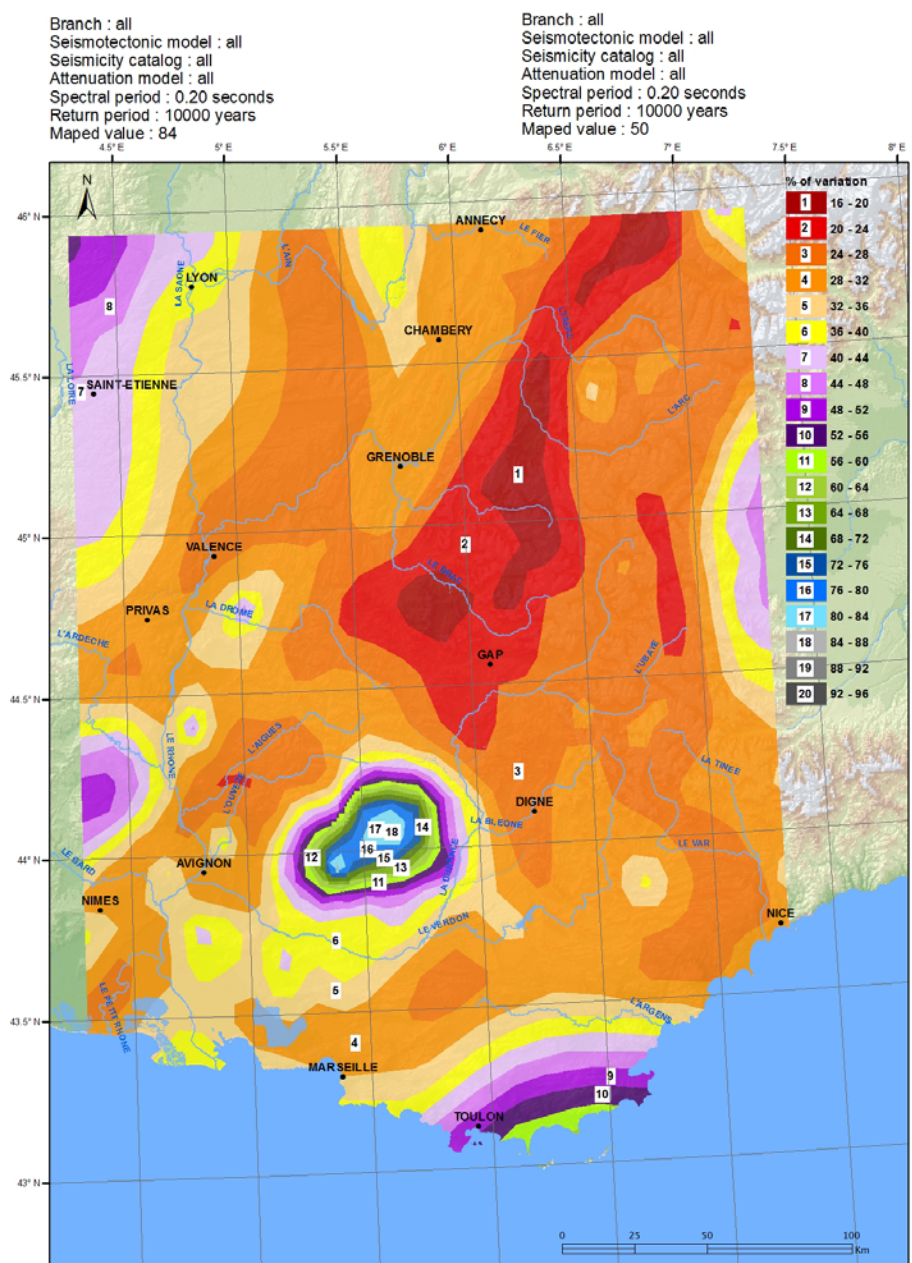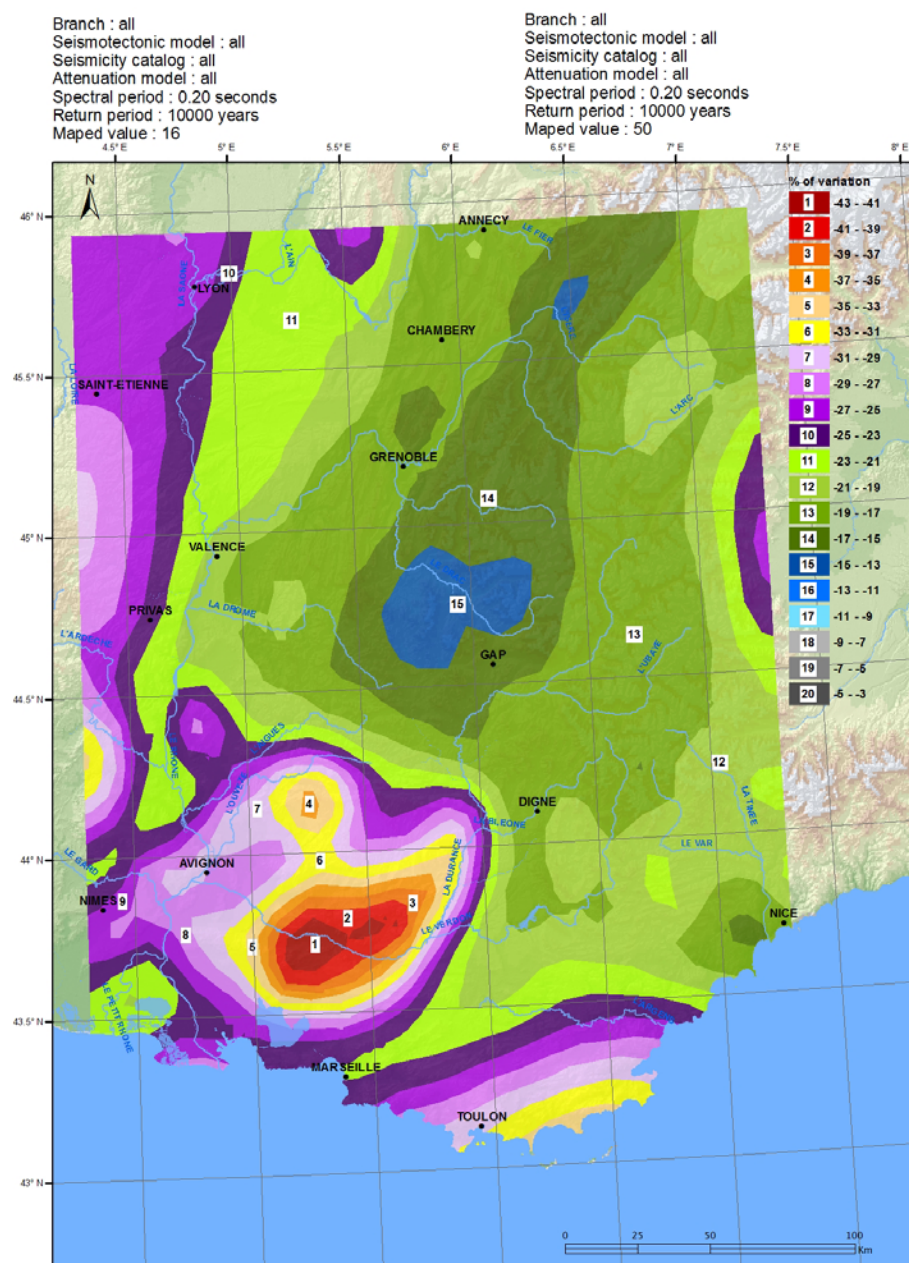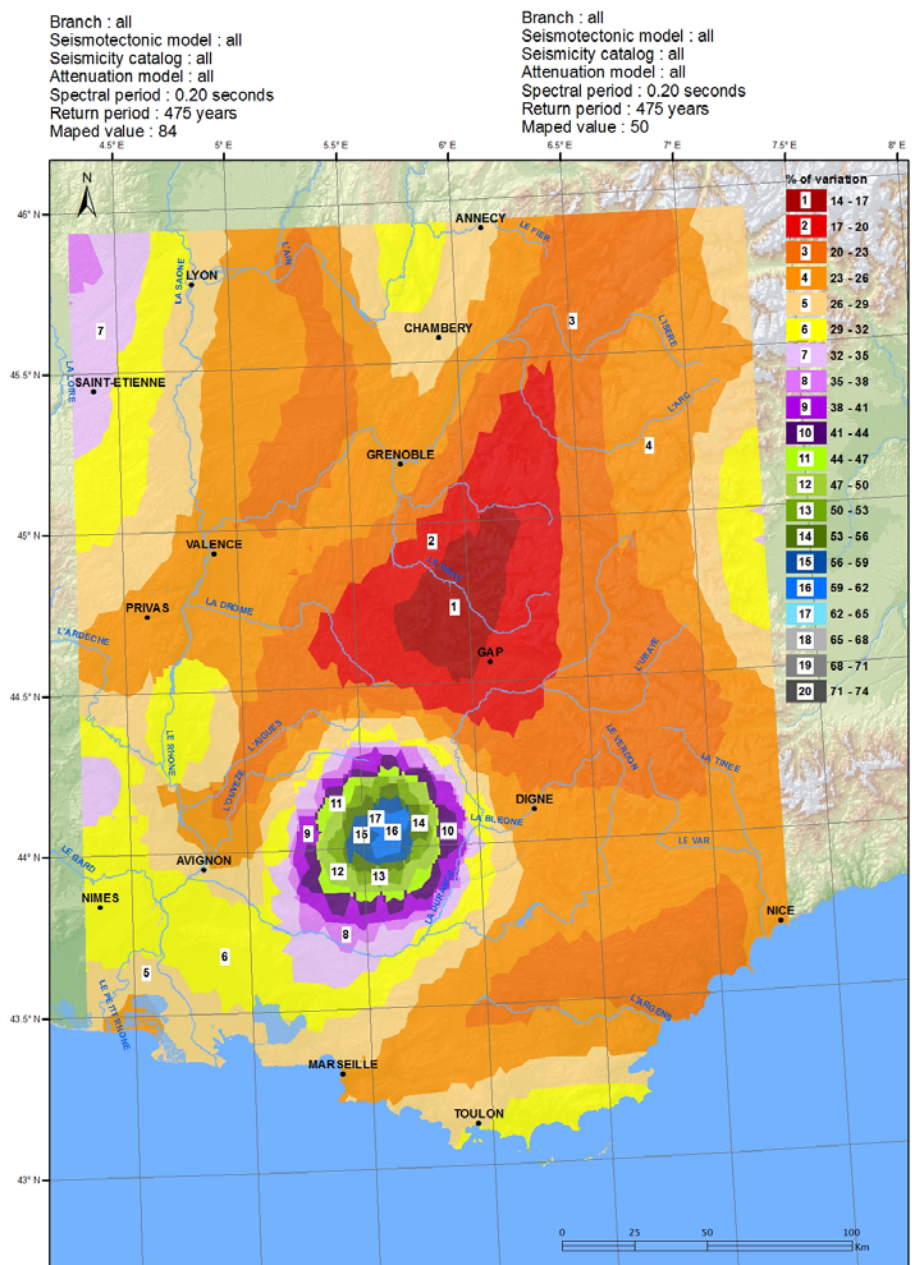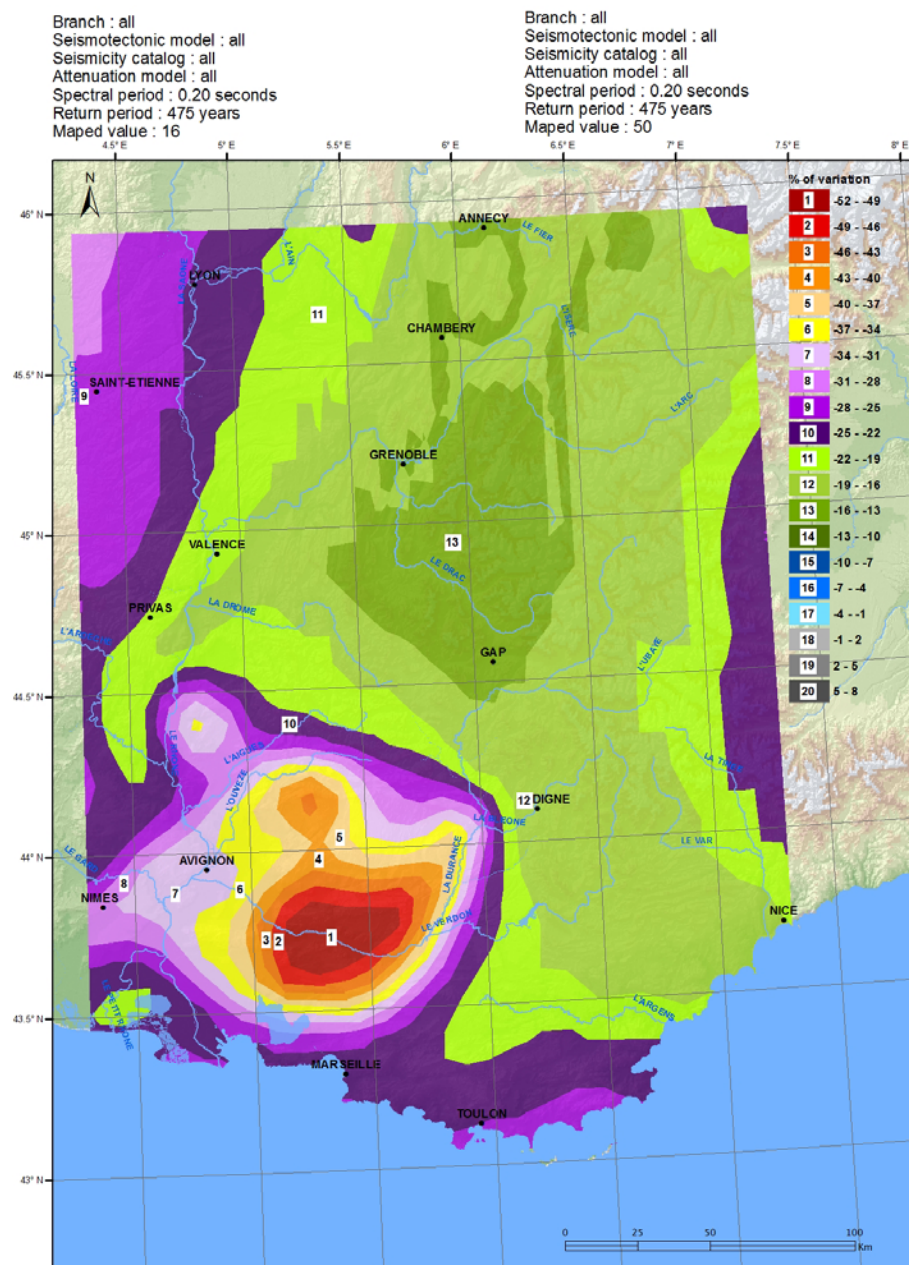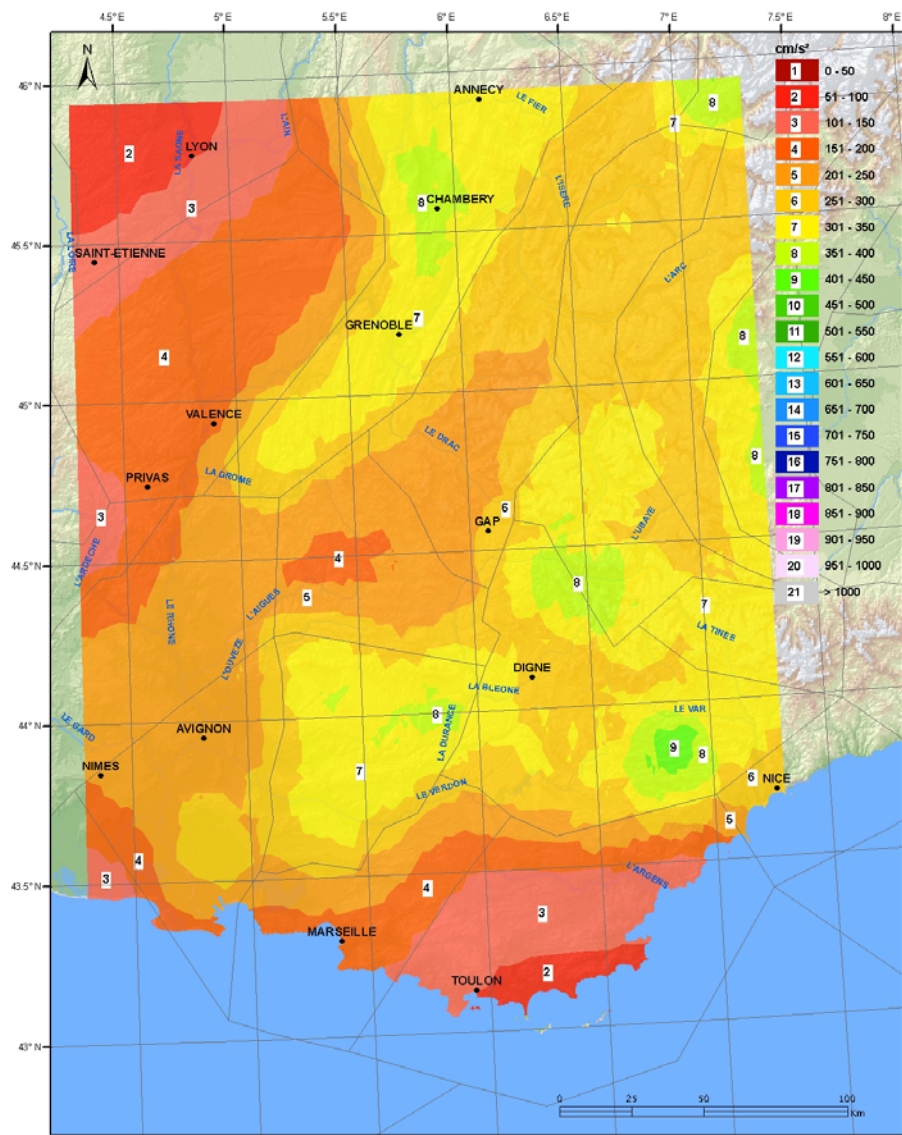
Figure 31 - Percentage of variation between percentile 16 and median (top) and between percentile 84 and median, at 0.2 s and two return periods (left: 475 years; right: 10000 years)

6.2.3 Sensitivity analysis of the seismotectonic model

In order to assess the influence of the seismotectonic model on the hazard estimation, we compare the results of sub-branches sharing the same catalog and GMPE for each of the three mains branches corresponding to the three seismotectonic models. For this comparison, we used the orginal catalog and the Boore & Atkinson (2008) GMPE for PGA and for a return period of 10000 years. Figure 32 presents the three mean maps obtained from the three seismotectonic models. The maps obtained from seismotectonic models 1 and 2 share some similitude. However, one can clearly see that the different interpretations lead to different hazard looking in detail at the two maps, especially where sources zones of model 2 are much based on the fault systems. The results from the third seismotectonic model are of course much more different since it is based on very large source areas which smoothes the hazard. For instance, the PGA for 10000 years return period varies from 51 to 450 cm/s² for the two first seismotectonic models (SM1 and SM2) and from 101 to 300 cm/s² for the third model (SM3).
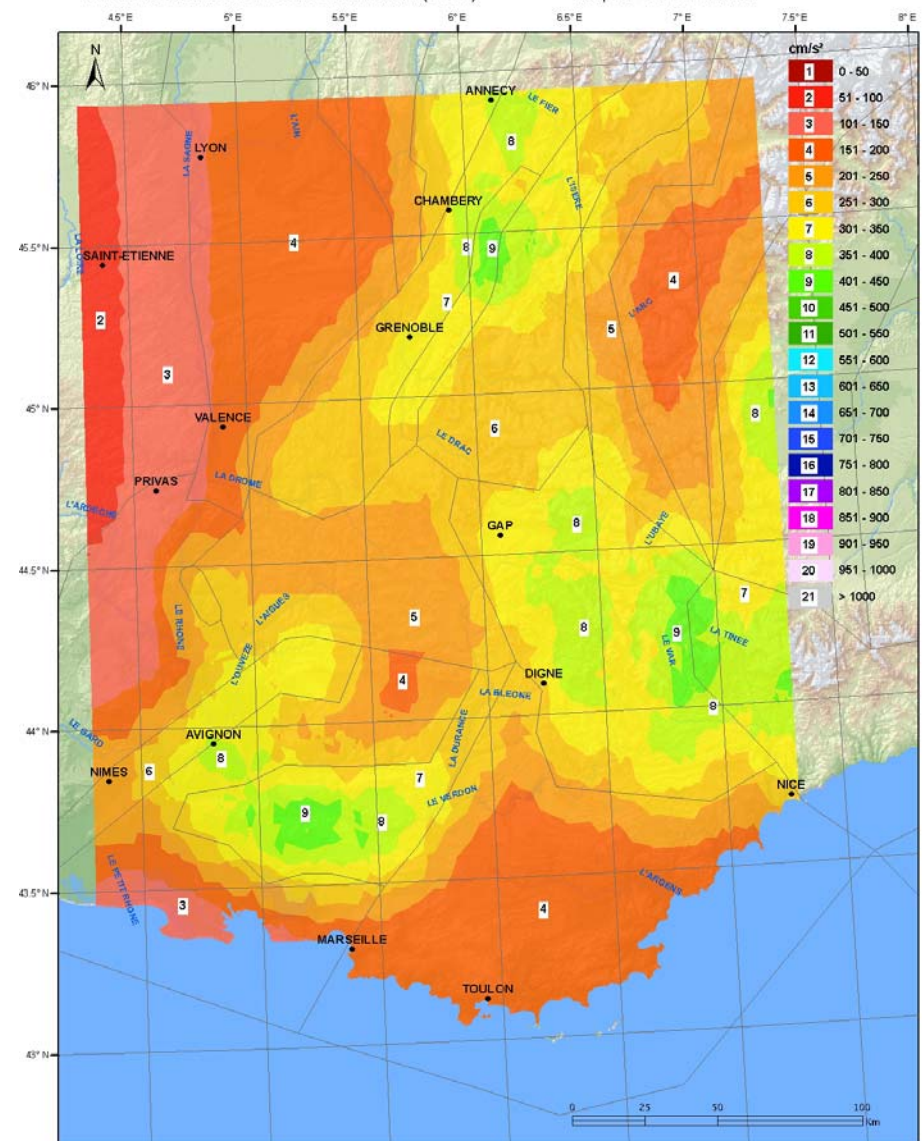
Figure 32 - Mean hazard maps for PGA at 10000 years return period using the original seismicity catalog and Boore & Atkinson (2008) GMPE for SM1 (top left), SM2 (top right), and SM3 (bottom left).

6.2.4 **Influence of the GMPE**

In order to assess the impact of using one or the other of the selected GMPEs, mean hazard maps are computed for PGA and 10000 years return preiod for the same seismotectonic model (SM1) and the same catalog (the original one). The four hazard maps computed with the four selected GMPEs are presented in Figure 33. The shapes of the maps are similar because they all result from the same seismotectonic model, but looking in detail at the four maps reveals that the use of one or the other GMPEs changes the regional variation pattern of the ground-motion. The PGA varies across the area of interest from 51 to 550 cm/s², from 51 to 350 cm/s², from 51 to 450 cm/s², and from 51 to 500 cm/s², using respectively, the Akkar & Bommer (2010), the Berge-Thierry et al. (2003), the Boore & Atkinson (2008), or the Zhao et al. (2006) model.
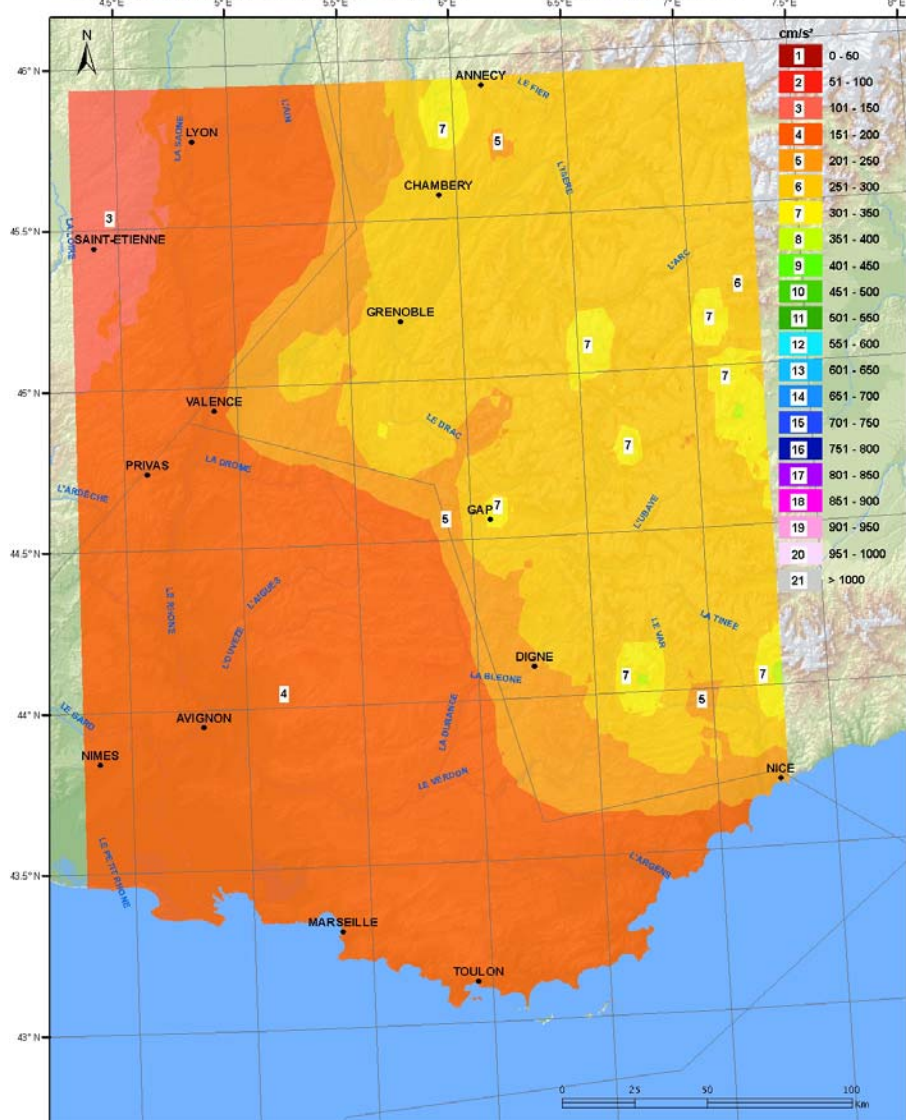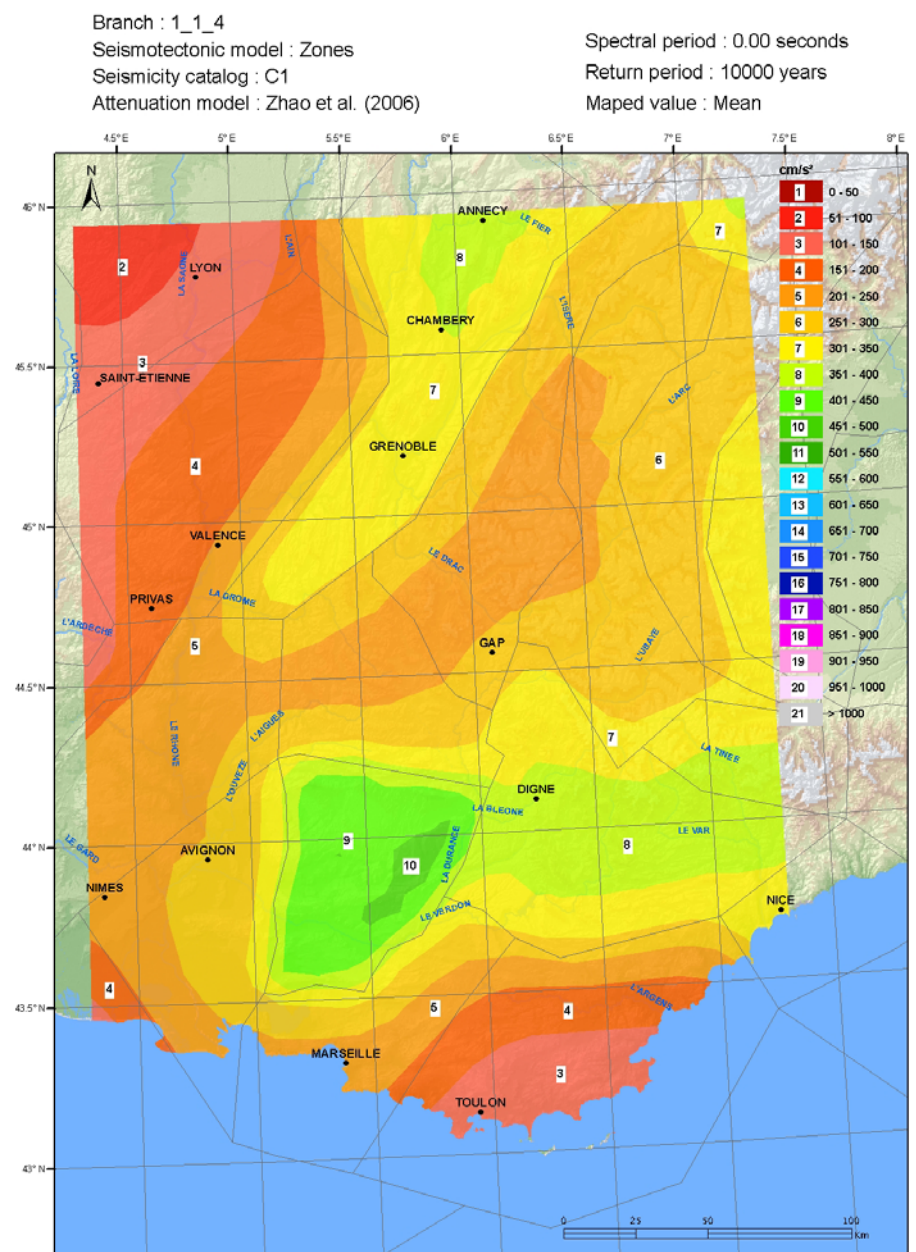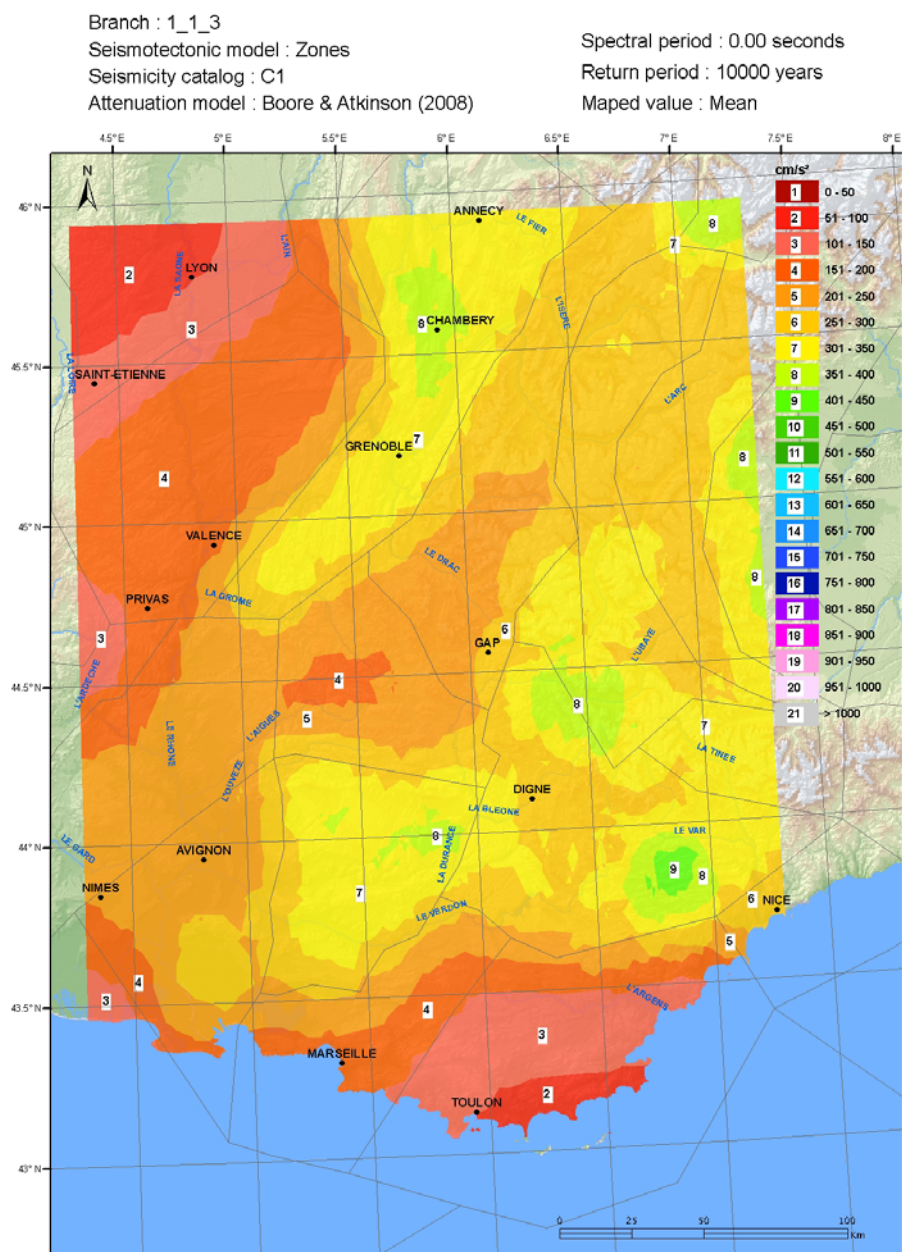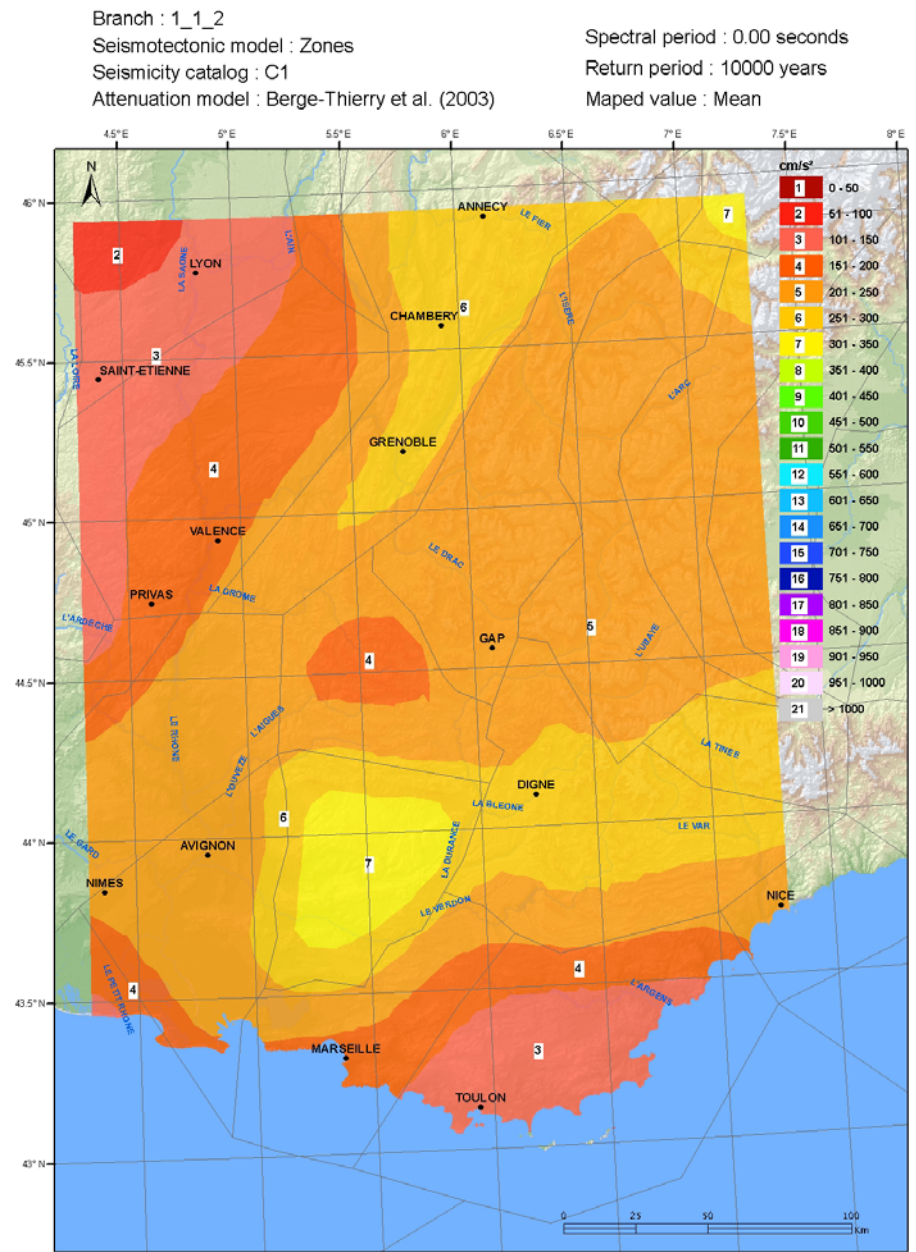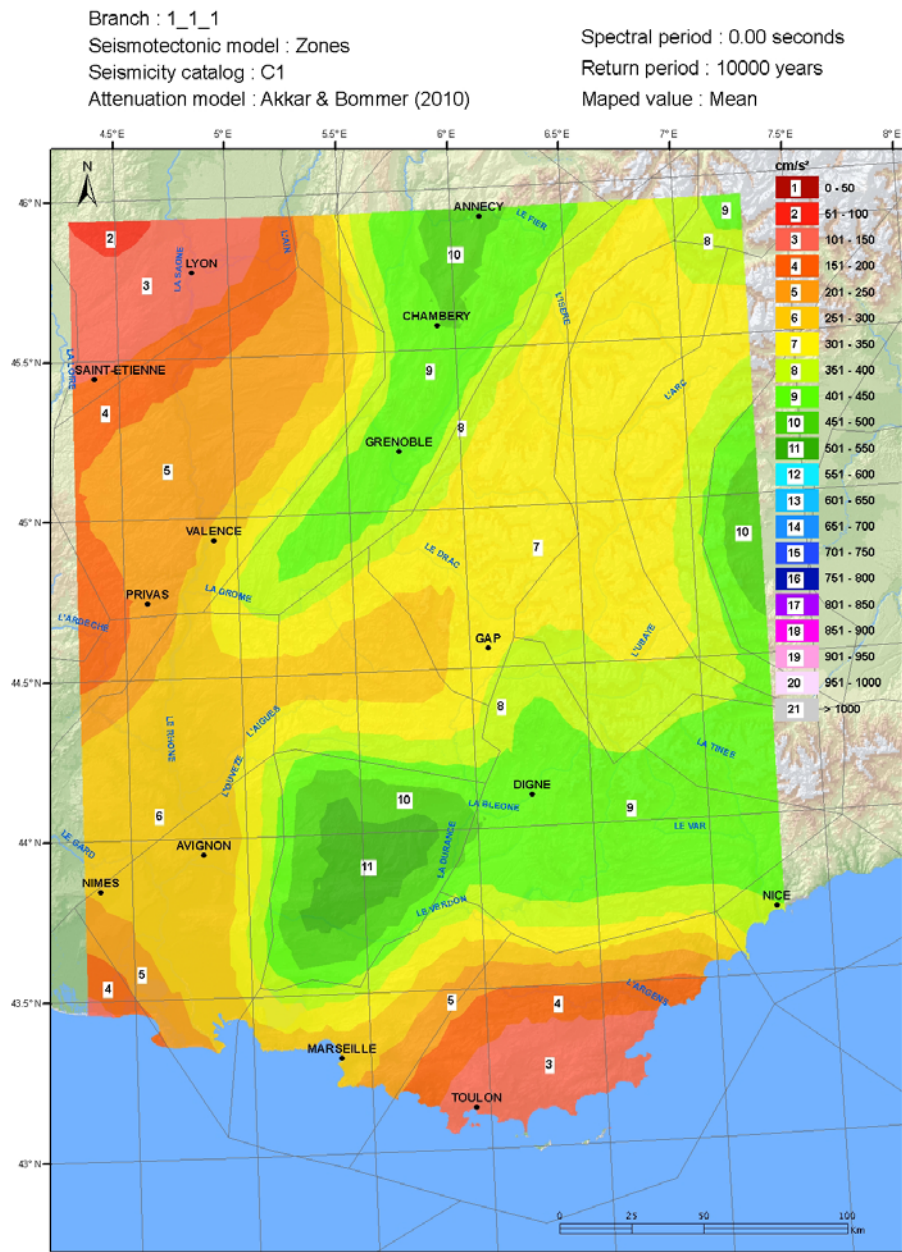
Figure 33 - Mean hazard maps for PGA at 10000 years return period using the original seismicity catalog and SM1, for Akkar & Bommer (2010) GMPE (top left), Berge-Thierry et al. (2003) GMPE (top right), Boore & Atkinson (2008) GMPE (bottom left), and Zhao et al. (2006) GMPE (bottom right).

6.2.5 Sensitivity analysis of zoning/zoneless approaches

6.2.5.1   Zoneless approach

The objective was to develop a zoneless to compare the results with the more classic zoning approach. The softwares used for the zoneless approach are the kergrid and kerry codes, originally developed by Woo (1996). This approach gives more weight to the epicenters location assuming that they could occur in the future following a distribution probability, function of the distance.

The zonless approach or kernel estimation method proposed by Woo (1996) intends to avoid the ambiguities related to the seismic zone definition as euclidian zones of uniform seismological character, especially for regions where the association between seismicity and individual faults is complex.

A probabilistic smoothing procedure is applied directly to the epicenters of the catalogue to calculate the activity rates at points of a grid acting as punctual seismic sources.

The contribution of each earthquake to the seismicity of the region of interest is smeared over a distance which can be magnitude dependent. Instead of defining the activity rate of each source using a Gütenberg-Richter recurrence relationship, individual rates are defined for each magnitude interval. These rates are calculated from the density and proximity of the epicenters lying within that magnitude range.

The kernel function is used to permit different magnitudes to have different distance dependencies in the equation that is applied to determine the contribution of each epicenter to the activity rate of each point source. By summing over all epicenters, the cumulative activity rate density is computed for each magnitude class, from the minimum magnitude of engineering interest (as in a zoning approach) up to the highest value observed in the catalogue. For each event, the cumulative activity rate density is updated at each point source of the grid.

Once the activity rate of each magnitude increment has been defined for each point source of the grid, an attenuation equation is employed and the hazard is calculated by summing over each point source as in the Cornell-McGuire zoning method.

To propagate the variability induced by the choice of the kernel function, three functions are adopted: two finite functions and one infinite function (Figure 34).

Finite Kernel function: The parameters to set for the kernel function are the minimum distance, R_{min} (km) up to which the function is constant and the maximum distance, R_{max}, from which the probability of occurrence is zero. The finite Kernel function is defined by:

$$K(M, x) = C/R_{min} \quad \text{if } R < R_{min}$$

$$= C/R \quad \text{if } R_{min} \leq R < R_{max}$$

$$= 0 \quad \text{in others case}$$

C is the normalization constant that ensures that the total probability of occurrence of an earthquake is equal to 1. The value of this constant is calculated by integrating the total area where the kernel function is defined:

$$\int_0^{2\pi}\int_0^{R_{min}}\frac{C}{R_{min}}RdRd\theta+\int_0^{2\pi}\int_{R_{min}}^{R_{max}}\frac{C}{R}RdRd\theta$$

$$=\frac{2\pi}{2R_{min}}CR_{min}^2+2\pi\ C(R_{max}-R_{min})=2\pi\ C\left(R_{max}-\frac{R_{min}}{2}\right)=1$$

and finally,

$$C = 1/[2\pi\ (R_{max} - 0.5\ R_{min})]$$

This function is chosen isotropic, i.e. independent of the spatial direction of the fault.

Infinite Kernel function: the parameters of this function, PL (> 1) and the bandwidth H (M), are defined by:

$$K (M, \mathbf{x}) = [\ (PL - 1)/\pi\ ]\ H(M)^{-2} [1 + r^2/H(M)^2]^{-PL}$$

$$H(M) = a\ \exp(bM)$$

PL   is normally defined in the interval 1.5 to 2.0.

We use the a and b paameters proposed by (Beauval et al., 2006), calibrated on French data:

$$H(M) = 0.26\ \exp(0.96 * M)$$

Figure 34: Comparison of the three kernel functions : finite (left) and infinite (right).
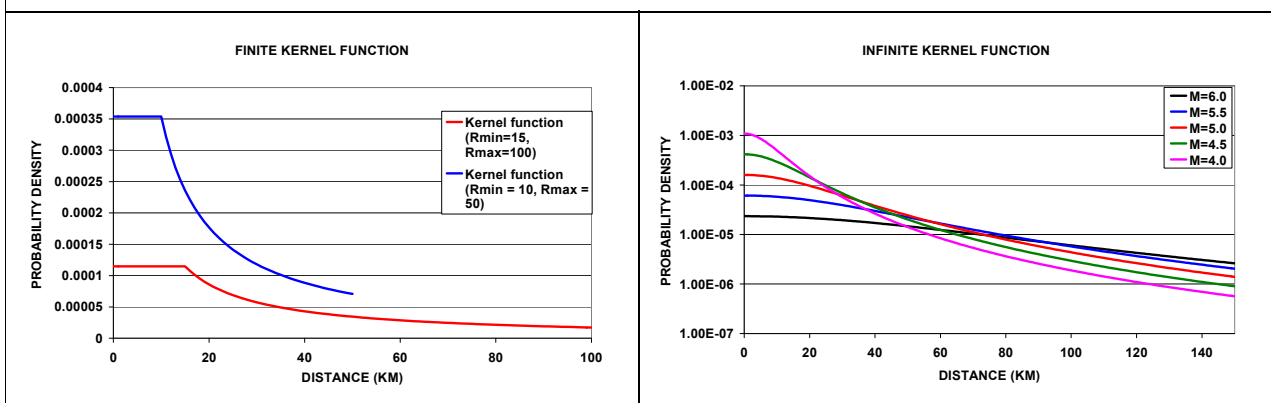
The first finite function (K1) is applied with the following parameters:

-   Rmin of kernel function: 10 km, which is approximately the size of the strongest earthquake rupture that can be expected in France, and is an approximation of the uncertainty of location of the epicenters;

- Rmax of the kernel function: 50 km, which is approximately the size of the smaller source areas.

For the second finite function (K2), the parameters are:

- Rmin of kernel function: 15 km, which corresponds to a slightly larger source size;

- Rmax of the kernel function: 100 km, which approximates the average size of source zones.

The infinite function (K3) is used with the following parameters:

- PL   of the kernel function: 1.5, which is the parameter that controls the degree of spatial smoothing;

- H(M) = $0.26*e^{0.96.M}$, where M is the magnitude, as suggested by Beauval et al. (2006).

The probability distribution of depths applied is:

Weights	0.2	0.5	0.2	0.1
Depth	5 km	10 km	15 km	20 km

The zoneless approach is only implemented using the Berge-Thierry et al. (2003) GMPE.

6.2.5.2   Comparison zning/zoneless results

The PGAs obtained with the original seismicity catalog are compared for seismotectonic model 1 and the three zoneless models (i.e., three kernel functions that smooth in different ways the seismicity around the point where the hazard is computed), in Figure 35 and Figure 36, for 475 and 10000 years return period, respectively.

The general shapes of the maps are similar at 475 years of return period. The differences between the zoneless approaches using different kernel functions are small. The kernel function 1, with a more limited range of distances concentrates more the hazard where large earthquakes occurred.

The differences are more significant at 10000 years of return period.
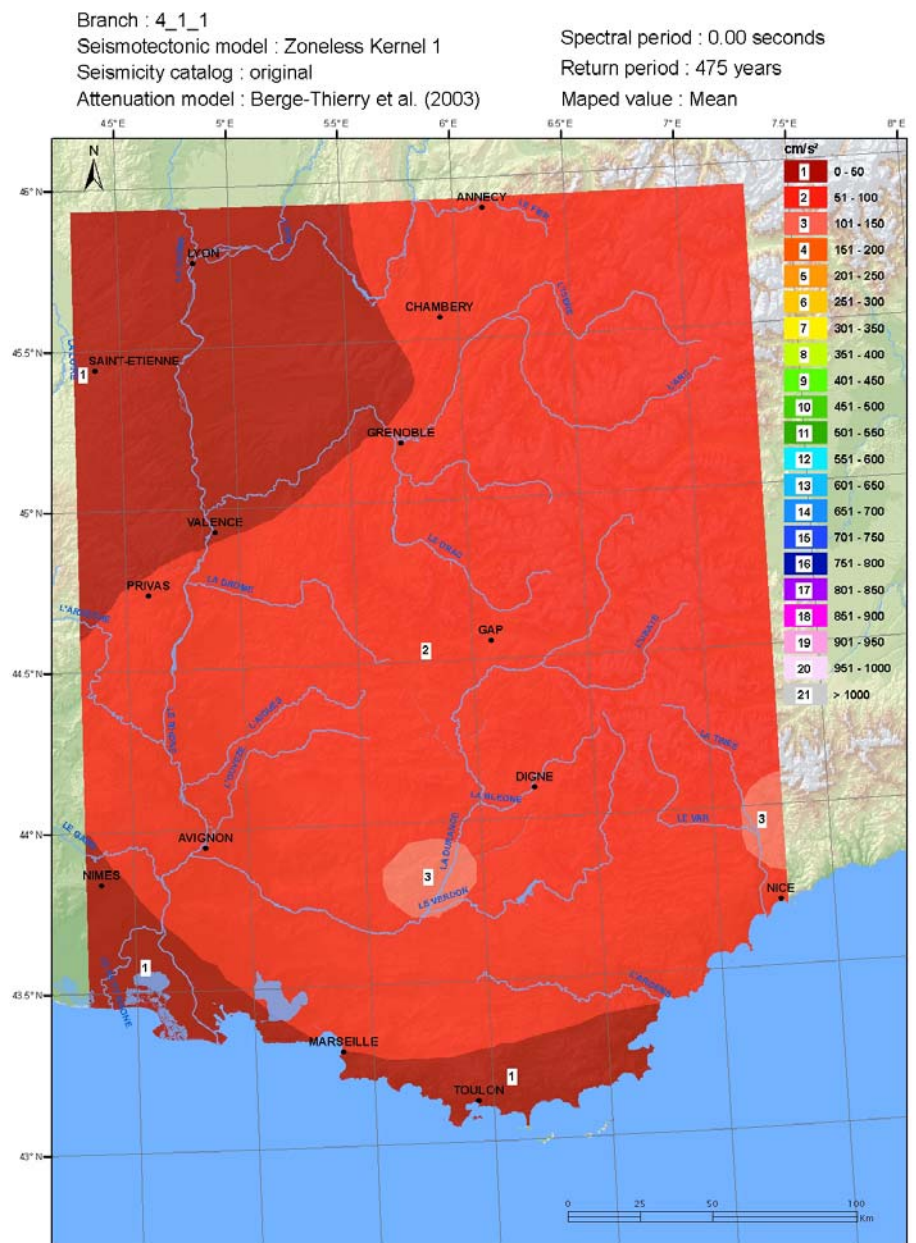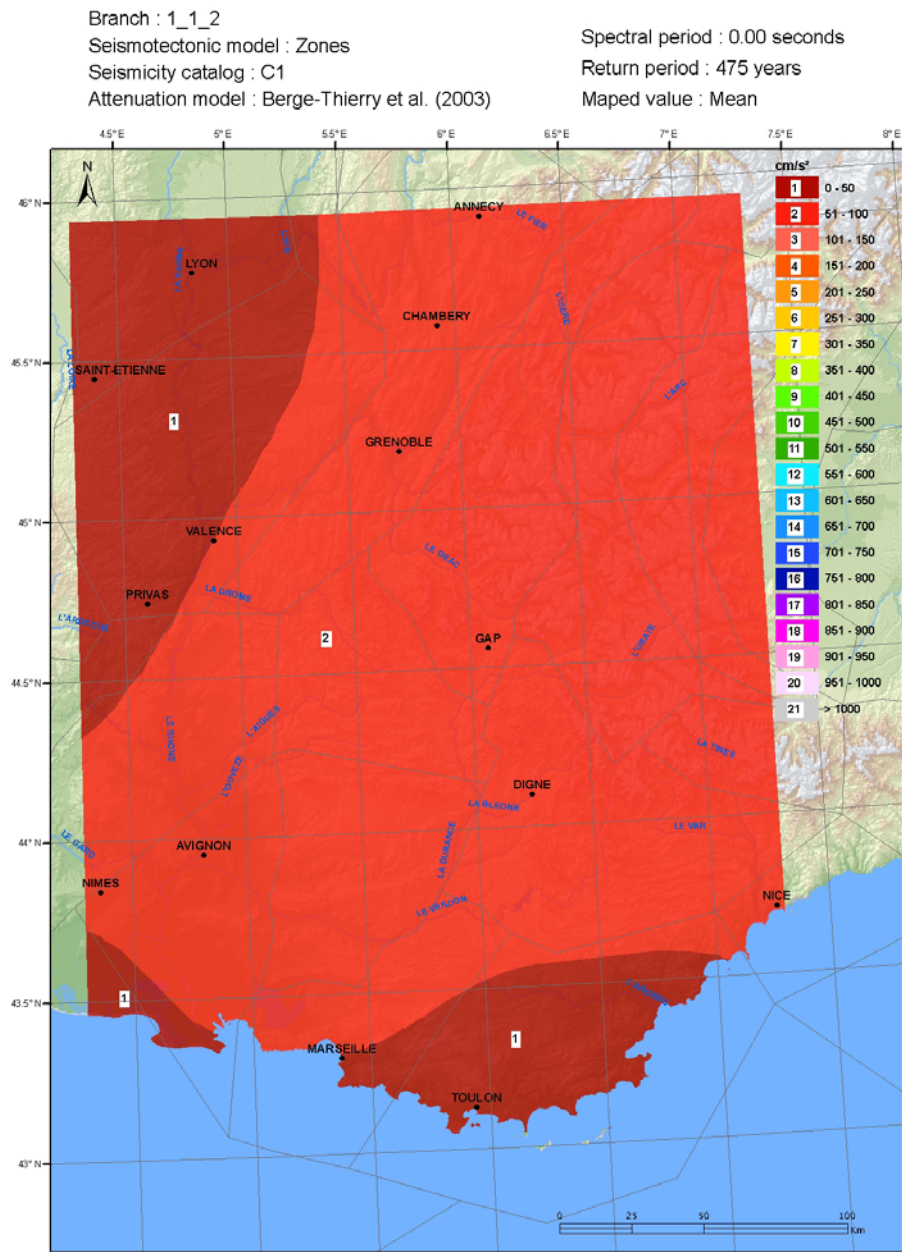
Figure 35 - Mean hazard maps for PGA at 475 years return period using the original seismicity catalog and Berge-Thierry et al. (2003) GMPE for SM1 (top left), Zoneless model 1 (top right), Zoneless model 2 (bottom left), and Zoneless model 3 (bottom right).
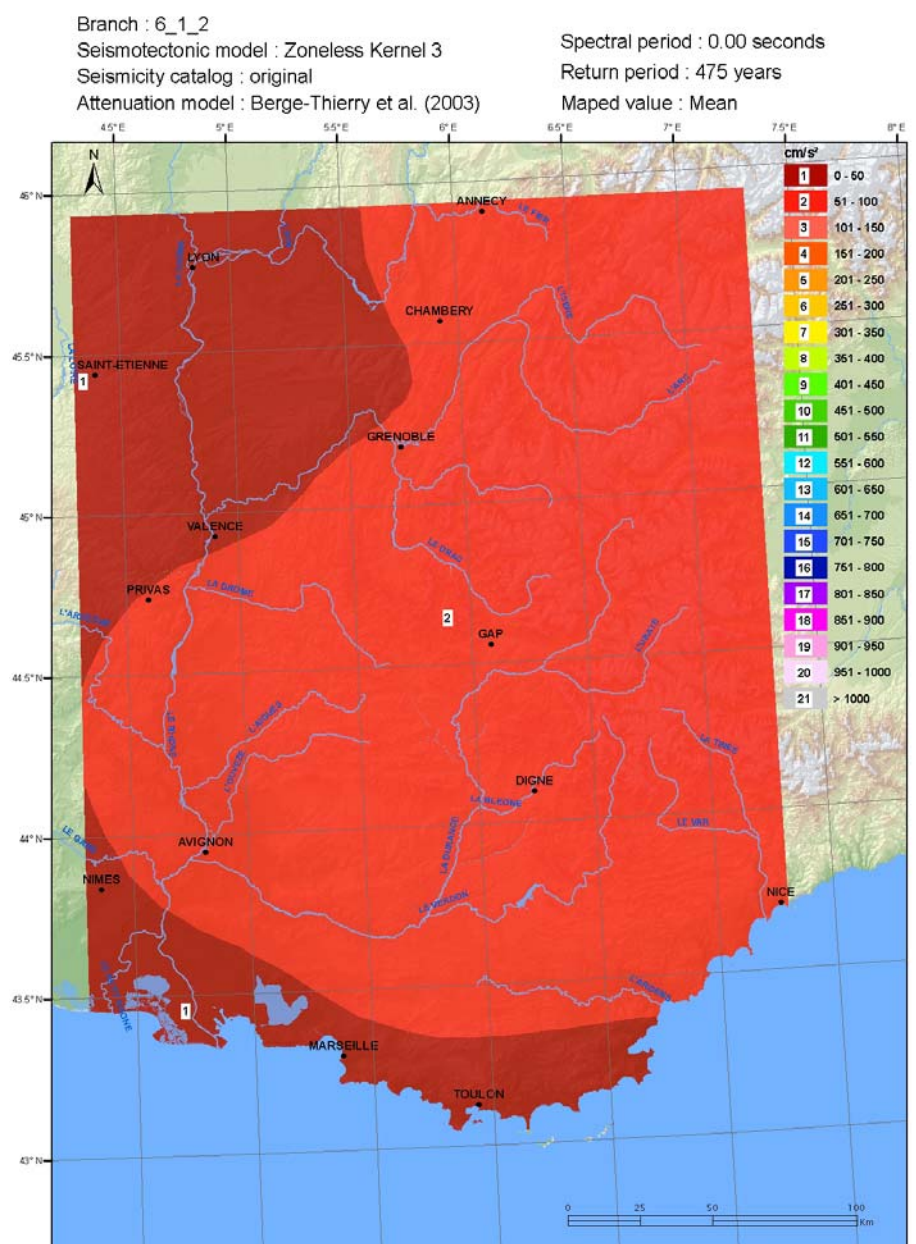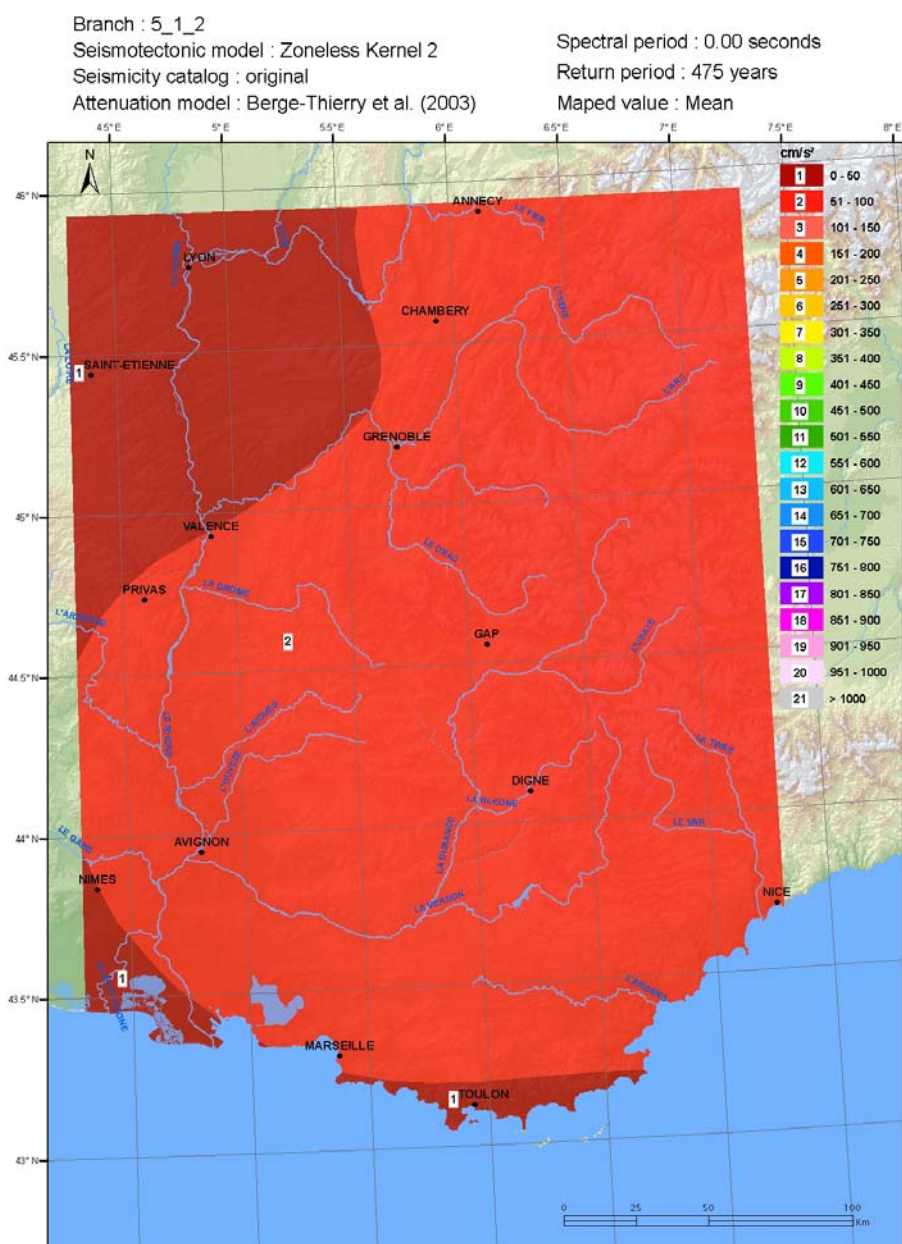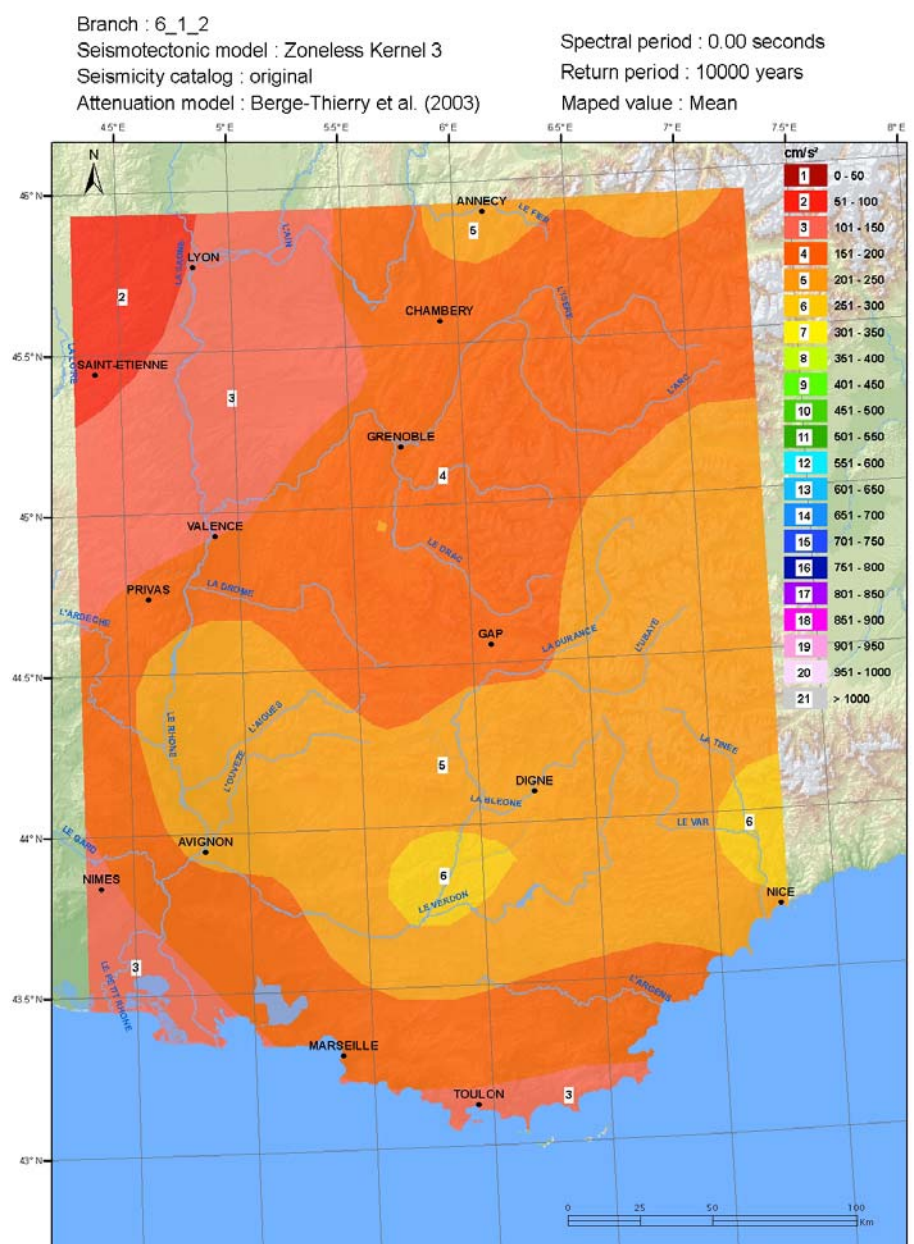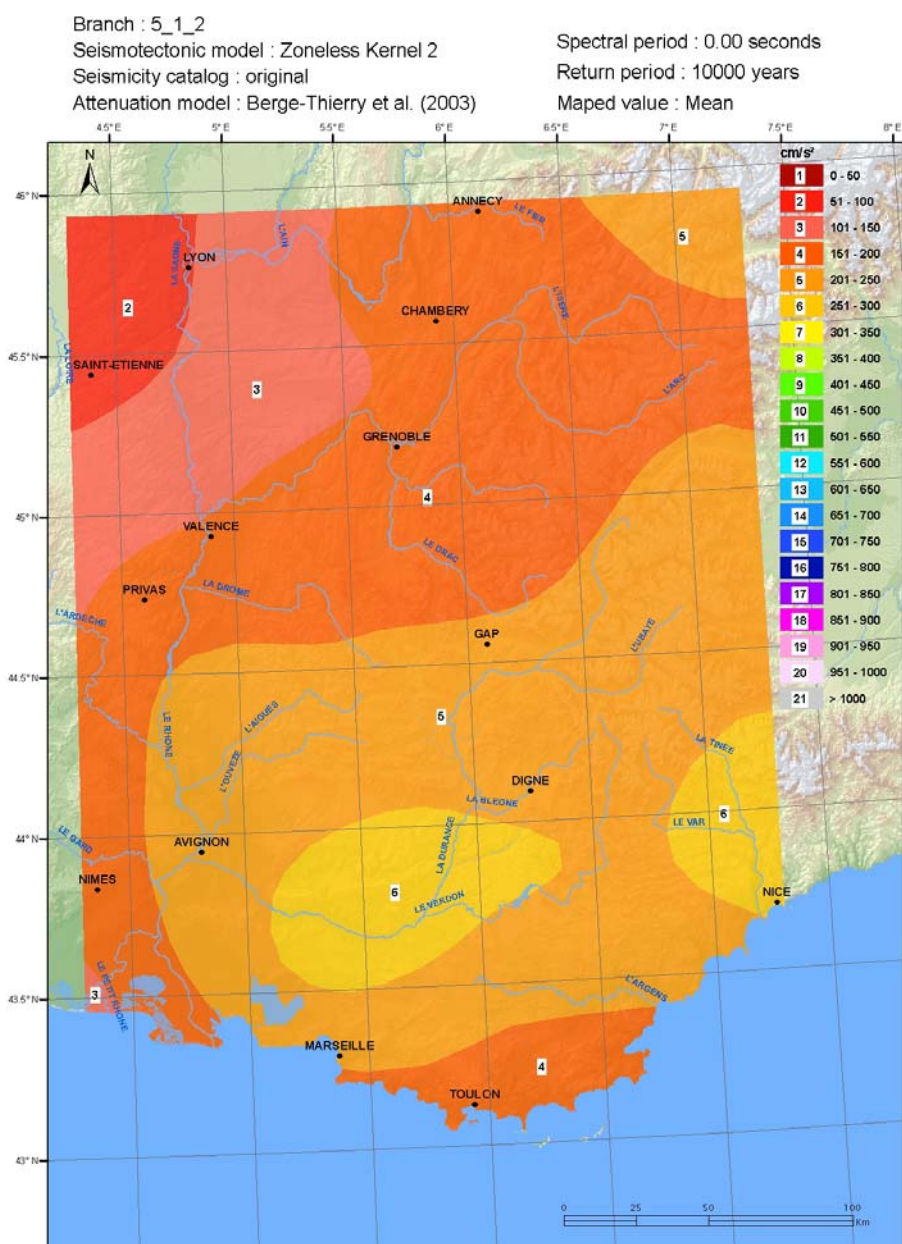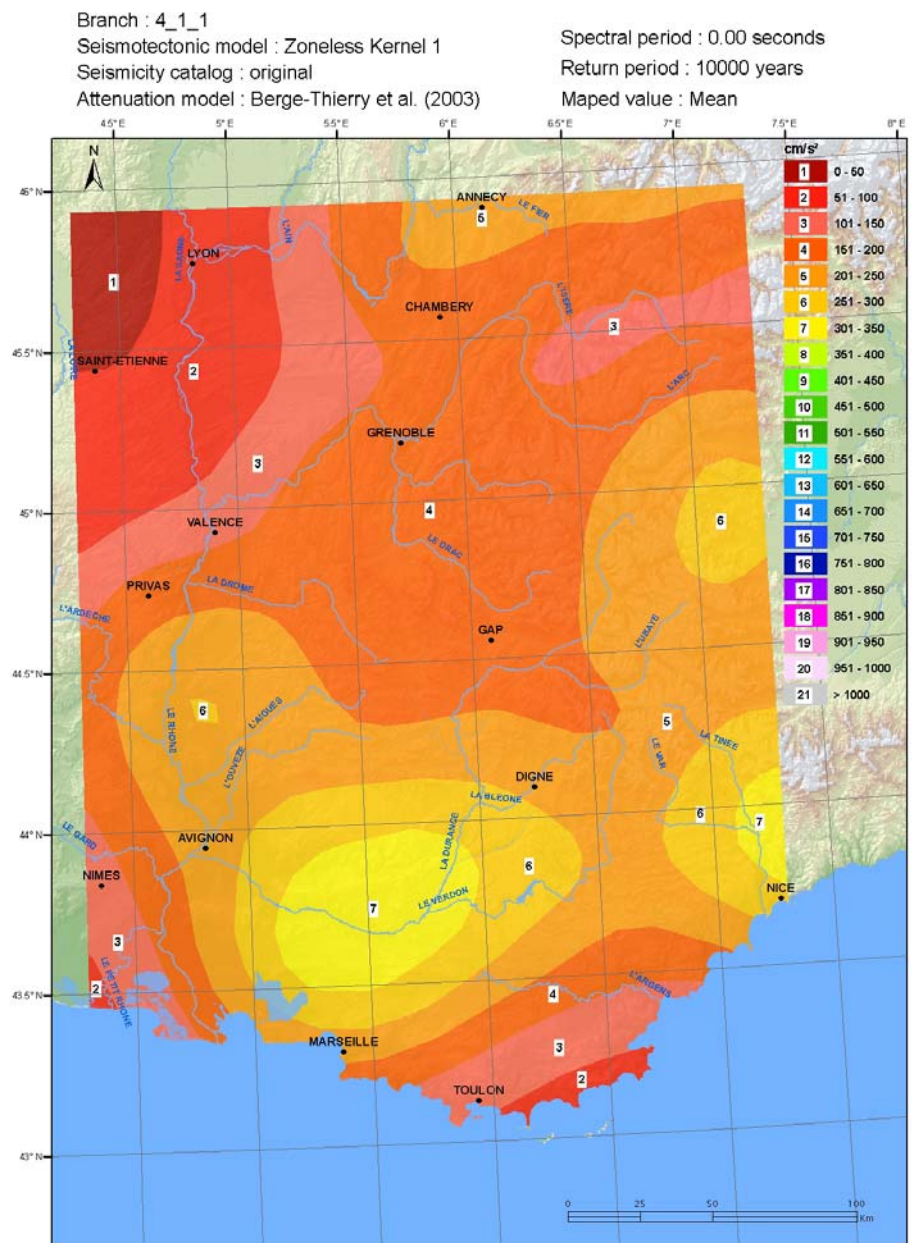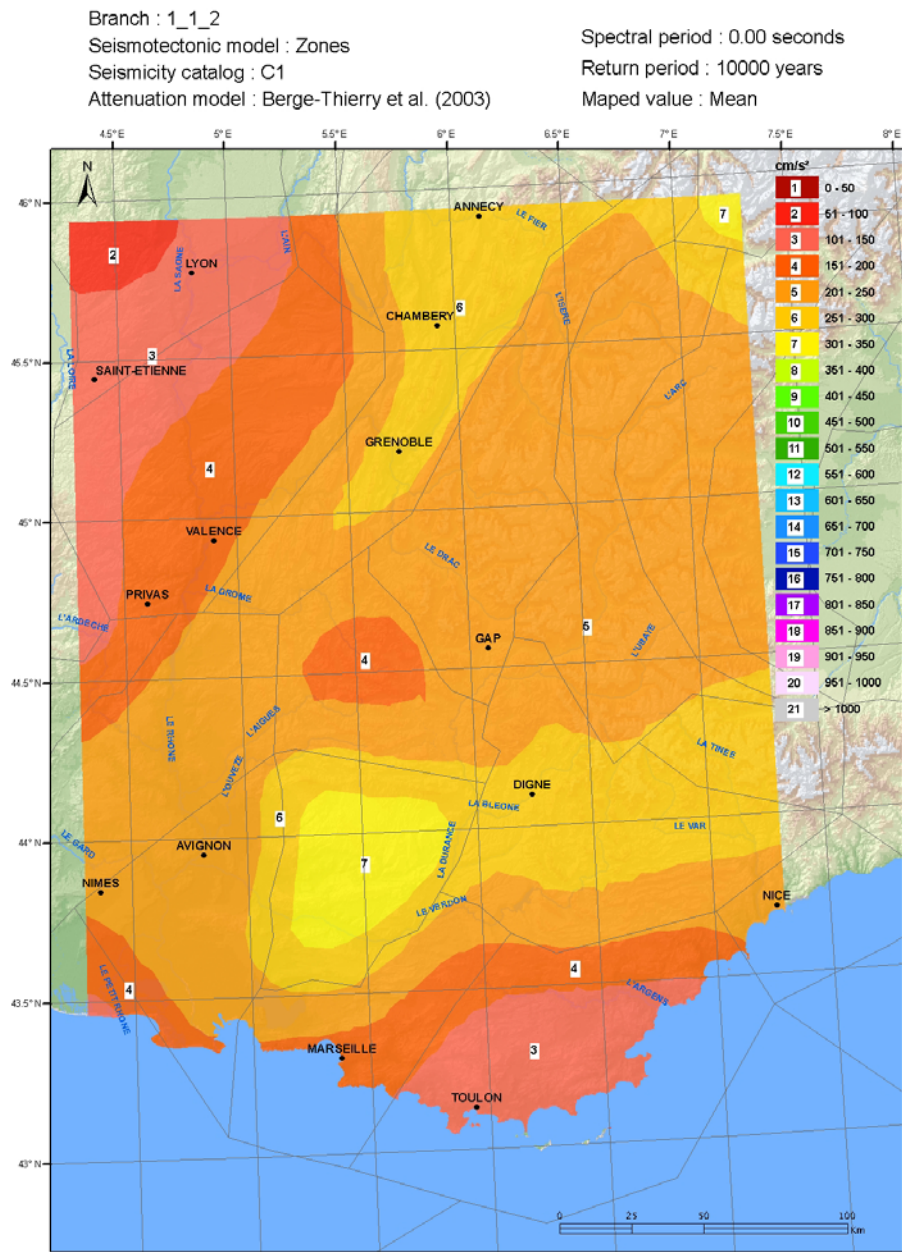
Figure 36 - Mean hazard maps for PGA at 10000 years return period using the original seismicity catalog and Berge-Thierry et al. (2003) GMPE for SM1 (top left), Zoneless model 1 (top right), Zoneless model 2 (bottom left), and Zoneless model 3 (bottom right).

6.3 Resultst at the 20 selected points of interest

6.3.1 Hazard curves

The numerical results provided on the DVD, allow the computation of hazard curves at any point of the grid covering the region of interest, or any of the 20 particular selected sites. Mean, median, percentiles 16% and 84% hazard curves are computed. However, any other percentile may also be computed going back to the individual outputs for any particular run. The format description of the numeric files is given in Annex 1. The hazard curves are plotted in annex 2 together with the uniform hazard response spectra at five return periods.

Figure 37 compares the mean, median and percentiles 16-84% and 5-95% hazard curves for PGA and at two particular points: OGMU and OGCA, which are accelerometric station locations. OGCA is close to the Provence region characterized by large historical events but few recorded ones, and hence seismicity parameters are not well constrained. This is also one of the region within the studied area were faults are partly identified but different interpretations still exist, and consequently were the seismotectonic models differ significantly. On the other hand, OGMU is located in Grenoble and the region is characterized by many recorded events and seismicity parameters are relatively well constrained. Consequently, the uncertainty is larger at OGCA compared to OGMU.
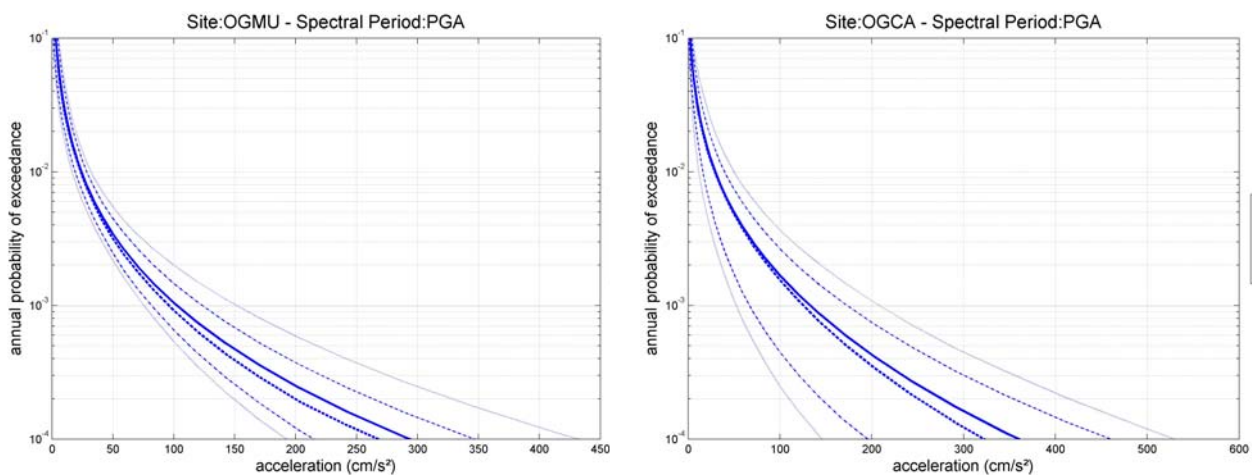
Figure 37 - Mean (solid line), median (dashed line), percentiles 16 and 84% (dashed-dotted lines), and percentiles 5 and 95% (dotted lines) hazard curves at stations OGMU (left) and OGCA (right) for PGA.

Figure 38 compares the mean hazard curves for PGA, 0.2 and 1.0 sec at stations OGMU and OGCA. The hazard curves are available in each point, for the 15 spectral periods common to the GMPEs.
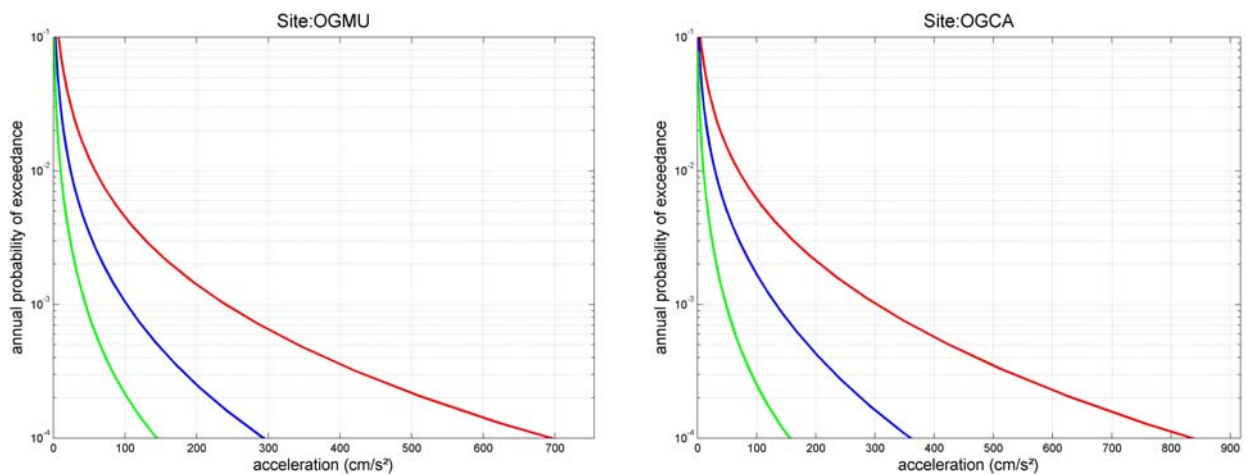
Figure 38 - Mean hazard curves at station OGMU (left) and OGCA (right), for PGA (blue), 0.2 sec (red) and 1.0 sec (green).

6.3.2 Uniform Hazard Spectra

The effect of the return period on the mean Uniform Hazard Spectra is illustrated in Figure 39 for sites OGMU and OGCA. The shape of the spectra is preserved with increasing return period but its amplitude increases. All the uniform hazard response spectra are plotted in annex 2, and available in numeric format on the DVD.
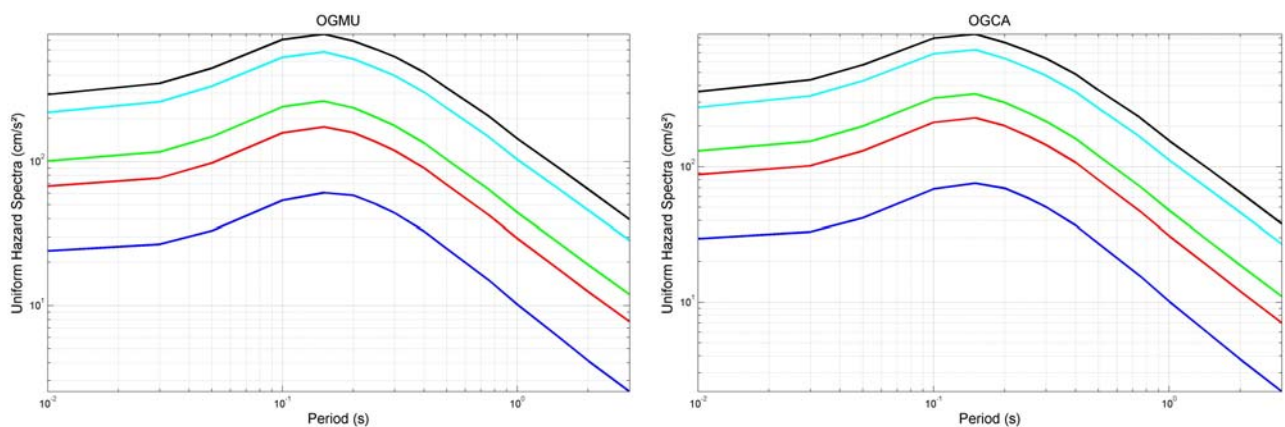
Figure 39 - Uniform Hazard spectra at site OGMU (left) and OGCA (right), for different return periods (blue: 100 years; red : 475 years ; green : 975 years ; cyan : 5000 years ; black : 10000 years).

The mean, median, and percentiles 16% and 84% PGA values, for two return periods 475 and 10000 years, are tabulated for each of the 20 selected sites in Table 15.

SITE	PGA (cm/s²)							
	475 years return period				10000 years return period			
	Mean	Median	16%	84%	Mean	Median	16%	84%
CALF	59.71	57.4	48.49	70.09	278.82	266.39	194.51	336.46
OGAG	71.78	69.03	57.97	84.4	307.33	278.84	216.28	411.61
OGAN	72.38	67.49	57.53	86.27	322.93	299.65	224.93	413.1

OGCA	87.4	84.29	44.34	114.55	359.57	321.54	194.98	458.91
OGMO	68.06	65.1	55.23	79.78	265.99	248.34	195.79	317.11
OGMU	67.33	63.72	54.54	80.91	293.31	266.71	214.15	346.71
STET	78.15	75.72	60.23	93.18	318.69	294.9	228.44	381.26
LYON	31.11	30.06	23.01	38.04	139	124.99	90.57	181.47
VALENCE	43.47	41.89	34.73	50.95	195.5	180.94	142.31	240.49
DIGNE	66.4	63.4	53.27	78.16	281.17	257.96	202.38	338.7
AVIGNON	62.77	61.02	41.26	77.7	246.97	233.27	166.91	298.36
NICE	62.13	59.35	48.38	73.25	267.89	230.9	189.94	318.88
MARSEILLE	41.31	40.08	30.88	49.06	177.42	156.84	121.85	219.4
ALBERTVILLE	68.43	65.76	56.94	79.58	273.5	253.42	214.27	323.04
DONZERE	68.7	59.97	40.94	104.05	326.37	247.68	173.52	405.16
GAP	63.76	62.17	53.42	73.22	271.7	253.42	201.6	323.77
DRAGUIGNAN	41.83	40.74	33.93	48.86	167.45	155.05	117.79	205.37
LA_MURE	62.3	60.69	52.82	71.38	262.47	244.96	203.31	312.48
VINON_SUR_VERDON	67.37	64.81	43.8	84.26	256.06	231.56	177.05	309.94
FOS_SUR_MER	48.14	46.39	35.61	58.6	190.39	174.4	137.72	230.65

Table 15 - Mean, median and percentiles 16% and 84% PGA values obtained at the 20 selected sites.

6.3.3 Influence of the seismotectonic model

The influence of the seismotectonic models on the mean hazard curves for PGA is shown in Figure 40. The sub-branches corresponding to the original seismicity catalog and to Boore & Atkinson (2008) GMPE, but for the three different seismotectonic models are compared. As already shown on the maps, the influence of the seismotectonic model is stronger at site OGCA than at site OGMU.

Figure 40 – Mean hazard curves at sites OGMU (left) and OGCA (right) for PGA, using Boore & Atkinson (2008) GMPE, and for SM1 (blue), SM2 (red), SM3 (green).

The influence of the seismotectonic model is also assessed on Uniform Hazard Spectra in Figure 41 for the two same sites for two return periods : 475 and 10000 years. The same conclusion is drawn, the seismotectonic model strongly impact the hazard at station OGCA.

Figure 41 - Uniform Hazard Spectra at site OGMU (left) and OGCA (right), for 475 (top) and 10000 (bottom) years return period, using Boore & Atkinson (2008) GMPE, and for the three seismotectonic models (SM1 : blue ; SM2 : red ; SM3 : green).

It appears that the seismotectonic models 1 and 2, give closer results than compared with seismotectonic model 3. This was expected since the third model is composed of very large sources (5 in total) corresponding to areas with homogeneous deformation, while the other two contain around 40 zones with homogeneous seismo-tectonic characteristics. The differences do not seem to depend very much on the return period, and are more related to the site position. Indeed, OGCA is located close to the Provence region where active fault systems are identified. In model 1 and 2, this zone is related to a high seismic activity, leading to large UHS amplitudes, while in the third model, this activity is spread over a large zone which is responsilble for a hazard dilution. On the contrary, close to OGMU, the seismic activity is denser

and spread over large areas and, consequently, dividing the region in small or large zones does not lead to large differences in the spectra amplitudes.

6.3.4 Influence of the GMPE

The influence of the GMPE on the hazard curves is assessed in Figure 42. The seismotectonic model 1 and the original seismicity catalog are used with the different GMPEs. The impact of the GMPEs is about the same for both sites OGMU and OGCA.
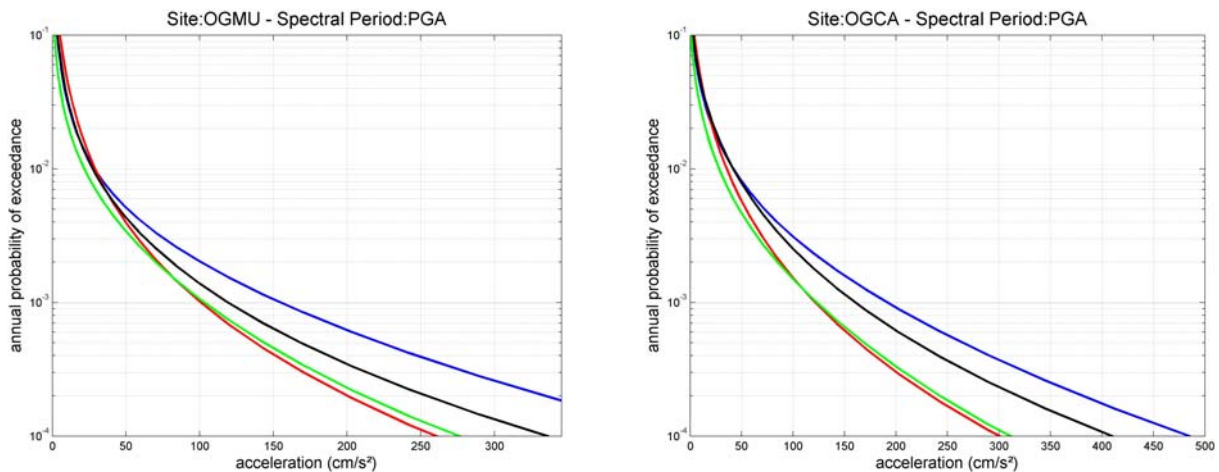
Figure 42 – Mean hazard curves at sites OGMU (left) and OGCA (right) for PGA, using SM1, and for Akkar & Bommer (2010) GMPE (blue), Berge-Thierry et al. (2003) GMPE (red), Boore & Atkinson (2008) GMPE (green), and Zhao et al. (2006) GMPE (black).

The impact of the GMPEs is further assessed on Uniform Hazard Spectra. Again, the seismotectonic model 1 and the original seismicity catalog are used, and the hazard spectra obtained using the four selected GMPEs are compared for sites OGMU and OGCA at two return periods: 475 and 10000 years (Figure 43). The two GMPEs leading the the higher hazard are Akkar & Bommer (2010) and Zhao et al. (2006) for spectral periods below about 0.5 sec whatever the return period. At higher spectral periods, the difference between the GMPEs is decreasing.
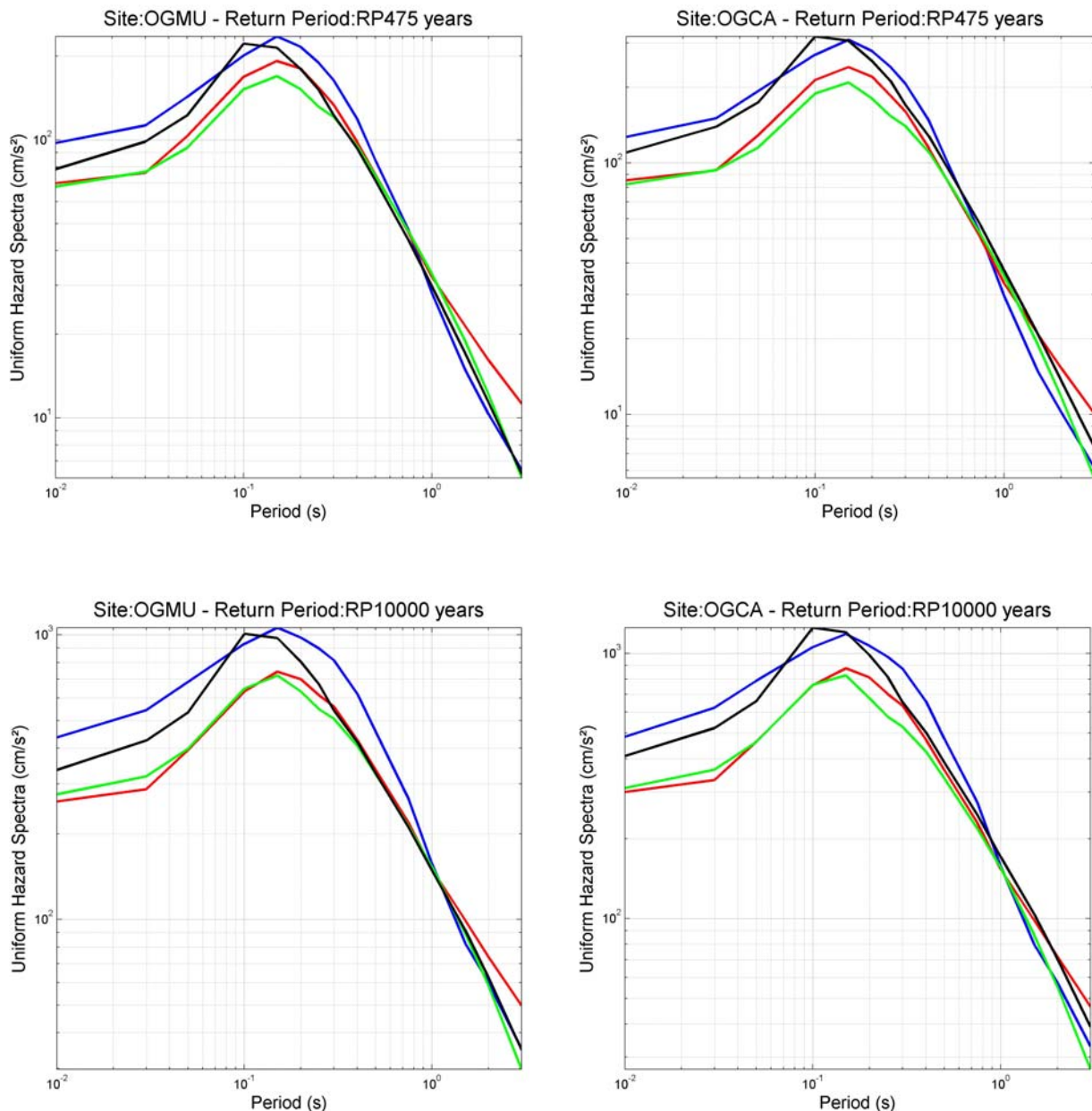
Figure 43 - Uniform Hazard Spectra at site OGMU (left) and OGCA (right), for 475 (top) and 10000 (bottom) years return period, for SM1, and for the four GMPEs (Akkar & Bommer (2010) : blue ; Berge-Thierry et al. (2003) : red ; Boore & Atkinson (2008) : green ; Zhao et al. (2006) : black).

6.3.5 **Comparison zoning/zoneless**

The mean hazard curves obtained for the three different seismotectonic models and the three different Zoneless models are compared in Figure 44. Since the Zoneless approach is implemented with Berge-Thierry et al. (2003) GMPE only, this is the reference model used for the comparison. The original seismicity catalog is also used. One can see that the three zoneless models give similar results at site OGMU and more different results at site OGCA. On the other hand, if one excludes SM3 at OGCA, the results for the zoning/zoneless approach are more different at site OGMU than at site OGCA.
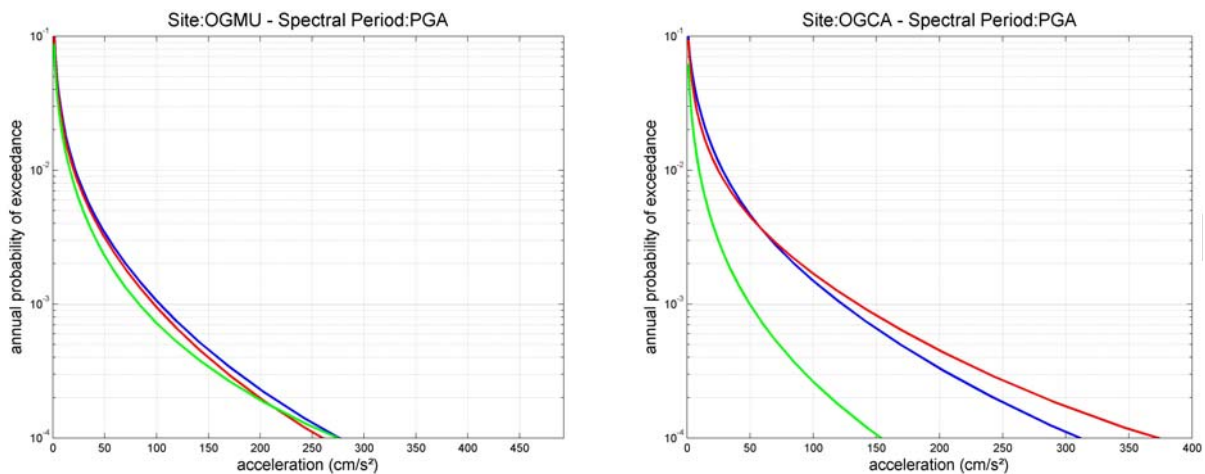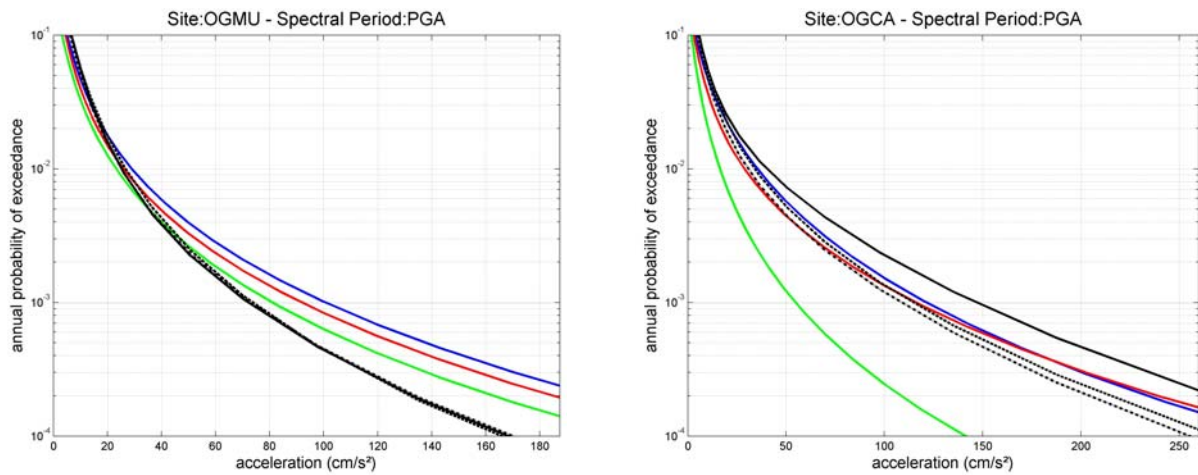
Figure 44 – Mean hazard curves at site OGMU (left) and OGCA (right) for PGA, using Berge-Thierry et al. (2003) GMPE, and for SM1 (blue), SM2 (red), SM3 (green), and the three Zoneless models (1 : solid black ; 2 : dashed black ; 3 : dashed-dotted black).

The same conclusions may be drawn from the comparison of the Uniform Hazard Spectra shown in Figure 45. The shapes of the spectra are almost the same but the amplitudes differ from one model (zoning/zoneless) to the other.
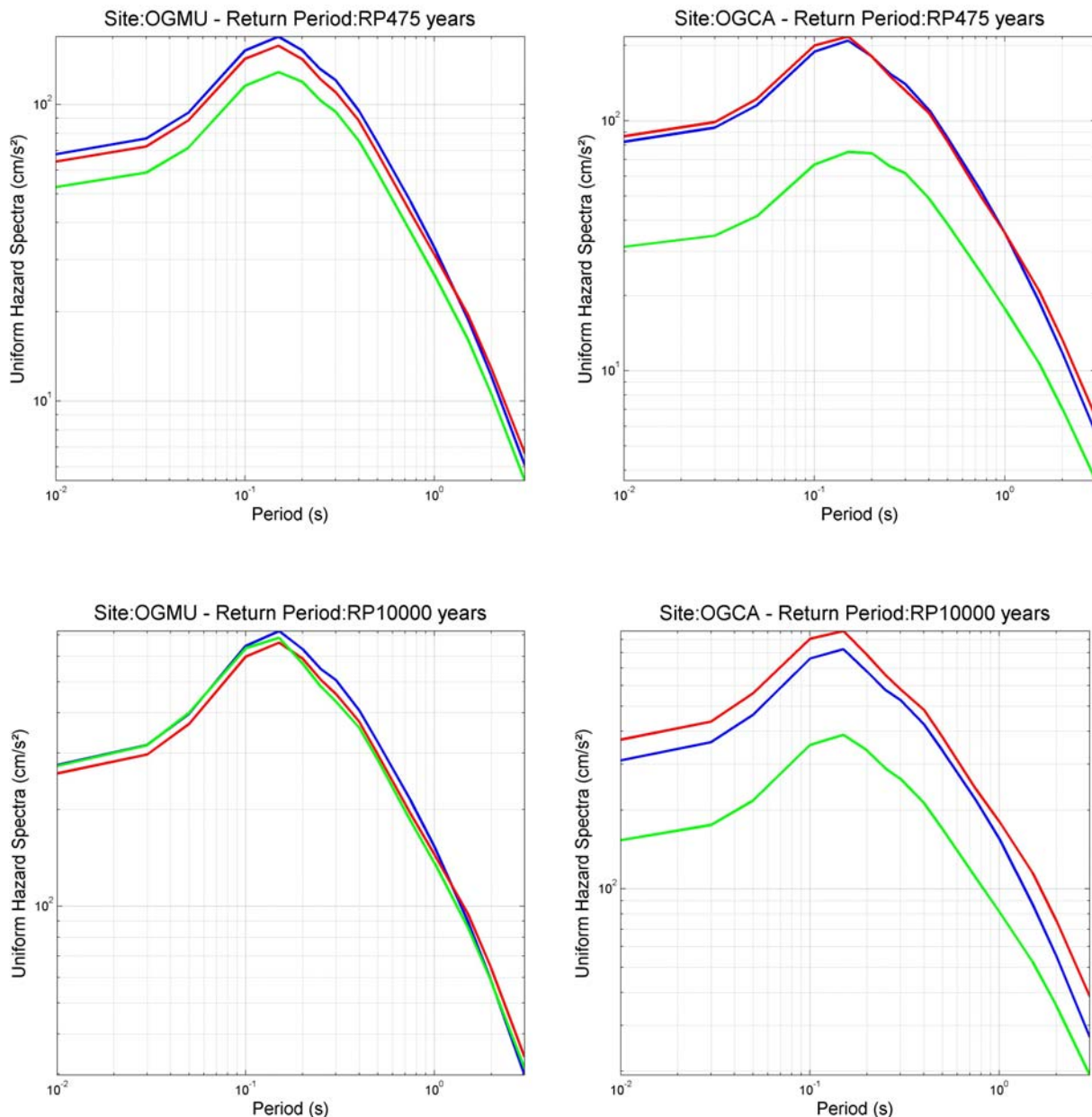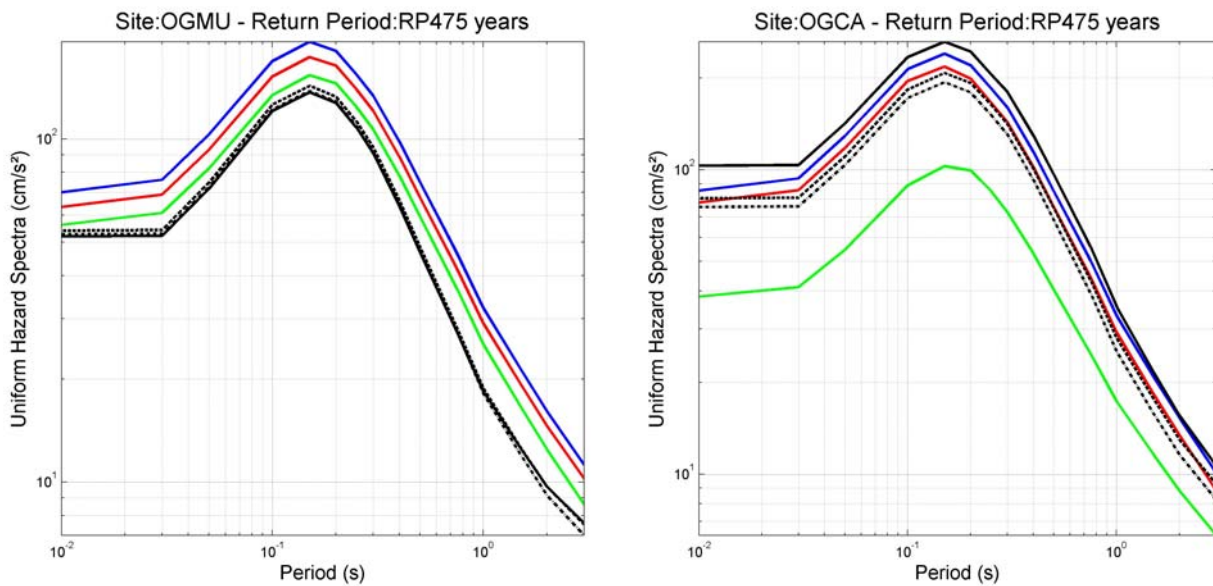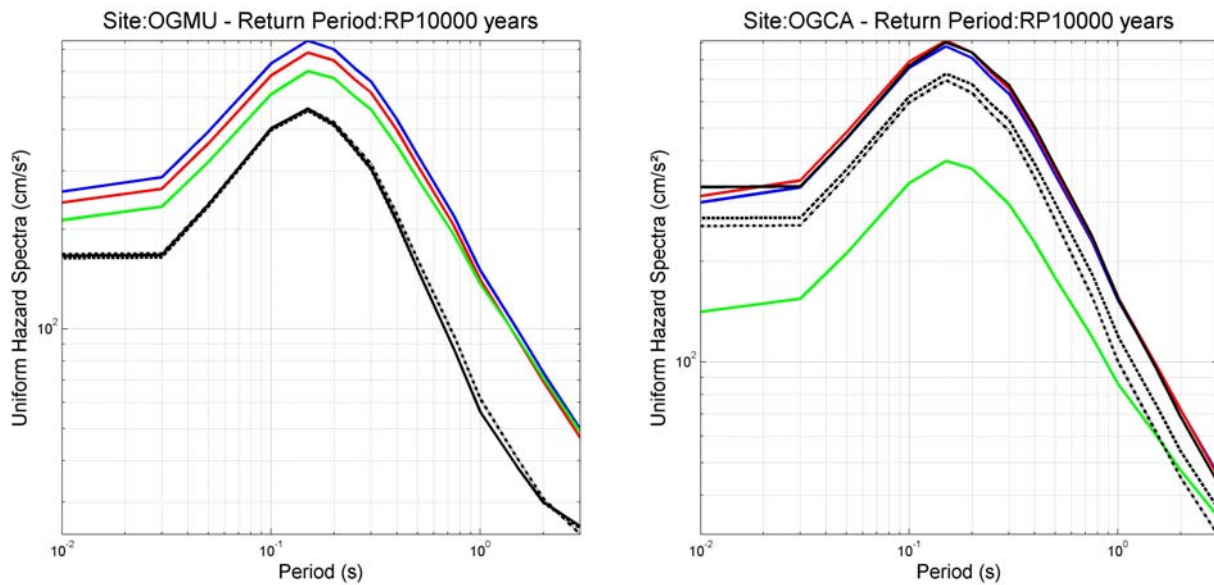
Figure 45 – Mean Uniform Hazard Spectra (UHS) at sites OGMU (left) and OGCA (right), for 475 (top) and 10000 (bottom) years return period, using Berge-Thierry et al. (2003) GMPE, and for SM1 (blue), SM2 (red), SM3 (green), and the three Zoneless models (1 : solid black ; 2 : dashed black ; 3 : dashed-dotted black).

6.4 Influence of the maximum magnitude estimation

For the region of interest, the differences in the mamximum magnitudes between our model and the model of Stucchi *et al.* (2011) was emphasized (section 4.8.2.1).

In order to test the influence of the maximum magnitude estimation, we used the seismotectonic model 1 with the original seismicity catalog and the Boore & Atkinson (2008) GMPE. We modified the maximum magnitude in our seismotectonic model by limiting the maximum magnitude to 6.3 in each seismic source. Figure 46 shows the mean hazard curves for a particular point (n° 508, located east of Grenoble). The geographical variations of estimated PGA corresponding to the two maximum magnitude models are shown in Figure 47.

Clearly, the assumption made on the maximum values influence the hazard at the largest return period of interest for this study. With a maximum magnitude comparable to the one's adopted in Italy a decrease of about 10-15% is observed in the Alps.

This suggests that the WP1 could implement a specfic task on the maximum magnitude in the region of interest.
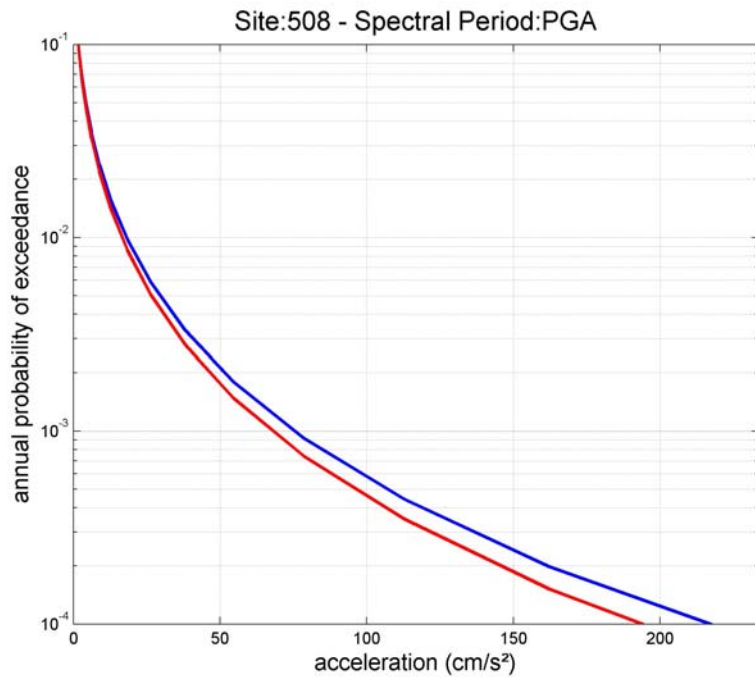
Figure 46 - Mean hazard curve for PGA, at the point 508 of the region of interest, and for SM1, the original catalog, the Boore & Atkinson (2008) GMPE. The blue curve corresponds to the original Mmax and the red curve corresponds to limited Mmax to a maximum value of 6.3.
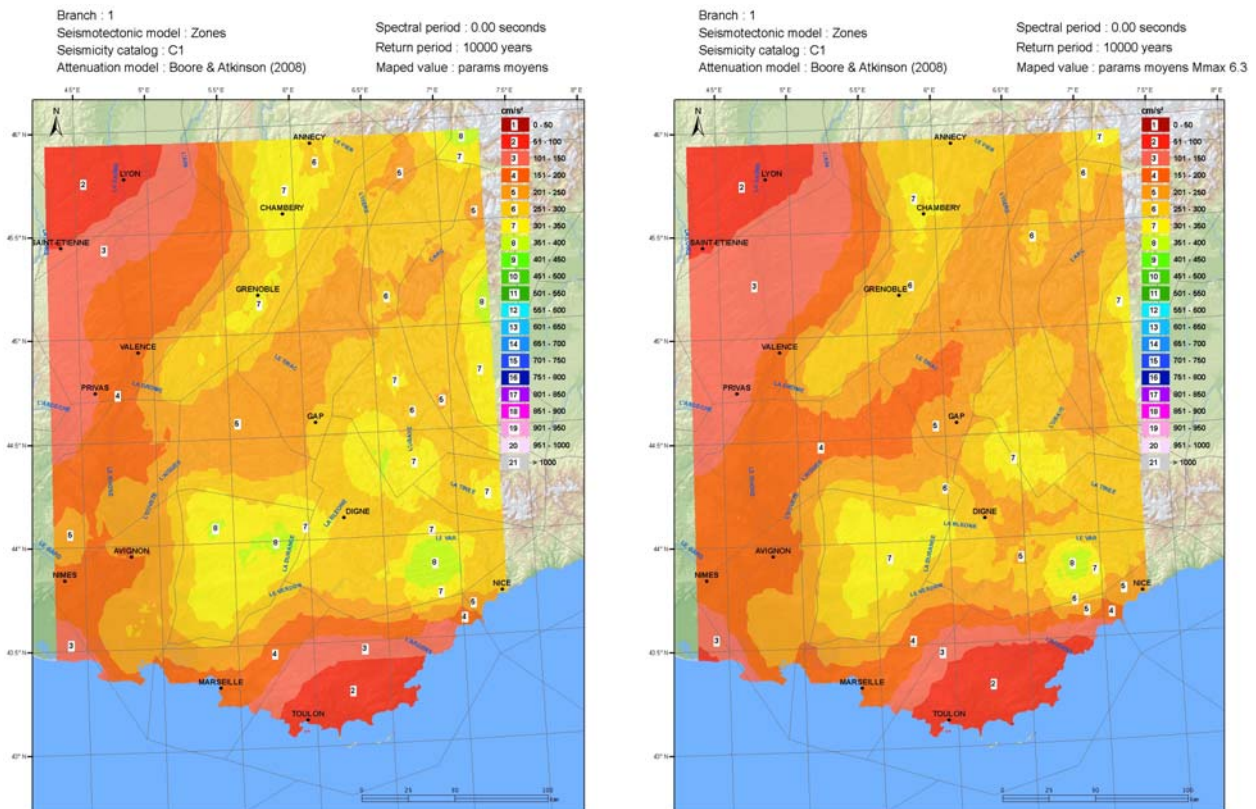
Figure 47 – Mean hazard maps for PGA using SM1, the original catalog, and the Boore & Atkinson (2008) GMPE. The map on the left corresponds to the original Mmax and the map on the right corresponds to limited Mmax to a maximum value of 6.3.

7.   Concluding remarks

The objective of the task 4-1 was to produce maps and hazard curves, based on available data and models and using current state of practice in the country, at the beginning of the project and to provide necessary inputs (maps, hazard curves and response spectra) to the others tasks of the project. The results of the initial PSHA will be used in the future to appreciate the benefits of SIGMA at the end of the project.

The PSHA level is comparable to a SSHAC level 2 (Budnitz et al., 1997). The conceptual logic tree tries to capture a representative range of possibilities, especially regarding the seismotectonic sources and ground motion prediction equations, based on the available data at the beginning of the project.The epistemic branches of the logic tree refer to the seismic source models, the GMPEs, the catalogue of seismicity and associated completeness periods and Gütenberg-Richter parameters, and to the maximum magnitudes. The other uncertainties represent the aleatory variability of the earthquakes distribution within the seismic source (location and depth), of the time of occurrence and of the ground motion. A zoneless model was implemented to compare the results obtained with the logic tree based on source zones models.

Three seismic area source models are used based on different criteria for thedelineation of the seismic sources. The model 1 is an area source model based on previous Geoter works ; the model 2 tries to better identify the fault systems in four regions (Provence faults system, the Tricastin cluster, the Belledone and the Nimes faults ; the model 3 is an area source model based on previous IRSN works, and significantly differs from model 1 and 2 by the large size of the seismic sources.

One of the challenge was to select a limited set of 4 GMPEs, verifying as much as possible the principle of mutual exclusiveness and collective exhaustiveness, and considering that the Berge-Thierry et al. (2003) GMPE was mandatory. The Akkar & Bommer (2010), Boore & Atkinson (2008, 2011) and Zhao et al. (2006) GMPEs are the other selected GMPEs.

All calculations were done considering a Mmin value Mw 4.5 and an integration up to 3σ of the GMPEs. Hazard curves were computed for all branches of the logic-tree at all common spectral periods of the GMPEs, using weights defined by the PSHA team.

For a given annual probability of exceedance, the mean, median and percentiles values of hazard curves were obtained by statistical treatment of all branches. They are used to build the maps and the uniform hazard spectra at 20 selected sites of interest and at 5 return periods from 100 years to 10.000 years.

The results at 475 years tends to be lower than those obtained in previous PSHA studies (MEDD 2002, AFPS 2006), while there is no reference to compare at 10.000 years. The percentage of variation from the median to the percentiles 16% and 84% varies from one site to the other, in large proportions (15-20% for the lower variability up to 70-75% for the larger).

All the results are made available to the SIGMA partners on a DVD. The hazard curves are available for 3 spectral periods (PGA, 0.2 and 1 second) at each point of the calculation grid. They are provided at the 15 common periods of the GMPEs together with the uniform hazard spectra, at the 20 selected sites.

Sensitivity analysis of the different hypothesis (seismoteconic model, zoneless approach, GMPEs, Catalogue of seismicity) was implemented using the results of individual branches or group of branches. A zoneless approach was implemented with the Berge-Thierry et al. (2003) GMPE, for comparison with the zoning approach. It introduces a significant variability which is a function of the location of historical events and the shape of the adopted kernel function.

All the results are not analyzed yet, which requires a significant post-processing effort. Different issues can be highlighted because they could be addressed in the workpackages of SIGMA :

- One of the weak points of the preliminary model comes from the earthquake catalog, the homogenization of the moment magnitude being not calibrated with appropriate procedures. While an instrumental catalogue is in preparation (in collaboration with the SI-Hex national program), a specific effort should be paid on the definition of the Mw magnitude of historical events that control the Gütenberg-Richter parameters. One solution could be to obtain the agreement from IRSN, to benefit from their works on the magnitude homogeneization of events of the Sisfrance database ;

- The introduction of three seismotectonic models, even established considering different criteria, does not affect significantly the hazard in some regions. We have observed, in higher PSHA level implemented for individual sites in the region of interest, that the consideration of a 3D fault model can significantly impact the hazard for sites located in the fault vicinity. In complement of the research works implemented for some individual faults, the WP1 could contribute in the development of more homogeneous fault model, at the scale of the region of interest, with 3D geometry description and activity parameters consistent with the use of a characteristic model ;

- In the Provence region, where the only strong known historical earthquake occurred in 1909, the introduction of an elapsed time model or a non poissonian model could also affect the hazard pattern. Such a model is planed for the Po plain PSHA implemented by the Italian group of SIGMA. It should be analyzed, in which part of the region of interest the state of knowledge allows the definition of the input parameters of such models ;

- The comparison of the results between zoning and zoneless approaches, advocates for the introduction of zoneless approach in the total logic tree. This implies to implement this model with the same GMPEs as those used in the zoning approach ;

- The thickness of the seismogenic layer remains a poorly determined parameter. The present models adopt a uniform and aleatory distribution within this layer. A conditional distribution function of the depth with magnitude size, could be introduced in the future, if the depth distribution can be better determined ;

- For the purpose of the comparisons between predictions and observations, and because most of recorded motions correspond to small earthquakes, new GMPEs with validity domain extended to low magnitudes should be integrated ;

- The preliminary model suffers from a limited number of epistemic branches. Additional epistemic branches should be included in the final PSHA to enlarge the range of possibilities. Their definition will result from the outputs of the SIGMA workpackages.

8. Bibliographie

ABRAHAMSON NA, BIRKHAUSER P, KOLLER M, MAYER-ROSA D, SMIT PM, SPRECHER C, TINIC S and GRAF R (2002) PEGASOS- A comprehensive probabilistic seismic hazard assessment for nuclear power plants in Switzerland. In: Proceedings of the 12 ECEE, London, 9-13 September 2002, paper no. 633

ABRAHAMSON N (2006) Seismic hazard assessment: problems with current practice and future developments. In: Proceedings of the 13 ECEE, Geneva, 3-8 September 2006, keynote address k2.

ABRAHAMSON N., ATKINSON G., BOORE D., BOZORGNIA Y., CAMPBELL K., CHIOU B., IDRISS I.M., SILVA W. and YOUNGS R. (2008). Comparisons of the NGA ground-motion relations. *Earthquake Spectra, Vol. 24, n° 1, p. 45-66.*

ABRAHAMSON N. and SILVA W. (2008). Summary of the Abrahamson and Silva NGA ground-motion relations. *Earthquake Spectra, Vol. 24, n° 1, p. 67-97.*

ABRAHAMSON N. and SILVA W. (2009).Erratum to "Summary of the Abrahamson and Silva NGA ground-motion relations". *Published on PEER NGA website.*

AKKAR S. and BOMMER J.J. (2007). Empirical prediction equations for peak ground velocity derived from strong-motion records from Europe and the middle East. *Bulletin of the Seismological Society of America, Vol. 97, n° 2, p. 511-530.*

AKKAR, S. and BOMMER, J.J., 2010. "Empirical Equations for the Prediction of PGA, PGV and Spectral Accelerations in Europe, the Mediterranean Region and the Middle East," Manuscript accepted for publication in Seismological Research Letters.

AMBRASEYS N. N. and JACKSON J. A. (1998). Faulting associated with historical and recent earthquakes in the eastern Mediterranean region. *Geophys. J. Int., 133, p. 390-406*

AMBRASEYS N. N. and FREE M.W. (1997). Surface-wave magnitude calibration for European earthquakes. *Journal of Earthquake Engineering., 1:1,1-22.*

ARVIDSSON, R.; GRÜNTHAL, G. (2010): The SHARE European seismic source zone model. 32nd General Assembly European Seismological Commission (Montpellier, France 2010).

AUTRAN A., BLES J.-L., COMBES P., CUSHING M., DOMINIQUE P., DUROUCHOUX C., GARIEL J.-C., GOULA X., MOHAMMADIOUN B. and TERRIER M. (1998). Probabilistic seismic hazard assessment in France ; Part one : seismotectonic zonation. *11th European Conference on Earthquake Engineering, 1998, Balkema, Rotterdam.*

BAKUN W.H. and SCOTTI O. (2006). Regional intensity attenuation models for France and the estimation of magnitude and location of historical earthquakes. Geophysical Journal International, 164, p. 596-610

BAIZE S., CUSHING M., LEMEILLE F., GRANIER T., GRELLET B., CARBON D., COMBES P. et HIBSCH C. (2002). Inventaire des indices de rupture affectant le quaternaire, en relation avec les

grandes structures connues en France métropolitaine et dans les régions limitrophes. *IRSN, Mémoires de la société géologique de France, n° 175, 143 p.*

BAIZE S., CUSHING M., LEMEILLE F., JOMARD H. (2011). Révision du zonage sismotectonique de la France pour l'évaluation de l'aléa sismique. *Proceedings du 8ème colloque national AFPS..*

BEAUVAL C. (2003). Analyse des incertitudes dans une estimation probabiliste de l'aléa sismique, exemple de la France. *Thèse de doctorat de l'université Joseph Fourier*, p.1-161, 74 fig., 15 tabl.

BEAUVAL C. and SCOTTI O. (2004). Quantifying sensitivities of PSHA for France to earthquake catalog. Uncertainties, truncation of ground-motion variability, and magnitude limits. *Bulletin of the Seismological Society of America*, Vol. 94, n° 5, p. 1579-1594

BEAUVAL C., BARD P.-Y., HAINZL S. and GUEGUEN P. (2008). Can strong-motion observations be used to constrain probabilistic seismic-hazard estimates ?. *Bulletin of the Seismological Society of America*, Vol. 98, n° 2, p. 509-520

BEAUVAL C., HAINZL S., SCHERBAUM F. (2006). Probabilistic seismic hazard estimation in low-seismicity regions considering non-Poissonian seismic occurrence. *Geophysical Journal International*, Vol. 164, p. 543-550

BEAUVAL C., SCOTTI O., BONILLA F. (2009). The role of seismicity models in probabilistic seismic hazard estimation: comparison of a zoning and a smoothing approach. *Geophysical Journal International*, vol. 165, p. 584-595, doi: 10.1111/j.1365-246X.2006.02945.x

BECKER A., FERRY M., MONECKE K. SCHNELLMANN M. and GIARDINI D. (2005). Multiarchive paleoseismic record of late pleistocene and holocene strong earthquakes in Switzerland. *Tectonophysics, 400, p. 153-177*

BERGE-THIERRY C., CUSHING E., SCOTTI O. and BONILLA F. (2004). Determination of the seismic input in France for the nuclear power plants safety : Regulatory context, hypothesis and uncertainties treatment. Proceedings of the CSNI Workshop on seismic input motions, incorporating recent geological studies, Tsukuba, Japan, 15-17 November, 14 p.

BERGE-THIERRY C., REY J. and LAVARENNE S. (2007). On the selection of time series representative of site specific seismic motion. Transactions, SMiRT 19, Toronto, August 2007. Transactions, SMiRT 19, Toronto, August 2007.

BEYER, K., and J.J. BOMMER, 2006, "Relationships between Median Values and Between Aleatory Variabilities for Different Definitions of the Horizontal Component of Motion." Bulletin of the Seismological Society of America," Vol. 96, No. 4A, pp. 1512-1522.

BLES J.-L., BOUR M., DOMINIQUE P., GODEFROY P., MARTIN C. et TERRIER M. (1998). Zonage sismique de la France métropolitaine pour l'application des règles parasismiques aux installations classées. Document BRGM n°279, p.1-56., 8 fig., 5 tabl.

BOMMER, J. J., F. SCHERBAUM, H. BUNGUM, F. COTTON, F. SABETTA, and N. A. ABRAHAMSON (2005). On the use of logic trees for groundmotion prediction equations in seismic hazard assessment. Bulletin of the Seismological Society of America 95 (2), 377–389.

BOMMER, J.J., P.J. STAFFORD, J.E. ALARCON & S. AKKAR (2007). The influence of magnitude range on empirical ground-motion prediction. Bulletin of the Seismological Society of America 97(6), 2152-2170.

BOMMER J.J., DOUGLAS J., SCHERBAUM F., COTTON F., BUNGUM H. and FAH D. (2010). On the selection of ground-motion prediction equations for seismic hazard analysis. *Seismological Research Letters, Vol. 81, n° 5, p. 783-793.*

BOMMER J.J., AKKAR S. and DROUET S. (2011). Extending ground-motion prediction equations for spectral acceleration to higher response frequencies. *Bulletin of Earthquake Engineering, in press.*

BOURGEOIS O., FORD M., DIRAISON M., LE CARLIER DE VESLUD C., GERBAULT M., PIK R., RUBY N. and BONNET S. (2005). Separation of riftng and lithospheric folding signatures in the NW-Alpine foreland. *International Journal Earth Sciences, 29 p.*

BRAUNMILLER J., DEICHMANN N., GIARDINI D., WIEMER S. and THE SED MAGNITUDE WORKING GROUP (2005). Homogeneous moment-magnitude calibration in Switzerland. Bulletin of the Seismological Society of America, Vol. 95, n° 1, p. 58-74

BOORE D.M. and ATKINSON G.M. (2008). Ground-motion prediction equations for the average horizontal component of PGA, PGV, and 5%-damped PSA at spectral periods between 0.01 and 10s. *Earthquake Spectra, Vol. 24, n° 1, p. 67-97.*

BRUNE J.N. (1970). Tectonic stress and the spectra of seismic shear waves from earthquakes. *Journal of Geophysical Research, Vol. 75, n° 26, p. 4997-5009.*

BRUNE J.N. (1971). Erratum to "Tectonic stress and the spectra of seismic shear waves from earthquakes". *Journal of Geophysical Research, Vol. 76, p. 5002.*

BUDNITZ, R.J. APOSTOLAKIS, G., BOORE, D.M., CLUFT, L.S., COPPERSMITH, K.J., CORNELL, C.A. & MORRIS, P.A. 1997: Recommendations for probabilistic seismic hazard analysis: guidance on uncertainty and use of experts. *U.S. Nuclear Regulatory Commission, NUREG/CR-6372.*

CAMPBELL K.W. (2003). Prediction of strong ground-motion using the hybrid empirical method and its use in the development of ground-motion (attenuation) relations in Eastern North America. *Bulletin of the Seismological Society of America, Vol. 93, n° 3, p. 1012-1033.*

CAMPBELL, K.W. & Y. BOZORGNIA (2008). NGA ground motion model for the geometric mean horizontal component of PGA, PGV, PGD and 5%-damped linear elastic response spectra at periods ranging from 0.1 s to 10.0 s. Earthquake Spectra 24(1), 139-171.

CAUZZI C. and FACCIOLI E. (2008). Broadband (0.05 to 20 s) prediction of displacement response spectra based on worldwide digital records. *Journal of Seismology, Vol. 12, n° 4, p. 453-475.*

CHIOU B.S.-J. and YOUNGS R.R. (2008). An NGA model for the average horizontal component of peak ground motion and response spectra. *Earthquake Spectra, Vol. 24, n° 1, p. 173-215.*

CHIOU, B.S-J., YOUNGS, R.R., ABRAHAMSON, N. & ADDO, K., (2010).Ground-motion attenuation Model for small-to-moderate shallow crustal earthquakes in California and its implication on regionalization of ground-motion prediction models. Earthquake Spectra 26(4), 907-926.

CLEMENT C., SCOTTI O., BONILLA L., BAIZE S., BEAUVAL C. (2004). Zoning versus faulting models in PSHA for moderate seismicity regions: preliminary results for the Tricastin nuclear site, France. *Bollettino di Geofisica Teorica ed Applicata, Vol. 45, n° 3, p. 187-204*

CLEMENT C., CARBON D., MARTIN C.., GUIGNARD P., and BELLIER O. (2009). Probabilistic seismic hazard assessment in Western Provence based on a faults seismotectonic model. *Proceedings colloque Provence 2009.*

CLOETINGH S. and the ENTEC Team (2002). The northern alpine foreland natural laboratory : Neotectonic hazard and the ENTEC project. ENTEC Spring Workshop, Vienna, 12 April 2002, 4 p.

CLOETINGH S., CORNU T., ZIEGLER P.A. and BEEKMAN F. (2006). Neotectonics and intraplate continental topography of the northern Alpine Foreland. *Earth-Science Reviews*, Vol. 74, p.127-196

CLOETINGH S., ZIEGLER P. A., BEEKMAN F., ANDRIESSEN P. A. M., HARDEBOL N. and DEZES P. (2005). Intraplate deformation and 3D rheological structure of the Rhine rift system and adjacent areas of the northern Alpine foreland. *International Journal Earth Sciences*, Vol. 94, n° 4, p. 758-778

CLOETINGH S., ZIEGLER P.A., BEEKMAN F., ANDRIESSEN P.A.M., MATENCO L., BADA G., GARCIA-CASTELLANOS D., HARDEBOL N., DEZES P. and SOKOUTIS D. (2005). Lithospheric memory, state of stress and rheology: neotectonic controls on Europe's intraplate continental topography. *Quaternary Science Reviews*, 24, p. 241-304

COTTON, F., F. SCHERBAUM, J. J. BOMMER, and H. BUNGUM (2006). Criteria for selecting and adjusting ground-motion models for specific target applications: Applications to Central Europe and rock sites. Journal of Seismology 10 (2), 137–156.

COTTON F., POUSSE G., BONILLA F. and SCHERBAUM F. (2008). On the discrepancy of recent European ground-motion observations and predictions from empirical models: analysis of KiK-net accelerometric data and point-sources stochastic simulations. *Bulletin of the Seismological Society of America, Vol. 98, n° 5, p. 2244-2261.*

CUSHING M., BELLIER O., NECHTSCHEIN S., SEBRIER M., LOMAX A., VOLANT PH., DERVIN P., GUIGNARD P and.BOVE L. (2007): A multidisciplinary study of a slow-slipping fault for seismic hazard assessment : the example of the Middle Durance Fault (SE France). *Geophys. J. Int.* doi: 10.1111/j.1365-246X.2007.03683.x

DELACOU B. (2004). Tectonique et géodynamique actuelle de l'arc alpin - Approche sismotectonique et modélisation numérique. *Thèse, Université de Neuchätel et Université de Nice Sophia-Antipolis, 182 p.*

DELACOU B., SUE C., CHAMPAGNAC J.-D. and BURKHARD M. (2004). Present-day geodynamics in the bend of the western and central Alps as constrained by earthquake analysis. *Geophysical Journal international, n° 158, p. 753-774*

DELACOU B., SUE Ch., NOCQUET J.-M., CHAMPAGNAC J.-D., ALLANIC C., BURKHARD M. (2009). Quantification of strain rate in the Western Alps using geodesy: comparisons with seismotectonics. *Swiss Journal of Geosciences, vol. 101, p. 377-385, DOI 10.1007/s00015-008-1271-3*

DELAVAUD E., COTTON F., AKKA S., SCHERBAUM F. BEAUVAL C., DROUET S. DANCIU L. SEGOU M., DOUGLAS J., BOMMER J., FACCIOLI E., BONILLA F., BUNGUM H., THEODULIDIS N. Toward a groud-motion logic tree for PSHA in Europe. Submitted to Journal os Seismology as a general paper.

DÈZES P. AND ZIEGLER P.A. (2002). Map of the European Mohorovicic discontinuity. EUCOR-URGENT homepage (http://comp1.geol.unibas.ch/).

DEZES P., SCHMID S.M. and ZIEGLER P.A. (2004). Evolution of the European Cenozoic Rift System: interaction of the Alpine and Pyrenean orogens with their foreland lithosphere. *Tectonophysics*, Vol. 389, p. 1-33

DELAVAUD E., COTTON F., AKKAR S., SCHERBAUM F., BEAUVAL C., DROUET S., DANCIU L., SEGOU M., DOUGLAS J., BOMMER J.J., FACCIOLI E., BONILLA F., BUNGUM H. and THEODULIDIS N. (2011). Toward a ground-motion logic tree for PSHA in Europe. *Submitted to Journal of Seismology as a general paper.*

DOUGLAS J., BUNGUM H. and SCHERBAUM F. (2006). Ground-motion prediction equations for southern Spain and southern Norway obtained using the composite model perspective. *Journal of Earthquake Engineering, Vol. 10, n° 1, p. 33-72.*DOUGLAS J. (2010). Ground-motion prediction equations 1964-2010. *Final report RP-59356-FR, BRGM, Orléans, France.*

DOUGLAS J., FACCIOLI E., COTTON F. and CAUZZI C. (2010). Selection of ground-motion prediction equations for GEM1. *GEM Technical Report E1, GEM Foundation, Pavia, Italy.*

DROUET S., COTTON F., BEAUVAL C. and AKKAR S. (2010). Regionally adjusted ground motion prediction equations (GMPE) for Europe. *Deliverable 4.2 of the SHARE European project.*

DROUET, S., COTTON, F. AND GUÉGUEN P. (2010). VS30, kappa, regional attenuation and Mw from accelerograms: application to magnitude 3–5 French earthquakes Geophysical Journal International, 182, 2, p. 880–898, DOI : 10.1111/j.1365-246X.2010.04626.x

DROUET S., NICOLAS M. AND HERNANDEZ B. (2007). Analyse de la base de données de mouvements forts Européenne: dans quelle mesure des effets de site sont contenus dans cette base? *7ème Colloque National AFPS 2007, 4-6 juillet 2007, Châtenat-Malabry, France.*

GIARDINI D., WIEMER S., FAHD. and DEICHMANN N. (2004). Seismic hazard assessment of Switzerland, 2004. *Report, Swiss Seismological Service*

GRUNTHAL G. and WAHLSTROM R. (2003). An Mw based earthquake catalogue for central, northern and northwestern Europe using a hierarchy of magnitude conversions. Journal of seismology, 7, p. 507-531

GRÜNTHAL, G.; WHALSTROM, R.; STROMEYER, D. (2009a): The unified catalogue of earthquakes in central, northern and northwestern Europe (CENEC)-updated and expanded to the last millenium. *Journal of seismology ; 13, 4,517-541.*

GRÜNTHAL, G.; STROMEYER, D. ; WHALSTROM, R.; (2009b): Harmonization check of Mw within the central, northern and northwestern European earthquake catalogue. *Journal of seismology ; 13, 4,613-632.*

GRÜNTHAL, G.; ARVIDSSON, R.; BOSSE, C. (2010): Earthquake model for the European-Mediterranean Region for the purpose of GEM1, Scientific *Technical Report* ; 10/04, *Deutsches GeoForschungsZentrum* GFZ, 35 p.

HINTERSBERGER, E., SCHERBAUM, F., HAINZL, S. (2007): Update of likelihood-based groundmotion model selection for seismic hazard analysis in western central Europe. - Bulletin of Earthquake Engineering, 5, 1, 1-16,

HOLLENDER F. (2005). Réunion "Faille de la Moyenne Durance" du 01 Octobre 2004 au Château de Cadarache. CEA/DEN/CAD/DTAP/CASI, Compte rendu de réunion, 8 p.

HOLLENDER F. (2007). Etude de définition du projet d'acquisition de nouveaux profils de sismique réflexion profonde. Réunion d'enclenchement - 27 novembre - Cadarache. Compte Rendu de Réunion, 60 p.

JIMÉNEZ, M.-J., GIARDINI, D. AND GRÜNTHAL, G.: The ESC-SESAME unified hazard model for the European-Mediterranean region. EMSC/CSEM Newsletter 19, 2-4, 2003.

KAKLAMANOS, J., L. G. BAISE, and D. M. BOORE (2011). Estimating unknown input parameters when implementing the NGA ground-motion prediction equations in engineering practice, Earthquake Spectra http://www.daveboore.com/pubs_online/eqs_revised_manuscript_final_08dec10.pdf

KIJKO, A., (2002). Seismic Hazard Assessment for Specified Area. Estimation of maximum regional magnitude Mmax. Theory for program Hn2, Release 2.08.

KIJKO A. (2002). Statistical estimation of maximum regional earthquake magnitude Mmax. Proceedings of the 12th European Conference on Earthquake Engineering. Londres, 2002.

KISSLING, E., SCHMID, S.M., LIPPITSCH,R., ANSORGE, J. & FÜGENSCHUH,B. (2006). Lithosphere structure and tectonic evolution of the Alpine arc: new evidence from high-resolution teleseismic tomography. In: Gee, D.G. & Stephenson, R.A. (eds) European Lithosphere Dynamics. *Geological Society, London, Memoirs*, 32, 129-145.

LAMBERT J., WINTER T., DEWEZ T.J.B. and SABOURAULT P. (2005). New hypotheses on the maximum damage area of the 1356 Basel earthquake (Switzerland). Quaternary Science Reviews, 24, p. 383-401

LE PICHON X., RANGIN C. (2010). Geodynamic of the France Southeast Basin: importance of gravity tectonics. Thematic issue edited by Le Pichon and Rangin, *Bull. Soc. géol. Fr.,* 2010, t. 181, no 6.

LEVRET A., BACKE J. C. and CUSHING M. (1994). Atlas of macroseismic maps for French earthquakes with their principal characteristics. Natural hazards, 10, p 19-46

LEVRET A., CUSHING M et PEYRIDIEU G. (1996). Recherche des caractéristiques de séismes historiques en France. Institut de Protection et de Sûreté Nucléaire, Vol. 1, 399 p., Vol. 2, Atlas de 140 cartes macrosismiques

MARCHANT R. (1993). The underground of the Western Alps. Thèse de Doctorat, Université de Lausanne, Mémoire de Géologie, n° 15, 3 p.

MARTIN Ch., COMBES Ph., SECANELL R., LIGNON G., CARBON D., FIORAVANTI A., GRELLET B. (2002). Révision du zonage sismique de la France. Etude probabiliste. Rapport GEOTER. GTR/MATE/0701-150.

MARTELET G., PAJOT G. et DEBEGLIA N. (2009). Nouvelle carte gravimétrique de la France : RCGF09 - Réseau et carte gravimétrique de la France, 2009. BRGM, Rapport, BRGM/RP-57908-FR, 77 p., 26 fig., 2 annexes

MOUROUX B., BRULHET J. (1997). La démarche scientifique de l'Andra, Site du Gard. In Etude du Gard Rhodanien, EDP Sciences ANDRA CNRS, Actes des Journées Scientifiques CNRS/ANDRA, Bagnols-sur-Cèze, 20, 21 octobre 1997.

MUSSON, R.M.W. [2009] "Ground motion and probabilistic hazard", Bull. Earthq. Eng., doi 10.1007/s10518-009-9108-7.

MUGNIER J.L., BERGERAT F., DAMOTTE B., GUELLEC S., NICOLAS A., POLINO R., ROURE F., TARDY M. and TRUFFERT C. (1996). Crustal structure of the Western Alps and their forelands. *Mémoires de la Société Géologique de France*, n° 170, p. 73-97

MUGNIER J.L., GUELLEC S., MENARD G., ROURE F., TARDY M. and VIALON P. (1990). A crustal scale balanced cross-section through the external Alps deduced from the ECORS profile. *Mémoires de la Société Géologique de France*, N.S., n° 156, p. 203-216

NICOLAS, A., HIRN, A., NICOLICH, R., POLINO, R. and ECORS-CROP Working Group, 1990. Lithospheric wedge in the western Alps inferred from the ECORS-CROP traverse. *Geology*, 18, 587-590.

NOCQUET J.-M., CALAIS E. (2004). Geodetic Measurements of Crustal Deformation in the Western Mediterranean and Europe. *Pure appl. geophys.*, 161, p. 661-681.

NOCQUET, J.M. & CALAIS, E. (2003). Crustal velocity field of Western Europe from permanent GPS array solutions, 1996–2001. Geophysical Journal International 154(1), 72–88.

PAPAZACHOS B.C., SCORDILIS E.M., PANAGIOTOPOULOS D.G., PAPAZACHOS C.B., KARAKAISIS G.F. (2004). Global relations between seismic fault parameters and moment magnitude of earthquakes. Bull. of the Geological Society of Greece, vol. 36, Proceedings of the 10th International Conrees, Thessaloniki, p. 1482-1489.

PFIFFNER, O., LEHNER, P., HEITZMANN, P., MUELLER, S. AND STECK, A., 1997. Deep structure of the Swiss Alps: results of NRP20. *Birkhäuser Verlag*, Basel.

PIQUARD V., (2010). Statistical study of seismic magnitudes. Rapport PHIMECA RT-1001BST003-001C.

RANGIN CL., LE PICHON X, HAMON Y., LOGET N., and CREPY A. (2010) Gravity tectonics in the SE Basin (Provence, France) imaged from seismic reflection data. *Bull. Soc. géol. Fr.,* 2010, t. 181, no 6, pp. 503-530.

REGNIER J., A. LAURENDEAU, A.-M. DUVAL et P. GUEGUEN (2010). "From heterogeneous set of soil data to Vs profile: Application on the French permanent accelerometric network (RAP) sites". Poster, 14ECEE, Ohrid, République de Macédoine, 30 aout-3 septembre 2010. Produit LCPC n°OP11R065/2010/ERA6/08.

REY J. and BERGE-THIERRY C. (2005). Propositions et recommandations pour la selection et la generation d'accélérogrammes integrant la variabilité des indicateurs du mouvement sismique. Rapport DEI/SARG/2005-022.

SCHERBAUM, F., F. COTTON, and P. SMIT (2004). On the use of response spectral reference data for the selection of ground-motion models for seismic hazard analysis: the case of rock motion. Bulletin of the Seismological Society of America 94 (6), 2,164–2,185.

SCHERBAUM F., COTTON F. and STAEDTKE H. (2006). The estimation of minimum-misfit stochastic models from empirical ground-motion prediction equations. *Bulletin of the Seismological Society of America, Vol. 96, n° 2, p. 427-445.*

SCHERBAUM, F., E. DELAVAUD, and C. RIGGELSEN (2009). Model selection in seismic hazard analysis: An information-theoretic perspective. Bulletin of the Seismological Society of America 99 (6), 3,234–3,247.

SINGH S.K, BAZAN E., and ESTEVA L. (1980). Expected Earthquake Magnitude from a Fault. Bulletin of the Seismological Society of America, Vol. 70, No. 3, pp. 903-914, June 1980.

SCHMID S. and KISSLING E. (2000). The arc of the western Alps in the light of geophysical data on deep crustal structure. *Tectonics*, Vol. 19, n°1, p. 62-85

TESAURO M., HOLLENSTEIN C., EGLI R., GEIGER A. and KAHLE H.-G. (2006). Analysis of central western Europe deformation using GPS and seismic data. *Journal of Geodynamics*, 42, p. 194-209

TARDY M., DEVILLE E., FUDRAL S., GUELLEC S., MENARD G., THOUVENOT F. et VIALON P. (1990). Interprétation structurale des données du profil de sismique réflexion profonde ECORS-CROP

Alpes entre le front Pennique et la ligne du Canavese (Alpes occidentales). *Mém. Soc. Géol. France*, N.S., n° 156, p. 217-226

TERRIER M. (2006). Identification et hiérarchisation des failles actives de la Région Provence-Alpes-Côte d'Azur, Phase 3 : Hiérarchisation des failles actives. BRGM, Rapport final, BRGM/RP-53930-FR, 216 p.

TERRIER M. et WINTER T. (2006). Nouvelles données sur le système de failles le Fare-Eguilles, implication en terme d'aléa sismique pour la région PACA (secteur de l'étang de Berre, Lambesc, Aix-en-Provence). Rapport BRGM/RP-55233-FR-Décembre 2006, 26 p.

TERRIER M., COURRIOUX G., MARTELET G., BITRI A., HANOT F. (2008). Etude de la faille de Salon-Cavaillon (région PACA, France). Rapport BRGM/RP-55989-FR, Février 2008.

THOUVENOT F., FRECHET J., JENATTON L. and GAMOND J. F. (2003). The Belledonne Border Fault: Identification of an active seismic strike-slip fault in the western Alps. *Geophys. J. Int.*, 155, p. 174-192.

THOUVENOT F., JENATTON L and GRATIER J.P. (2009). 200-m-deep earthquake swarm in Tricastin (lower Rhône Valley, France) accounts for noisy seismicity over past centuries. *Terra Nova*, 21, 203–210.

TORO G., ABRAHAMSON N.A. and SCHNEIDER J.F. (1997). Model of strong ground motions from earthquakes in Central and Eastern North America: best estimates and uncertainties. *Seismological Research Letters, Vol. 68, n° 1, p. 41-57.*

VAN HOUTTE C., DROUET S. and COTTON F. (2011). Analysis of the origins of K (kappa) to compute hard rock to rock adjustment factors for GMPEs. *Bulletin of the Seismological Society of America, in press.*

VIGNY C., CHERY J., DUQUESNOY T., JOUANNE F., AMMANN J., ANZIDEI M., AVOUAC J.-P., BARLIER F., BAYER R., BRIOLE P., CALAIS E., COTTON F., DUQUENNE F., FEIGL K. L., FERHAT G., FLOUZAT M., GAMOND J.-F., GEIGER A., HARMEL A., KASSER M., LAPLANCHE M., LE PAPE M., MARTINOD J., MENARD G., MEYER B., RUEGG J.-C., SCHEUBEL J.-M., SCOTTI O., VIDAL G. (2002). GPS network monitors the Western Alps' deformation over a five-year period : 1993-1998. *Journal of Geodesy,* Vol. 76, p. 63 – 76.

WALPERSDORF A., BAIZE S., CALAIS E., TREGONING P., NOCQUET J.-M. (2006). Deformation in the Jura Mountains (France). First results from semi-permanent GPS measurements. *Earth and Planetary Science Letters*, 245, p. 365-372.

WELLS D. L. and COPPERSMITH K. J. (1994). New empirical relationships among magnitude, rupture length, rupture with, rupture area, and surface displacement. *Bulletin of the Seismological Society of America, Vol. 84, n° 4, p. 974-1002*

WESNOUSKY S.G. (2008). Displacement and Geometrical Characteristics of Earthquake Surface Ruptures: Issues and Implications for Seismic-Hazard Analysis and the Process of Earthquake Rupture. *Bull. Seismo. Soc. Am.,* 98, 4, p. 1609-1632

ZHAO J.X., ZHANG J., ASANO A., OHNO Y., OOUCHI T., TAKAHASHI T., OGAWA H., IRIKURA K., THIO H.K., SOMERVILLE P.G., FUKUSHIMA Y. and FUKUSHIMA Y. (2006). Attenuation relations of strong ground motion in Japan using site classification based on predominant period. *Bulletin of the Seismological Society of America, Vol. 96, n° 3, p. 898-913.*

ZIEGLER P. A. and DEZES P. (2006). Crustal evolution of western and central europe. European Lithosphere Dynamic, Memoir of the Geological Society, London, Vol. 32, p. 43-56

ZIEGLER P.A. and DEZES P. (2005). Neogene uplift of Variscan massifs in the Alpine foreland : timing and controlling mechanisms. n: J.H. Behrmann, M. Granet, S. Schmid and P.A. Ziegler (Editors), EUCOR-URGENT Special Issue. *International Journal of Earth Sciences*, Volume 94, Number 4, p. 594 - 614.

ZIEGLER P.A., DEZES P. (2007). Cenozoic uplift of Variscan Massifs in the Alpine foreland : timing and controling mechanisms. *Global and Planetary Change*, 58, p. 237-269.

SIGMA. WP4 T4-1.

Probabilistic analysis for France's southeast ¼

to produce a preliminary

« classical » hazard map

<u>Annex 1 : Structure and format</u>

<u>of the numerical results</u>

Type of document :	**identification :**
Final report	Report GTR/ARE/0212-924

1. **Structure of the directories**

The results are separated into two different directories :

- *maps_3SP*. This directory contains results for a grid of 858 points covering the South-East of France. PSHA is computed for 3 spectral periods : PGA, 0.2 and 1.0 sec.
- *sites_15SP*. This directory contains results for 20 points of interest distributed homogeneously within the calculation grid described above. PSHA is computed for 15 spectral periods : PGA, 0.03, 0.05, 0.1, 0.15, 0.2, 0.25, 0.3, 0.4, 0.5, 0.75, 1.0, 1.5, 2.0, and 3.0 sec.

In each of these directories, two sub-directories are created :

- *logic_tree*. This directory contains the results corresponding to the logic-tree implemented in the study. The results for the total logic tree and for the different individual branches are included.
- *zoneless_for_comparison*. This directory contains the results of the zoneless approach which are not included in the logic-tree, but allows us to compare the zoning and zoneless approaches.

Under these directories, the structure follows the logic-tree structure :

- A first level of directories refers to the seismotectonic model used (*M1*, *M2*, or *M3*) for the zoning approach (used in the logic tree), or to the Kernel function used (*Zl1*, *Zl2*, or *Zl3*) for the zoneless approach.
- A second level of directories refers to the seismicity catalogue used : *C1* for the original catalogue, and *C2* for the synthetic one.
- A third level of directories refers to the GMPE used : *L1*, *L2*, *L3*, or *L4*.
- In the directory *logic_tree* there is another directory : *statistics_logic_tree*, which contains the results of the whole logic-tree (i.e. combination of the different sub-branches using the weights defined at each node : seismotectonic model, catalogue, GMPE).

At the end of the above-described structure, one may find 4 types of files :

- *.gra* files : which contain the hazard curves for the different calculation points at the different spectral periods.
- *.iap* files : which are build from interpolation of the hazard curves at five different return periods : 100, 475, 975, 5000, and 10000 years. For each calculation point, the acceleration level reached at the five return periods and for the different spectral periods are reported. These files may be used to plot the Uniform Hazard Spectra.
- *.dat* files : which contain a subset of values reported in the *.iap* files. They are only present under the *maps_3SP* directory, and they contain the acceleration level obtained for a given spectral period and a given return period for every points of the calculation grid. These files may be used to build the acceleration maps.
- *.jpg* files : which are plots of either hazard curves, Uniform Hazard Spectra, or maps of acceleration levels.

2. **Files format**

2.1 **Hazard curve files**

The names of the *.gra* files contain the type of statistical values indicated in the files :

- *avg* : for the mean values.
- *median* : for the median values.
- *per05*, *per16*, *per84*, or *per95* : for the different fractiles.

The names also include the sub-branch information. For example, a file name including *M2_C1_L4* correspond to results for the seismotectonic model 2, the seismicity catalogue 1 and the GMPE 4. For the results of the whole logic-tree, the filename contains *final_stats*. In all cases, except for the Zoneless approach at the 20 sites of special interest, the .gra files contain the results for all the calculation points. For the Zoneless approach at the 20 sites of special interest, there is one *.gra* file per site, in which case, the name of the site is included in the filename. A typical example of file name is *per16_nopond_M1_C1_L1.DAT.001.gra* which corresponds to the centile 16% of the sub-branch related to the first seismotectonic model (*M1*), the original seismicity catalogue (*C1*) and the first GMPE (*L1*).

The *.gra* files have a 8 lines header. They are composed of several blocks for each calculation point and each spectral period. The first line of a block contains the longitude and latitude of the current calculation point, and eventually information on the site (site name, site type : *sta_RAP* for RAP stations or *ville* for cities). Then for each points, there are as many sub-blocks as the number of spectral periods investigated (3 for the maps, and 15 for the sites). Each sub-block starts with a line including *INTENSITY* followed by either the number of the spectral period considered (from 1 to 3 for the maps, and from 1 to 15 for the sites) or the value of the spectral period. Each sub-block is then composed of 3 columns : acceleration level (in cm/s²), annual probability of exceedance, and an unused column filled with zeros. An example, of such a file is provided below :

```
    PROGRAM GEOSIS2 VERSION    1.00                          |
                                                             |
    Date : 2012/01/04                                        |
                                                             | HEADER
                                                             |
                                                             |
INTENSITY versus EXPECTED EXCEEDANCE RATE                    |
   4.30000    43.05000                                       | Longitude and latitude of the first point
INTENSITY   1 IA                                             | First spectral period
1.00000E+00  7.98986E-02  0.00000E+00                        |
1.43845E+00  6.74369E-02  0.00000E+00                        |
2.06914E+00  5.27664E-02  0.00000E+00                        |
2.97635E+00  3.80997E-02  0.00000E+00                        |
4.28133E+00  2.54252E-02  0.00000E+00                        |
6.15848E+00  1.57656E-02  0.00000E+00                        |
8.85867E+00  9.13513E-03  0.00000E+00                        |
1.27428E+01  4.95990E-03  0.00000E+00                        | Hazard curve for the first point and the first
```

```
1.83298E+01  2.51660E-03  0.00000E+00          | spectral period
2.63665E+01  1.18556E-03  0.00000E+00          | acceleration (cm/s²), probability
3.79269E+01  5.15751E-04  0.00000E+00          | The last column is not used
5.45560E+01  2.08085E-04  0.00000E+00          |
7.84760E+01  7.94478E-05  0.00000E+00          |
1.12884E+02  2.96840E-05  0.00000E+00          |
1.62378E+02  1.11356E-05  0.00000E+00          |
2.33572E+02  4.08771E-06  0.00000E+00          |
3.35982E+02  1.37409E-06  0.00000E+00          |
4.83293E+02  3.89026E-07  0.00000E+00          |
6.95193E+02  8.47951E-08  0.00000E+00          |
1.00000E+03  1.24184E-08  0.00000E+00          |
INTENSITY   2 IA                                | Second spectral period
1.00000E+00  9.51848E-02  0.00000E+00          | Hazard curve for the first point and the second
1.49190E+00  9.08635E-02  0.00000E+00          | spectral period
…
   4.42000    43.05000                          | Longitude and latitude of the second point
INTENSITY   1 IA                                | First spectral period
1.00000E+00  8.25057E-02  0.00000E+00          | Hazard curve for the second point and the first
1.43845E+00  6.98236E-02  0.00000E+00          | spectral period
2.06914E+00  5.48382E-02  0.00000E+00
2.97635E+00  3.97901E-02  0.00000E+00
4.28133E+00  2.67210E-02  0.00000E+00
…
```

2.2 Uniform Hazard Spectra files

The file names of the *.iap* files are formatted in the same way as the *.gra* files (see first 2 paragraphs of section **Erreur ! Source du renvoi introuvable.**). These files are only included in the directory *sites_15SP*. A typical example of file name is : *acceleration_avg_nopond_M1_C1_L1.DAT.001.gra.iap* which includes the name of the *.gra* file (*avg_nopond_M1_C1_L1.DAT.001.gra*) used to build the *.iap* file with the prefix and suffix *acceleration_*, and *.iap*, respectively. The file name given above corresponds to the mean of the sub-branch related to the first seismotectonic model (*M1*), the original seismicity catalogue (*C1*) and to the first GMPE (*L1*).

The *.gra* files are composed of several blocks for each calculation point. The first line of the blocks is a header line filled with the string :

<div align="center">*longitude   latitude site*</div>

The second line of the blocks gives the latitude, longitude and site name of the actual calculation point. The third line of the blocks is another header line filled with the following string :

<div align="center">*SP   RP100   RP475   RP975   RP5000   RP10000   (ans)*</div>

Where *SP* refers to spectral period, *RP* to return period (5 distinct return periods) and *ans* to years. Then the following lines of the blocks contain the spectral period value and the five acceleration levels (in cm/s²) corresponding to the five return periods. An example, of such a file is provided below :

```
longitude latitude    site                      | First header line
6.92183   43.75280 CALF                          | longitude latitude and name of the first calculation point
```

SP	RP100	RP475	RP975	RP5000	RP10000 (ans)		Second header line
0.01	25.65	81.11	129.24	308.66	415.91		
0.03	27.59	91.55	150.58	384.65	527.76		
0.05	32.45	113.64	189.17	479.52	651.53		
0.1	48.21	163.41	266.61	651.31	877.01		
0.15	62.52	197.45	312.86	740.33	993.55		Acceleration levels (in cm/s²) at the five return periods
0.2	61.84	187.15	292.02	682.01	921.02		(columns) and for the spectral periods considered (lines)
0.25	55.87	166.70	260.05	622.73	851.25		for the first point
0.3	49.62	147.36	229.98	561.69	779.56		
0.4	36.17	109.17	170.88	423.65	595.69		
0.5	25.35	78.48	123.44	309.53	438.26		
0.75	14.42	44.63	69.88	179.20	262.69		
1	8.32	26.35	41.23	104.68	152.19		
1.5	4.40	13.93	21.75	54.92	79.96		
2	2.88	9.66	15.37	39.66	57.50		
3	1.72	6.00	9.55	23.82	33.77		
longitude	latitude	site					First header line
6.54000	44.78800	OGAG					longitude latitude and name of the second point
SP	RP100	RP475	RP975	RP5000	RP10000 (ans)		Second header line
0.01	29.29	80.48	120.77	259.15	339.03		
0.03	31.88	92.69	143.47	326.16	433.40		
0.05	37.74	115.93	181.87	414.18	546.84		
0.1	55.30	161.54	247.79	546.00	714.97		
0.15	71.36	194.63	290.52	621.56	810.97		Acceleration levels (in cm/s²) at the five return periods
0.2	70.45	182.99	267.83	561.27	734.57		(columns) and for the spectral periods considered (lines)
0.25	63.38	162.54	237.41	503.76	665.34		for the second point
0.3	56.25	142.86	207.98	444.60	592.93		
0.4	41.28	106.23	154.89	333.36	447.45		
0.5	29.65	78.60	115.55	252.58	341.77		
0.75	17.71	47.83	70.65	157.94	218.22		
1	10.49	29.01	43.02	96.77	133.69		
1.5	5.66	15.77	23.50	53.48	74.31		
2	3.74	11.00	16.69	39.05	54.48		
3	2.30	7.03	10.71	24.63	33.87		

…

2.3 Files for plotting the maps

The *.dat* files contain a subset of the values tabulated in the *.iap* files. They contain the acceleration levels for a given spectral period, and a given return period at each calculation point (the longitude and latitude of the calculation points are also included in the files). These files are only included in the directory *maps_3SP*, and they are build only for a limited number of cases (corresponding to the maps included in the report GTR/ARE/0112-898).

The file names of the *.dat* files include the information related to the branch of the logic-tree they are associated with. The file names start with three integers separated by _. These numbers correspond to the seismotectonic model (1 for SM1, 2 for SM2, 3 for SM3, 4 for kernel 1 of the zoneless approach, 5 for kernel 2, and 6 for kernel 3), then to the catalogue used (1 for the original and 2 for the synthetic

catalogue), and finally to the GMPE used (1 for L1, 2 for L2, 3 for L3, and 4 for L4). Then the file names contain the same information in a more explicit way :

- *SM1*, *SM2*, *SM3*, *SM_ZI1*, *SM_ZI2*, *SM_ZI3* for the seismotectonic models 1, 2 or 3, and the Zoneless approaches 1, 2 or 3.
- *C1 or C2 for the original or the synthetic seismicity catalogue, respectively.*
- *AM1*, *AM2* or *AM_L2*, *AM3*, *AM4* for the 4 different GMPEs used
- For the results of the whole logic tree, the above mentionned parameters are replaced by *all* (see the *.dat* files in the *maps_3SP/statistics_logic_tree* directory).

The file names also include the information of the spectral period and the return period considered :

- *SP0_00*, *SP0_20*, or *SP1_00* for PGA, 0.2 and 1 sec, respectively
- *RP100*, *RP475*, *RP975*, *RP5000*, *RP10000* for return periods 100, 475, 975, 5000, or 10000 years, respectively.

The last part of the file name refers to the type of statistical value included in the file : mean, median or centiles (*mean*, *median*, *per16* or *per84*). All the information included in the file name is repeated in a more explicit way within the file in one header line. A typical example of file name is : *1_1_1_SM1_C1_AM1_SP0_00_RP10000_mean.dat* which correponds to the mean PGA values at 10000 years return period, computed for the sub-branch related to the first seismotectonic model (*SM1*), the original seismicity catalogue (*C1*) and to the first GMPE (*AM1*). An example, of such a file is provided below :

Branch : 1_1_1 ; Seismotectonic model : Zones ; Seismicity catalog : C1 ; Attenuation model : Akkar & Bommer (2010) ; Spectral period : 0.00 seconds ; Return period : 10000 years ; Maped value : Mean
4.30000,43.05000,71.95
4.42000,43.05000,77.20
4.54000,43.05000,86.43
4.66000,43.05000,102.16
4.78000,43.05000,129.73
4.90000,43.05000,164.58
5.02000,43.05000,195.57
5.14000,43.05000,224.64
5.26000,43.05000,240.67
5.38000,43.05000,233.02
5.50000,43.05000,186.42

The first header line summarizes the branch from which the values are coming from. The branch identification code (*1_1_1* in the example) is the same as described in the file name (see paragraphs above). The Seismotectonic model code is :

- *Zones* for seismotectonic model 1
- *Fault systems* for seismotectonic model 2
- *Large zones* for seismotectonic model 3
- *Zoneless kernel 1* (or 2 or 3) for the different zoneless approaches.

The seismicity catalogue code is still *C1* or *C2* for the original or the synthetic catalogue. The GMPEs, spectral period and return period are explicitly written in the header line, as well as the type of statistical

value included in the file. The rest of the file is formatted in three columns, separated by comas and including the longitude, the latitude and the acceleration level (in cm/s²). The files include one header line and 858 lines corresponding to each of the points of the calculation grid.

2.4 Image files

Some results are plotted and included as images (*.jpg* files). The filenames are coherent with the codes given in sections **Erreur ! Source du renvoi introuvable.** to **Erreur ! Source du renvoi introuvable.**. Such files are provided for acceleration maps (in this case the filename includes the name of the *.dat* file from which the map has been drawn, moreover, all the information are written within the image), hazard curves, or uniform hazard spectra (for the two latter cases the file name include explicitly the site name, the spectral period or the return period. In each case legends are provided in the figures refering to the filenames from which the plots have been drawn). Under the directory *maps_3SP/statistics_logic_tree*, some of the maps show the difference in % between two results. In these cases, the filename of the map includes both filenames of the *.dat* files from which the difference has been computed.

POLE GEO-ENVIRONNEMENT
3, rue Jean Monnet
34830 Clapiers - France
Tél : + 33 (0)467591811
Fax : + 33 (0)467591824
Email : geoter@geoter.fr
Site Web : http://www.geoter.fr

SIGMA. WP4 T4-1.

Probabilistic analysis for France's southeast ¼

to produce a preliminary

« classical » hazard map

Annex 2 : Hazard curves and

Uniform Hazard spectra at the

20 sites of special interest

Type of document :	identification :
Final report	Report GTR/ARE/0212-924

The results of the logic-tree (3 seismotectonic models, 2 seismicity catalogues, 4 GMPEs, and uncertainty propagation) are presented hereafter at each selected site.

Each sheet contents the PGA hazard curves and the uniform hazard response spectra at 5 return periods.
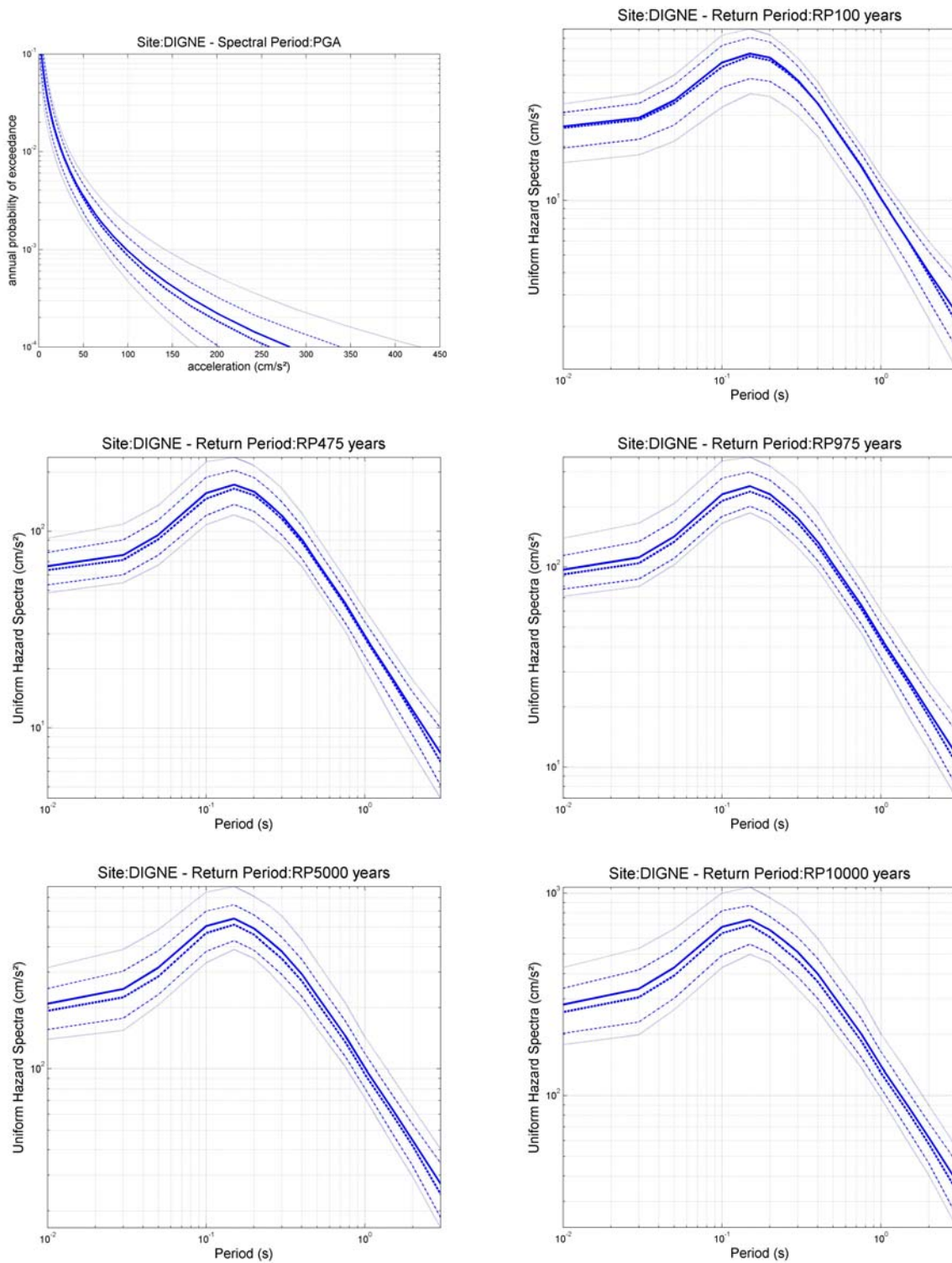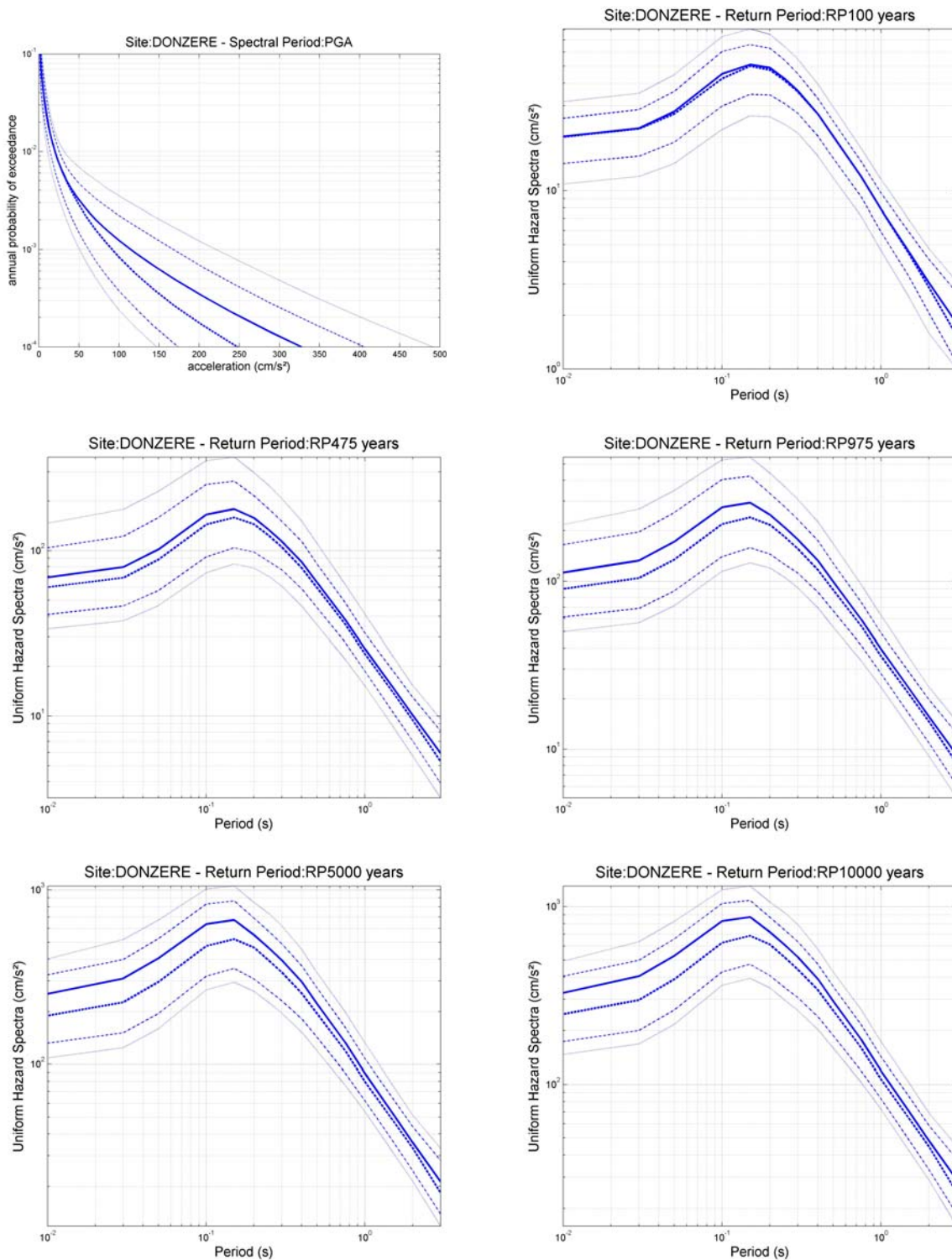
Albertville
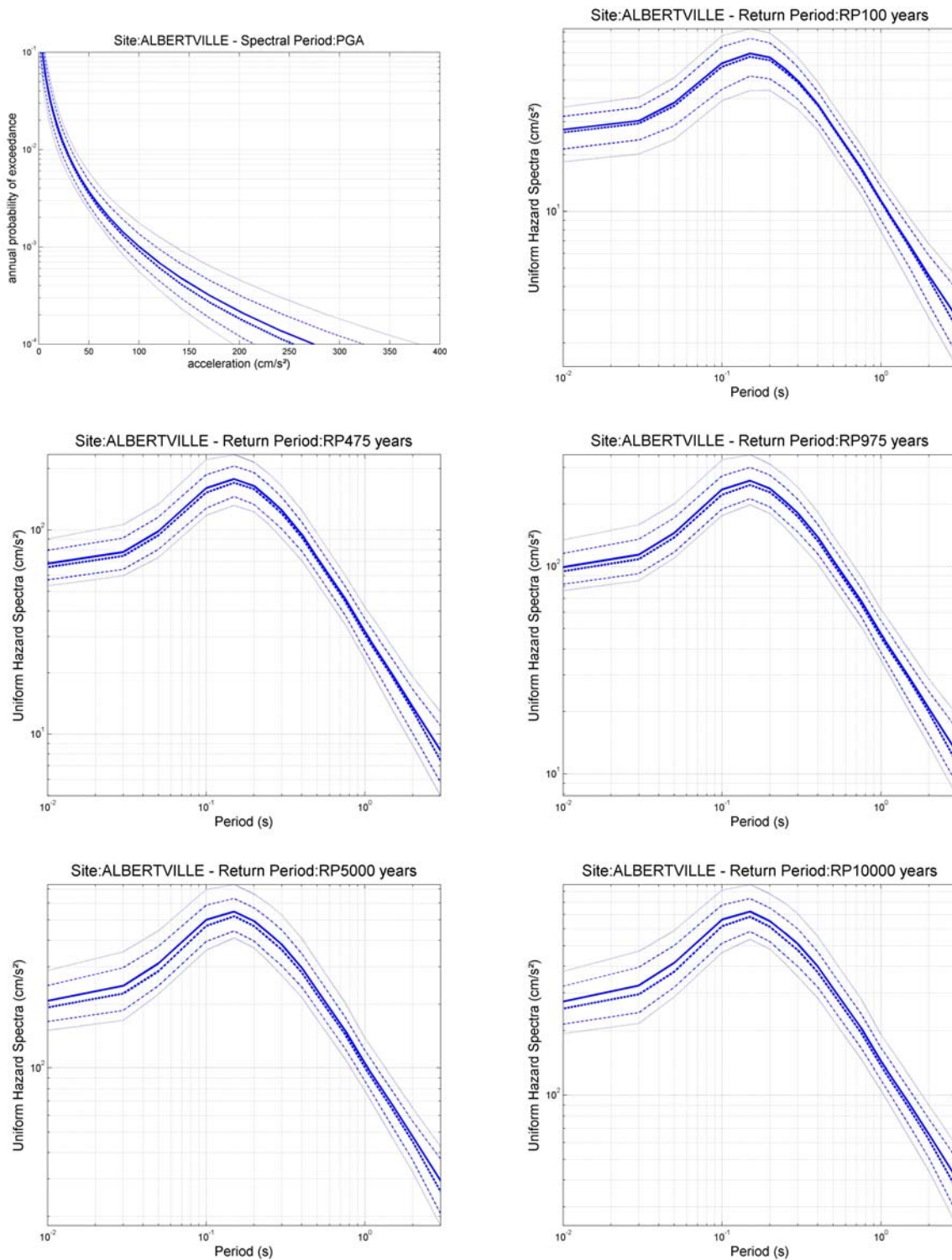
Figure 1 – Hazard curves for PGA (top left), and Uniform Hazard Spectra for 5 different return periods (from 100 years : top right, to 10000 years : bottom right) at site Albertville. Mean : thick solid line, median : thick dashed line, centiles 14-86% : thin dashed lines, and centiles 5-95% : thin dotted lines.

Avignon
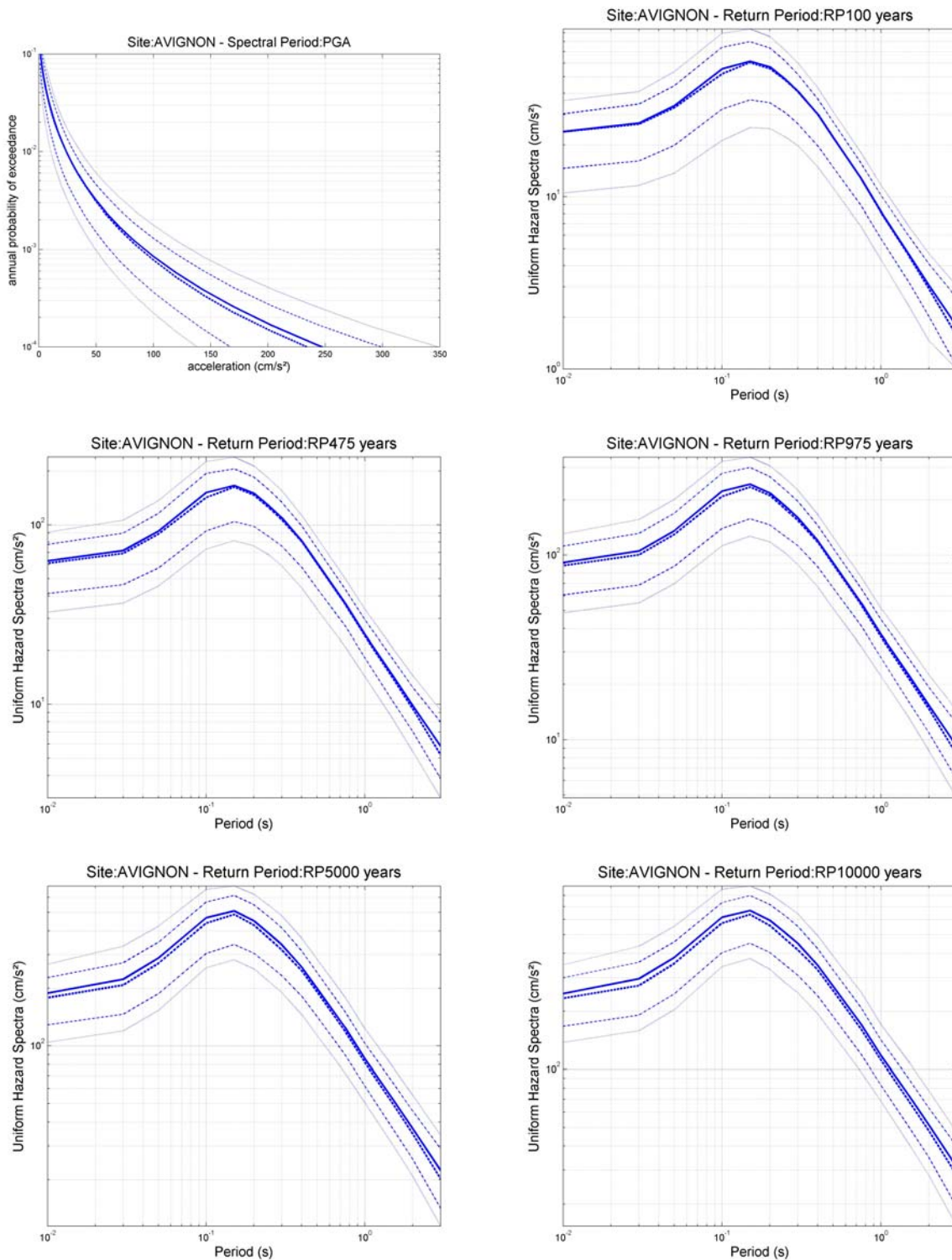
Figure 2 – Hazard curves for PGA (top left), and Uniform Hazard Spectra for 5 different return periods (from 100 years : top right, to 10000 years : bottom right) at site Avignon. Mean : thick solid line, median : thick dashed line, centiles 14-86% : thin dashed lines, and centiles 5-95% : thin dotted lines.
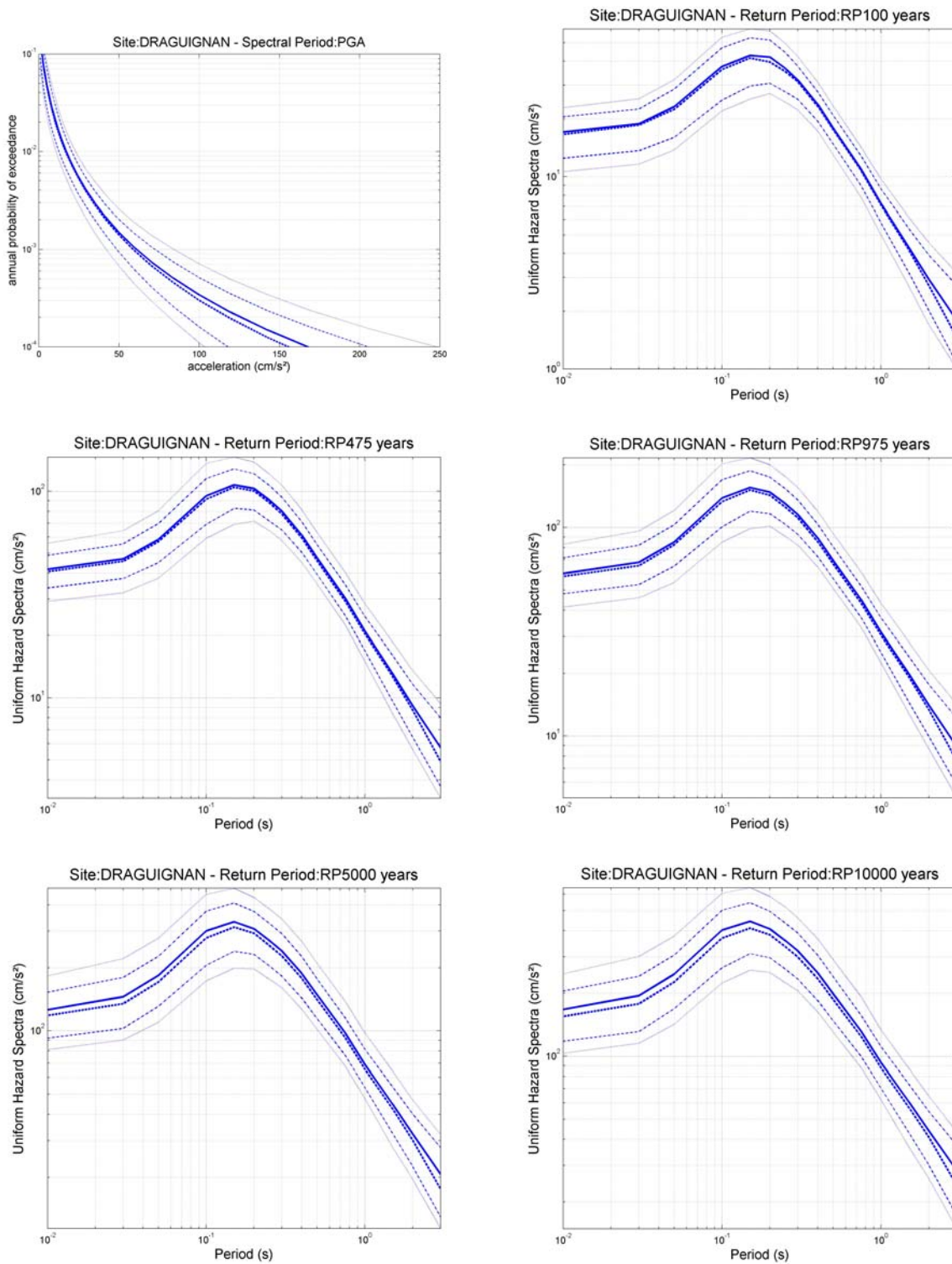
CALF
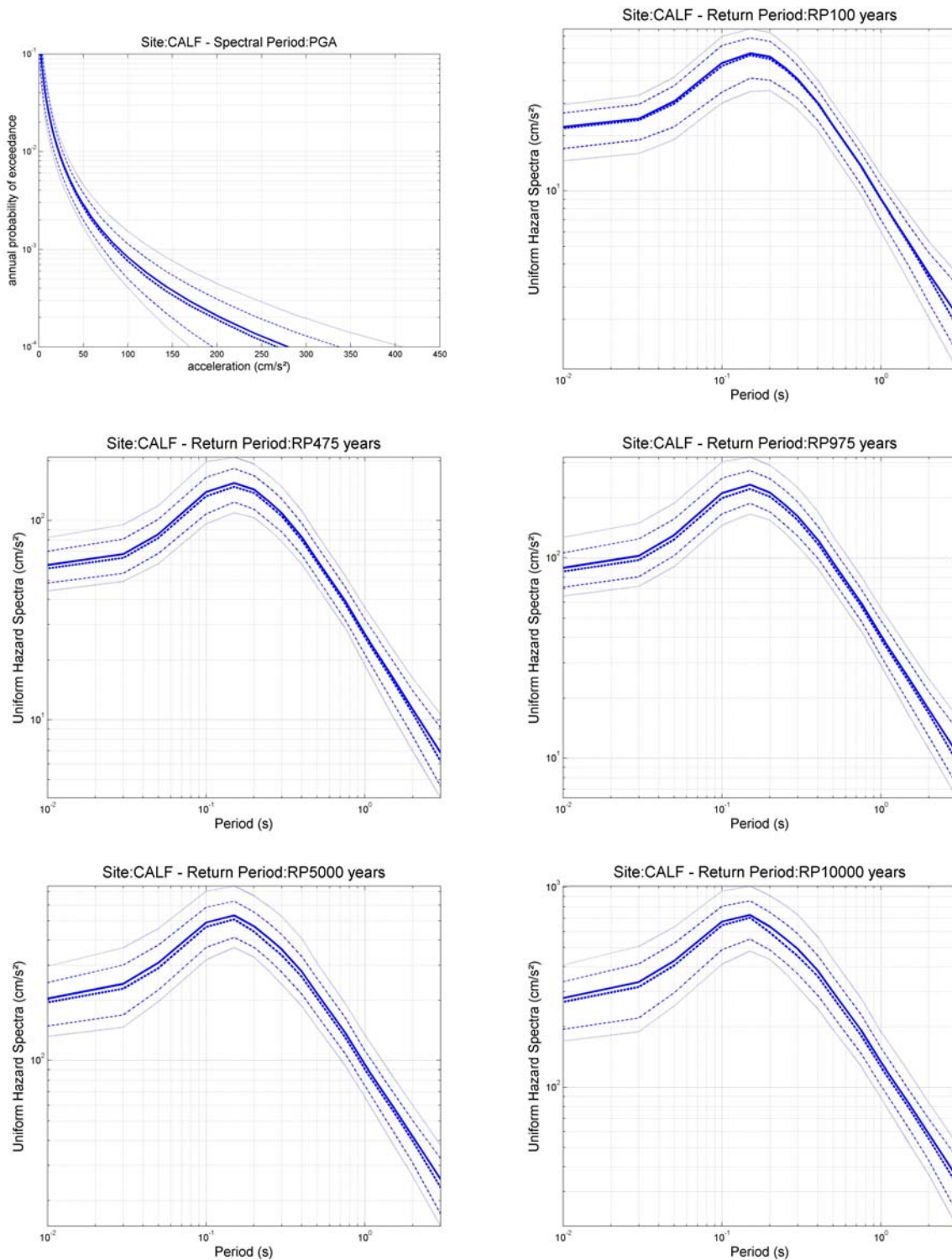
Figure 3 – Hazard curves for PGA (top left), and Uniform Hazard Spectra for 5 different return periods (from 100 years : top right, to 10000 years : bottom right) at site CALF. Mean : thick solid line, median : thick dashed line, centiles 14-86% : thin dashed lines, and centiles 5-95% : thin dotted lines.
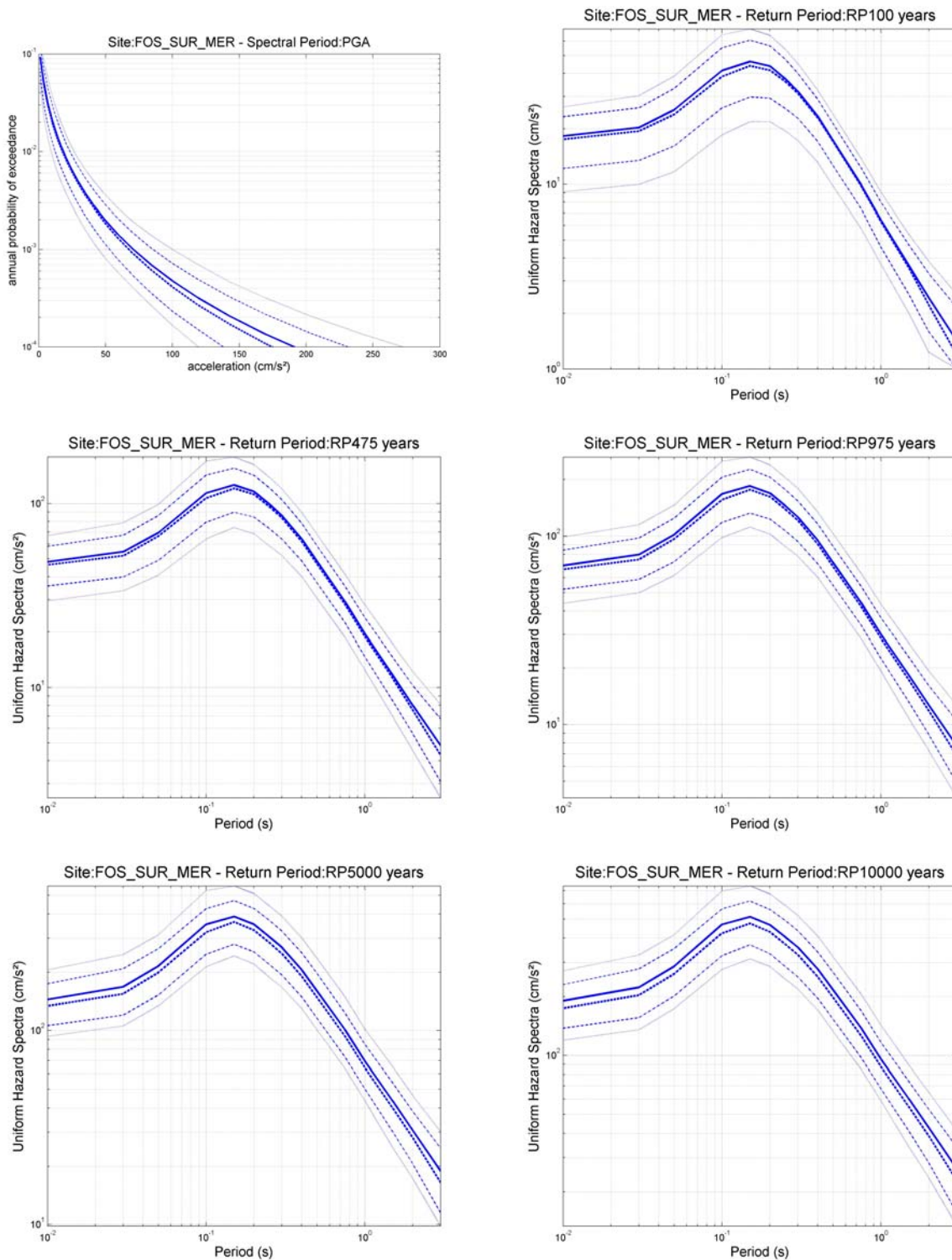
Digne

Figure 4 – Hazard curves for PGA (top left), and Uniform Hazard Spectra for 5 different return
periods (from 100 years : top right, to 10000 years : bottom right) at site Digne.
Mean : thick solid line, median : thick dashed line, centiles 14-86% : thin dashed
lines, and centiles 5-95% : thin dotted lines.

Donzere

Figure 5 – Hazard curves for PGA (top left), and Uniform Hazard Spectra for 5 different return periods (from 100 years : top right, to 10000 years : bottom right) at site Donzere. Mean : thick solid line, median : thick dashed line, centiles 14-86% : thin dashed lines, and centiles 5-95% : thin dotted lines.
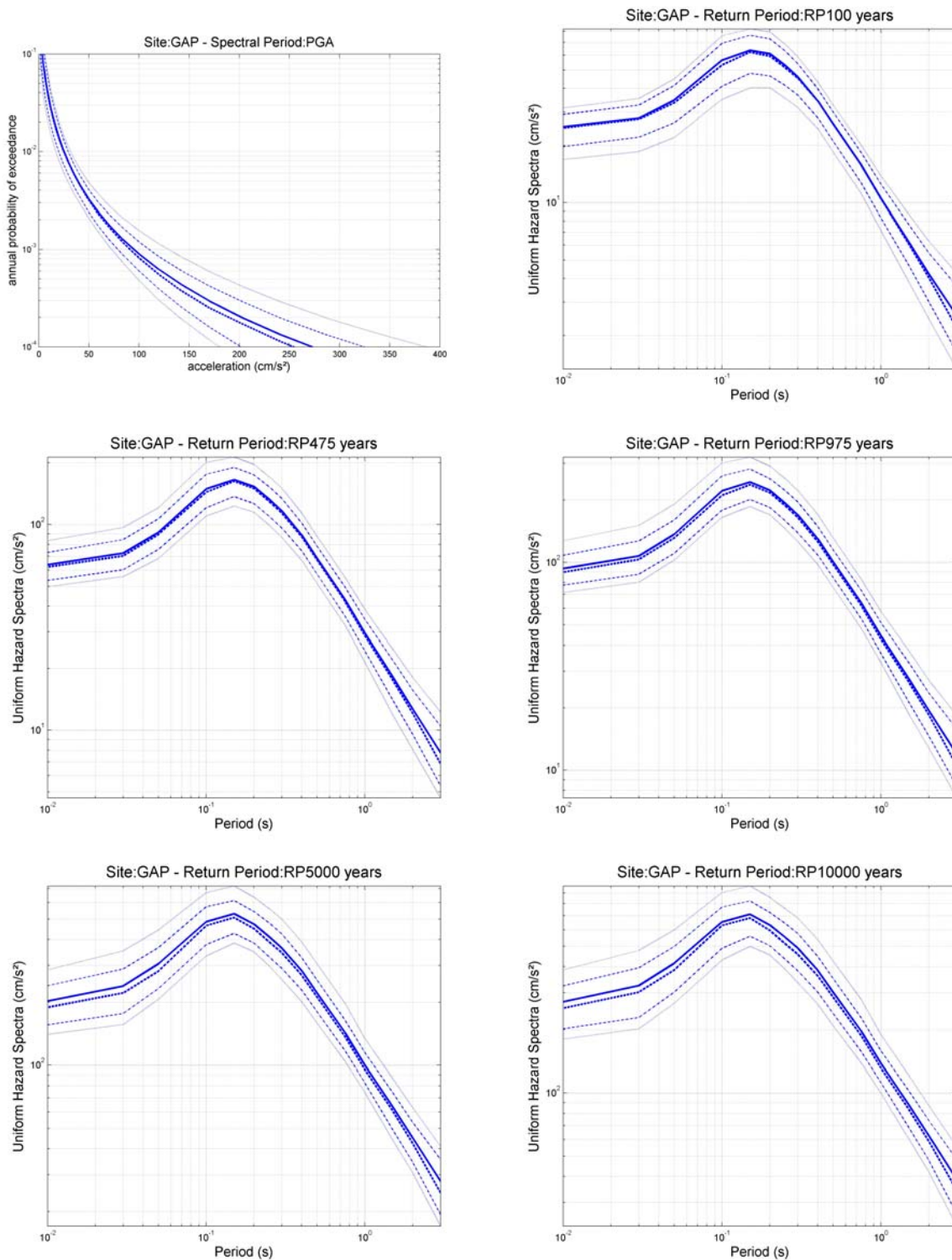
Draguignan

Figure 6 – Hazard curves for PGA (top left), and Uniform Hazard Spectra for 5 different return periods (from 100 years : top right, to 10000 years : bottom right) at site Draguignan. Mean : thick solid line, median : thick dashed line, centiles 14-86% : thin dashed lines, and centiles 5-95% : thin dotted lines.
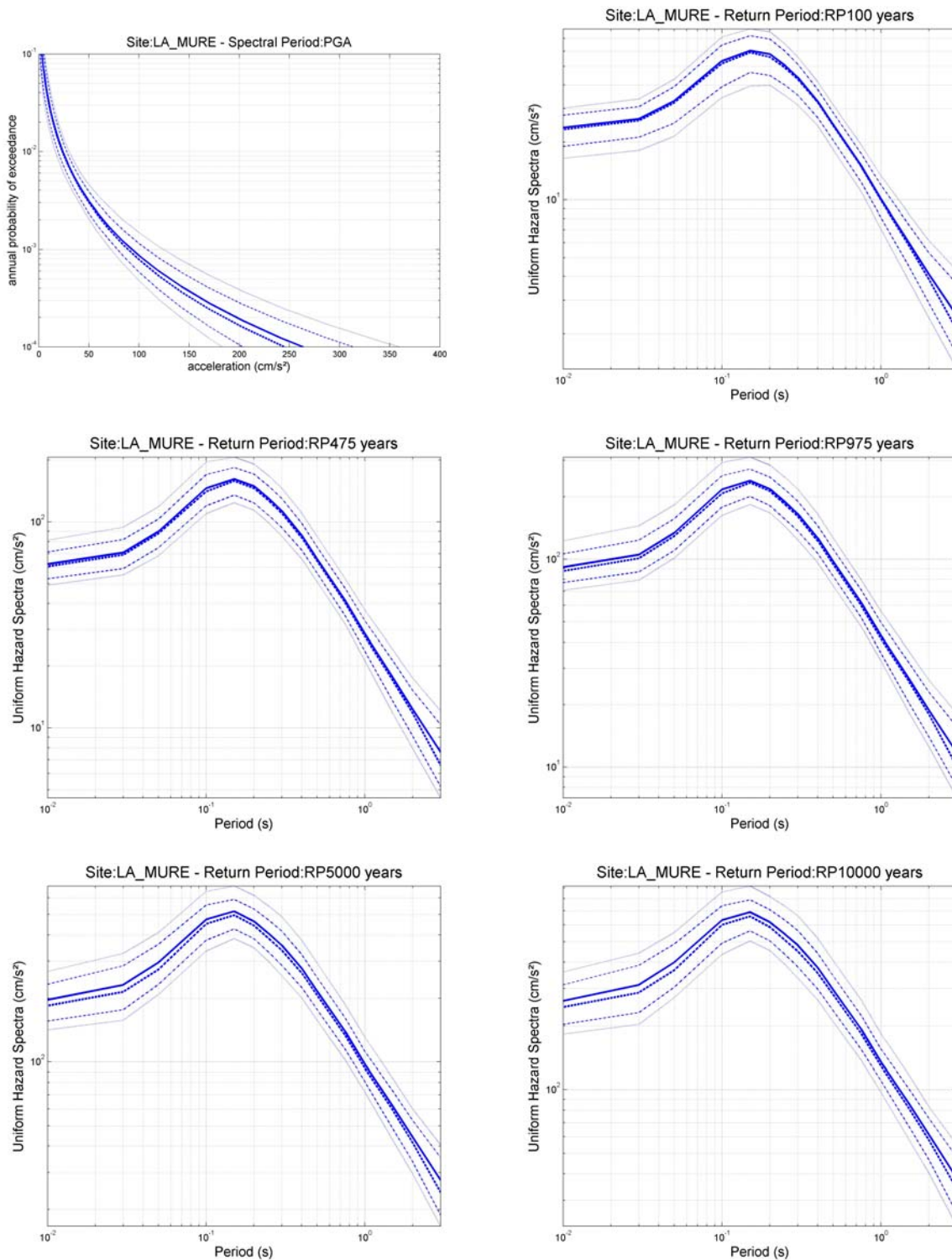
Fos-sur-Mer

Figure 7 – Hazard curves for PGA (top left), and Uniform Hazard Spectra for 5 different return periods (from 100 years : top right, to 10000 years : bottom right) at site Fos-sur-Mer. Mean : thick solid line, median : thick dashed line, centiles 14-86% : thin dashed lines, and centiles 5-95% : thin dotted lines.

Gap

Figure 8 – Hazard curves for PGA (top left), and Uniform Hazard Spectra for 5 different return periods (from 100 years : top right, to 10000 years : bottom right) at site Gap. Mean : thick solid line, median : thick dashed line, centiles 14-86% : thin dashed lines, and centiles 5-95% : thin dotted lines.
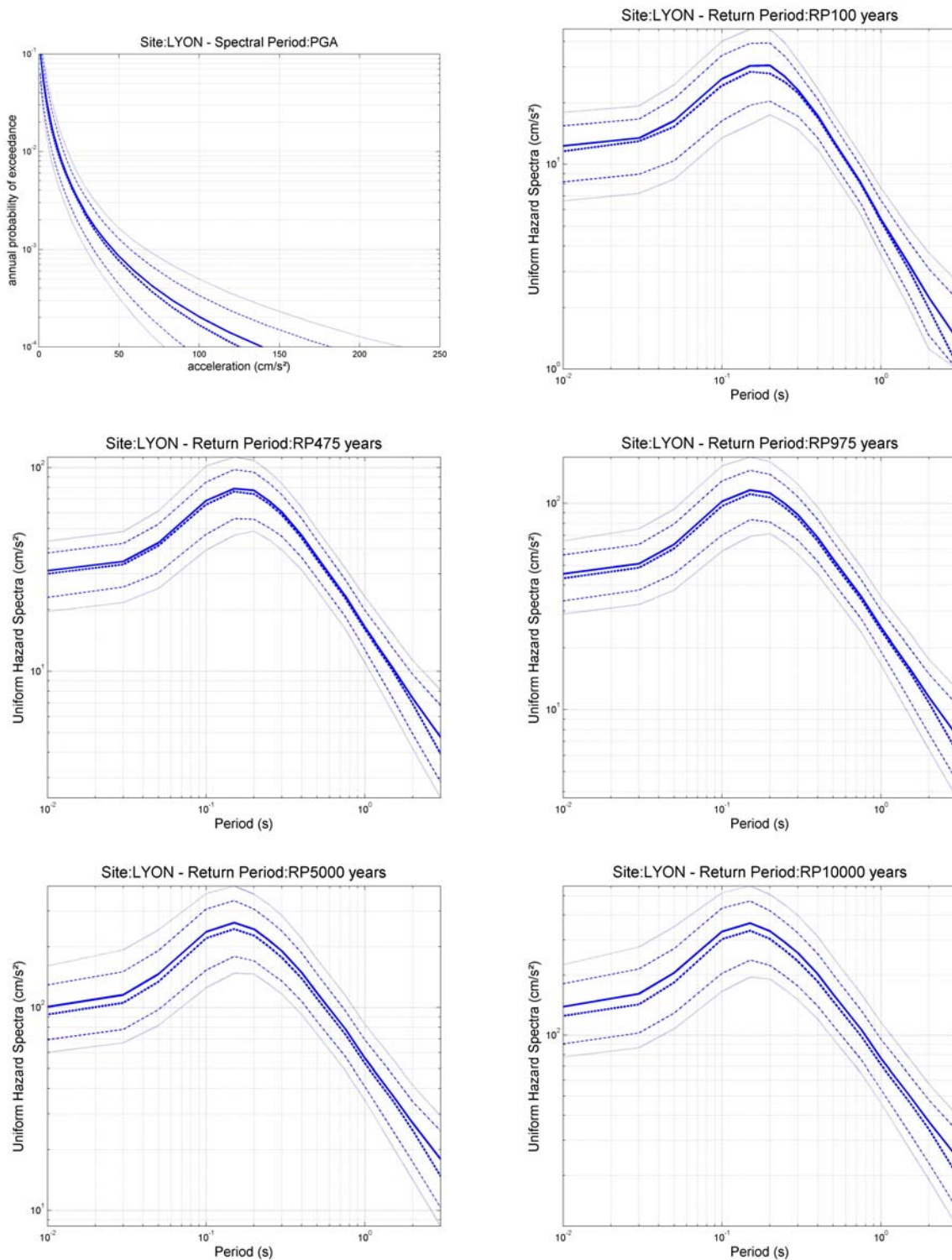
La Mure

Figure 9 – Hazard curves for PGA (top left), and Uniform Hazard Spectra for 5 different return periods (from 100 years : top right, to 10000 years : bottom right) at site La Mure. Mean : thick solid line, median : thick dashed line, centiles 14-86% : thin dashed lines, and centiles 5-95% : thin dotted lines.
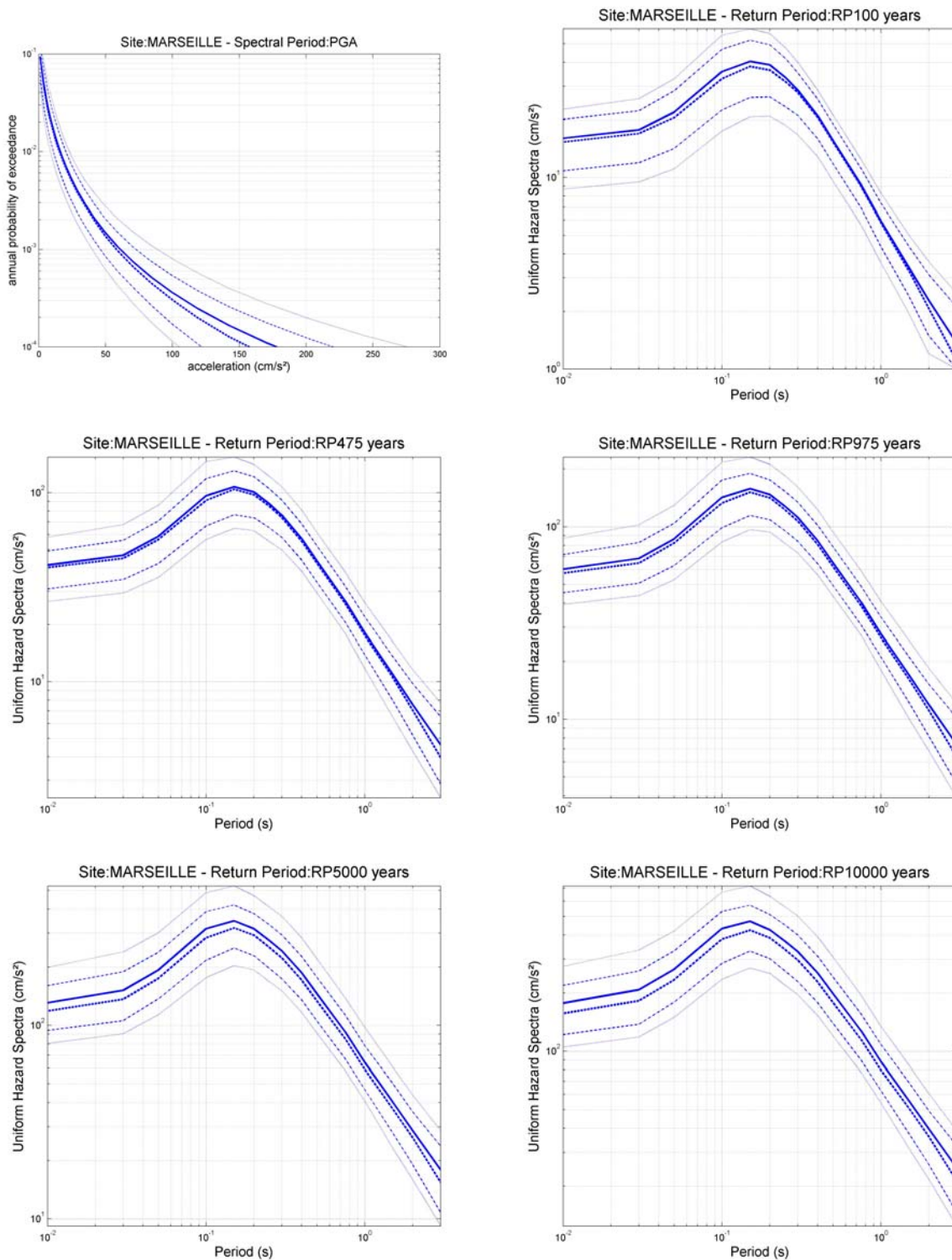
Lyon

Figure 10 – Hazard curves for PGA (top left), and Uniform Hazard Spectra for 5 different return periods (from 100 years : top right, to 10000 years : bottom right) at site Lyon. Mean : thick solid line, median : thick dashed line, centiles 14-86% : thin dashed lines, and centiles 5-95% : thin dotted lines.

Marseille

Figure 11 – Hazard curves for PGA (top left), and Uniform Hazard Spectra for 5 different return periods (from 100 years : top right, to 10000 years : bottom right) at site Marseille. Mean : thick solid line, median : thick dashed line, centiles 14-86% : thin dashed lines, and centiles 5-95% : thin dotted lines.
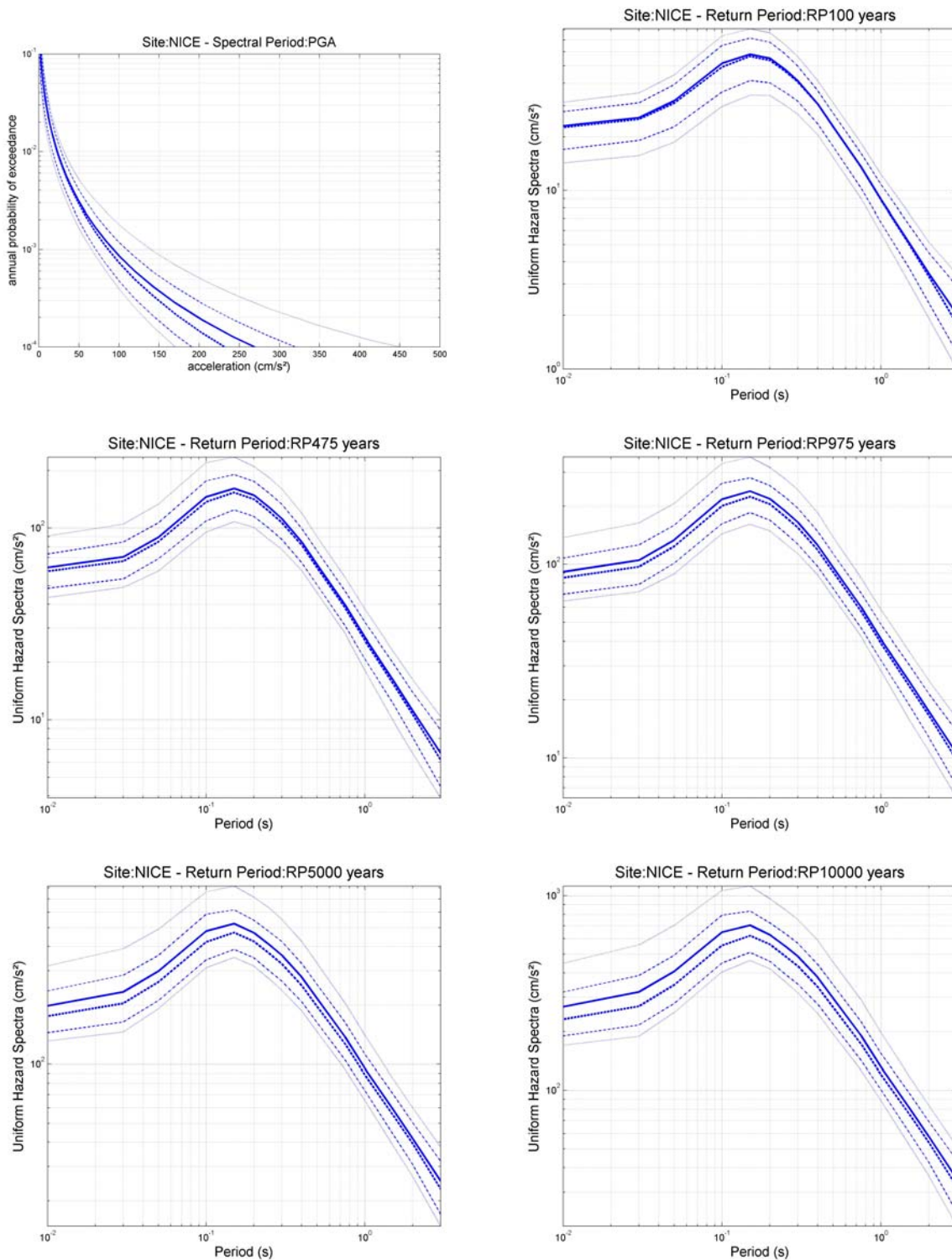
Nice

Figure 12 – Hazard curves for PGA (top left), and Uniform Hazard Spectra for 5 different return periods (from 100 years : top right, to 10000 years : bottom right) at site Nice. Mean : thick solid line, median : thick dashed line, centiles 14-86% : thin dashed lines, and centiles 5-95% : thin dotted lines.
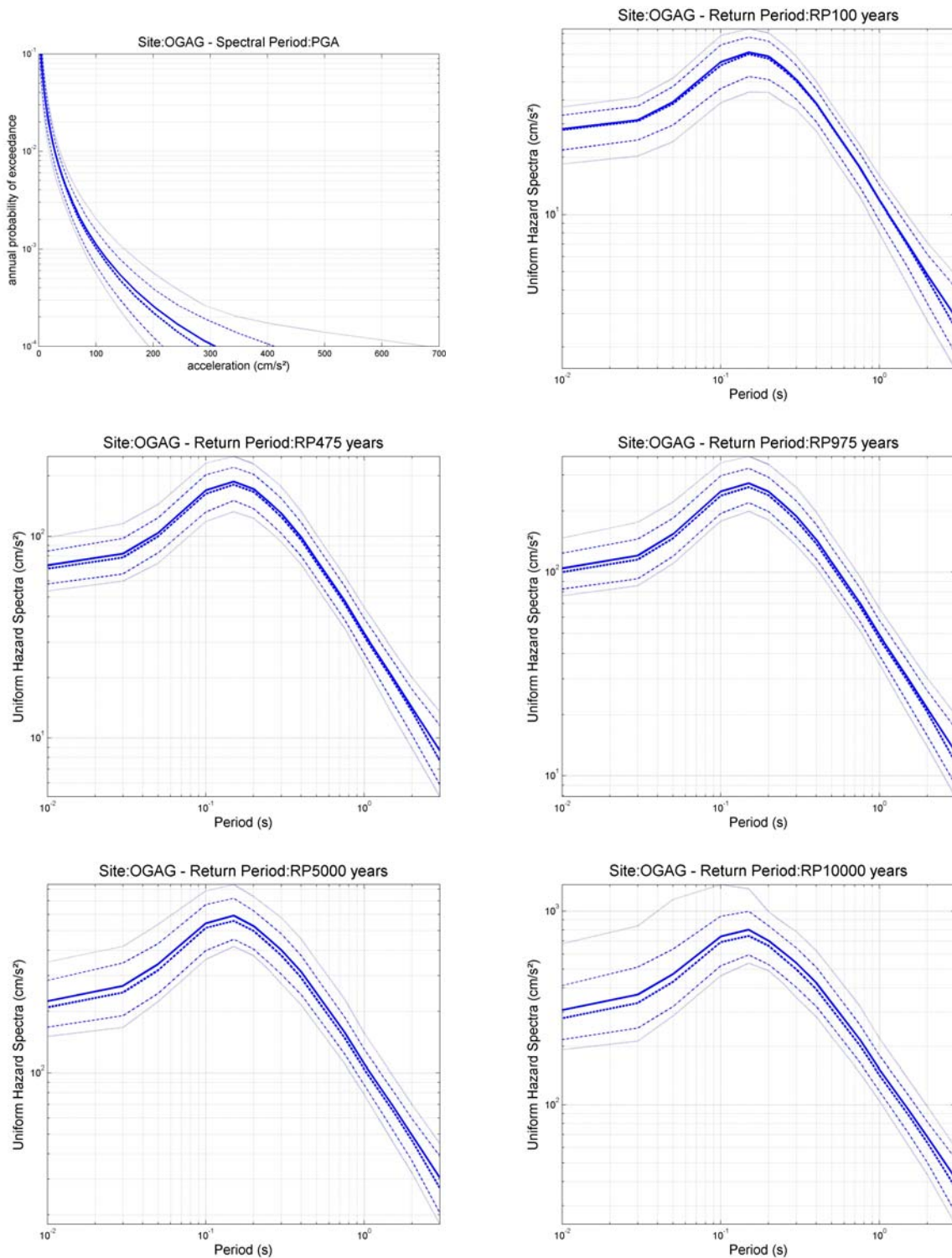
OGAG

Figure 13 – Hazard curves for PGA (top left), and Uniform Hazard Spectra for 5 different return periods (from 100 years : top right, to 10000 years : bottom right) at site OGAG. Mean : thick solid line, median : thick dashed line, centiles 14-86% : thin dashed lines, and centiles 5-95% : thin dotted lines.

OGAN

Figure 14 – Hazard curves for PGA (top left), and Uniform Hazard Spectra for 5 different return periods (from 100 years : top right, to 10000 years : bottom right) at site OGAN. Mean : thick solid line, median : thick dashed line, centiles 14-86% : thin dashed lines, and centiles 5-95% : thin dotted lines.
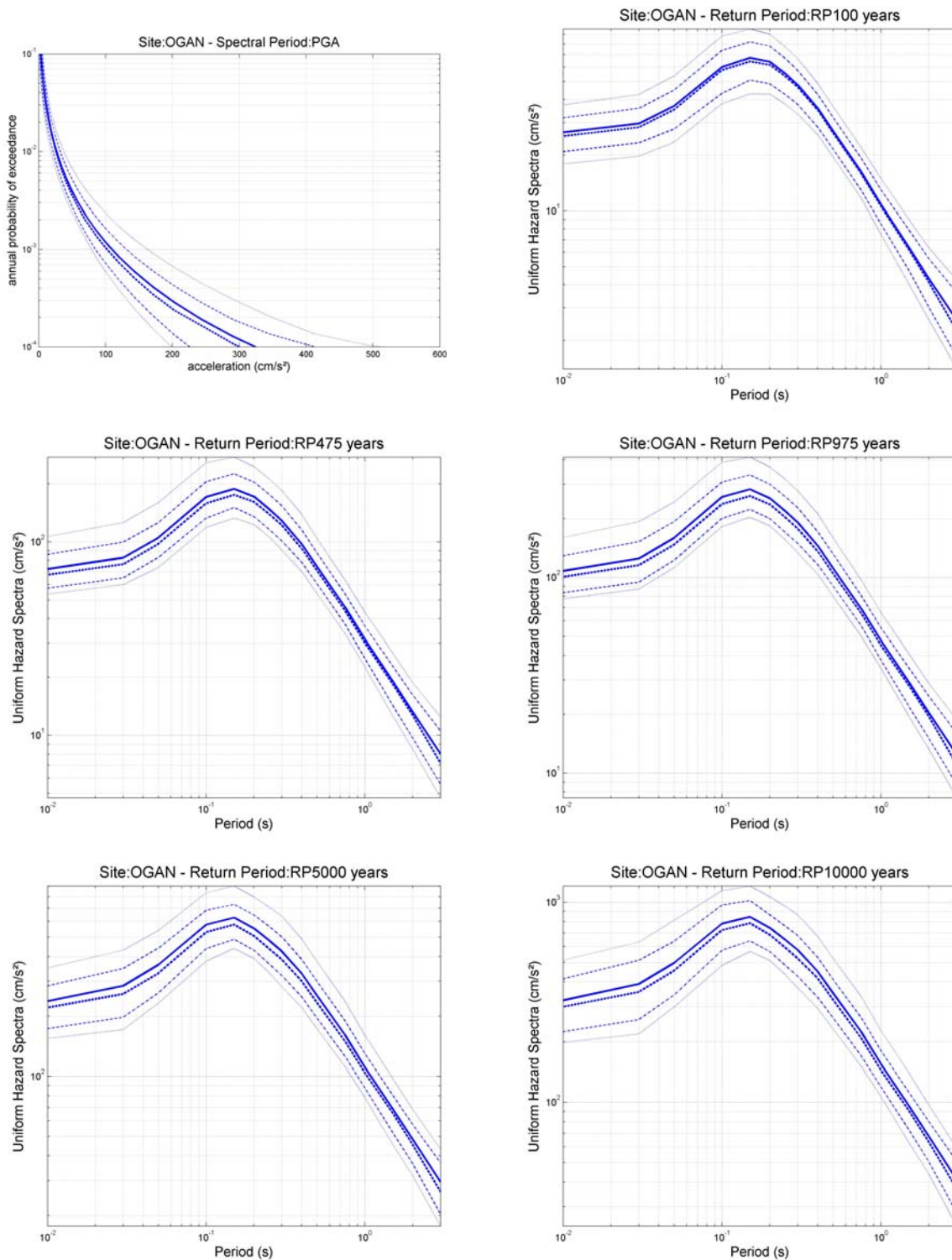
OGCA

Figure 15 – Hazard curves for PGA (top left), and Uniform Hazard Spectra for 5 different return periods (from 100 years : top right, to 10000 years : bottom right) at site OGCA. Mean : thick solid line, median : thick dashed line, centiles 14-86% : thin dashed lines, and centiles 5-95% : thin dotted lines.
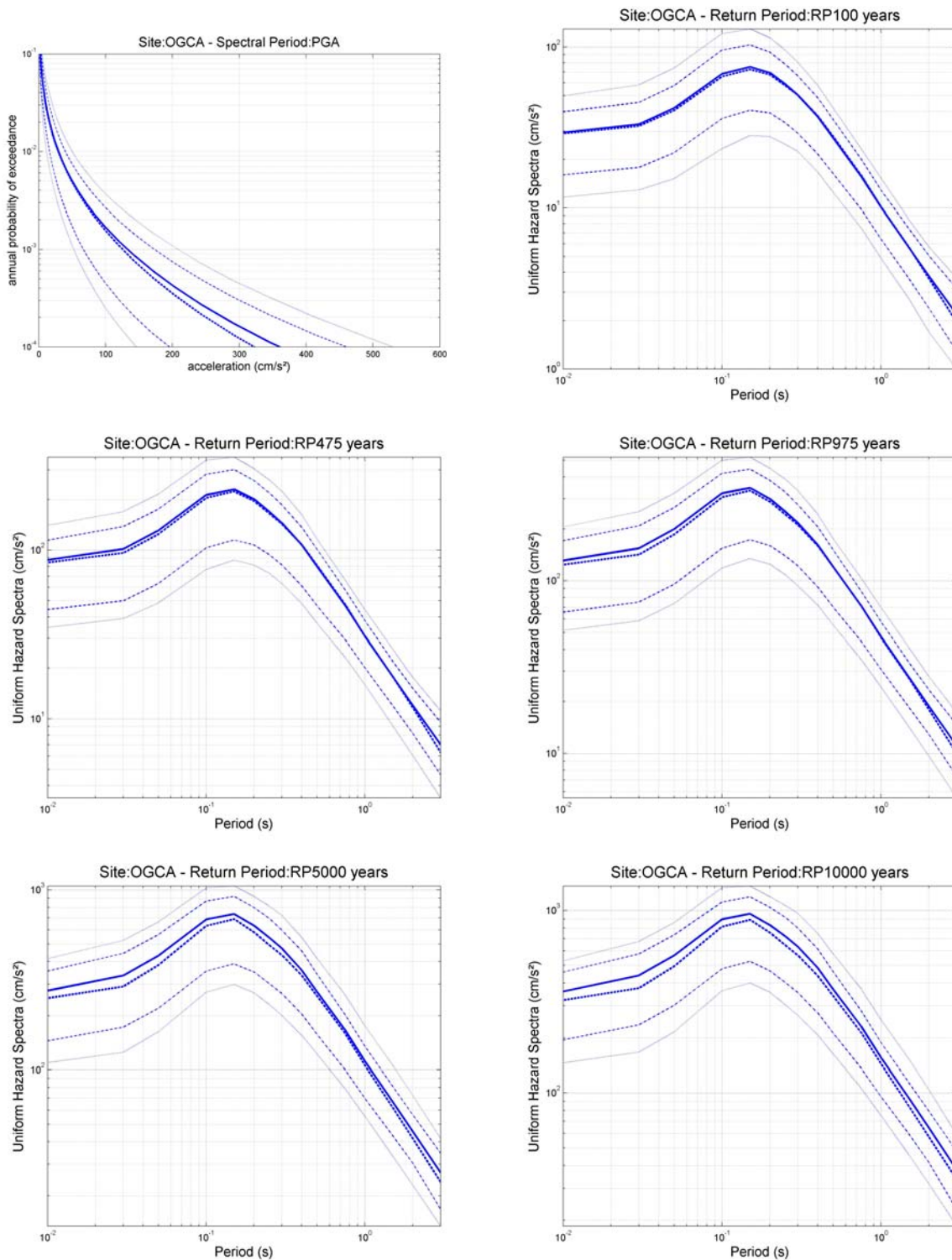
OGMO

Figure 16 – Hazard curves for PGA (top left), and Uniform Hazard Spectra for 5 different return periods (from 100 years : top right, to 10000 years : bottom right) at site OGMO. Mean : thick solid line, median : thick dashed line, centiles 14-86% : thin dashed lines, and centiles 5-95% : thin dotted lines.

OGMU

Figure 17 – Hazard curves for PGA (top left), and Uniform Hazard Spectra for 5 different return periods (from 100 years : top right, to 10000 years : bottom right) at site OGMU. Mean : thick solid line, median : thick dashed line, centiles 14-86% : thin dashed lines, and centiles 5-95% : thin dotted lines.
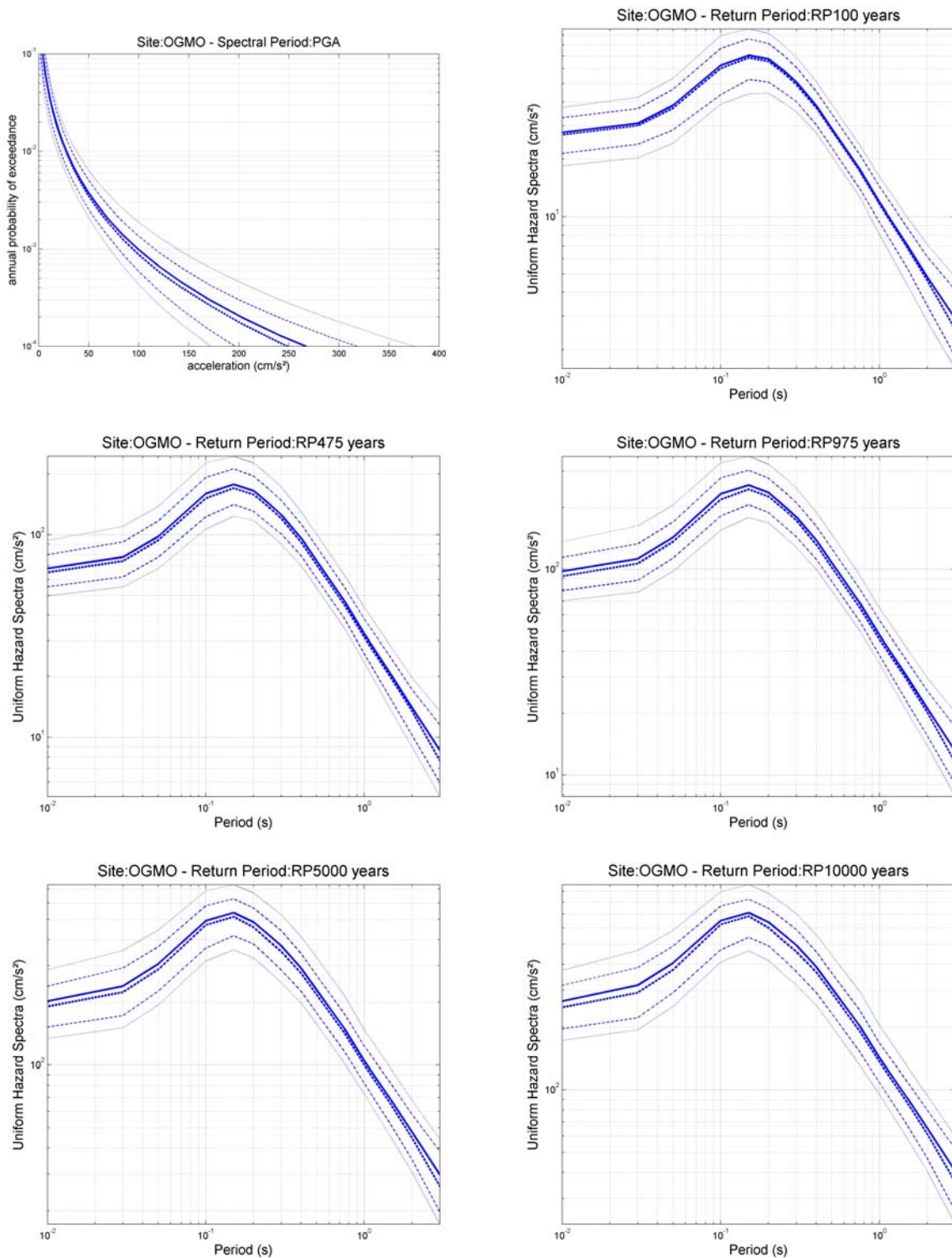
STET

Figure 18 – Hazard curves for PGA (top left), and Uniform Hazard Spectra for 5 different return periods (from 100 years : top right, to 10000 years : bottom right) at site STET. Mean : thick solid line, median : thick dashed line, centiles 14-86% : thin dashed lines, and centiles 5-95% : thin dotted lines.
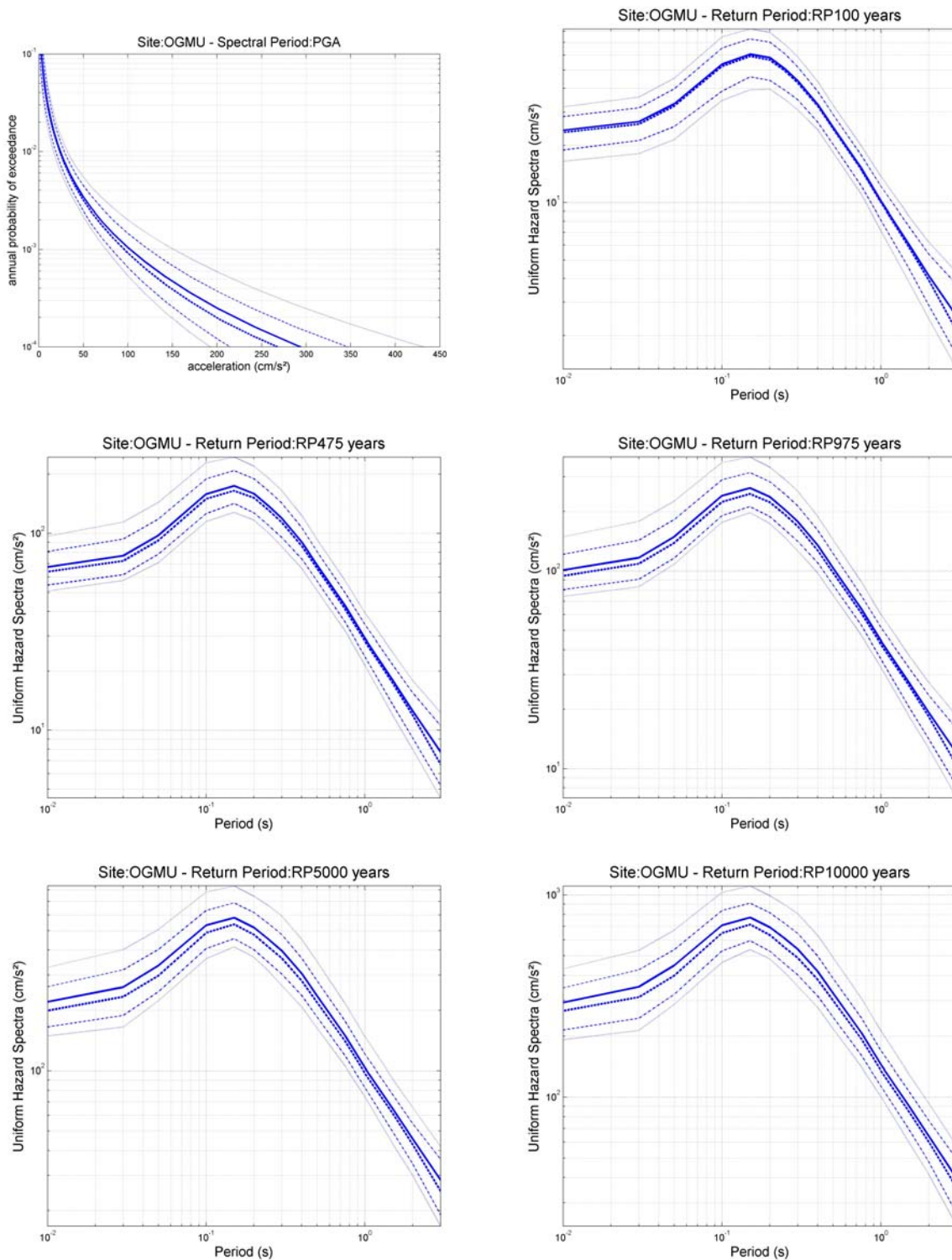
Valence

Figure 19 – Hazard curves for PGA (top left), and Uniform Hazard Spectra for 5 different return periods (from 100 years : top right, to 10000 years : bottom right) at site Valence. Mean : thick solid line, median : thick dashed line, centiles 14-86% : thin dashed lines, and centiles 5-95% : thin dotted lines.
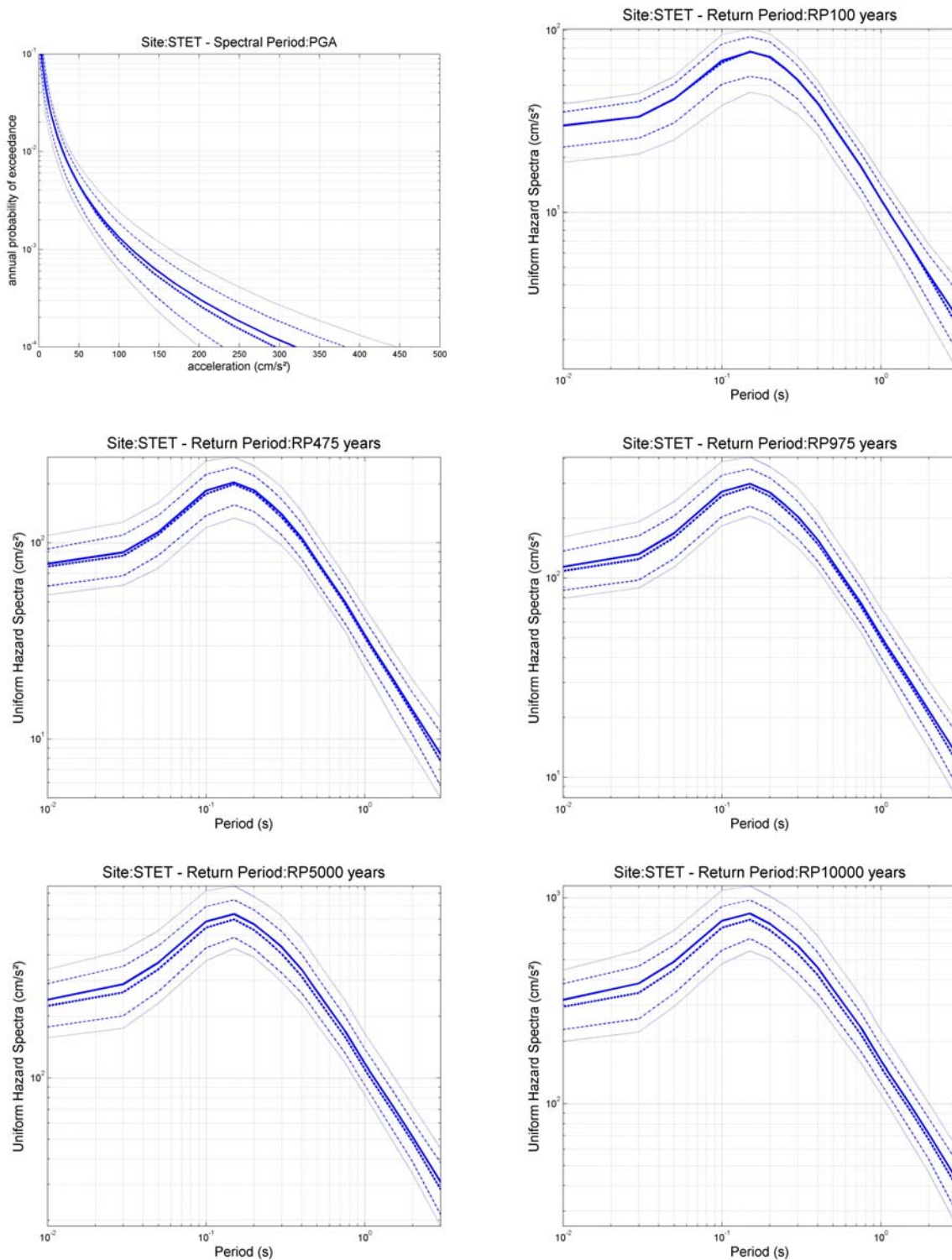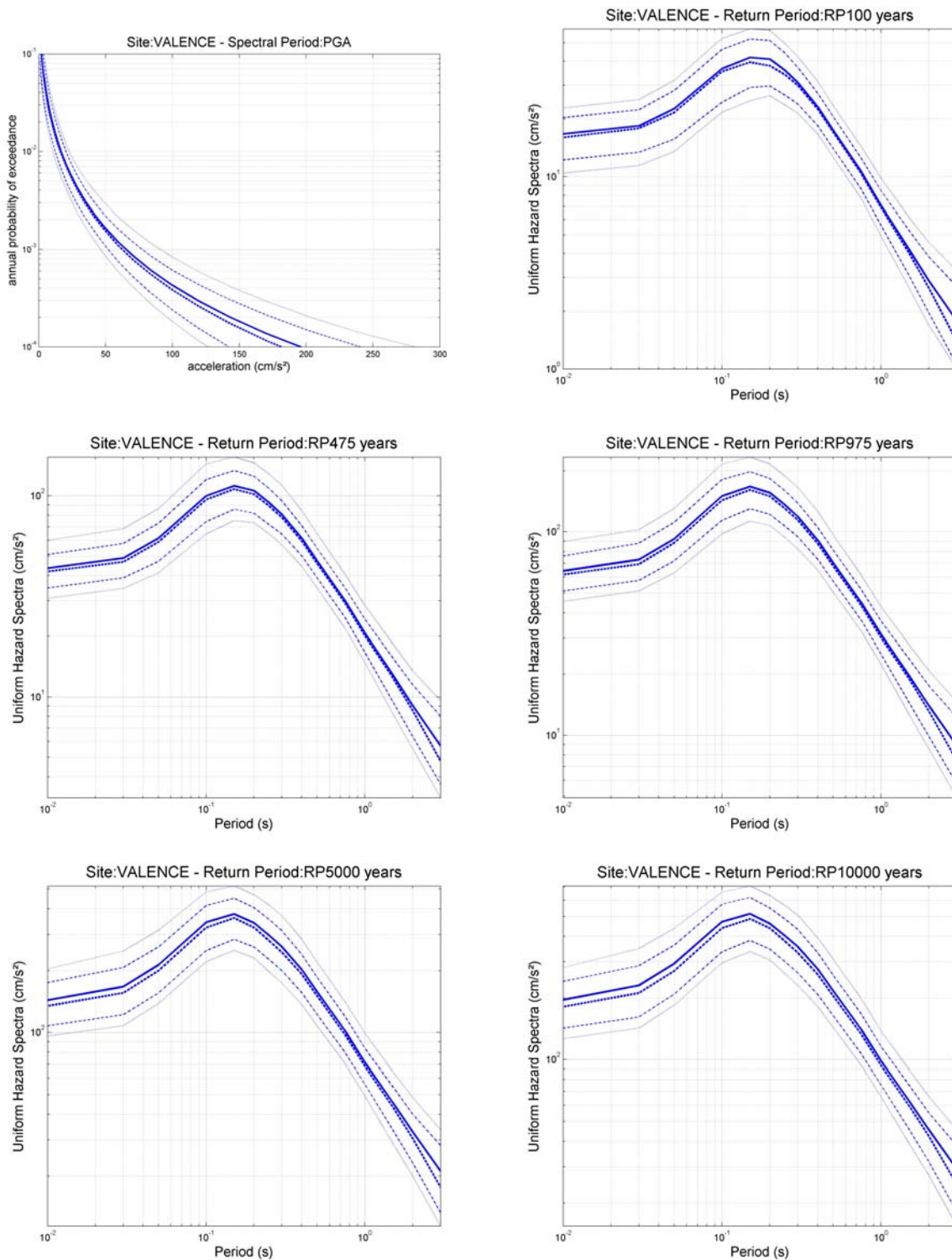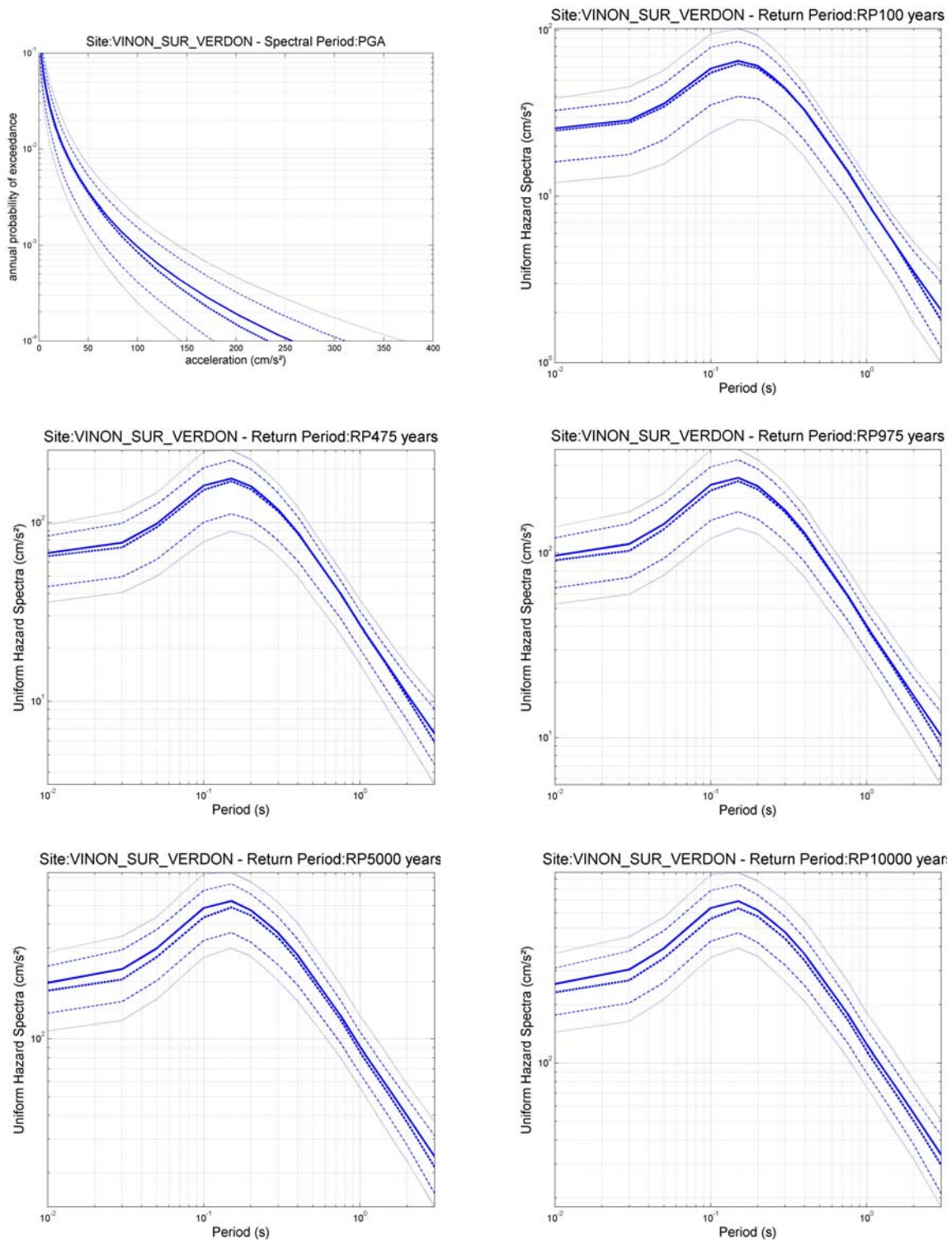
Vinon-sur-Verdon

Figure 20 – Hazard curves for PGA (top left), and Uniform Hazard Spectra for 5 different return periods (from 100 years : top right, to 10000 years : bottom right) at site Vinon-sur-Verdon. Mean : thick solid line, median : thick dashed line, centiles 14-86% : thin dashed lines, and centiles 5-95% : thin dotted lines.

Comments on deliverable D4-1

Preliminary PSHAs at selected sites, based on state of the art earthquake source models and attenuation relationships, considering both outcropping bedrock and soil conditions

Frank Scherbaum
University of Potsdam
Potsdam, May 8, 2012

1 Introduction

The report SIGMA-2012-D4-129, Version 01, covers those aspects of seismic hazard analysis in the Po plain which relate to new results or were modified, clarified or newly implemented by the technical integration team since the last meeting of the scientific committee.

The coverage of this rather heterogeneous set of aspects is excellently done and very well presented. There are only a few issues where I believe further clarification is needed. Therefore, most of the points I raise are touching upon details. For easier reference I am numbering them consecutively.

2 Previous studies and available input

On page 16 the authors write (citations are given in Times New Roman12 font):

Each SSZ in ZS9 was parameterized through (Working Group, 2004):

- its geometry, as well as an uncertainty range associated to its boundaries;

- its characteristic (uniform) seismogenic depth; its predominant focal mechanism;

- a subset of earthquakes from the CPTI04 catalogue (CPTI Working group, 2004b, see Sec. 2.1) "associated" to each SSZ, together with estimates of the completeness intervals;

- minimum (Mmin) and maximum (Mmax) magnitudes. *Mmin* was taken equal to 4.76 in nearly all SSZs while two values of *Mmax* were defined for each SSZ, namely *Mmax1* = largest observed magnitude included in the appropriate event subset of CPTI04 (see Figure 6), and *Mmax2 ≥ Mmax1,* conservatively estimated at 6.14 for all the zones where *Mmax1* would be less than *Mmax2* (except for the "volcanic" zones 922, 928 and 936, not concerned with this study).

In this context, I have the following questions:

1) Was the concept of a characteristic depth chosen because of the seismic hazard code or because the Working Group believed that a single depth would adequately describe the depth distribution for the purpose of hazard calculations?

2) Given that the observational period of seismicity (however long it may be) is finite, what is the justification for taking the largest observed magnitude Mmax1 as a legitimate estimate of maximum magnitude?

3) What is the reason for giving the magnitude values at a precision of 2 digits?

4) What is the rationale for judging a magnitude of 6.14 as conservative?

Further down on page 16, the standard Cornell´s method is mentioned.

5) Does this refer to the original approach in which the aleatory variability of ground motion was ignored?

3 Tool for PSHA: outline of CRISIS 2008

This chapter describes the main features of CRISIS 2008 and outlines its potential. The validation exercises done through PEER and within the GEM project provide confidence that the code performs well on the benchmark problems. However, what I miss and what seems to become relevant for the discussion in chapter 5.4 is

6) a discussion of the influence of the approximation of a continuous depth distribution of earthquake source through a single or a small set of characteristic depths on the hazard curve. Since the PDF of the square of the hypocentral distances involves the convolution of the PDF of the epicentral distances and the PDF of the depth distribution, representing the depth distribution simply by a single value ignores the „smoothing“ of the PDF of the hypocentral distances in comparison to the PDF of the epicentral distributions. I am concerned that the validity of this approximation may need to be tested, in particular for sites close to boundaries of seismic source zones.

4 Concepts for new seismic source zone model

This chapter is very clear and provides an excellent summary of the progress made in terms of refinement of SSZ models. The only questions which arose for me are related to a) the magnitude conversions and b) to the treatment of the depth distributions.

Equations 5 and 6 on page 48 list two linear relations between moment magnitude and M_l and m_b, respectively. A recent PhD at the ETh Zurich by Falko Bethmann (2011) entitled „Magnitude scaling relations and attenuation in thick sediments“, which is now partially published in BSSA (Bethmann et al., 2011), illustrates nicely how attenuation can affect the relationship between local magnitude and moment magnitude so that a linear relationship such as equation 5 would no longer be justified.

This could possibly affect the determination of seismicity parameters for the Po plain as well. Here I simply want to flag this issue for potential consideration. From page 49:

6) „The influence of the uncertainty introduced by the conversions on the variability of the frequency-magnitude correllations **will possibly be discussed** in a future deliverable". it has not become clear to me if the authors plan to spend further efforts on the issue of magnitude conversions. If they do (in addition to accounting for the uncertainty in the magnitude conversions) it might be worth looking at the issue of the potential non-linearity of the conversion equations.

Another issue in chapter 4 is the representation of continuous focal depth distributions through single selected characteristic depth values and corresponding weights in Figure 31.

7) It has not become clear to me how it is going to be ensured that the focal depth distributions are properly accounted for in the hazard calculations.

To illustrate my concern, the assignment of the relative weights is unclear to me. Taking for example the uppermost left panel in Fig. 31, the depth bin at 14 km seems to be as heavily loaded as the depth bin at 25 km (which receives a weight of 30% while the depth bin at 14 km receives 0%). Furthermore, some of the SSZ models in Table 10 on page 66 are represented only by single values, the rationale for which cannot be judged at all since none of the corresponding focal depth distributions is shown.

5 Parametric SHA at selected sites

This chapter explores the influence of the PSHA analysis with respect to some components of the hazard model for a small set of selected sites. Although this is not a comprehensive analysis, which would have been outside the scope of this deliverable, it discloses some of the more subtle sensitivity aspects of the PSHA results. I can only second the statement of the authors that „These results are of considerable interest and will be further explored in forthcoming PSHAs".

My only critical comment which I have with respect to this chapter (again) relates to the treatment of depth. As discussed on page 80, the authors discover consistently higher short period spectral ordinates by the CF08 GMPE which they attribute to the presence of SSZs at 6 km depth. Close to the end of page 80 they write „To explore this aspect in more detail, some alternative analyses were also performed modifying the SSZ model for the purpose of decreasing the possible influence of nearest (= most shallow) areal source."

8) My concern with this statement is that it seems to aim at the reduction of the influence of shallow seismicity (which may be a real feature) rather than its adequate incorporation, which in my opinion would be the appropriate perspective.

Concluding remarks

Overall, I found this is a very clear and well documented report, which is excellently presented.

Although I have flagged a total of 8 issues, most of them are of cosmetic nature. My main concerns are with

a) the justification of the maximum observed magnitude as Mmax and

b) the possible non-linearity of the magnitude conversion relation and

c) the treatment of the focal depth distribution in the hazard calculations.

References

Bethmann, Falko (2011). *Magnitude scaling relations and attenuation in thick sediments: application to the induced seismicity beneath the city of Basel, Switzerland.* PhD thesis, ETH Zürich.

Bethmann, Falko, Nicholas Deichmann, and P. Martin Mai (2011). Scaling Relations of Local Magnitude versus Moment Magnitude for Sequences of Similar Earthquakes in Switzerland, *Bulletin of the Seismological Society of America, 101*(2), 515-534.

Project SIGMA

Preliminary PSHAs at selected sites, based on state of the art earthquake source models and attenuation relationships, considering both outcropping bedrock and soil conditions

(Ref : SIGMA-2012-D4-29, 4/25/2012)

Jean B. Savy
May 8, 2012

1. Scope of the work reviewed

This is a review of the research work documented in EDF Ref: SIGMA-2012-D4-29, also presented as part of Work Package WP4, "Seismic Models", under the identification DI_4-1.

The first section of the report states the objective of the study as using existing recent seismic hazard studies to identify the areas that need improvements, to use it later, as basis for a second phase where the said improvements will be fully implemented. The phase presently reviewed is therefore considered only as a preliminary study.

 The stated areas of investigations are:

- Building an updated model of earthquake source zones of regional relevance in the Po Plain with respect to existing model ZS9.
- Selection of GMPEs through the use of a regional set of strong motion data,
- The application of non-stationary earthquake occurrence models in the hazard analysis
- Carry out a set of parametric analyses based on the previous ingredients,
  including a first, simple assessment of local response on deep soil sediments at some selected sites.

2. General comments and general conclusions

The document reflects the thoroughness of review performed to bring in the latest in research and development in the relevant scientific areas, and in accounting for the most recent data.

In order to determine if the study reach its goals of identifying needed research items, I asked the following questions:

- Question 1: Are the approaches, methods, existing studies and databases used in this work relevant and appropriate to derive conclusions as to the need of further research?
  Answer: Yes.

- Question 2: Did the study consider the impact of improvements on both level, and uncertainty in hazard results?
  Answer: Not convincingly

- Question 3: Are the conclusions convincingly documented?
  Answer: No.

- Question 4: Is there a clear plan for the actual improvements that will be implemented in phase II?
  Answer: No.

- Question 5: What is missing in this preliminary study?
  Answer: Disaggregation, consideration of alternate models in SSZs, and discussion on validity of PMPE models. Presentation of hazard results, and more specifically presentation of annual probabilities

Since there is no presentation of what will be done with the results of this study, and we do not know what actual improvements will be implemented, my conclusions are only based on the present document without assumptions on phase II. The main points of concern identified are:

- Overall, it is not clear how the various types of uncertainties will be handled in Phase II, in terms of their characterization, and also how they are going to be handled in the use of the CRISIS software (assuming it is the one that will be used). Before this task is complete there should be a clear and complete description of the methods, data and codes that will be implemented and used in Phase II.
- The uncertainty in zones' boundaries is not properly taken into account. Apparently SZ9 model is a consensus model, and the version used as starting point does not have epistemic uncertainty. This is a very critical point as the selected sites reside close to those boundaries. No alternative zones are used, aside for the smoothed seismicity. An alternative was developed to include a better representation of the subduction slab, but this is not sufficient to reflect the real epistemic uncertainty around the zones boundaries. In the present context it is not inconceivable that accounting for these uncertainties, would lower considerably the estimate of the hazard.
- There is no detailed description of how uncertainty in the seismicity parameters is handled in the computation software CRISIS. Given a certain seismicity database, parameters a's and b's (of G-R relationship) are not independent parameters. At least statistically they are correlated through the data. We need to know how the couples (a,b) will be selected, how many couples, and how it is used in CRISIS. (similar comment to comments made in May and November 2011 related to use of CRISIS by GEOTER)
- The choice of maximum magnitudes Mmax is based on a weak rationale and for the background it is not consistent with GEOTER's study assumptions for the western part of Piedmont and Italian Alps. GEOTER estimates are substantially higher. Given the very small probabilities assigned to large earthquakes, these differences would not affect hazard

results for return periods in the range of 10^3 years, but it might have a large impact for 10^4 years and larger.

- Presentation of the results is not standard. It is customary to present results in terms of annual probabilities, and this helps comparison between studies. Presenting results for 30yr life may be a local practice or a necessity, but it would be most helpful to also generate annual probability results, not only for a couple of spectral frequencies, but also for PGA, even though PGA is not used anymore in many design codes, but it is still used and it gives a quick idea of the seismic hazard at a site.
- Missing is a set of comparisons between the selected GMPEs, on the basis of actual ground motion data (PGA, and a couple of frequencies), for several magnitudes most relevant to the sites, and not only comparison based on Frank Scherbaum's LLH values.
- Also missing is a disaggregation of the hazard estimates for the 3 selected sites. Disaggregation is an important ingredient in the identification of zones, parameters, and GMPEs that have the greatest impact on the results. For GMPEs it can be used to determine if the models' ranges of validity are adequate, and it should be used as one of the input in the assignments of weights. We note that the task of selecting a formal process for the determination of those weights has been identified as a necessary additional task elsewhere in SIGMA, that when completed should be used in this study's Phase II.

3. A few comments on the form

On the form, I find the reviewed document rather well presented and well written with substantial and relevant references to previous works, but too verbose, which sometimes weakens clarity and does not help understanding the ideas developed.

4. Detailed comments

1) Maximum magnitude

Mmax should be consistent with our understanding of the geology and of the geometry of the tectonic blocs that drive locally plate motions. There is no explanation of the rational for selecting M6.5 for the SSZs of table 9, and the assigned uncertainties seems arbitrary. It is obviously true that Mmax in a specific SSZ has to be greater (or equal?) than the largest observed event, but given the size of the area, and the rarity of 6.5's, we also have to determine whether some of the postulated geologic structure are capable of generating such magnitudes. Before going further in the study, it would be helpful to analyze in detail the fault selected, and to present the rationales for the Mmax selections.

It could result that some SSZ would have Mmax greater than 6.5, such as the subduction slab (because of its potentially large geographical area- See comment below), but it could also lead to lower Mmax in some SSZs.

Somehow, the estimates of seismicity rates in this study and in GEOTER's study should be analyzed and made consistent. If they are not reconcilable, because of different interpretations of the data, or use of different models, at a minimum, both models should be considered as alternatives, with appropriate weights.

for the Piedmont, and Italian Alps SSZs:

    This Study: Mmax-min = 6.14 Mmax-max = 6.14

GEOTER: 6.70   7.20

2) <u>Use of 30 yr life instead of annual probabilities</u>

Considering that the authors wanted to use non-stationary occurrence models, it is reasonable to use the life time (30yrs here) as the reference time for estimating hazard. However, this creates difficulties for comparing with other similar or previous studies which use annual probabilities. It is possible to translate the results into annual probability of exceedance by making approximations. For example, a p30=10^{-4} probability in 30yrs, can be reasonably equated to a p1=10^{-3} annual probability, assuming some equivalent constant annual rate p1, and annual Bernoulli trials.

p30 = 1 – (1-p1)^{30} , so that a 10^{-4} (constant) annual probability corresponds to 10^{-3} 30yr life probability

p1 = 1 – (1-p30)$^{1/30}$, similarly, the (constant) annual probability p1 that gives a 10^{-4} 30yr life probability is p1= 3.3 10^{-6}

Therefore, we have to use the 10^{-3} probability of exceedance in 30yrs (5. 10^{-3} for 50yrs),to obtain an estimate of 10^{-4} annual probability of exceedance.
To get a very approximate estimate of the 10^{-4} PGA estimate for the NVL site, I used figure 53, page 77 which gives 0.1g to 0.3g for UH1, HazGrid and HazFX-BPT, disregarding DBM and MPS04 as extremes. The figure is for 0.06 probability of exceedance in 30yrs which corresponds to 2. 10^{-3} annually. Further (back of the envelop estimate) assuming that the slope of the hazard curve is similar at zero period as it is at 0.2sec, (from figure 52), we obtain 0.4g to 0.6g range of PGA for 10^{-4} annual probability (10,000 years return period) and 0.30g to 0.5g for 4.10^{-4} (2500years return period). These results, if confirmed, seem to be on the high side for this region of low seismicity, with only a potential for rare large events. It points out the need to investigate more thouroughly the zonation assumptions as well as those of the GMPEs.

3) <u>Zonations</u>

The starting point for this study is the existing ZS9, which appears to be a consensus map, as presented in Table 1, page 17, and Figure 6, page 15. Much work was devoted to the formulation of this map, but as it is presented, there is no consideration of uncertainty in the drawing of the zones. DI_4-1 reports on one improvement, that of considering the subduction slab, but it fails to characterize this epistemic uncertainty or to indicate how it will be handled in the next phase. Although this is not absolutely needed for this study, Phase II should consider carefully that aspect of the problem.

4) <u>No disaggregation</u>

Disaggregation is an important tool to narrow down the number of issues that are the most important and have the most impact on hazard estimates. It is a standard of any PSHA or preliminary studies. Results of disagreggation should identify the dominant sources of hazard and it should be used to judge on the adequacy of the models, their applicability range and their limitations. Specifically, in the weighting of

selected GMPEs, as an additional input to the ranking and
LLH scores.

5) <u>Subduction slab addition to the ZS9 model</u>
   There is a good discussion on the segregation of events in depth, and how the
   subduction slab can be characterized (pages 44-45). Two points here can be made:
   - Is it possible to show some focal mechanisms that demonstrate clearly the
     existence of the slab
   - From figure 21, p. 45, and given the explanations in the document, I
     estimate the maximum possible size of the slab to be approximately
     100kmx35km or 3,500km^2 in area.
     Using Wells and Coppersmith correlation relation of Rupture Area (RA)
     versus Magnitude (Wells D. and Coppersmith K.,BSSA, Vol. 84, No. 4, pp
     974-1002, Aug. 1994, Table 2A p 990), we obtain an estimate of **M**7.5 to
     M8 for the maximum ever possible on the slab. The maximum allowed in
     this study is **M**6.5 without much explanation for this choice.

6) <u>Selection of parameters of the G-R relationship</u>
   As mentioned above, a's and b's cannot be selected independently. It is necessary
   to explain how these parameters are selected and how they are used in the version
   of CRISIS being used in this task.

7) <u>High b values (p. 64)</u>
   Can it be explained why some b values are high, in particular for zones 916, 911
   and 908. Is there a possible physical reason for this, or possibly an over-correction
   for incompleteness, or perhaps, under-estimation of magnitudes of the larger
   earthquakes?

8) <u>Proximity of selected sites to SSZ boundaries(pages 45-46, and table 10
   p.66)</u>
   Because the selected sites are close to the boundaries of the SSZ (TRT- near SSZ
   911 boundary, NVL and CAS – near 912's), the exact location of the boundaries,
   and the contrast in seismicity rates between the host zones and neighboring zones
   are critical parameters affecting the estimate of the hazard. But the boundaries are
   at best uncertain, and rather arbitrary, for lack of resolution in the geology, so that it
   is very important to factor this uncertainty. It is absolutely necessary for the phase II
   study to include this epistemic uncertainty, and a more complete sensitivity analysis
   in this first phase is also needed.

9) <u>How is depth of earthquakes handled at the slab location (p66, table 10)?</u>
   Is it correlated with magnitude?
   Are large earthquakes allowed to be in the top layer?
   How does the version of CRISIS used in this study handle depth?
   We already discussed at length this issue in the review of GEOTER's work. It
   needs to be clarified here too.

10) <u>Need to explain how the uncertainty in Mmax is handled in the version of CRISIS</u>

The document does not give much information on this issue which requires some clear and complete documentation.

11) <u>Show a full display comparison of the selected GMPEs</u>

The document presents a very good discussion on the ranking of existing GMPEs, but it would also be very useful to show how each and all the models compare with the local data. The ranking with LLH measure is an abstract concept that does not give full account of the actual weight to assign each model, which will require also some judgment. As was mentioned above, a judgment must be made as to the importance of validity ranges, and what happens outside of the ranges of magnitude, distance and other factors in the data. A large part of that judgment by experts will rely on comparisons of models at various magnitudes, distance, and at various frequencies that are the most important for a particular site (hence need for disaggregation). Therefore the selection of GMPE's weights will not necessarily be the same for all sites. Note that the specific task of developing practical and reasonable methods of assigning those weights will be the object of another task in SIGMA, thus requiring close interaction with the work in Phase II of this task.

12) <u>Disaggregation</u>

Figures 43, 44 and 45 p.71 and p.72 show results for each SSZ and the combined results, but it does not show complete disaggregation. At a minimum, a disaggregation in terms of magnitude and distance is needed, but also a clear display of the relative contribution of each SSZ. (Not all SSZ's need to be shown, but only those contributing significantly to the final hazard). Figure 43 shows that SSZ 911, and to a lesser extent the subduction slab dominate the hazard confirming the concern about the importance of location of site with respect to SSZ zone boundaries

13) <u>Earthquake occurrence models</u>

Section 5.3, p. 75, describes seven occurrence models which are fitted to a limited number of years of data. This is an interesting exercise in the fact that it brings new ideas to this area of research, but the comparison that are shown in the study are not convincing for selecting one model over another, especially for the fact that it only relies on limited amount of data, and the medium-to-large events have occurrence rates orders of magnitudes smaller than the extent of the data. Therefore the practical range of validity of the models, as tested, and as fitted, may not be appropriate for a PSHA for which the dominant events are likely to be in the range of magnitudes 5.5 and above, and for return periods in the hundreds, if not thousands of years. All the models analyzed are worthy of consideration, but, again, careful weighting needs to be applied.

14) <u>Results of sensitivity analysis is questionable, if not doubtful (page 78)</u>

The report concludes

"*It is apparent that the variability introduced by the different models of earthquake occurrence in time, all within a consistent smoothed seismicity type of*

*representation, significantly exceeds the others. On the other
hand, the variability associated to the SSZ models, i.e. old ZS9 model vs. its present, deeply
revised version, is quite modest or negligible. This result was not so obvious…"*
Based on my previous comments, I do not find it obvious that the sensitivity to zonation boundaries would be negligible.

15) <u>V/H ratio (p. 83-84-85)</u>
V/H ratio is an important parameter in design the study and characterization of which, could be the subject of a new task or sub-task elsewhere in SIGMA. For coherence across SIGMA, this group should remain updated on progress in characterization of V/H, and possibly contribute to the selection of method and tools to estimate V/H at a particular site.

Respectfully submitted, May 8, 2012.

Jean Savy